DETERMINATION OF ELASTIC CONSTANTS FOR GEOSYNTHETICS USING IN-AIR BIAXIAL TENSION TESTS

by

Henry Nathaniel Haselton

A thesis submitted in partial fulfillment
of the requirements for the degree

of

Master of Science

in

Civil Engineering

MONTANA STATE UNIVERSITY
Bozeman, Montana

April 2018

ACKNOWLEDGEMENTS

I would like to thank my girlfriend Linnaea, my parents Eliza and George, my sister Sarah and all of my friends for being very supportive and helpful to me throughout all my years of school and the writing this thesis. I would like to thank Dr. Steve Perkins for his great contributions, continued assistance and advice throughout the entire research and writing process.

I would like to thank Eli Cuelho for designing and building the biaxial testing device as well as his advice pertaining to using the device and other equipment at the Western Transportation Institute (WTI). I would like to thank Stephen Valero and Hanes Geo for providing the geosynthetics used for testing. I would like to thank the folks at WTI for allowing us to use the lab facilities and store the geosynthetic materials. I would like to thank Beker Cuelho for assisting me with the initial lab testing and showing me how to operate testing equipment. I would like to thank Emily Schultz for all of the lab testing she conducted. I would like to thank Dr. Mark Owkes for his assistance with MATLAB and the least squares approximation technique.

I would like to thank the funding sources, the National Science Foundation (award number 1635029) and the Geosynthetic Institute for providing funding used during the first year of this project. I would also like to thank the College of Engineering for a graduate teaching assistant position for my second year of graduate school.

TABLE OF CONTENTS

TABLE OF CONTENTS CONTINUED

LIST OF TABLES

Table Page

LIST OF TABLES CONTINUED

Table Page

LIST OF TABLES CONTINUED

Table Page

LIST OF FIGURES

Figure Page

LIST OF FIGURES CONTINUED

Figure Page

LIST OF FIGURES CONTINUED

Figure Page

LIST OF FIGURES CONTINUED

Figure Page

LIST OF FIGURES CONTINUED

Figure Page

LIST OF FIGURES CONTINUED

Figure Page

LIST OF FIGURES CONTINUED

Figure Page

LIST OF FIGURES CONTINUED

Figure Page

LIST OF FIGURES CONTINUED

Figure Page

ABSTRACT

Geosynthetics are polymeric membranes used for structural reinforcement for many geotechnical applications such as reinforced pavement. Geosynthetics have been shown to increase the service life of roadways in a variety of field tests. The knowledge of geosynthetics and design methodologies could be improved with a better understanding of geosynthetic material properties. To better understand how geosynthetics perform in field loading situations, geosynthetic tensile resilient material properties are needed. The properties of geosynthetics of interest for this thesis are the resilient tensile modulus of elasticity and Poisson's Ratio (elastic constants) in both material directions. Modulus of elasticity has been traditionally calculated using wide-width uniaxial tests, which is a poor representation of field loading conditions due to the unrestrained sides of the material. Biaxial tension tests are a better representation of field loading conditions and thus were implemented for determination of elastic constants pertaining to different geosynthetic materials. Biaxial tension tests were performed on cruciform shaped samples using a custom device built by the Western Transportation Institute at Montana State University to test geosynthetic samples. A biaxial testing procedure was created using conclusions from a uniaxial testing program implemented to examine the resilient response of geosynthetics after being subjected to four types of loading (cyclic stress relaxation, monotonic stress relaxation, cyclic creep and monotonic creep) over different durations of time. The conclusions of the uniaxial testing program, the available literature and ASTM D7556 were synthesized to create a biaxial testing procedure. Biaxial tension tests were performed in three modes of loading to simulate loading conditions and loadings where a geosynthetic experiences loading in both directions simultaneously. The biaxial tension tests generated stress and strain data used to calculate the elastic constants of six biaxial geogrids and two woven geotextiles. The elastic constants were calculated using an orthotropic linear elastic constitutive model with a least squares approximation. The elastic constants calculated for each geosynthetic material were shown to represent the resilient behavior of geosynthetics in different field loading situations with more realistic boundary conditions than previous uniaxial tests used to characterize the resilient response of geosynthetics.

CHAPTER ONE

INTRODUCTION

Background

Geosynthetics are defined by ASTM D4439 as

> A planar product manufactured from polymeric material used with soil, rock, earth, or other geotechnical engineering related material as an integral part of human-made project, structure, or system (ASTM, 2017).

Geosynthetics are currently used in many geotechnical applications for structural reinforcement of soil. Common geosynthetic applications include retaining structures, roads, constructed slopes and load transfer platforms. For roadways, geosynthetics are placed at the bottom of or within the base course layer to provide reinforcement. This reinforcement can allow less base course to be used and/or can extend the service life of the roadway (Cuelho, 1998).

The performance of geosynthetics used for structural reinforcement of soil is dependent on tensile strength as well as other mechanisms (Koerner, 2012). In roads, as well as other applications, geosynthetics are subjected to a biaxial mode of loading, meaning the material experiences load simultaneously in both principal material directions. In applications such as long retaining walls, the direction perpendicular to the retaining wall face experiences loading, while the orthogonal direction is a direction of plane strain. Load still develops in this direction due to the Poisson effect, which impacts the stiffness and strength of the material in the direction being loaded.

Geosynthetics in applications such as roadways, experience repetitive loading over long durations of time that make the material experience some combination of stress relaxation and creep. The resilient response of the geosynthetic when loaded in tension repetitively is of interest in these applications.

Previous Work on Geosynthetics

The tensile properties of geosynthetics have primarily been studied using wide width tensile tests and other types of uniaxial load devices. Geotextiles have been tested for quality control as well as material properties using the wide-width strip method outlined in ASTM D4595. Geogrids have been tested in a similar manner to determine tensile properties with the Multi-Rib Tensile Method outlined by ASTM D6637. Wide-width cyclic uniaxial tension tests have been performed in the past in order to simulate loads experienced by geosynthetics in road applications (Cuelho et al., 2005). This test was created to obtain more realistic geosynthetic material properties for pavement design and is outlined by ASTM D7556. These tests, as well as all types of uniaxial tests, are less representative of field loading conditions because of the unrestrained sides of the material. The results from uniaxial tests are often used simply as index tests because they cannot accurately characterize how geosynthetics will perform in field applications.

Some design methods for field applications use load-strain material models for geosynthetics based on orthotropic linear elastic models. These orthotropic linear elastic models and other more advanced orthotropic elastic-plastic models have not been calibrated from appropriate tensile tests involving

controlled stress and strain boundaries. In order to calibrate these material models with appropriate test data, an advanced testing device that can apply loads simultaneously in two material directions is necessary. A biaxial testing device of this nature has been built by the Western Transportation Institute at Montana State University and was used for this research project.

Scope of Work

The goal of this research is to conduct biaxial tests in a manner that simulates a resilient load-strain response of geosynthetics that is representative of their response in applications such as wheel loading in roads. Initially uniaxial wide width tensile tests were performed on a woven geotextile and a geogrid to create a procedure for the experimental biaxial testing device. Biaxial tests were then conducted to determine elastic constants for an orthotropic linear elastic constitutive model of these materials. The material properties desired from biaxial tests were the modulus of elasticity in both principal directions and the in-plane Poisson's ratio.

CHAPTER TWO

LITERATURE REVIEW

Introduction

Biaxial tests have been used for determining material response and properties on a variety of materials in the past. Many structural membranes used for building materials have been tested using biaxial samples and yielded useful results. For geosynthetics, far fewer biaxial tests have been conducted and have yielded inconclusive results. In the past, different types of uniaxial tests have been performed on geosynthetics because a less complex testing device is necessary. Literature from uniaxial testing on geosynthetics was examined as well for this literature review.

Uniaxial Testing of Geosynthetics

A variety of uniaxial testing procedures have been developed for both geogrids and geotextiles for the application of structural reinforcement of soil. Some tests are simply used as index tests while others are intended to provide insight into the performance of the geosynthetic in field applications. Tensile tests on geosynthetics can provide information such as the tensile stress vs. strain, ultimate strength, strain at failure and modulus of elasticity (Koerner, 2012). Several testing standards exist for determining the in-air material properties for geosynthetics including ASTM D1682, D751, D4632, D4595, D6637 and D7556 (Koerner, 2012). For determination of the modulus of elasticity, it is desirable to use significantly wide samples to reduce the effects of necking

that occurs in uniaxial tension tests. The use of wide samples in comparison to their length reduces the Poisson effect (necking) of the sample and thus allows for more realistic stress and strain measurements. This concept was used for testing geotextiles to calculate modulus values because geotextiles (especially nonwovens) are susceptible to necking.

Cuelho et al. (2005) examined the resilient response of geosynthetics subjected to repetitive loading to simulate field loading conditions to which geosynthetics are subjected in reinforced flexible pavements. Cyclic wide width tensile tests were performed for this study on a variety of geotextiles and geogrids. The objective of this study was to document the modulus or stiffness of the material after the application of a large number of cyclic loads and to examine how this modulus varies as the material is cycled at progressively higher values of load and strain. The resilient response of geosynthetics was simulated by applying 1000 cycles of load at progressively larger values of permanent strain (Figure 1). The modulus at each permanent strain level was calculated using the slope of the last 10 cycles (Figure 2). The tests were performed under displacement control such that load was cycled to produce ±0.1% strain centered around the chosen value of permanent strain. This type of loading caused stress-relaxation during cyclic loading and is illustrated in Figure 1 for tests performed on a biaxial geogrid. The modulus remained relatively constant as permanent strain increased for geogrids (Geosynthetic D-G on Figure 2) while the modulus increased as permanent strain increased for geotextiles (Geosynthetic A-C on Figure 2). Only cyclic stress relaxation

tests were performed in this study. No cyclic creep tests, monotonic stress relaxation tests or monotonic creep tests were performed for this study.

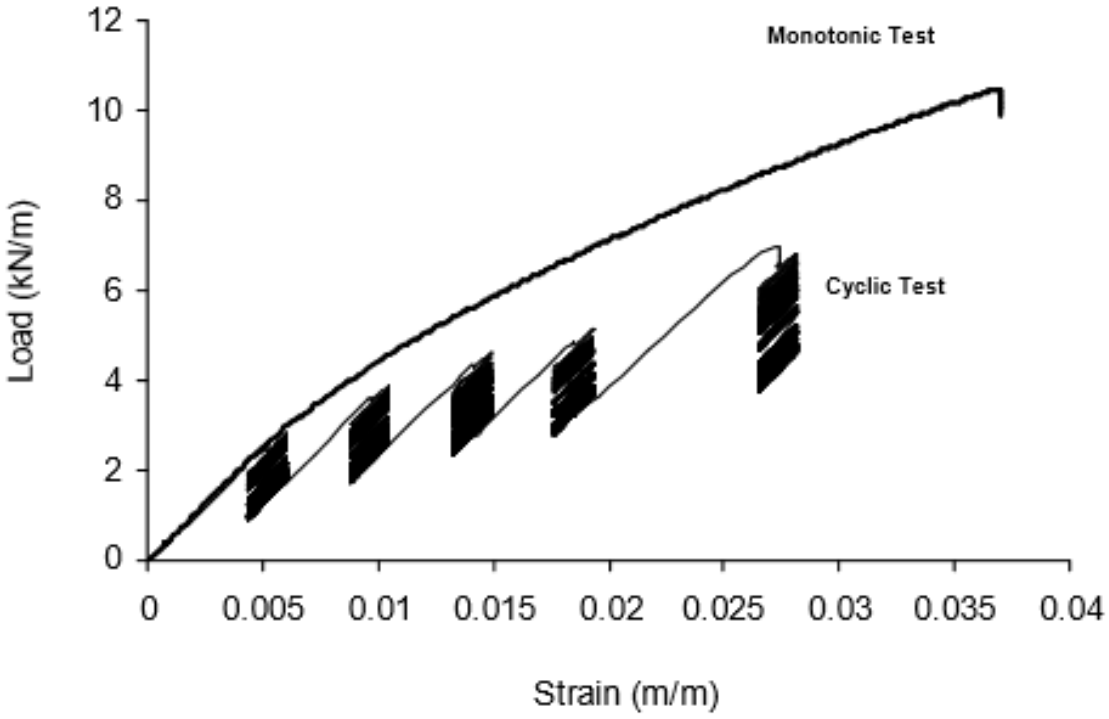

Figure 1 Cyclic and monotonic wide-width tension tests on biaxial geogrid, machine direction (Cuelho et al., 2005)

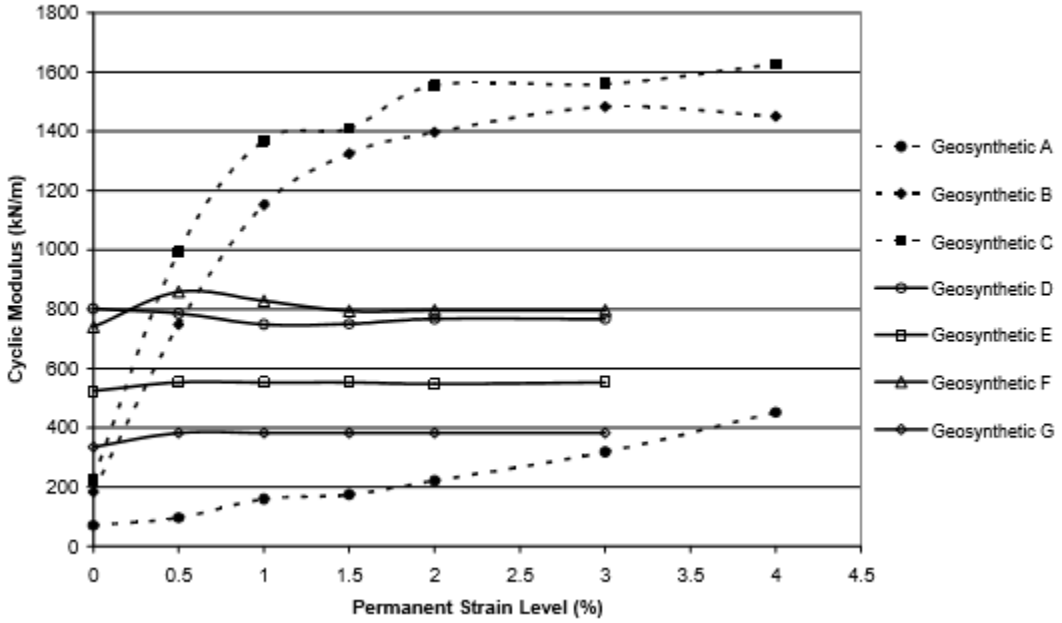

Figure 2 Cyclic tensile modulus versus permanent strain, machine direction (Cuelho et al., 2005)

Biaxial Testing of Structural Membranes and Fabrics

Structural membrane materials generally consist of fibers made from a variety of polymers ranging from natural fibers to polyethylene that are woven in two perpendicular directions (Beccarelli 2015). Fabrics used for structural membranes are similar in material composition and manufactured structure to some woven geotextiles, making them of interest for this literature review. The need for biaxial tests for structural membranes dates back to the early 1900s when high strength textiles were tested for use in German dirigible airships (Haas, Dietzius, 1913). In the 1950s, it was recognized by several researchers that uniaxial tests were not sufficient for testing certain fabrics. Checkland et al. (1958); Reichardt et al. (1953) and Klein (1959) performed biaxial tests

on fabrics to examine load-strain response. The advantages of using cruciform shaped samples to minimize effects of material griping and yield a uniform stress field in the interior portion of the sample was identified by Klein (1959). Biaxial testing for high-strength fabrics used in inflatable radar domes was examined by Krause and Bartolotta (2001). Cruciform shaped specimens were tested using an in-plane biaxial load frame to examine the highly nonlinear properties of these materials. A uniform strain field was observed in the interior section of the biaxial sample (Figure 3)

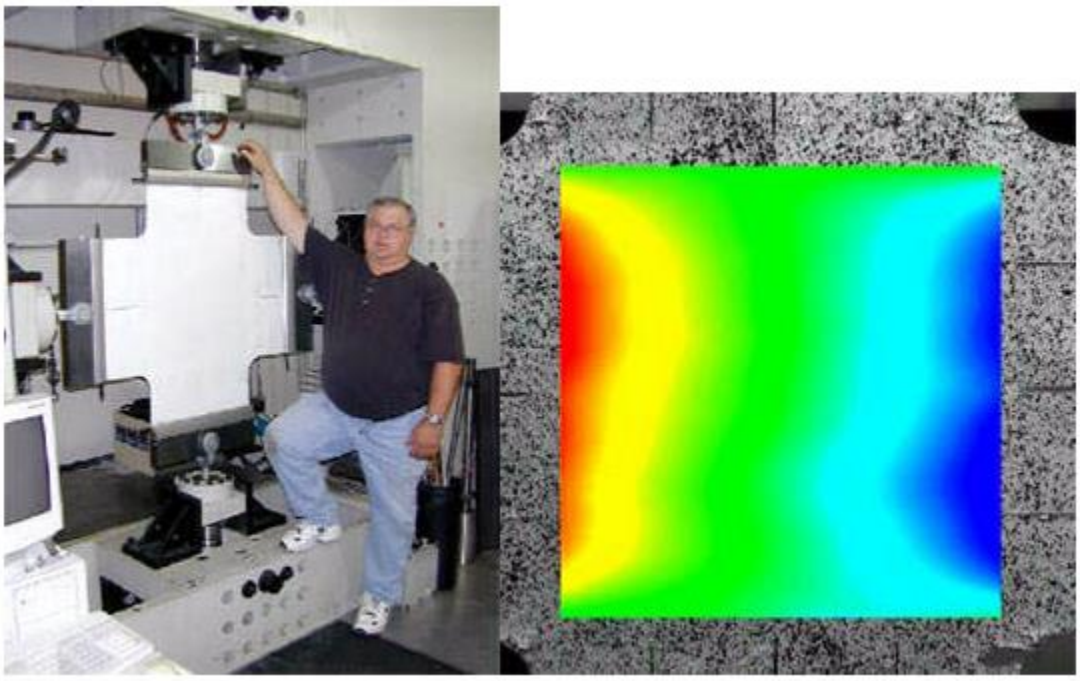

Figure 3 Left: Biaxial Testing Device Used for Testing High-Strength Fabrics Right: Strain Field from Equal Loading along both axes (Krause & Bartolotta, 2001)

The importance of fabric shape, load application, material gripping and strain measurement in biaxial tests was examined by Bridgens and Gosling (2003). Cruciform samples were used to reduce distortion seen from tests on rectangular samples in earlier

studies. A finite element program was used to analyze cruciform shaped samples with a variable number of slits along the cruciform arms (Figure 4).

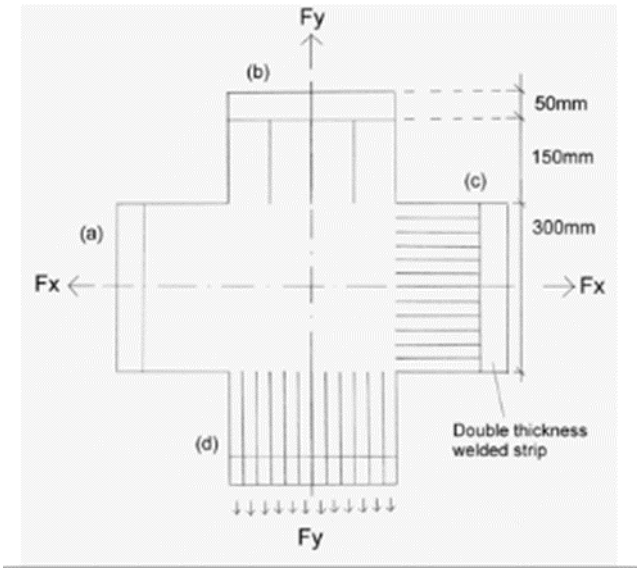

Figure 4 Cruciform Shaped Biaxial Sample with Slits along Cruciform Arms (Bridgens and Gosling, 2003)

The interior section of the cruciform was 300 mm by 300 mm. A uniform stress field was observed in the center of the interior section, with effects from the grips becoming noticeable around 100 mm from the center (Figure 5).

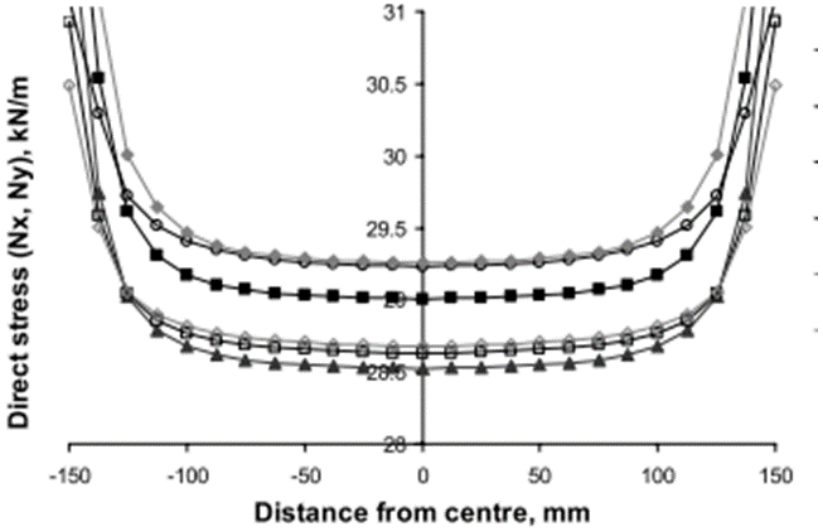

Figure 5 Stress Distribution in Interior Portion of Biaxial Sample (Bridgens and Gosling, 2003)

The sample with no slits along the arms gave the least variation in stress across the interior section. The model also showed a stress reduction occurring between the stress applied at the grip and the stress in the interior of the sample. This reduction was less significant when the slits were placed in the arms of the cruciform shape. The model showed arms with eleven slits had the lowest stress reduction ratio. Bridgens and Gosling (2003) recommended using cruciform shaped biaxial samples with eleven slits and a gauge length of 200 mm for samples with interior dimensions of 300 mm by 300 mm.

Despite the fact that membrane materials have been tested in biaxial devices for decades, very few testing standards exist to outline testing procedures. The American Society of Civil Engineers (ASCE) and Structural Engineering Institute (SEI) created a testing standard for tensile membrane structures in 2010 (ASCE/SEI 55-10, 2010). An orthotropic linear elastic constitutive model is recommended for determining the elastic

constants of membrane materials from biaxial tension tests on cruciform shaped samples (ASCE/SEI 55-10, 2010). In order to solve for the elastic constants from measured stress and strain data, the least squares method is recommended (ASCE/SEI 55-10, 2010). The Membrane Structures Association of Japan created a Testing Method for Elastic Constants of Membrane Materials (MSAJ, 1995) that is referenced as an outline in many biaxial testing studies that proceeded it. The testing standard outlines a detailed testing procedure including testing device specifications, test specimen specifications, test procedures and methods for calculating the elastic constants of materials tested. The Japanese standard recommends a biaxial testing device that is capable of applying loads simultaneously in perpendicular directions such that the location of the center point of the cruciform shaped specimen remains constant (MSAJ, 1995). The recommend test specimen size is outlined in

. The recommended distance between initial standard points for measurement of displacement was between 20 and 80 mm or at least 10 crossing yarns for a range of strain measurement of -10 % to 20 %.

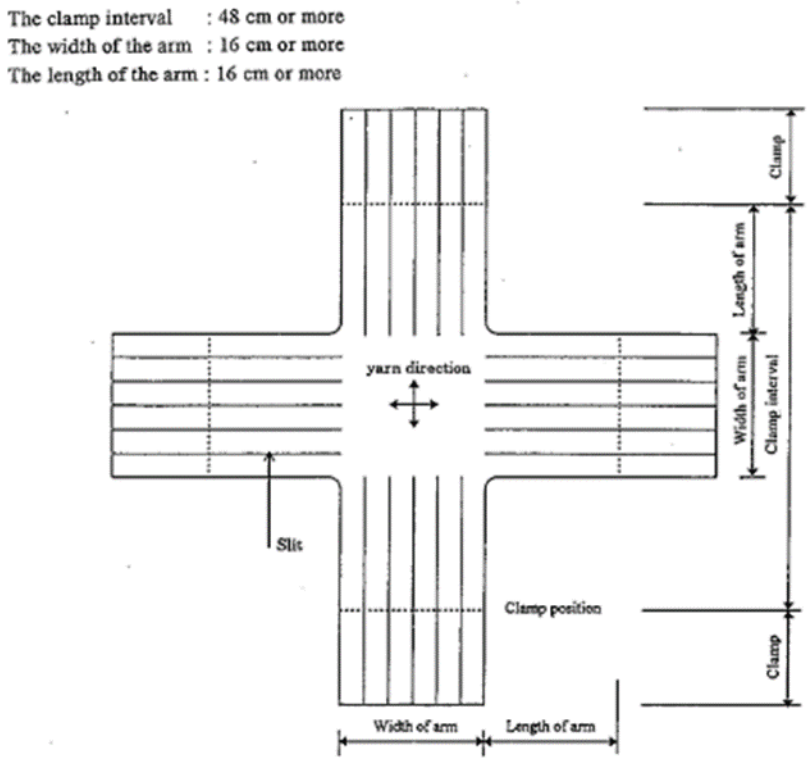

Figure 6 Biaxial Sample Dimensions for Japanese Testing Standard (MSAJ, 1995)

The Japanese testing standard also specifies slits being cut on the cruciform arms to minimize the load reduction that occurs between the grip where the load is applied and the interior portion of the sample where displacement is measured. The applied loading procedure for testing membranes in the Japanese standard is not applicable for the resilient response desired for the geosynthetics tested in this thesis but the same material constants can be calculated from both testing procedures. From the measured loads and displacements, stress and strain values for both material directions are used to calculate elastic constants using a linear elastic orthotropic constitutive model (MSAJ, 1995). Two methods for calculating the four elastic constants (Elastic modulus in machine direction (MD) and cross-machine direction (XMD) and Poisson's ratio relating MD to XMD and

XMD to MD directions) are used in the Japanese testing standard. The first method is a Least-Squares Method that can be used to minimize the stress or strain terms of governing equations (see Chapter Three of Thesis) using multiple load ratios. The other suggested method is the Best Approximation Method or minimax method. Both methods will be discussed further in proceeding sections of this thesis. Multiple tests and load ratios are needed to calculate the elastic constants since only three independent equations are available to calculate four unknowns for the selected linear elastic orthotropic model.

A number of testing programs and studies have been performed on structural membranes in order to determine their elastic constants from biaxial laboratory testing. The Japanese testing standard was referenced in a significant number of studies as an outline for the testing procedure and a guide for calculating elastic constants. Bridgens and Gosling (2010) examined the Japanese testing standard in detail. In this paper, different methods for calculating elastic constants from biaxial tests performed on a Ferrari 1202 PVC-polyester membrane were examined. The Japanese testing standard outlines a procedure with multiple load ratios applied to the same material over the course of one test. The load ratios are defined as the ratio of the load applied in each perpendicular direction of a biaxial tension test. If equal load is applied in both directions, the load ratio is 1:1. In the Japanese testing standard, load ratios of 0:1 and 1:0 are specified in the testing procedure. The Japanese testing standard recommends not using data in the direction of zero load for calculation of elastic constants. Bridgens and Gosling (2010) examined differences in elastic constants when the data from these load ratios was included. The Japanese testing standard uses an equation to relate Poisson's

ratio in both directions referred to as the reciprocal constraint ($\nu_{12} * E_2 = \nu_{21} * E_1$). Bridgens and Gosling (2010) examined the difference in elastic constants when this equation was not used.

When coated woven fabrics used for structural membranes are subjected to high loads over sustained periods of time, they develop some residual strain due to creep. In the Japanese testing standard nothing is done to account for this residual strain in the material so Bridgens and Gosling (2010) also examined the effect of removing this strain from their data. Significant variation in values of the elastic constants calculated was observed between the different analysis approaches examined by Bridgens and Gosling (2010). The results are shown in Table 1.

Table 1 Elastic Constants Using Different Calculation Methods (Bridgens and Gosling, 2010)

Test data used to determine elastic constants	Reciprocal constraint aplied? †	Warp stiffness, 'E_x' (kN/m)	Fill stiffness, 'E_y' (kN/m)	Poisson's ratio warp-fill, 'ν_{xy}'	Poisson's ratio fill-warp, 'ν_{yx}'	Sum of strain differences squared, 's'
Ferrari 1202 PVC-polyester						
All load ratios, with residual strain	No	350	414	-0.17	-0.32	0.7347
	Yes	339	431	-0.22	-0.27	0.7393
All load ratios, residual strain removed	No	744	787	0.42	0.76	0.0439
	Yes	818	718	0.63	0.55	0.0522
All load ratios, creep removed, 0:1 & 1:0 zeroed	No	1157	919	0.29	0.17	0.0165
	Yes	1132	935	0.25	0.20	0.0167
Single load ratio 1:1	No	500	500	0.60	0.64	0.0019
	Yes	5482	4021	-3.00	-2.20	0.0019
Single load ratio 2:1	No	4560	4916	0.01	-6.14	0.0016
	Yes	1211	4561	0.01	0.04	0.0016
Single load ratio 1:2	No	502	500	1.13	0.50	0.0003
	Yes	3781	1016	0.59	0.16	0.0003
Single load ratio 1:0	No	1253	8468	0.75	- *	0.0018
	Yes	1109	10000	0.70	- *	0.0013
Single load ratio 0:1	No	9999	806	- *	1.23	0.0007
	Yes	515	790	- *	1.21	0.0008
Verseidag B18089 PTFE-glass						
All load ratios, residual strain removed	No	764	603	1.12	0.84	0.0728
	Yes	752	611	1.08	0.88	0.0730

† 'Constraint' refers to whether the reciprocal relationship (Formula 2) has been applied. If 'No' then all four elastic constants are independent.
* For load ratios of 0:1 and 1:0 only one value of Poisson's ratio must be considered, the other is multiplied by zero in all calculations.

The variation in results highlights the complex behavior of structural membrane fabrics and the possible over-simplification of representing this material with the linear

elastic orthotropic model. Bridgens and Gosling (2010) concluded that use of the reciprocal constraint had only a small effect on the calculated values for elastic constants in comparison to the effect of removing residual strain. The removal of residual strain was discussed in more detail by Bridgens and Gosling (2004). Beccarelli (2015) also referenced the Japanese testing standard for calculating elastic constants from biaxial tension tests. Craenenbroeck et al. (2015) used the testing procedure outlined in the Japanese standard as well as variations of this procedure to calculate elastic constants for structural membranes. It was found that when a loading protocol that mimicked field-loading conditions for membranes was used instead of the standard protocol, a variation in elastic constants occurred (Craenenbroeck et al., 2015).

The in-plane biaxial tests on structural membranes provided useful information regarding biaxial testing devices, biaxial sample size/setup and use of stress and strain data to calculate elastic constants with an orthotropic linear elastic constitutive model. The specifics about loading procedure effects on elastic constants and membrane behavior in general are slightly less applicable since a significantly different testing procedure was used on significantly different materials for this thesis.

Biaxial Testing of Geosynthetics

The three most notable biaxial tests on geosynthetics have been conducted by Kupec and McGown (2004), McGown et al. (2004) and Hangen et al. (2008). All three of these studies were performed on biaxial geogrids.

Kupec and McGown (2004) used cruciform shaped samples of a biaxial geogrid to conduct sustained loading tests in the testing device shown in Figure 7.

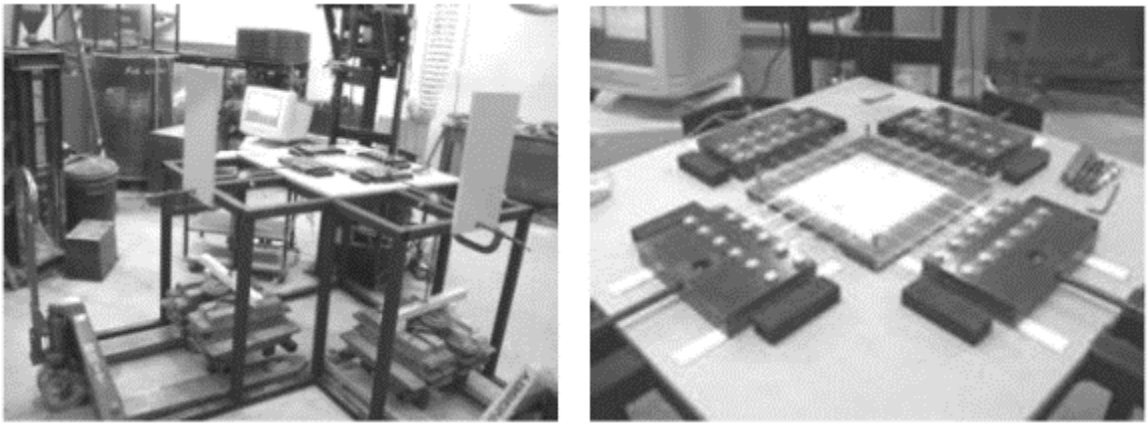

Figure 7 Biaxial Testing Device used for Sustained Loading Tests on Biaxial Geogrids (Kupec & McGown, 2004)

Uniaxial sustained creep tests were also performed on the same material at the same level of applied stress (30% and 50% of the nominal strength of the material). A stiffer response was observed for materials tested biaxially in comparison to uniaxially (Figure 8).

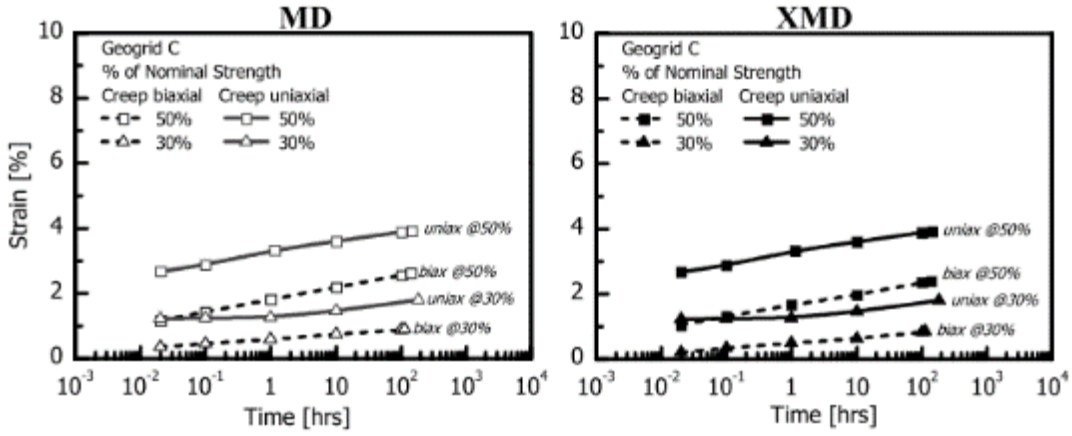

Figure 8 Results from Biaxial and Uniaxial Sustained Loading Tests (Kupec & McGown, 2004)

McGown et al. (2004) commented on the need for a more rigorous design approach using laboratory data for soil reinforcement using geogrids. To better understand the material response of geogrids, McGown et al. (2004) conducted constant rate of strain biaxial and uniaxial tests on biaxial geogrids over shorter durations of time to examine any differences in stiffness. Biaxial tests were performed on cruciform-shaped specimens with slit cruciform arms as shown in Figure 9.

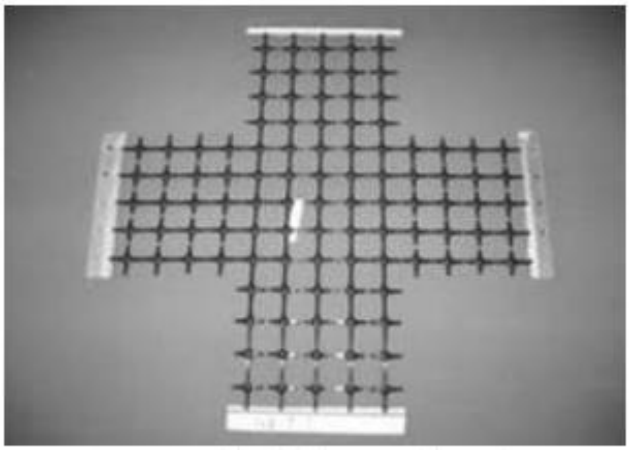

Figure 9 Biaxial Geogrid Specimen for Biaxial Test (McGown et al., 2004)

Under a constant rate of deformation of 1 mm/min, a slightly stiffer response was observed for geogrids tested biaxially in comparison to uniaxially (Figure 10), (McGown et al., 2004). The increased stiffness for biaxial tests in comparison to uniaxial tests was much less significant for constant rate of strain tests than it was for sustained loading tests. McGown et al. (2004) attributed the increased stiffness of geogrids in biaxial loading in comparision to uniaxial loading to the behavior of the junctions of the geogrid. McGown et al. (2004) concluded that when junctions are subjected to biaxial load/strain conditions they will react with an increased stiffness compared to their reaction from uniaxial load/strain conditions because the junctions are required to strain simultaneously in two directions.

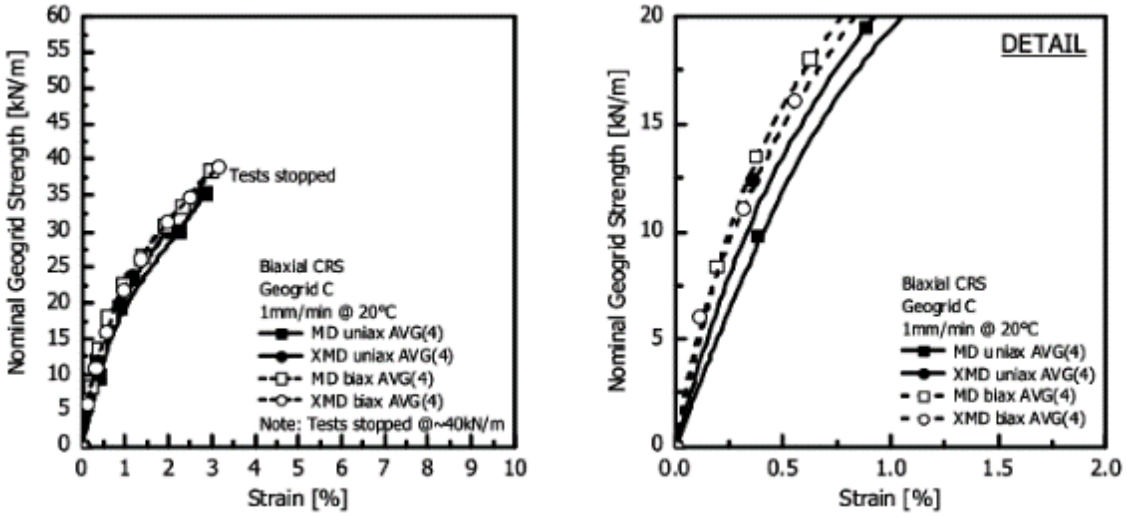

Figure 10 Biaxial and Uniaxial Constant Rate of Strain Tests on a Biaxial Geogrid (McGown et al., 2004)

Hangen et al. (2008) examined the importance of several factors in biaxial tests. The loading and clamping arrangement of biaxial samples was investigated, as well as the sample size and shape. It was concluded that samples should be tested in the shape of a cruciform with the center point of the sample staying stationary. This is accomplished by applying equal displacements in all four directions. To eliminate effects of clamping, the length of the cruciform arms need to be sufficiently long with the cross-direction ribs being snipped (Hangen et al., 2008). Hangen et al. (2008) mimicked the testing procedures used by Kupec and McGown (2004) and McGown et al. (2004) for constant rate of strain tests and sustained loading tests on the same biaxial geogrids and did not observe the increased stiffness reported by the previous studies. Hangen et al. (2008) concluded that the increased stiffness reported previously was likely due to loading and clamping errors and not a result of biaxial loading conditions. The conflicting results

reported by Hangen (2008) and McGown et al. (2004) and Kupec and McGown (2004) highlight the need for additional biaxial testing.

Synthesis of Literature Review

The literature examined for this thesis was helpful for the process of creating a biaxial testing procedure for geosynthetics that could be used to simulate a resilient response of geosynthetics subjected to relatively low biaxial loads. The procedure for Determining Small-Strain Tensile Properties of Geogrids and Geotextiles by In-Air Cyclic Tension Tests (ASTM D7556) was most applicable for the desired resilient response of geosynthetics. A form of this procedure was adopted using other information regarding biaxial testing devices, sample specifications and calculation of elastic constants for biaxial samples of geosynthetics using in-plane biaxial tension tests. Limitations of the biaxial testing device available for this thesis also were examined and modifications were made to the testing procedure and data analysis to best utilize the testing equipment and data collection systems available.

CHAPTER THREE

THEORY

Constitutive Equations

An orthotropic linear elastic model was used to describe the behavior of geosynthetics subjected to biaxial tension tests. For the entirety of this thesis, stress will be expressed as force per length, as dividing by the thickness of the geosynthetic to get the true units of stress is not commonly done for geosynthetics. The inputs for the constitutive equations are the stress and strain measured in both principle directions of the material. The constitutive equations are used to calculate four elastic constants for the material. The elastic constants calculated are the modulus of elasticity in both material directions and Poisson's ratio in both material directions. Only three of the elastic constants are independent when the reciprocal constraint is applied (Equation (9)). The orthotropic linear elastic constants were calculated using the general relationship between stress and strain shown in Equation (1). For biaxial loading, the general form of the equation can be reduced to Equation (2) because the material is in a state of plane stress. A further simplification resulting in Equation (3) can be made assuming biaxial samples are in a state of pure tension. Equation (3) was used for calculation of the three independent elastic constants for geosynthetics. The three independent elastic constants that were solved for are the modulus of elasticity in both directions (E_1 and E_2) and Poisson's Ratio (ν_{12}). These elastic constants appear in terms in the stiffness matrix, which are defined in

Equations (4), (5), (6) and (7). Poisson's ratios for orthotropic materials are related by Equation (9) and constrained via Equation 0.

$$(1)\ \sigma_i = C_{ij}\varepsilon_j$$

$$(2)\ \begin{bmatrix}\sigma_1\\ \sigma_2\\ \tau_{12}\end{bmatrix} = \begin{bmatrix}C_{11} & C_{12} & 0\\ C_{21} & C_{22} & 0\\ 0 & 0 & C_{66}\end{bmatrix}\begin{bmatrix}\varepsilon_1\\ \varepsilon_2\\ \gamma_{12}\end{bmatrix}$$

$$(3)\ \begin{bmatrix}\sigma_1\\ \sigma_2\end{bmatrix} = \begin{bmatrix}C_{11} & C_{12}\\ C_{21} & C_{22}\end{bmatrix}\begin{bmatrix}\varepsilon_1\\ \varepsilon_2\end{bmatrix}$$

$$(4)\ C_{11} = \frac{E_1}{1-\nu_{12}\nu_{21}}$$

$$(5)\ C_{22} = \frac{E_2}{1-\nu_{12}\nu_{21}}$$

$$(6)\ C_{12} = \frac{\nu_{21}E_1}{1-\nu_{12}\nu_{21}}$$

$$(7)\ C_{21} = \frac{\nu_{12}E_2}{1-\nu_{12}\nu_{21}}$$

$$(8)\ C_{12} = C_{21}$$

$$(9)\ \nu_{12} = \nu_{21}\frac{E_1}{E_2}$$

$$(10)\ \nu_{12}\nu_{21} < 1$$

The orthotropic stress-strain relationship results in Equations (11) and (12). These equations are derived simply from converting the matrix form of Equation (3) to algebraic form. These two equations contain three independent unknowns (E_1, E_2, ν_{12}) so they cannot be directly solved. Instead numerical methods must be introduced in order to determine "best fit" values for these three elastic constants that satisfy Equations (11) and (12). Biaxial test data provides the stress and strain inputs for Equations (11) and (12).

$$(11)\qquad \sigma_1 = \frac{E_1}{1-\nu_{12}\nu_{21}}\varepsilon_1 + \frac{\nu_{21}E_1}{1-\nu_{12}\nu_{21}}\varepsilon_2$$

$$(12)\qquad \sigma_2 = \frac{\nu_{12}E_2}{1-\nu_{12}\nu_{21}}\varepsilon_1 + \frac{E_2}{1-\nu_{12}\nu_{21}}\varepsilon_2$$

Numerical Methods

The constitutive equations used to solve for the elastic constants results in a system of equations that is indeterminate for a single biaxial test since only Equations (11) and (12) are available for solving three independent elastic constants. To solve for the elastic constants, additional tests must be conducted at varied load ratios. This allows additional equations to be generated in the form of equations (11) and (12) with different values for stress and strain inputs (MSAJ, 1995). Once additional load ratios are used, numerical methods can be implemented to determine what set of elastic constants best fits the measured stress and strain responses for multiple load ratios. The most common approach for solving this system of equations is a least squares approximation. The least squares approach is outlined in the Japanese testing standard and has been implemented for numerous studies using biaxial tension tests to calculate elastic constants for membrane materials.

The least squares method was examined in a more general format to confirm the method outlined in the Japanese testing standard was applicable. The least squares technique is useful when there is a positive correlation between x and y that cannot accurately be predicted by polynomial interpolation or other approximation techniques (Chapra, Canale, 1998). In the case of biaxial tension tests, there is a positive relationship between measured stress and strain values that can be related by the elastic constants in the orthotropic linear elastic model. A least squares regression uses an approximating function that does not necessarily pass through all data points but generally predicts the trend of the data (Chapra, Canale, 1998). In order to provide a unique approximation that

"best" fits the given data, a minimization of the sum of the squares of the residuals is used as shown in Equation (13) (Chapra, Canale, 1998).

$$S = \sum(y_{i,measured} - y_{i,model})^2 \quad (13)$$

A general least squares approach for a given data set tries to approximate the data using an approximating function in the form of Equation (14). The approximating function for general leas squares is required to have a linear dependence on its parameters ($a_1, a_2 \ldots a_n$) (Chapra, Canale, 1998). The least squares approximating function (Equation (14)) approximates function values (y) using the parameters ($a_1, a_2, \ldots, a_n$) and basis functions ($z_1, z_2, \ldots, z_m$), where the parameters are the unknowns and the basis functions are a function of the x values.

$$\text{Given Data: } (x_i, y_i) \text{ for } i = 1, \ldots, n$$

$$\text{Approximating Function: } f(x) = a_1 z_1 + a_2 z_2 + \cdots + a_m z_m \quad (14)$$

As mentioned previously, the goal of the approximating function is to minimize the error (residuals) between the data values for y and the approximated values or f (x) values. To minimize the residuals, a function is defined as follows (Chapra, Canale, 1998),

$$S_r = \sum_{i=1}^{n} (y_i - f(x_i))^2 \quad (15)$$

To solve for the parameters in the approximating function (a_1, a_2 and a_n) the partial derivatives of S_r with respect to a_1, a_2 and a_n are set equal to zero (Chapra, Canale, 1998).

$$\frac{\partial S_r}{\partial a_1} = \frac{\partial S_r}{\partial a_2} = \frac{\partial S_r}{\partial a_n} = 0 \quad (16)$$

The general least squares approach can be applied to stress and strain data from biaxial tension tests to solve for the elastic constants in an orthotropic linear elastic constitutive

model. The least squares approach can be used to minimize the residuals in the stress term or in the strain term for a given data set from biaxial tension tests. The method to minimize the stress term, as shown in the Japanese Testing Standard, uses Equations (11) and (12), which are rewritten using equations (4) -(7) to be in a linear form as required for general least squares. The stress term for each direction (σ_1, σ_2) are written as a function of the strain terms $(\varepsilon_1, \varepsilon_2)$ and parameters (C_{11}, C_{12}, C_{22}) in the same format as Equation (14).

$$\sigma_1 = C_{11}\varepsilon_1 + C_{12}\varepsilon_2 \tag{17}$$

$$\sigma_2 = C_{21}\varepsilon_1 + C_{22}\varepsilon_2 \tag{18}$$

The following equation is written in the form of Equation (15) (MSAJ, 1995) using the measured values of stress and strain from a biaxial test.

$$S = \sum\{(C_{11}\varepsilon_1 + C_{12}\varepsilon_2 - \sigma_1)^2 + (C_{21}\varepsilon_1 + C_{22}\varepsilon_2 - \sigma_2)^2\} \tag{19}$$

The partial derivatives of S with respect to the parameters in the approximating function (C_{11}, C_{12}, C_{22}) are set equal to zero according to Equation (16) (MSAJ, 1995).

$$\frac{\partial S}{\partial C_{11}} = \frac{\partial S}{\partial C_{22}} = \frac{\partial S}{\partial C_{12}} = 0 \tag{20}$$

A matrix is setup to solve for the three constants (C_{11}, C_{12}, C_{22}) by taking the partial derivatives shown above as equal to zero and is shown in Equation 21.

$$\begin{bmatrix} \sum(\varepsilon_1^2) & \sum(\varepsilon_1\varepsilon_2) & 0 \\ \sum(\varepsilon_1\varepsilon_2) & \sum(\varepsilon_2^2 + \varepsilon_1^2) & \sum(\varepsilon_1\varepsilon_2) \\ 0 & \sum(\varepsilon_1\varepsilon_2) & \sum(\varepsilon_2^2) \end{bmatrix} \begin{bmatrix} C_{11} \\ C_{12} \\ C_{22} \end{bmatrix} = \begin{bmatrix} \sum(\sigma_1\varepsilon_1) \\ \sum(\sigma_1\varepsilon_2 + \sigma_2\varepsilon_1) \\ \sum(\sigma_2\varepsilon_2) \end{bmatrix} \tag{21}$$

The summation terms of stress and strain are calculated using the measured values of stress and strain from the biaxial tension tests for which the elastic constants are desired. The elastic constants are calculated using Equations (4), (5) and (6) or (7) since there are only three independent elastic constants and three equations. The elastic constants from a least squares stress minimization can be calculated as:

$$E_2 = C_{22} - \frac{C_{12}^2}{C_{11}} \tag{22}$$

$$\nu_{12} = \left[\frac{C_{11}}{C_{22}}\left(1 - \frac{E_2}{C_{22}}\right)\right]^{0.5} \tag{23}$$

$$E_1 = \frac{\nu_{12}^2 E_2}{1 - \frac{E_2}{C_{22}}} \tag{24}$$

$$\nu_{21} = \nu_{12}\,\frac{E_2}{E_1} \tag{25}$$

The same process can be utilized to minimize the strain terms to solve for the elastic constants and is outlined in the Japanese Testing Standard. Rearranging Equations (11) and (12) leads to Equations (26) and (27).

$$\varepsilon_1 = \frac{\sigma_1}{E_1} - \frac{\sigma_2}{E_2}\nu_{21} \tag{26}$$

$$\varepsilon_2 = \frac{\sigma_2}{E_2} - \frac{\sigma_1}{E_1}\nu_{12} \tag{27}$$

If constants E_{11}, E_{22}, E_{12} and E_{21} are defined slightly differently than C_{11}, C_{22} and C_{12} previously used for the stress minimization approach, the same least squares method can be used (MSAJ, 1995).

$$E_{11} = \frac{1}{E_1} \tag{28}$$

$$E_{22} = \frac{1}{E_2} \tag{29}$$

$$E_{12} = \frac{\nu_{12}}{E_1} = E_{21} = \frac{\nu_{21}}{E_2} \tag{30}$$

$$S = \sum[\{(E_{11}\sigma_1 - E_{12}\sigma_2) - \varepsilon_1\}^2 + \{(E_{22}\sigma_2 - E_{12}\sigma_1) - \varepsilon_2\}^2] \tag{31}$$

$$\frac{\partial S}{\partial E_{11}} = \frac{\partial S}{\partial E_{22}} = \frac{\partial S}{\partial E_{12}} = 0 \tag{32}$$

It should be noted that a typo was made in the strain minimization equation shown in the Japanese testing standard and has been corrected for this thesis in Equation (31). It is also noteworthy that Bridgens and Gosling (2010) had an error in the strain minimization equation shown in their appendix. Equation (32) allows the elastic constants to be solved for in the same manner as Equation (20) did for the stress minimization approach.

The general least squares approach described thus far in this section requires a linear relationship between the parameters E_{11}, E_{22}, E_{12}, C_{11}, C_{22}, C_{12} and the approximating function. This requirement was met for both the stress and strain minimization approaches, meaning the methodology used is justified. The parameters solved from the least squares approach (E_{11}, E_{22}, E_{12}, or C_{11}, C_{22}, C_{12}) then allowed for the elastic constants to be solved based upon how the parameters were defined. For the stress minimization approach, an additional least squares approach was used to ensure the validity of the approaches discussed thus far. Instead of using Equations (17) and (18), to define the stress terms, Equations (11) and (12) were used for a stress minimization. By doing this the parameters that were adjusted to minimize the error between the approximating function and the data were simply the elastic constants (E_1, E_2, ν_{12}). By doing this the approximating function was no longer related linearly to the parameters. This meant that a more complex nonlinear least squares approach had to be used to solve for the elastic constants. This approach resulted in the same values for elastic constants as

the linear least squares approach for a given data set of stress and strain values. The nonlinear approach is shown in Appendix A.

Several other methods for calculating the elastic constants from biaxial tension tests are presented in MSAJ (1995) and Bridgens and Gosling (2004). The Japanese testing standard also mentions the best approximation or minimax method for calculating elastic constants. The elastic constants calculated using this method showed no notable difference between the least squares technique (MSAJ, 1995). The best approximation method was much more difficult to understand and apply and was not used in any literature encountered for biaxial tension tests. For these reasons, this method was not implemented for this research. The third method presented in the Japanese testing standard is a multi-step linear approximation of material constants on the nonlinear extension curves. This method is recommended for use when load-extension curves are clearly not well represented by a linear line. For this thesis, the stress and strain data used was over small regions of strain such that load-extension curves were well represented with linear lines, meaning this approach was not necessary. Bridgens and Gosling (2004) and Bridgens and Gosling (2010) examine some modifications to the Japanese testing standard methods for calculating elastic constants for membrane materials. These modifications are discussed in the literature review section of this thesis and are not applicable for the analysis of geosynthetics in this thesis.

The solver in Microsoft Excel was also experimented with for calculating the elastic constants. The solver used in Microsoft Excel uses the Generalized Reduced Gradient (GRG) nonlinear algorithm. Initially this approach was desired because of its

simplicity and ability to produce a unique value for elastic constants using only one value of stress and strain in each material direction. After further analysis of this approach, it was seen to be inadequate because of the strong dependence on initial guess values used for elastic constants. The solver will converge on a possible combination of elastic constants near the guessed values that satisfy Equations 11 and 12 with some amount of error. This solution for the elastic constants is not a unique or a "best" fit solution. For these reasons, the least squares approaches were used for solving for the elastic constants of geosynthetics from biaxial tension tests.

CHAPTER FOUR

TESTING PROCEDURE DEVELOPMENT

Testing Procedure Objective

The goal of this research project was to quantitatively describe the mechanical resilient behavior of geosynthetics subjected to repetitive loading in multiple directions that simulates field loading conditions in applications such as reinforced pavements. In repetitive loading applications such as roads, it is expected that geosynthetics experience both cyclic creep and cyclic stress relaxation. In ASTM D7556, only cyclic stress relaxation is used to create a resilient response in geosynthetics. It was hypothesized that the resilient response seen after cyclic loading could also be achieved from sustained monotonic loading. It was thought that if a material was held at a constant value of strain and the load was allowed to relax as it does in cyclic stress relaxation, that this would create the same resilient response. It was also hypothesized that subjecting a material to stress relaxation and/or creep would both simulate the same resilient response. The time necessary for a geosynthetic to exhibit "resilient" behavior was also of interest for developing a biaxial tension test procedure for geosynthetics that simulates a resilient response.

Initially, it was desired to use the biaxial device to examine resilient response under the types of loads discussed above. The ability to control load and strain with the biaxial testing device was insufficient to carry out precise and repeatable cyclic tests. It was also discovered that the interior portion of the biaxial sample experienced a

combination of mostly stress relaxation with some creep when it was held at a constant displacement. It was not possible to limit the loading to only stress relaxation or only creep. Due to these limitations with the biaxial testing device available for this project, uniaxial wide-width tension tests were performed to examine differences in material resilient response from four types of loading, namely cyclic stress relaxation, monotonic stress relaxation, cyclic stress creep and monotonic stress creep.

Uniaxial Testing Overview

Uniaxial wide width tensile tests were performed using several modes of loading to establish a testing procedure using the biaxial device. (You have probably noticed that I have changed a lot of sentences like this where you start the sentence with an outcome, pause with a comma, then describe how you got to the outcome. I prefer to write the sentence in the order of the events that took place. I do not know if one is more correct than the other. I think that the sequential approach is more technically clean and to the point.) The goal of the uniaxial testing program was to examine differences in material response when a material was allowed to relax or creep by being subjected to cyclic loading or monotonic loading. The conclusions of the uniaxial tests were critical for showing that the biaxial testing device was capable of producing data that was representative of field loading conditions and could be used for determining elastic constants. Wide width tensile tests were performed using four different methods. Tests were performed as cyclic stress relaxation tests, cyclic creep, monotonic stress relaxation and monotonic creep tests. These four types of tests were performed using ASTM D7556

as a guideline when applicable. The widths and gauge lengths used for the uniaxial wide width tests on both the woven geotextile and biaxial geogrid were approximately 200 millimeters. The time necessary for the material to relax/creep was also examined using wide-width tensile tests.

Uniaxial Testing Device

The uniaxial wide width tensile tests were performed using a servo-hydraulic load frame (made by MTS Systems Corporation) controlled by an MTS control unit shown in Figure 11. The material was gripped by Curtis "Geo-Grips, which are designed specifically for gripping geosynthetics in tension and are shown in Figure 12. The programmable control unit and load frame had internal linearly varying differential transducers (LVDTs) and load cells that were used to calculate load and displacement. The programmable control unit for this device allows very precise procedures to be

followed accurately such as the procedure outlined by ASTM D7556. The programmable control unit allows cyclic loads to be applied precisely in a repeatable manner.

Figure 11 Uniaxial Testing Device

Figure 12 Curtis Geo-Grips Used for Wide Width Tensile Tests

Stress Relaxation

Monotonic stress relaxation occurs in a geosynthetic material when it is held at a fixed value of strain and stress in the material is allowed to dissipate or relax. Stress relaxation occurring in a material subjected to cyclic loading centered around a constant

value of strain is referred to as cyclic stress relaxation. Cyclic stress relaxation test procedures and methodology used for determination of resilient modulus values are outlined in ASTM D7556. No testing standards exist for sustained loading tests or monotonic stress relaxation tests used for determination of resilient modulus. It was hypothesized that monotonic stress relaxation tests and cyclic stress relaxation tests would result in similar values of resilient modulus. This hypothesis was never tested in a laboratory setting thus it was examined for this research.

Cyclic stress relaxation tests were performed on a biaxial geogrid and a woven geotextile according to the procedure in ASTM D7556. This procedure involved loading the material monotonically to 0.5 % strain, then applying 1000 cycles of load corresponding to ±0.1 % strain. The material was next loaded monotonically to 1.0 % strain then subjected to the same load cycles as at the previous level of permanent strain. This process was repeated for permanent strain levels of 1.5, 2.0, 3.0 and 4.0 % strain.

Monotonic stress relaxation tests were performed on the same biaxial geogrid and woven geotextile as cyclic stress relaxation tests. The procedure outlined above in ASTM D7556 was adopted for monotonic stress relaxation tests except instead of applying 1000 cycles at each value of permanent strain, the strain was held constant for a predetermined amount of time.

Creep under Sustained Load

Creep occurs in a geosynthetic material when it is subjected to a constant stress. As with stress relaxation, creep can be achieved by applying cyclic and monotonic loads.

The resilient modulus in geosynthetics subjected to monotonic or cyclic creep has not been studied previously and thus was also examined in a laboratory setting for this thesis. Due to time constraints, the majority of uniaxial wide width tensile tests were performed as stress relaxation tests. The results from creep tests were slightly less important because of the small amount that occurs in the biaxial testing device as compared to stress relaxation. It was also difficult to determine a procedure that would allow results to be directly compared to stress relaxation data. This problem was especially pronounced for cyclic creep tests because there is no guideline for what load should be cycled. Time constraints on the project also limited the amount of creep tests that were performed.

Creep tests were performed using a procedure that was intended to match as closely as possible the procedure used for stress relaxation tests. The material was initially loaded monotonically to a permanent strain value of 0.5 % then allowed to creep (either monotonically or by the application of load cycles). This process was continued for permanent strain limits of 1.0, 1.5, 2.0, 3.0 and 4.0 % strain. The issue encountered in this procedure was that the programmable uniaxial testing device procedures must either be displacement or load controlled for the entirety of a procedure. Precise permanent strain limits were desired for comparison to stress relaxation tests, but since load must be held constant for creep tests, this presented some procedural difficulties. This along with the desire to examine the effects of the length of time a material is allowed to creep or relax led to the development of a slightly different procedure for creep tests. The procedure that followed was to conduct creep tests starting at a single value of 4.0 % permanent strain. The material was loaded to this value of permanent strain and allowed

to creep for a period of 24 hours. Single cycles of load were applied at various times throughout the 24-hour period so that a resilient modulus versus time relationship could be developed.

Effect of Stress Relaxation and Creep Duration

The effect of the duration of time a geosynthetic was allowed to creep or relax on the resilient modulus was of interest for developing a biaxial testing procedure. To examine this effect, single stage (initially loaded monotonically to a permanent strain of 4.0 %) 24-hour tests were performed as described in the creep section. Stress relaxation tests were performed in a similar manner, where the material was loaded monotonically to a permanent strain value of 4.0 % then stress relaxation was induced either cyclically or monotonically. The results of all uniaxial testing are presented in Chapter 5 of this thesis. A summary of all uniaxial wide width tensile tests performed is shown below in Table 2.

Table 2 Summary of Uniaxial Testing

Test Type	Permanent Strain Values (%)	Time @ Each Level of Permanent Strain	Materials Tested (Number of Trials)
Cyclic Stress Relaxation	0.5, 1.0, 1.5, 2.0, 3.0, 4.0	16.67 Minutes	Biaxial Geogrid (4), Woven Geotextile (3)
Cyclic Stress Relaxation	4.0	24 Hours	Biaxial Geogrid (1), Woven Geotextile (1),
Monotonic Stress Relaxation	0.5, 1.0, 1.5, 2.0, 3.0, 4.0	10 Minutes	Biaxial Geogrid (3), Woven Geotextile (6),
Monotonic Stress Relaxation	0.5, 1.0, 1.5, 2.0, 3.0, 4.0	20 Minutes	Biaxial Geogrid (1), Woven Geotextile (1),
Monotonic Stress Relaxation	4.0	60 Minutes	Biaxial Geogrid (1), Woven Geotextile (1),
Monotonic Stress Relaxation	4.0	24 Hours	Biaxial Geogrid (1), Woven Geotextile (1),
Cyclic Creep	4.0	24 Hours	Biaxial Geogrid (1), Woven Geotextile (1),
Monotonic Creep	0.5, 1.0, 1.5, 2.0, 3.0, 4.0	10 Minutes	Woven Geotextile (1)
Monotonic Creep	4.0	60 Minutes	Biaxial Geogrid (1), Woven Geotextile (1),
Monotonic Creep	4.0	24 Hours	Biaxial Geogrid (1), Woven Geotextile (2),

CHAPTER FIVE

UNIAXIAL TESTING RESULTS AND INTERPRETATION

Uniaxial Testing Results

As discussed in Chapter Four, uniaxial tests (wide width tensile tests) were performed on a biaxial geogrid and a woven geotextile in their cross-machine direction. Uniaxial tests were performed using multiple procedures for examination of different effects as described in Chapter Four and summarized in Table 2. The raw data obtained from uniaxial tests was displacement and load, which were used to calculate strain and line load (stress) from the dimensions of the specimen tested. The stress vs. strain data was used to calculate a modulus for a given level of permanent strain as the initial slope of the stress vs. strain plot after stress relaxation or creep. The uniaxial modulus values at a certain level of permanent strain could then be compared from different types of loading to examine any differences.

Cyclic Stress Relaxation

Cyclic stress relaxation tests were performed according to ASTM D7556 as described in Chapter Four. The cycles were performed at a rate of 1 hertz such that the total cycle time for 1000 cycles at a given level of permanent strain was 16.67 minutes. The load that was cycled corresponded to ±0.1 % strain. The results for a biaxial geogrid and woven geotextile are shown below in Figure 13 and Figure 14.

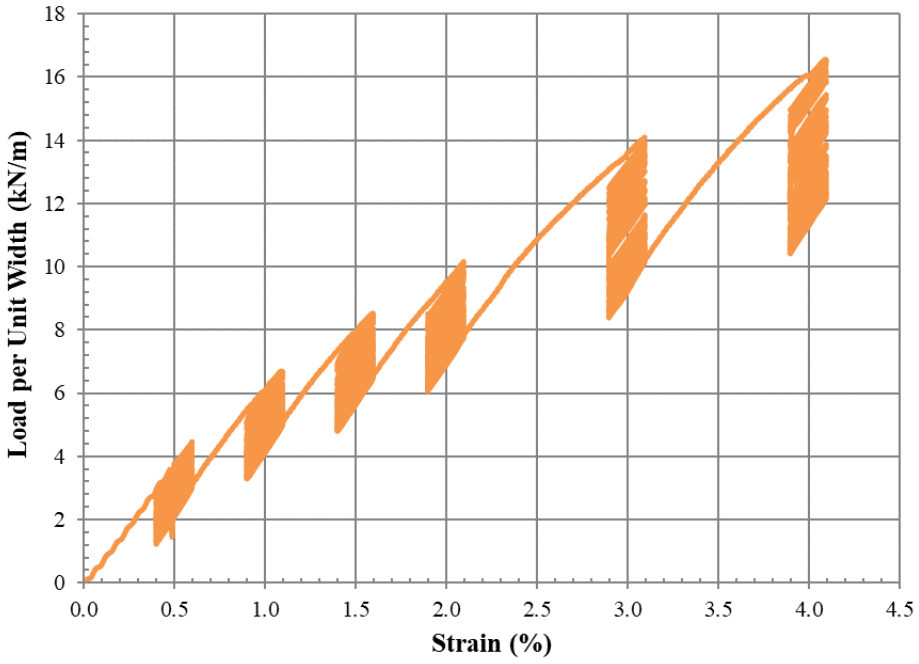

Figure 13 Cyclic Stress Relaxation Test on a Biaxial Geogrid

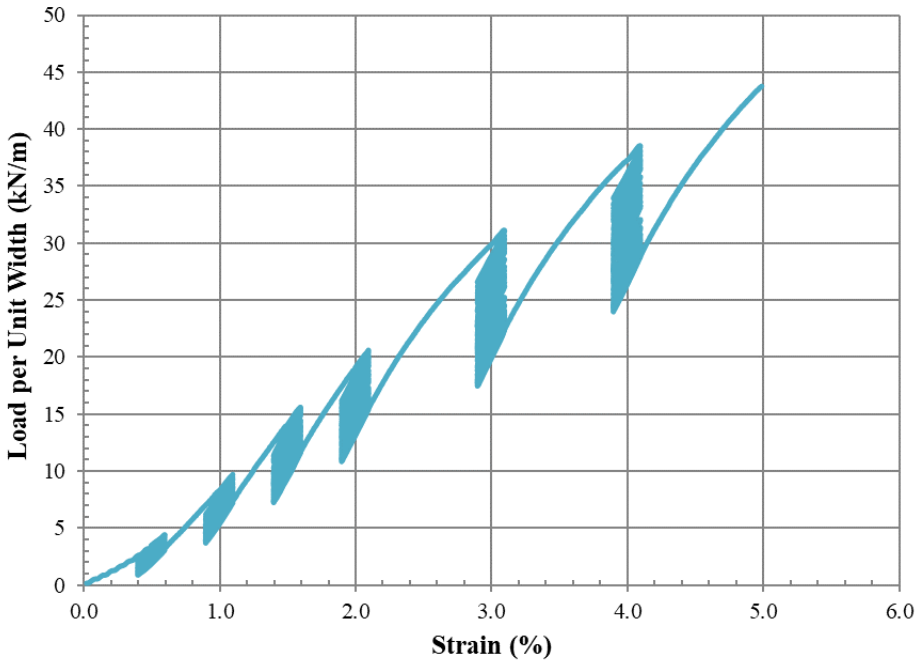

Figure 14 Cyclic Stress Relaxation Test on Woven Geotextile

From the cyclic stress relaxation tests a modulus value was calculated at each level of permanent strain. There are several methods available for calculating a modulus value from cyclic stress relaxation tests. All methods involve taking the slope of the line load (stress) vs. strain plot at each level of permanent strain after relaxation. According to ASTM D7556, the modulus should be calculated as a cyclic modulus, which is obtained from the last ten cycles of each of the six cyclic load steps. The cyclic modulus uses an equivalent force per unit width, which is calculated as the maximum force in a cycle minus the minimum force in a cycle divided by width of the tested specimen. The width of the geogrids is not simply measured but is taken as the number of tensile elements per unit width divided by the number of tensile elements being tested (Figure 15).

11.2 Calculate the equivalent force per unit width expressed in N/m (lbf/in.) of width:

11.2.1 *Test Methods A and B*—Use Eq 2:

$$\alpha_f = [(P_2 - P_1)/N_r] \times N_t \qquad (2)$$

where:

α_f = equivalent force per unit width, N/m (lbf/in.),
P_2 = observed maximum force for the cycle, N (lbf),
P_1 = minimum tensile load at the end of the cycle, N (lbf),
N_r = number of tensile elements being tested, and
N_t = number of tensile elements per unit width, equal to N_c/b (see 11.2.2).

Figure 15 Equivalent Force per unit Width Equation (ASTM 2016)

The number of tensile elements per unit width is determined by examining full width rolls of the specified geogrid (ASTM, 2016). For geotextiles, the width of the tested specimen can simply be measured.

A modulus from wide-width cyclic stress relaxation tension tests can also be calculated using the initial portion of the permanent loading line after cycles have been

applied. The modulus from the initial portion of the permanent loading can be calculated as a secant modulus or using a linear approximation (best fit linear trendline). The secant modulus and linear trendline modulus are calculated using the initial 0.2% strain of the permanent loading stress-strain curve. The secant modulus was calculated using an average of five points at the beginning and end of the 0.2% strain interval. The initial reloading of geosynthetics after stress relaxation exhibits linear behavior, thus the three methods mentioned for calculating the slope of the linear (modulus) should be equivalent. The only reason for any differences would arise from the cyclic modulus being calculated as the average slope of 10 cycles, while the secant and linear approximation are only from the single permanent loading curve. Slight differences in value could also arise from the material response not being perfectly linear or erroneous data points. Since the modulus values from cyclic relaxation tests are meant to be comparable to modulus values from monotonic tests, the modulus was only calculated using the initial portion of the permanent loading curve at each level of permanent strain after stress relaxation. The modulus was calculated at each level of permanent strain after relaxation for all cyclic stress relaxation trials from the initial 0.2 % strain of the permanent loading curve. The modulus at each level of permanent strain for each trial is summarized in Table 3 and Table 4 with an associated average, standard deviation and coefficient of variability for both the biaxial geogrid and woven geotextile. The standard deviation and coefficient of variability was calculated for tests that had multiple trials performed so that inherent variability of identical tests could be compared to the variability between dissimilar tests

later in the Analysis of Uniaxial Testing Section. Trial 2 from Table 3 was omitted because of errors in the testing procedure.

The average modulus value at each level of permanent strain is shown in Figure 16 and Figure 17 for the biaxial geogrid and woven geotextile. All of the modulus values for the biaxial geogrid remain relatively constant as permanent strain increases, which is consistent with what Cuelho et al. (2005) observed. On the contrary, modulus values for the woven geotextile increase as permanent strain increases for all types of loading examined, which is also consistent with what Cuelho et al. (2005) observed.

Table 3 Cyclic Stress Relaxation Test Results from Biaxial Geogrid

Strain	Modulus (kN/m)				Average Modulus (kN/m)	Standard Deviation	Coefficient of Variability
	Trial 1	Trial 3	Trial 4	Trial 5			
0.5 %	905	889	875	888	889	10.6	1.20 %
1.0 %	873	828	843	849	848	16.2	1.91 %
1.5 %	849	811	829	833	831	13.6	1.64 %
2.0 %	850	816	836	840	836	12.5	1.49 %
3.0 %	890	876	880	873	880	6.6	0.75 %
4.0 %	-	-	-	-	-	-	-
Average Coefficient of Variability							1.40 %

Table 4 Cyclic Stress Relaxation Test Results from Woven Geotextile

Strain	Modulus (kN/m)			Average Modulus (kN/m)	Standard Deviation	Coefficient of Variability
	Trial 1	Trial 2	Trial 3			
0.5%	1213	1170	1125	1170	36.0	3.08 %
1.0%	1852	1799	1809	1820	22.9	1.26 %
1.5%	2214	2166	2216	2199	23.2	1.05 %
2.0%	2294	2238	2284	2272	24.5	1.08 %
3.0%	2418	2390	2405	2404	11.6	0.48 %
4.0%	2446	2385	2398	2410	26.4	1.10 %
Average Coefficient of Variability						1.34 %

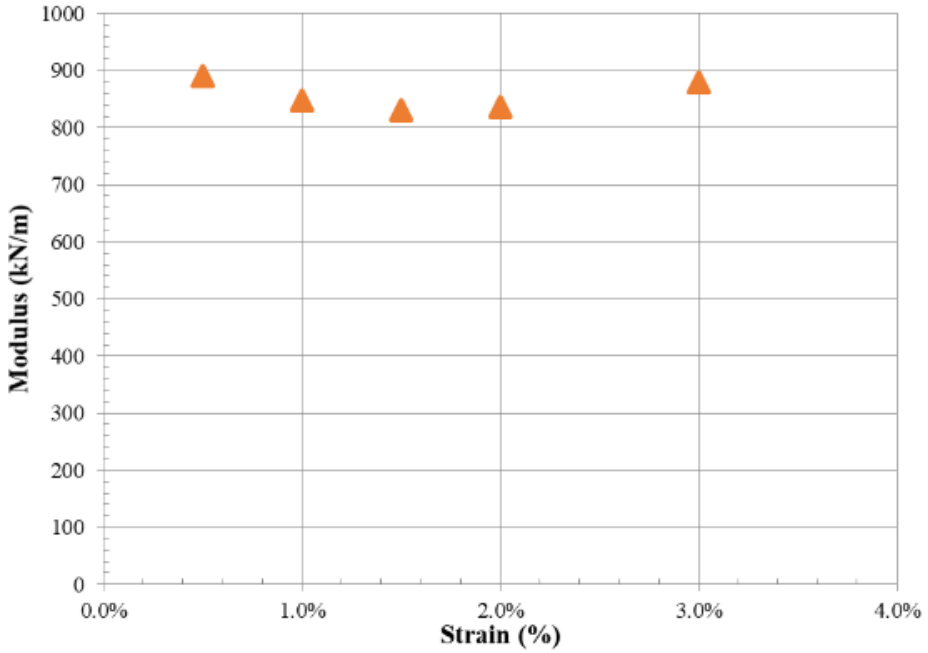

Figure 16 Modulus vs. Strain for Cyclic Stress Relaxation Tests on a Biaxial Geogrid

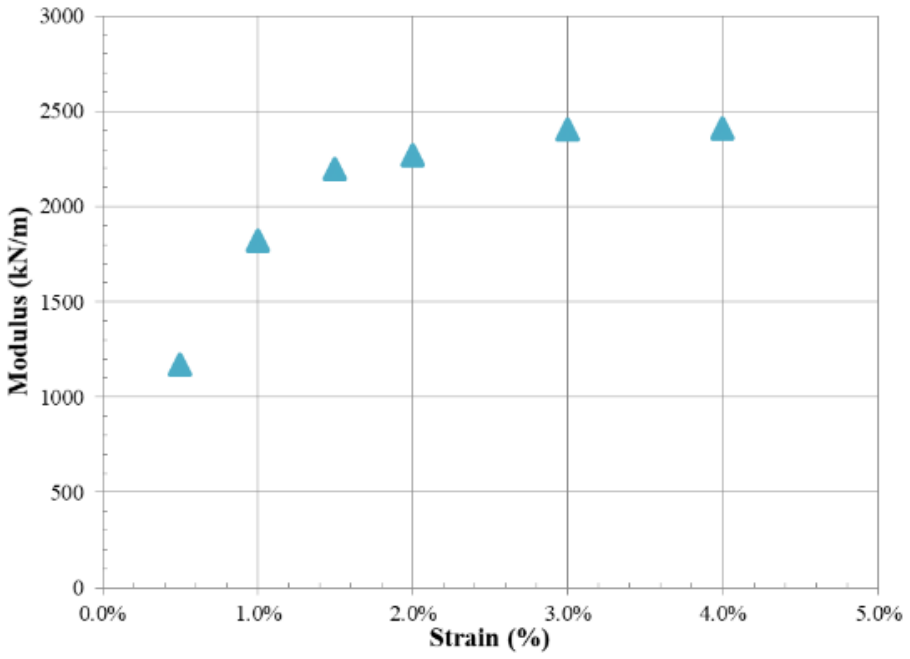

Figure 17 Modulus vs. Strain for Cyclic Stress Relaxation Tests on a Woven Geotextile

Cyclic stress relaxation tests were also performed over a 24-hour period starting at a permanent strain of 4.0%. Tests were performed in this manner to further examine the time necessary to simulate a "resilient response". The resilient modulus after different relaxation times was examined over a 24-hour period to determine an adequate time of relaxation. For 24-hour tests, the material was initially loaded monotonically to 4.0 % strain. This level of permanent strain was the highest value examined in all uniaxial tests and thus was used to examine the effect of cycle/hold time on modulus values. Similar 24-hour tests were also performed as monotonic relaxation, monotonic relaxation and cyclic creep. The 24 hour cyclic stress relaxation results from tests performed on a biaxial geogrid and woven geotextile are shown in Figure 18 and Figure 19, respectively.

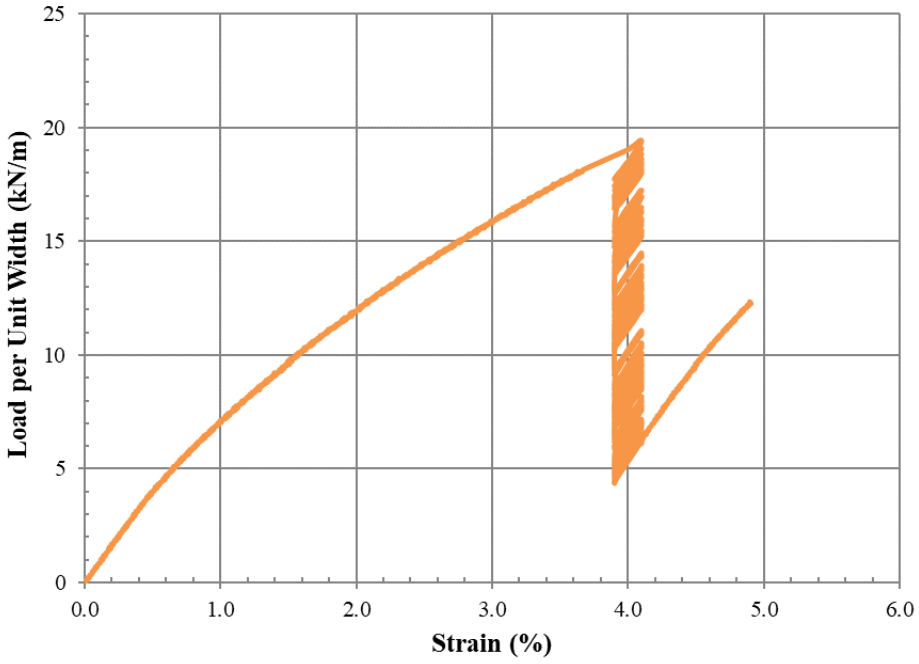

Figure 18 Cyclic Stress Relaxation 24 hr. Test Results from Biaxial Geogrid

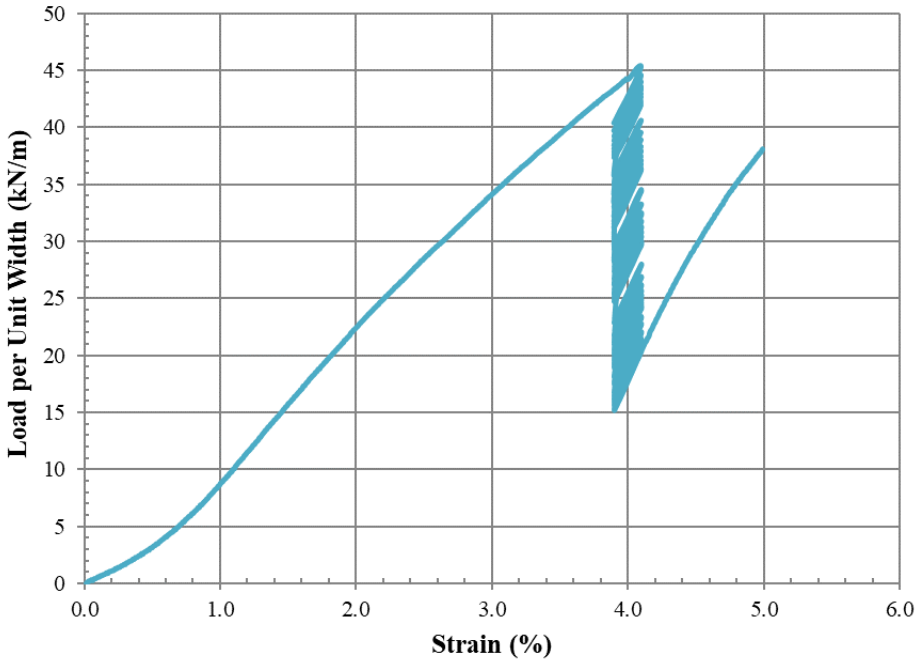

Figure 19 Cyclic Stress Relaxation 24 hr. Test Results from Woven Geotextile

Modulus was calculated using the slope of a cycle at various times along the 24-hour interval. and is plotted in Figure 20 and Figure 21 for the biaxial geogrid and woven geotextile respectively.

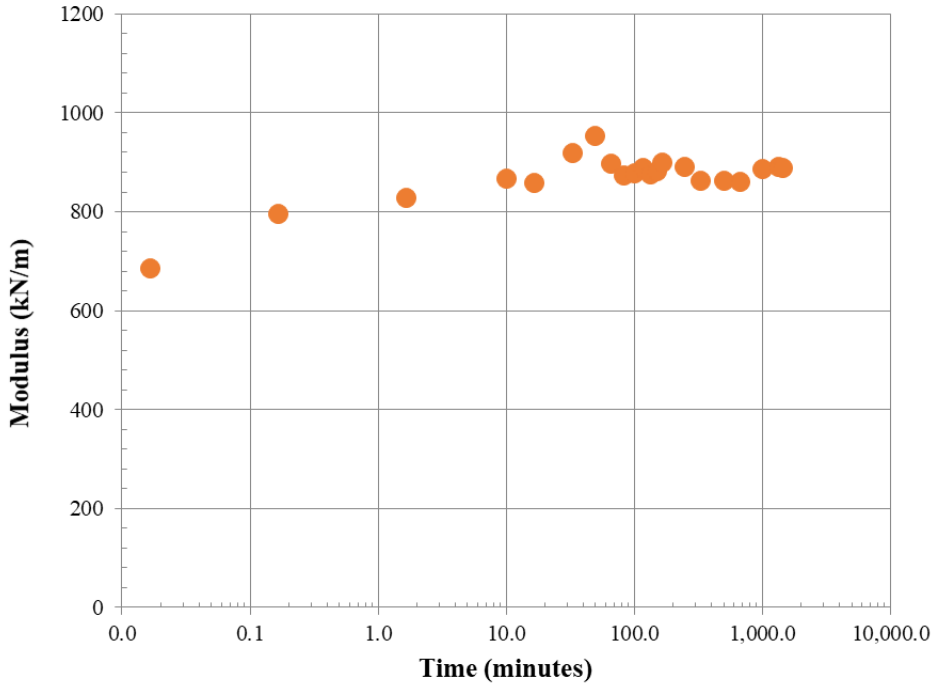

Figure 20 Modulus at 4.0 % Strain for 24-hour Cyclic Stress Relaxation Test Results from Biaxial Geogrid

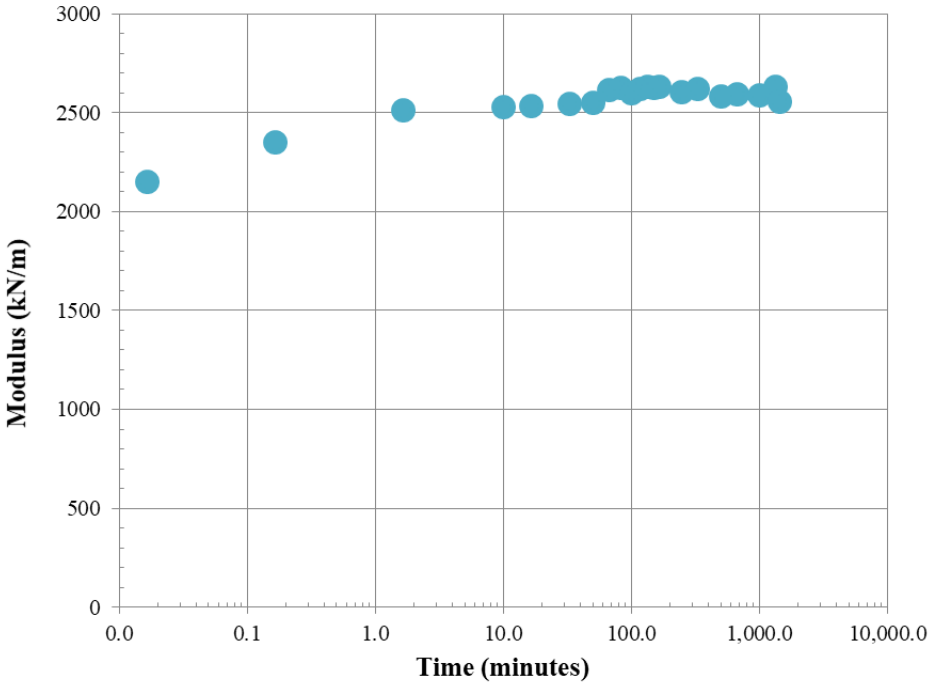

Figure 21 Modulus at 4.0 % Strain for 24-hour Cyclic Stress Relaxation Test Results from Woven Geotextile

The modulus values after 24 hours of cyclic stress relaxation are shown below in Table 5.

Table 5 Results from Cyclic Stress Relaxation Tests at 4.0 % Strain after 24 Hours

Strain	Time	Modulus (kN/m)	
(%)	(Hours)	Biaxial Geogrid	Woven Geotextile
4.0%	24	889	2556

Monotonic Stress Relaxation

Monotonic stress relaxation tests were performed using the same methodology as the cyclic stress relaxation tests except that at each level of permanent strain the material was held at a constant strain and the load was allowed to dissipate as shown in Figure 22

and Figure 23 for the biaxial geogrid and woven geotextile respectively. Monotonic stress relaxation tests were performed on the same biaxial geogrid and woven geosynthetic as the cyclic stress relaxation tests. Multiple trials were performed using a hold time of 10 minutes at each level of permanent strain.

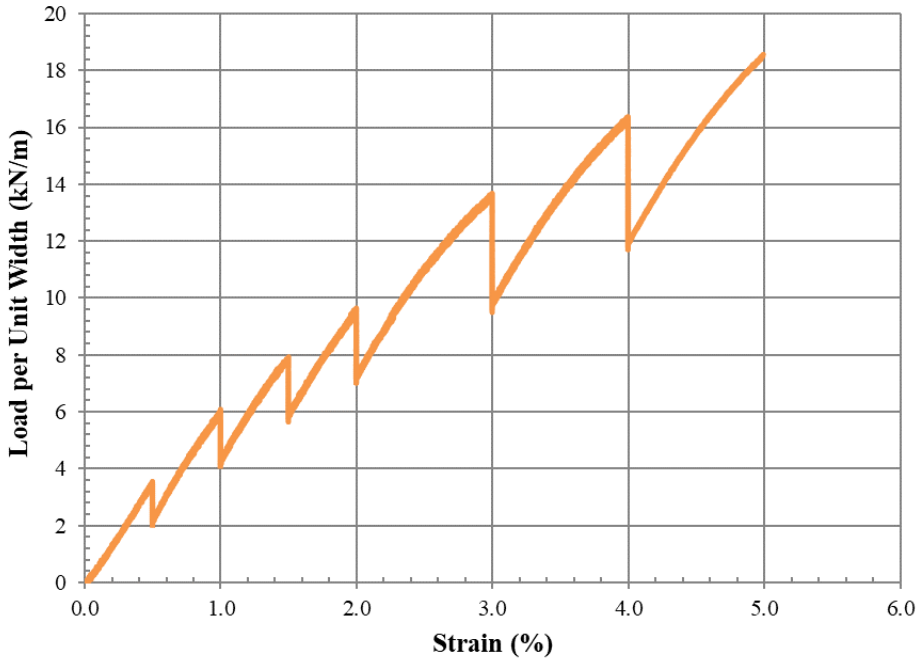

Figure 22 Monotonic Stress Relaxation (10-minute hold time) Test Results from Biaxial Geogrid

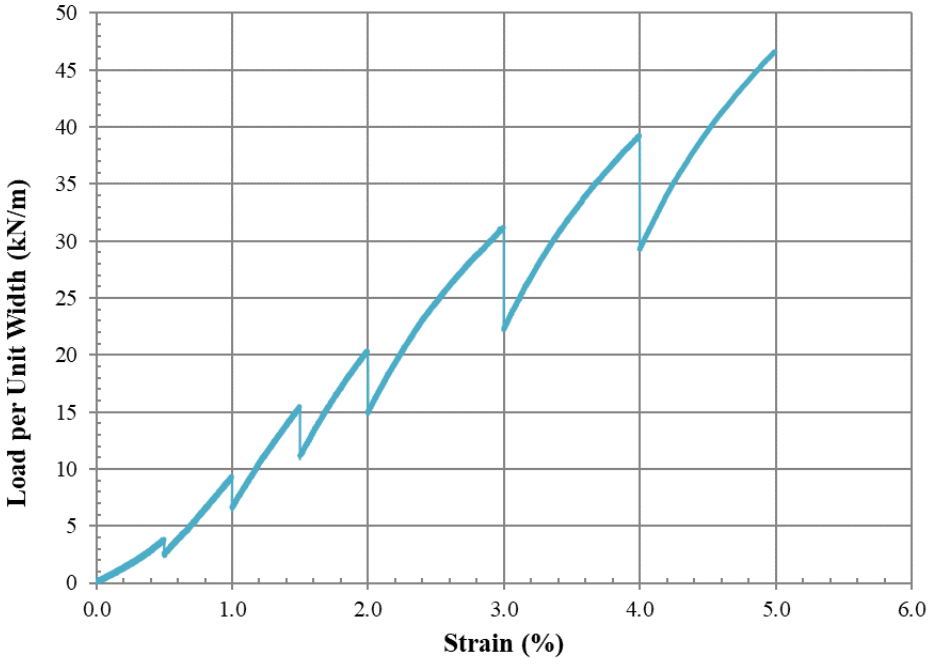

Figure 23 Monotonic Stress Relaxation Test (10-minute hold time) Results from Woven Geotextile

The modulus at each level of permanent strain for each trial was calculated for both the biaxial geogrid and woven geotextile and is shown in Table 6 and Table 7. The coefficient of variability was again calculated to get an idea of the inherent variability for identical trials. Trial 2 from Table 7 was omitted because it was determined to be an outlier.

Table 6 Monotonic Stress Relaxation Test Results from Biaxial Geogrid

Strain	Modulus (kN/m)			Average Modulus (kN/m)	Standard Deviation	Coefficient of Variability
	Trial 1	Trial 2	Trial 3			
0.5%	843	847	842	844	2.1	0.25 %
1.0%	822	809	813	815	5.3	0.65 %
1.5%	800	801	820	807	9.0	1.11 %
2.0%	785	797	812	798	11.1	1.39 %
3.0%	795	819	794	803	11.8	1.47 %
4.0%	828	814	821	821	5.5	0.67 %
Average Coefficient of Variability						0.92 %

Table 7 Monotonic Stress Relaxation Test Results from Woven Geotextile

Strain	Modulus (kN/m)					Average Modulus (kN/m)	Standard Deviation	Coefficient of Variability
	Trial 1	Trial 3	Trial 4	Trial 5	Trial 6			
0.5%	1090	1007	1281	1319	1188	1177	116.4	9.89 %
1.0%	1749	1676	1934	1865	1867	1818	92.7	5.10 %
1.5%	2012	2029	2060	2049	2089	2048	26.6	1.30 %
2.0%	2114	2083	2132	2151	2155	2127	26.3	1.24 %
3.0%	2221	2208	2246	2242	2216	2227	14.8	0.66 %
4.0%	2229	2209	2357	2299	2274	2274	52.6	2.31 %
Average Coefficient of Variability								3.42 %

Additionally, one trial for both materials was performed using a 20-minute hold time for each level of permanent strain to examine the effect of relaxation time on modulus. These trials are shown in Figure 24 and Figure 25 for the biaxial geogrid and woven geotextile respectively. The modulus at each level of permanent strain is shown for monotonic stress relaxation tests with hold times of both 10 and 20 minutes on Figure 26 and Figure 27 for the biaxial geogrid and woven geotextile, respectively. The modulus plotted for 10-minute hold times is an average from Table 7.

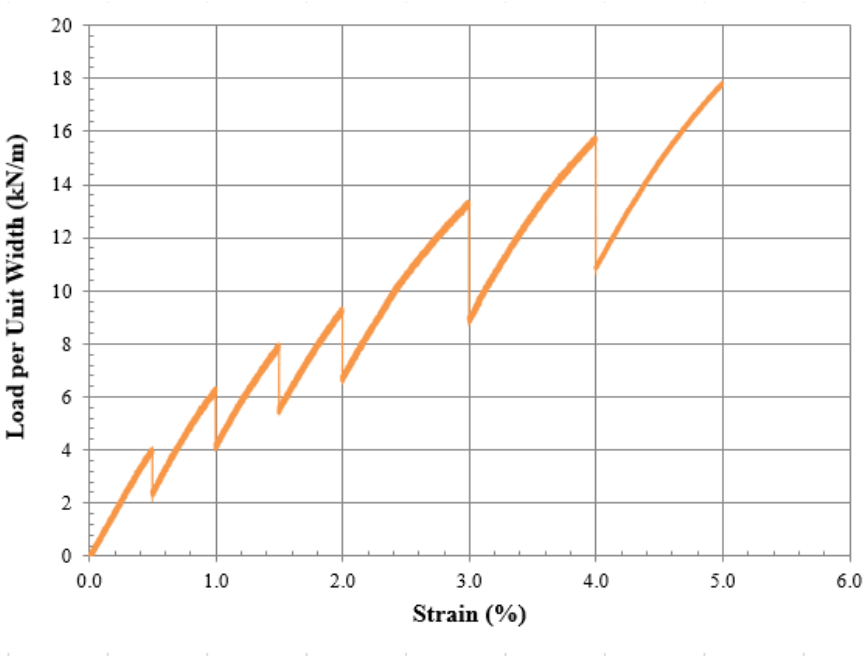

Figure 24 Monotonic Stress Relaxation Test (20-minute hold time) Results from Biaxial Geogrid

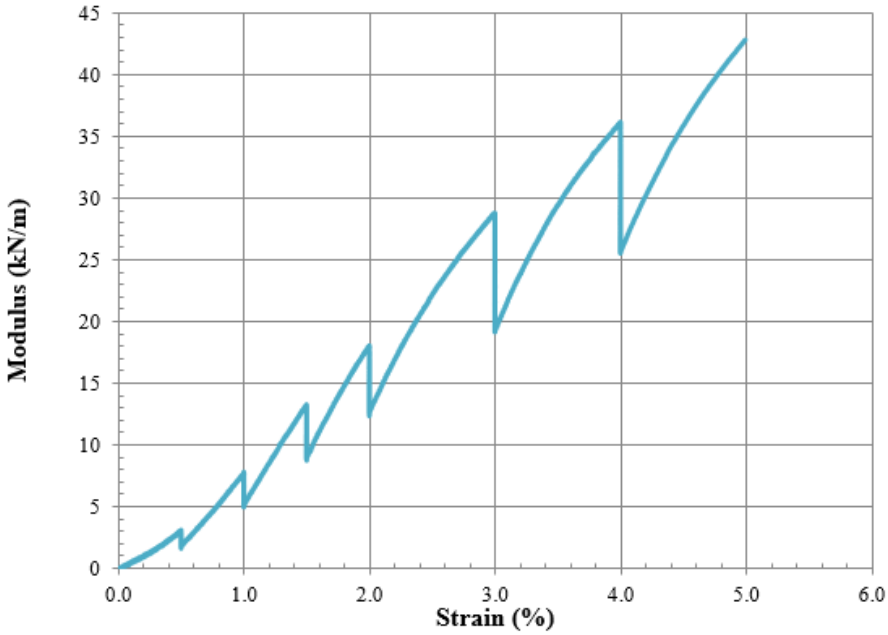

Figure 25 Monotonic Stress Relaxation Test (20-minute hold time) Results from Woven Geotextile

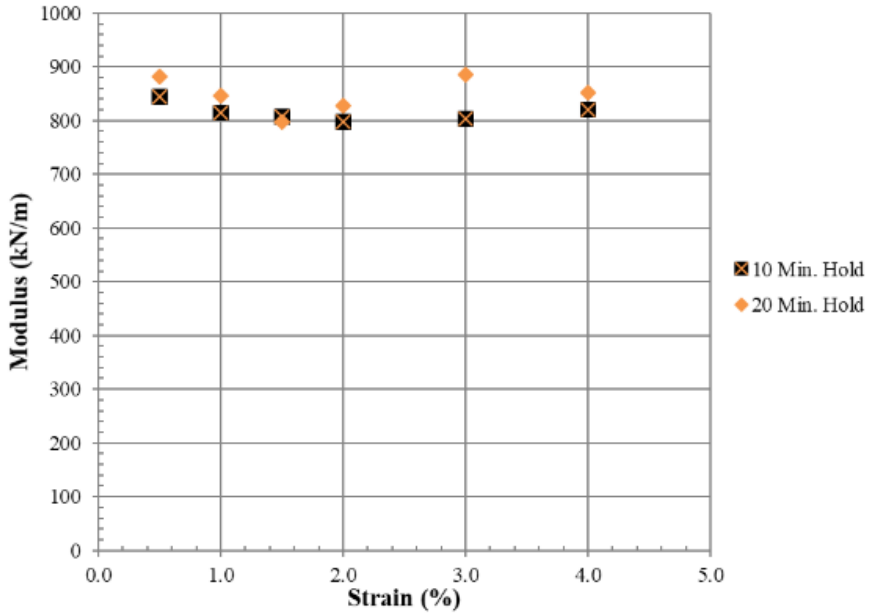

Figure 26 Average Modulus from Monotonic Stress Relaxation Test Results from Biaxial Geogrid

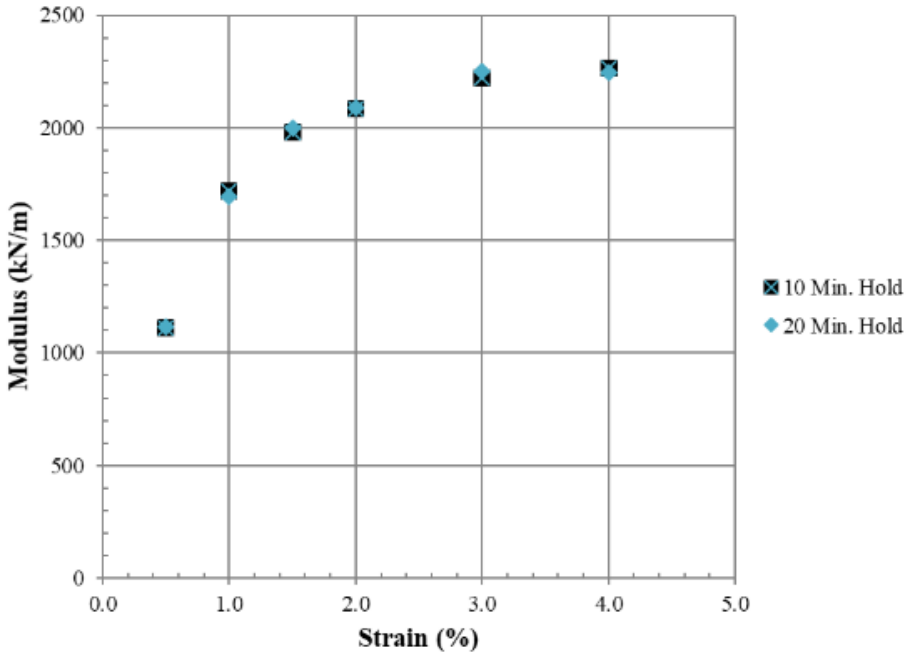

Figure 27 Average Modulus from Monotonic Stress Relaxation Test Results from Woven Geotextile

A 24 hour monotonic stress relaxation test was performed on both materials by loading the material to a permanent strain of 4.0 % then allowing the material to relax for 24 hours as shown in Figure 28 and Figure 29 for the biaxial geogrid and woven geotextile, respectively.

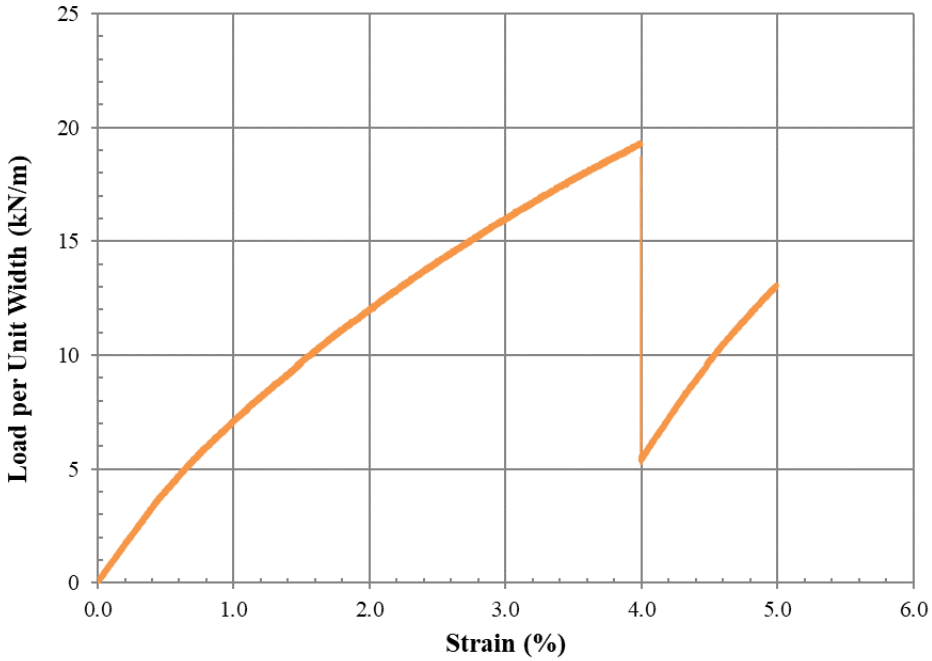

Figure 28 Monotonic Stress Relaxation 24 hr. Test Results from Biaxial Geogrid

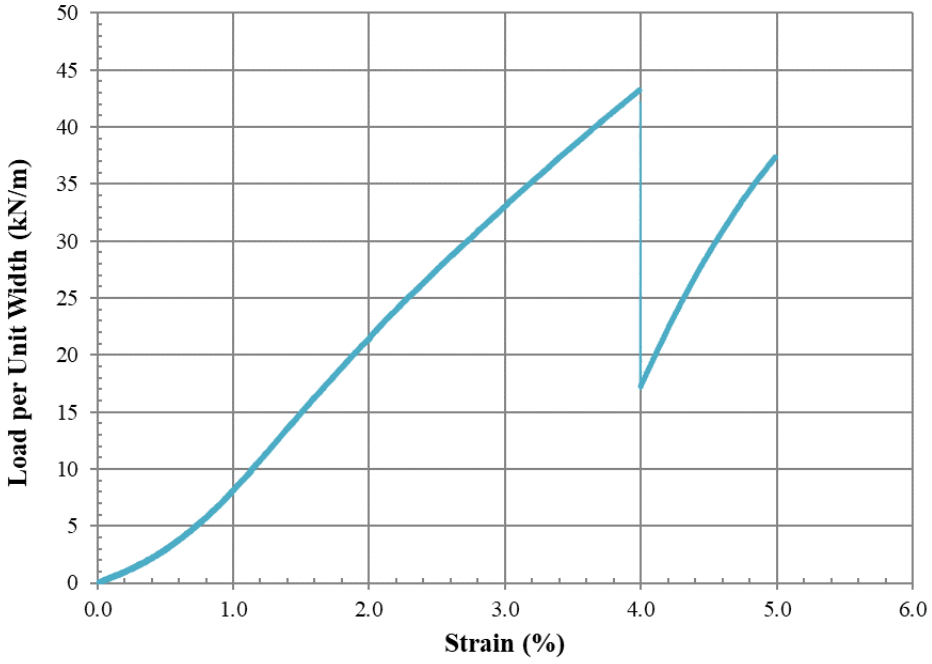

Figure 29 Monotonic Stress Relaxation 24 hr. Test Results from Woven Geotextile

The modulus for 24-hour monotonic stress relaxation tests is shown below in Table 8.

Table 8 Monotonic Stress Relaxation Test Results at 4.0 % Strain after 24 Hours

Strain	Time	Modulus (kN/m)	
(%)	(Hours)	Biaxial Geogrid	Woven Geotextile
4.0%	24	863	2504

One additional monotonic stress relaxation test was performed to further examine the effect of time on the resilient modulus value. This test was performed similar to the 24-hour tests except that a single cycle was applied at various times over the period of one hour such that modulus could be calculated. This type of test was performed on the

biaxial geogrid and woven geotextile and is shown in Figure 30 and Figure 31 respectively.

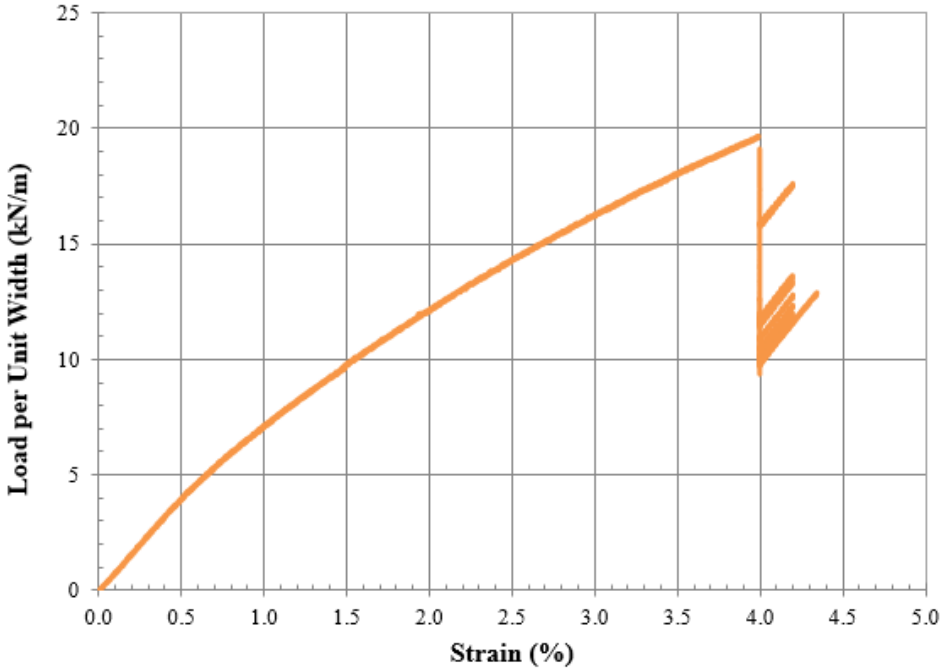

Figure 30 Monotonic Relaxation 1 hr. Test Results from Biaxial Geogrid

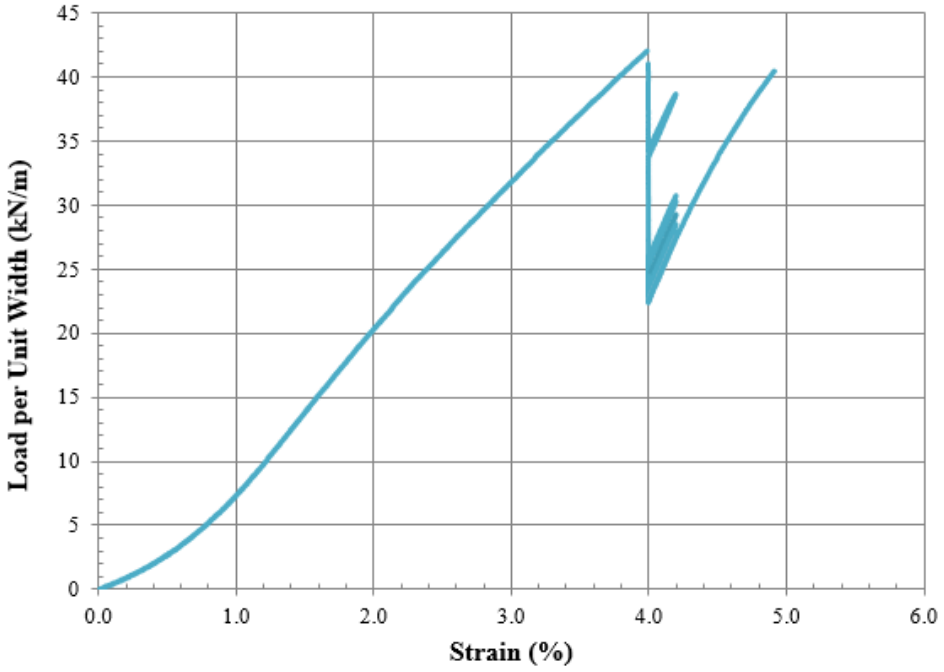

Figure 31 Monotonic Relaxation 1 hr. Test Results from Woven Geotextile

The modulus calculated at different times is shown in Table 9 and Figure 32 and Figure 33 for the biaxial geogrid and woven geotextile respectively.

Table 9 Monotonic Stress Relaxation Test Results at 4.0 % Strain

Strain	Time	Modulus (kN/m)	
(%)	(Minutes)	Biaxial Geogrid	Woven Geotextile
4.00%	1	852	2240
4.00%	10	894	2408
4.00%	16.67	916	2421
4.00%	20	913	2430
4.00%	30	915	2452
4.00%	40	905	2450
4.00%	50	910	2462
4.00%	60	909	2472

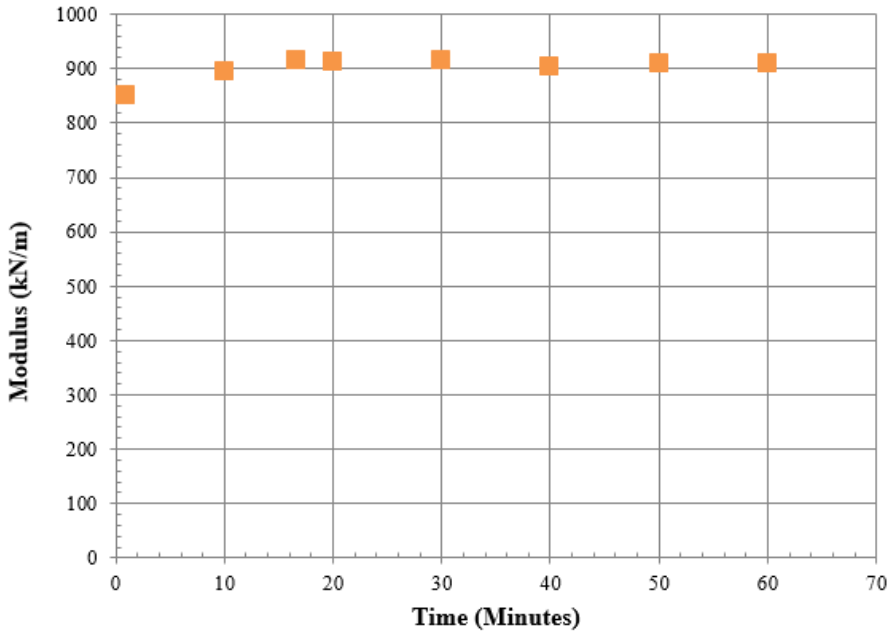

Figure 32 Monotonic Stress Relaxation Test Results at 4.0 % Strain over 60 Minutes from Biaxial Geogrid

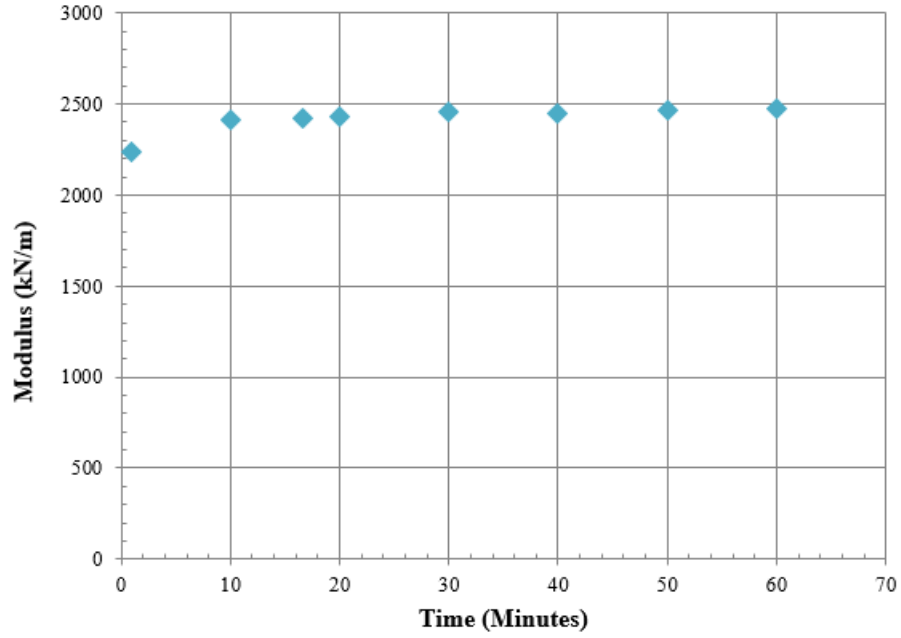

Figure 33 Monotonic Stress Relaxation Test Results at 4.0 % Strain over 60 Minutes from Woven Geotextile

Cyclic Creep

Cyclic creep tests were examined slightly differently than cyclic and monotonic stress relaxation for reasons outlined in Chapter Four of this thesis. This test was performed on the same biaxial geogrid and woven geosynthetic that were tested using cyclic and monotonic stress relaxation tests. The cyclic creep tests were not performed using six levels of permanent strain, instead they were performed by initially loading the material monotonically to 4.0% strain then allowing the material to creep for 24 hours as seen in Figure 34 and Figure 35 for the biaxial geogrid and woven geotextile respectively.

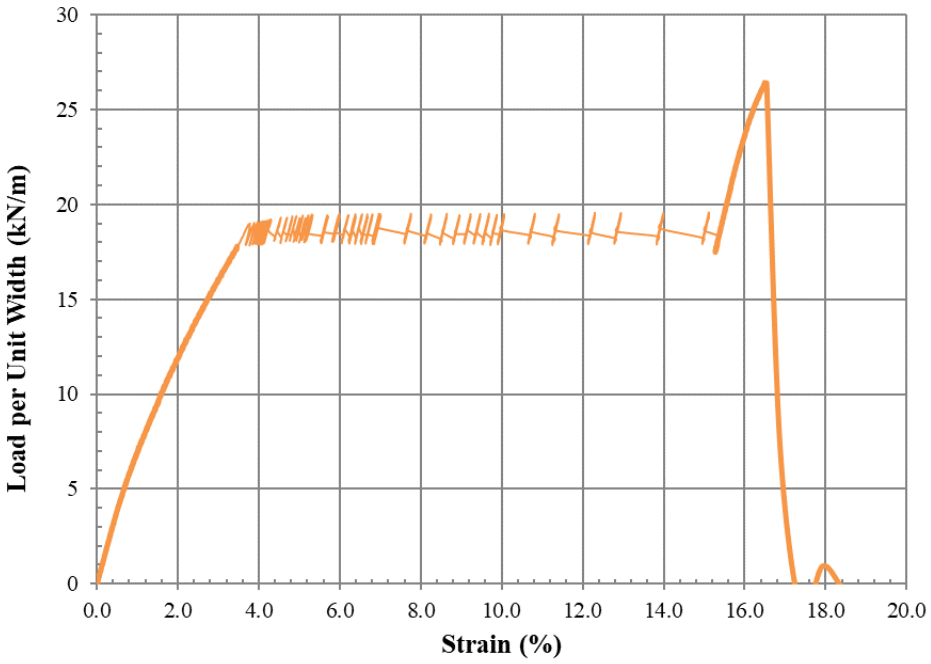

Figure 34 Cyclic Creep 24 hr. Test Results from Biaxial Geogrid

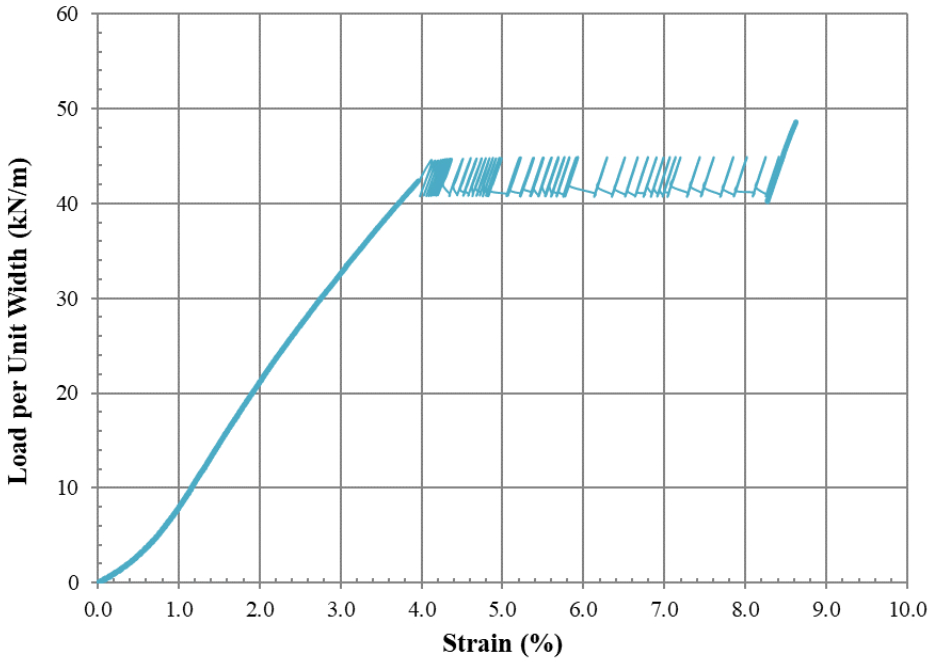

Figure 35 Cyclic Creep 24 hr. Test Results from Woven Geotextile

The modulus was calculated using the slope of the cycles over various times over the 24-hour period as shown in Figure 36 and Figure 37. The modulus value at 24 hours for the cyclic creep tests is shown in Table 10.

Table 10 Modulus from Cyclic Creep Tests at 4.0 % Strain after 24 Hours

Strain	Time	Modulus (kN/m)	
(%)	(Hours)	Biaxial Geogrid	Woven Geotextile
4.0%	24	897	2511

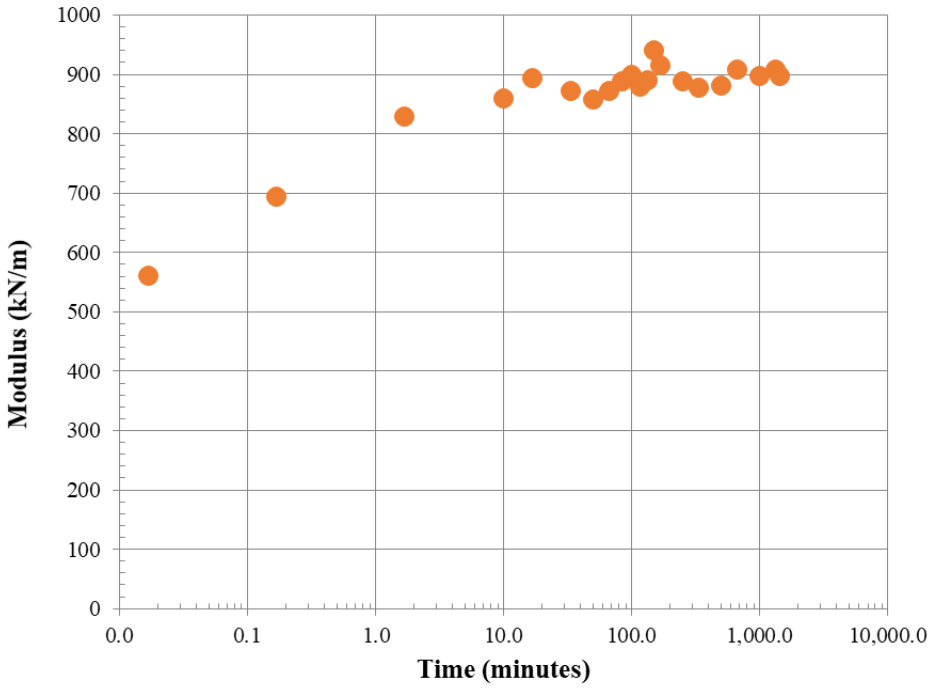

Figure 36 Modulus from Cyclic Creep Tests on Biaxial Geogrid

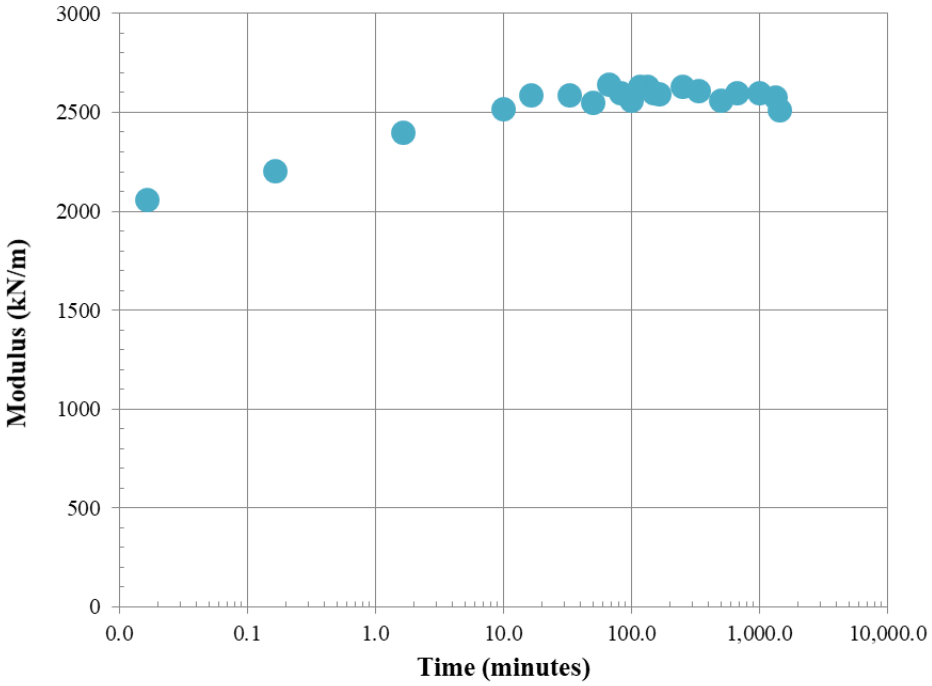

Figure 37 Modulus from Cyclic Creep Tests on Woven Geotextile

Monotonic Creep

A monotonic creep test was performed using 6 levels of permanent strain in a similar manner as the monotonic stress relaxation tests for the woven geotextile. At each level of permanent strain, the load was held constant and material was allowed to creep for 10 minutes. This test was performed on the woven geotextile and the results are shown below in Figure 38.

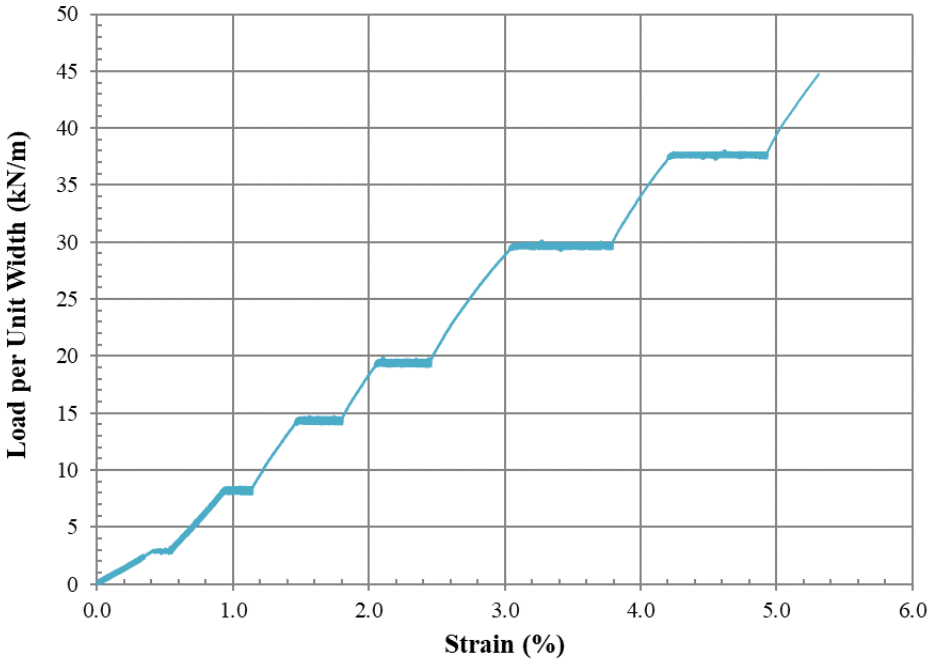

Figure 38 Monotonic Creep Test Results from Woven Geotextile

The modulus was calculated from Figure 38 at each level of permanent strain and is shown in Table 11 and Figure 39.The level of permanent strain was taken as the strain before the material was allowed to creep.

Table 11 Modulus from Monotonic Creep Test on a Woven Geotextile

Strain (%)	Modulus (kN/m)
0.5%	1323
1.0%	2006
1.5%	2211
2.0%	2289
3.0%	2326
4.0%	2362

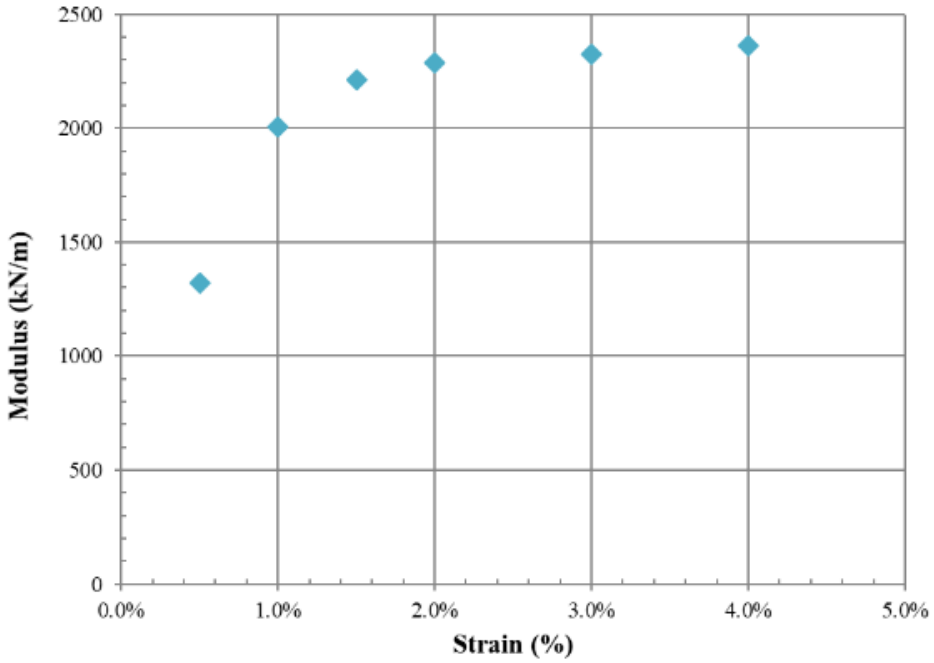

Figure 39 Modulus from Monotonic Creep Test on a Woven Geotextile

Monotonic creep tests were also performed over 24 hours on the same biaxial geogrid and woven geotextile tested previously as shown in Figure 40 and Figure 41 respectively. Monotonic creep tests were performed in a similar manner as the 24-hour

monotonic stress relaxation tests where the material was loaded to a permanent strain of 4.0 % then allowed to creep for 24 hours.

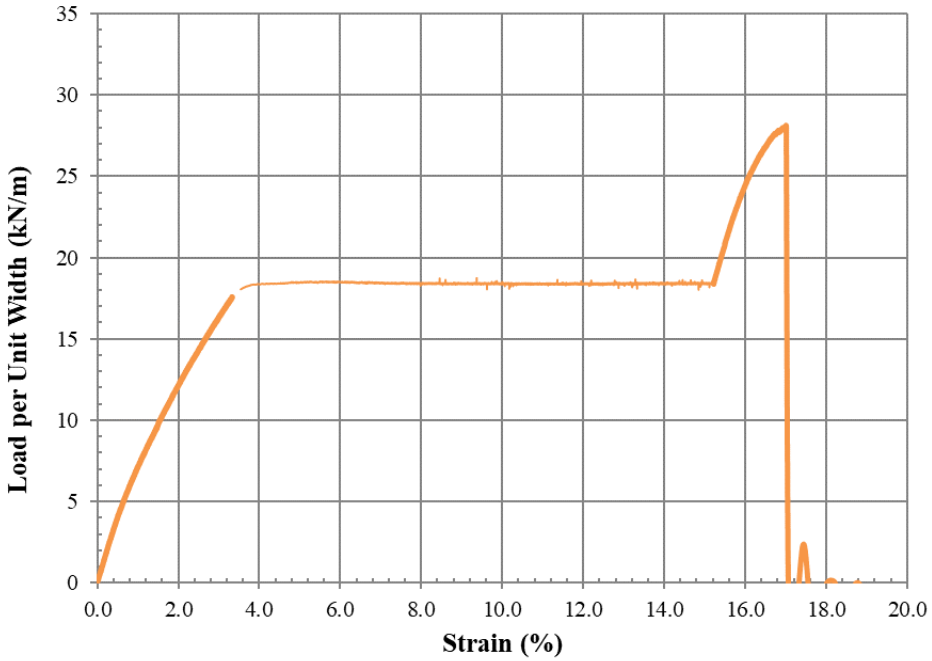

Figure 40 Monotonic Creep 24 hr. Test Results from Biaxial Geogrid

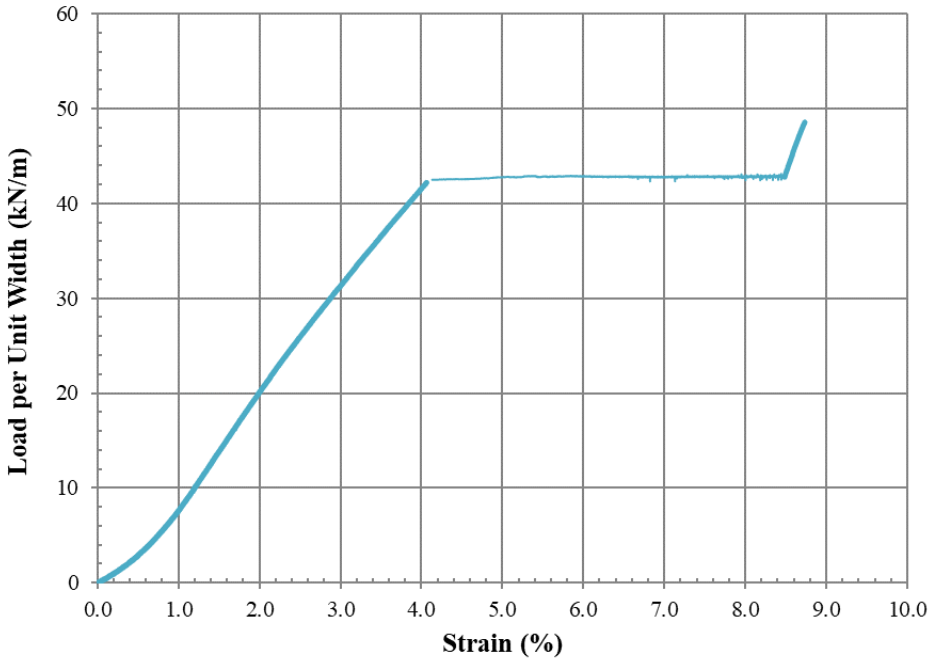

Figure 41 Monotonic Creep 24 hr. Test Results from Woven Geotextile

Two trials were performed on the woven geotextile, the modulus from each is shown in Table 12. The average modulus value of the two trials on the woven geotextile and the trial on the biaxial geogrid is shown in Table 13.

Table 12 Modulus from Monotonic Creep Tests at 4.0 % Strain at 24 Hours from Woven Geotextile

Strain	Modulus (kN/m)		Average Modulus (kN/m)	Standard Deviation	Coefficient of Variability
(%)	Trial 1	Trial 2			
4.0%	2435	2556	2496	60.1	2.41%

Table 13 Modulus from Monotonic Creep Tests at 4.0 % Strain at 24 hours

Strain	Time	Modulus (kN/m)	
(%)	(Hours)	Biaxial Geogrid	Woven Geotextile
4.0%	24	857	2496

One additional monotonic creep test was performed on the biaxial geogrid and woven geotextile over the duration of one hour and is shown in Figure 42 and Figure 43 respectively. The material was initially loaded to approximately 4.0 % strain (actually closer to 3.0 % strain due to the uniaxially testing device limitations for creep tests, this issue is discussed in more detail earlier in Chapter Four, Creep Under Sustained Load section), then it was allowed to creep for a period of one hour.

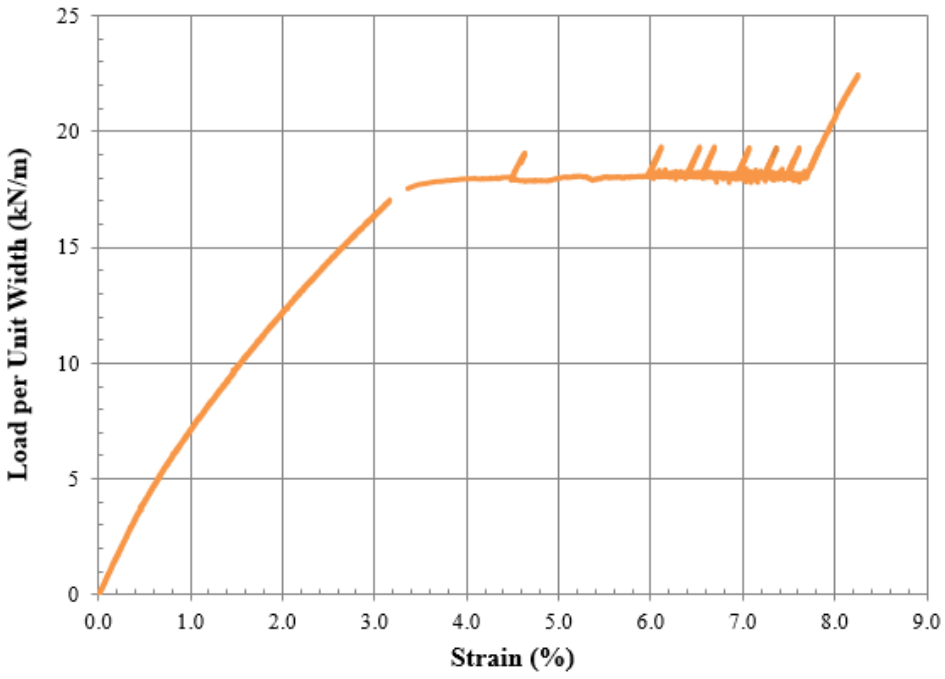

Figure 42 Monotonic Creep 1 hr. Test Results from Biaxial Geogrid

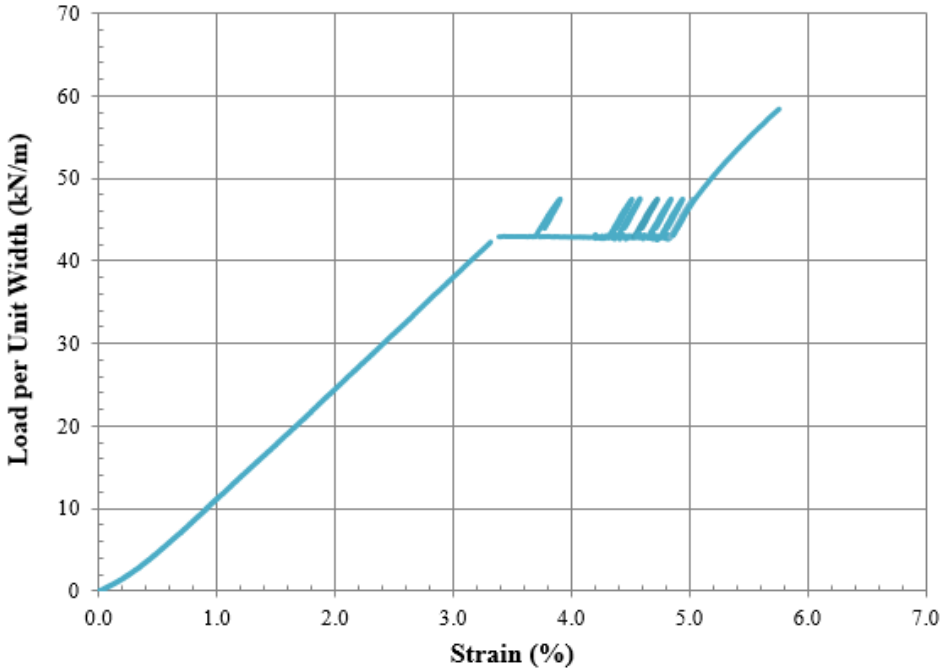

Figure 43 Monotonic Creep 1 hr. Test Results from Woven Geotextile

The modulus was calculated from the single cycles at different times and is shown below in Table 14 and Figure 44 and Figure 45 for the biaxial geogrid and woven geotextile respectively.

Table 14 Monotonic Stress Creep Test Results at 4.0 % Strain

Strain	Time	Modulus (kN/m)	
(%)	(Minutes)	Biaxial Geogrid	Woven Geotextile
4.00%	1	761	2218
4.00%	10	837	-
4.00%	16.67	855	2363
4.00%	20	869	2440
4.00%	30	873	2373
4.00%	40	877	2407
4.00%	50	856	2450
4.00%	60	892	2449

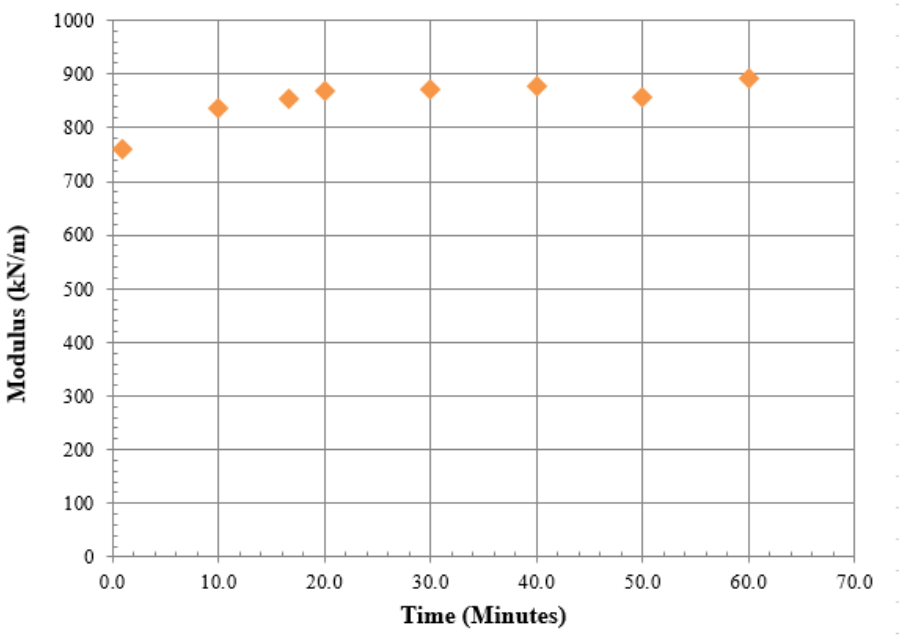

Figure 44 Monotonic Creep Test Results at 4.0 % Strain over 60 Minutes from Biaxial Geogrid

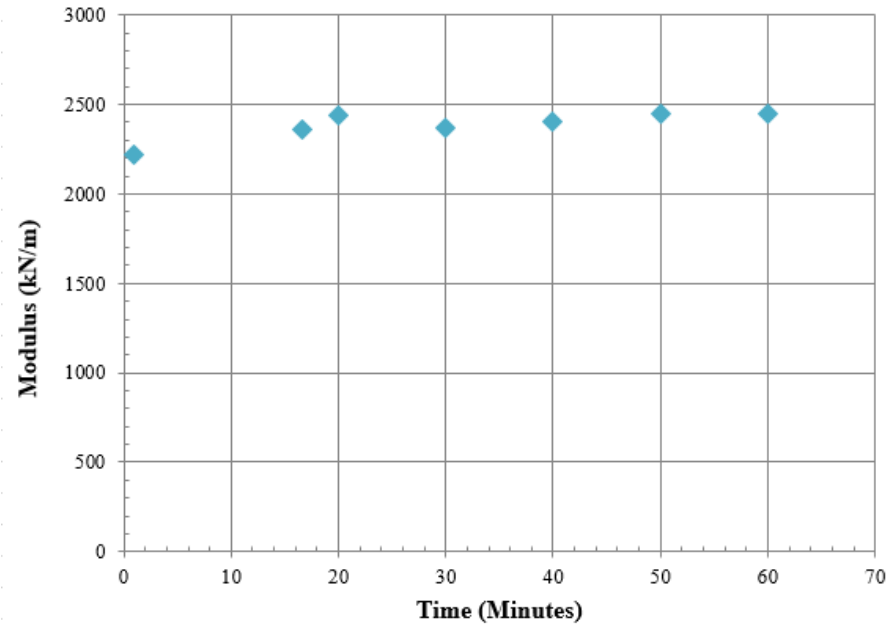

Figure 45 Monotonic Creep Test Results at 4.0 % Strain over 60 Minutes from Woven Geotextile

Analysis of Uniaxial Testing

The goal of the uniaxial testing program was to examine the resilient response of geosynthetics subjected to different types of loading over different durations of time to help develop a biaxial testing procedure using the biaxial device available. To do this, it was necessary to examine the resilient response from cyclic and monotonic stress relaxation and creep tests. It was also necessary to determine an adequate time to allow the material to relax/creep at each level of permanent strain such that the resilient response measured adequately described the resilient response expected in field loadings. The modulus from tests performed at six levels of permanent strain are compared on Figure 46 and Figure 47 for the biaxial geogrid and woven geotextile, respectively. The tests that were loaded initially to 4.0 % permanent strain were allowed to relax or creep for 24 hours are also shown on Figure 46 and Figure 47.

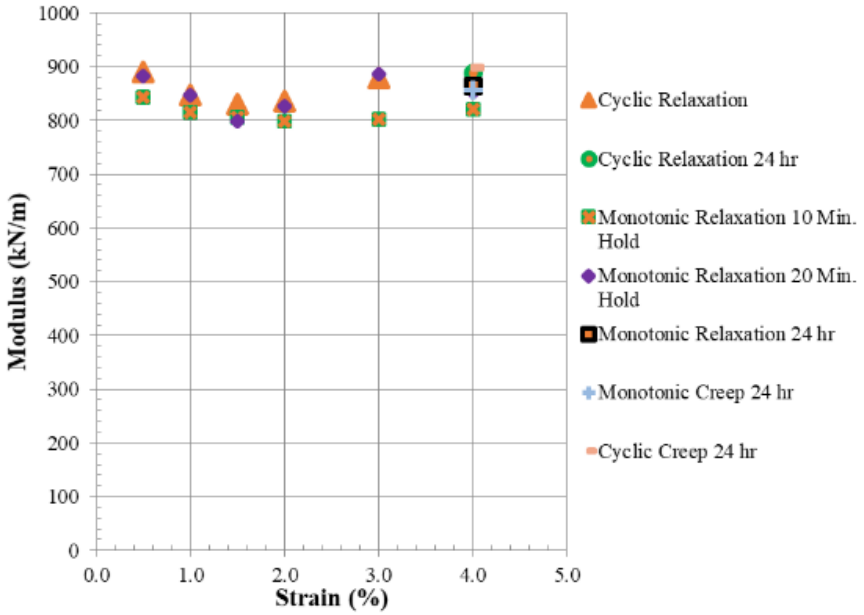

Figure 46 Comparison of Modulus Values from Cyclic Relaxation and Monotonic Relaxation Tests on a Biaxial Geogrid

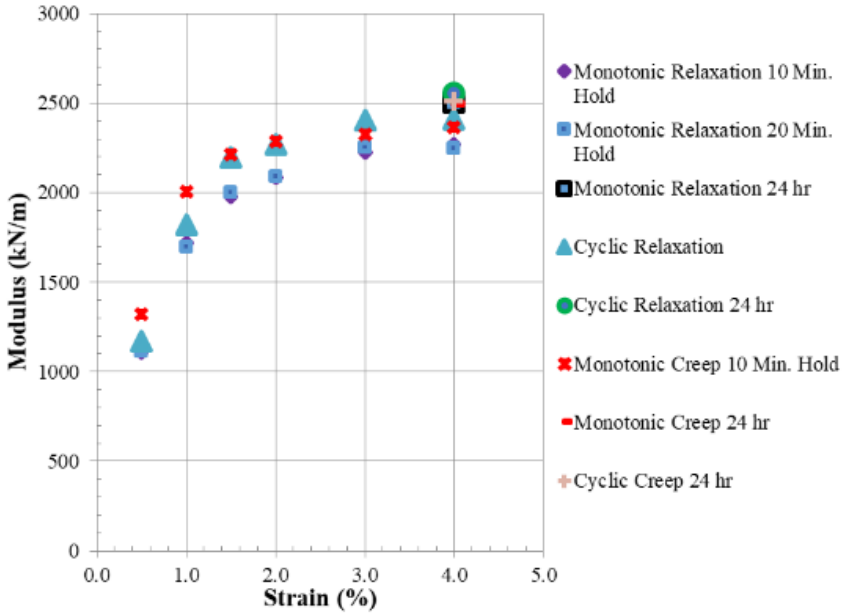

Figure 47 Comparison of Modulus Values from Cyclic Relaxation, Monotonic Relaxation and Monotonic Creep Tests on a Woven Geotextile

Cyclic and monotonic stress relaxation tests were performed extensively on both the biaxial geogrid and woven geotextile. For each of these types of tests, multiple trials were performed on each material such that a modulus was calculated at five or six levels of permanent strain. The modulus values could then be examined statistically to see the coefficient of variability that represents the variation in modulus values from the same type of test. This baseline variability should not increase when the modulus from different types of tests are compared if these modes of loading in fact are equivalent. Examining Table 3, Table 4, Table 6, Table 7 and Table 12 the variability of modulus values for cyclic stress relaxation (Table 3 and Table 4), monotonic stress relaxation (Table 6 and Table 7) and monotonic creep (Table 12) is observed. The coefficient of variability for modulus values from identical tests ranged from 0.25 % to 9.89 %.

To first examine the difference between cycling a material over small strains (±0.1 %) versus holding the material under a sustained strain (monotonic relaxation), the average modulus value for each level of permanent strain from cyclic stress relaxation (1000 cycles) and monotonic stress relaxation (10 minute holds) were compared as shown below in Table 15 and Table 16 for the biaxial geogrid and woven geotextile respectively.

Table 15 Comparing Average Modulus Values from Cyclic and Monotonic Stress Relaxation (10 Min. Hold) on a Biaxial Geogrid

Strain	Average Modulus	Standard	Coefficient of
	(kN/m)	Deviation	Variability
0.5%	867	11.3	1.30 %
1.0%	831	8.3	1.00 %
1.5%	819	5.9	0.72 %
2.0%	817	9.5	1.16 %
3.0%	841	19.2	2.29 %
4.0%	-	-	-
Average Coefficient of Variability			1.29 %

Table 16 Comparing Average Modulus Values from Cyclic and Monotonic Stress Relaxation (10 Min. Hold) on a Woven Geotextile

Strain	Average Modulus	Standard	Coefficient of
	(kN/m)	Deviation	Variability
0.5%	1173	3.8	0.33 %
1.0%	1819	0.8	0.05 %
1.5%	2123	75.5	3.55 %
2.0%	2199	72.4	3.29 %
3.0%	2315	88.9	3.84 %
4.0%	2342	68.0	2.91 %
Average Coefficient of Variability			2.33 %

The average modulus value from cyclic relaxation tests was also compared to the modulus value from the monotonic stress relaxation test with 20 minutes holds for both the biaxial geogrid and woven geotextile as shown in Table 17 and Table 18.

Table 17 Comparing Average Modulus Values from Cyclic and Monotonic Stress Relaxation (20 Min. Hold) on a Biaxial Geogrid

Strain	Average Modulus (kN/m)	Standard Deviation	Coefficient of Variability
0.5%	886	3.6	0.41 %
1.0%	848	0.6	0.08 %
1.5%	814	16.2	1.98 %
2.0%	832	4.1	0.49 %
3.0%	883	3.2	0.36 %
4.0%	-	-	-
Average Coefficient of Variability			0.66 %

Table 18 Comparing Average Modulus Values from Cyclic and Monotonic Stress Relaxation (20 Min. Hold) on a Woven Geotextile

Strain	Average Modulus (kN/m)	Standard Deviation	Coefficient of Variability
0.5%	1142	27.9	2.45 %
1.0%	1758	62.2	3.54 %
1.5%	2100	98.8	4.70 %
2.0%	2180	92.2	4.23 %
3.0%	2328	76.7	3.29 %
4.0%	2328	81.3	3.49 %
Average Coefficient of Variability			3.62 %

Modulus values from cyclic and monotonic stress relaxation tests at 4.0 % strain over 24 hours were calculated as shown in Table 5 and Table 8. These values are compared in Table 19 and Table 20 for the biaxial geogrid and woven geotextile, respectively.

Table 19 Comparing Modulus Values from 24 Hr. Cyclic and Monotonic Stress Relaxation on a Biaxial Geogrid

Strain	Average Modulus (kN/m)	Standard Deviation	Coefficient of Variability
4.00%	876	12.9	1.47%

Table 20 Comparing Modulus Values from 24 Hr. Cyclic and Monotonic Stress Relaxation on a Woven Geotextile

Strain	Average Modulus (kN/m)	Standard Deviation	Coefficient of Variability
4.00%	2530	26.1	1.03%

Using the same data compared in Table 19 and Table 20 with the addition of the data from Table 10 and Table 13, the modulus at 4.0 % strain can be compared from cyclic and monotonic stress relaxation and creep. This is shown below in Table 21 and Table 22 for the biaxial geogrid and woven geotextile respectively.

Table 21 Comparing Modulus Values from 24 Hr. Cyclic and Monotonic Stress Relaxation and Creep on a Biaxial Geogrid

Strain	Average Modulus (kN/m)	Standard Deviation	Coefficient of Variability
4.00%	876	16.8	1.92%

Table 22 Comparing Modulus Values from 24 Hr. Cyclic and Monotonic Stress Relaxation and Creep on a Woven Geotextile

Strain	Average Modulus (kN/m)	Standard Deviation	Coefficient of Variability
4.00%	2517	23.5	0.93%

Observing the coefficient of variability in Table 21 and Table 22 it can be concluded that the modulus values calculated from all four types of testing examined are equivalent. This statement of equivalency is based upon the fact that identical tests performed actually had a larger coefficient of variability in some instances as is seen in Table 3, Table 4, Table 6, Table 7 and Table 12. Although the cyclic and monotonic stress relaxation tests with six stages of permanent strain were not performed over identical times, the coefficients of variability for the modulus comparisons made in Table 15, Table 16, Table 17 and Table 18 are all very similar to those computed for identical tests. This indicates that geosynthetics will have the same resilient response after stress relaxation that is induced by small strain cycles or constant strain relaxation (monotonic relaxation). It is also noted that for the biaxial geogrid a hold time of 20 minutes instead of 10 minutes has modulus values that are more comparable to cyclic relaxation modulus values.

Comparisons were made to determine an adequate time of holding/cycling to simulate a resilient response. Examination of monotonic stress relaxation and creep tests performed at 4.0 % strain over one hour (Figure 32, Figure 33, Figure 44 and Figure 45) showed that a time of 20 minutes simulates the desired resilient response. This was examined a little further by comparing the modulus at 4.0 % strain at 24 hours and 20 minutes for monotonic relaxation (see Table 8 and Table 9 for modulus values being compared) and monotonic creep (see Table 13 and Table 14). These comparisons are shown in Table 23, Table 25 Table 24, Table 26 for the biaxial geogrid and woven geotextile, respectively.

Table 23 Comparing Modulus Values from 20 Min. and 24 Hr. Monotonic Stress Relaxation on a Biaxial Geogrid

Strain	Average Modulus	Standard	Coefficient of
	(kN/m)	Deviation	Variability
4.00%	888	25.0	2.82%

Table 24 Comparing Modulus Values from 20 Min. and 24 Hr. Monotonic Stress Relaxation on a Woven Geotextile

Strain	Average Modulus	Standard	Coefficient of
	(kN/m)	Deviation	Variability
4.00%	2467	37.1	1.50%

Table 25 Comparing Modulus Values from 20 Min. and 24 Hr. Monotonic Creep on a Biaxial Geogrid

Strain	Average Modulus	Standard	Coefficient of
	(kN/m)	Deviation	Variability
4.00%	863	6.2	0.72%

Table 26 Comparing Modulus Values from 20 Min. and 24 Hr. Monotonic Creep on a Woven Geotextile

Strain	Average Modulus	Standard	Coefficient of
	(kN/m)	Deviation	Variability
4.00%	2468	27.8	1.13%

The comparisons made in Table 23, Table 24, Table 25 and, Table 26 show that after 20 minutes of relaxation or creep both geosynthetics examined exhibit modulus values that are equivalent to that after 24 hours. The modulus at 4.0 % strain after 20 minutes for both monotonic stress relaxation and creep was additionally compared to the modulus at 4.0 % strain after 24 hours from all four types of loading examined and is

shown in Table 27 and Table 28 for the biaxial geogrid and woven geotextile respectively.

Table 27 Comparing Modulus Values from 20 Min. Monotonic Creep and Relaxation, 24 Hr. Monotonic and Cyclic Stress Relaxation and Creep on a Biaxial Geogrid

Strain	Average Modulus	Standard	Coefficient of
	(kN/m)	Deviation	Variability
4.00%	881	20.0	2.27%

Table 28 Comparing Modulus Values from 20 Min. Monotonic Creep and Relaxation, 24 Hr. Monotonic and Cyclic Stress Relaxation and Creep on a Biaxial Geogrid

Strain	Average Modulus	Standard	Coefficient of
	(kN/m)	Deviation	Variability
4.00%	2490	43.1	1.73%

The comparisons made in Table 27 and Table 28 show that after 20 minutes of relaxation or creep the resilient modulus calculated is equivalent to that of a resilient modulus after 24 hours. Table 27 and Table 28 also again demonstrate that all four types of loading are equivalent for calculation of a resilient modulus. Equivalency is based upon the fact that the coefficients of variability observed when comparing dissimilar types of tests is within the range of coefficients of variability that were calculated for identical tests with multiple trials.

Conclusions from Uniaxial Testing

It has been shown in this chapter of this thesis that the four forms of loading examined (Cyclic Stress Relaxation, Cyclic Creep, Monotonic Stress Relaxation and Monotonic Creep) result in equivalent resilient responses of two different geosynthetic

materials. It has also been shown that a time of 20 minutes results in an equivalent resilient response as a time of 24 hours for the two different geosynthetics examined. The biaxial geogrid examined for uniaxial testing was deemed representative of the other biaxial geogrids that were examined in the biaxial testing program. The woven geotextile examined in the uniaxial testing program was also deemed representative of the woven geotextiles that were examined using biaxial tension tests. Thus, a biaxial testing procedure was created using the knowledge gained from the uniaxial testing program described in this chapter. The fact that the biaxial device cannot produce purely stress relaxation was not important for simulating a resilient response of geosynthetics. The combination of mostly stress relaxation and some stress creep that occurs in biaxial samples from monotonic tests at multiple permanent strain limits is representative of a resilient response. A time of 20 minutes at each level of permanent strain was used for biaxial tests because this was shown to be an adequate time to generate a resilient response.

CHAPTER SIX

BIAXIAL TESTING

Biaxial Testing Methods

The uniaxial testing program was conducted to develop a biaxial testing procedure that could be used to simulate the resilient response of geosynthetics. The resilient response for biaxial tension tests is characterized by a more complex model than uniaxial testing as outlined in the Theory section of this thesis. This more complex model provides a better representation of field loading conditions of geosynthetics than uniaxial tests. The biaxial testing procedure developed for this research was based upon ASTM D7556 with the findings from the uniaxial testing program implemented. This meant that tests were performed at six permanent strain limits of 0.5, 1.0, 1.5, 2.0, 3.0 and 4.0 % strain with a hold time of 20 minutes at each level of permanent strain. The material experienced mostly stress relaxation with some creep during this 20-minute time period.

Three modes of biaxial tension tests were performed to calculate elastic constants that represent geosynthetics in different field loading situations. Tests where both perpendicular directions were pulled in tension by an equal displacement will be referred to as Mode 1 biaxial tests. Tests where the Machine Direction (MD), referred to as the Y or 2-Direction in this thesis, was held at a constant displacement while the Cross-Machine Direction (XMD), referred to as the X or 1-Direction in this thesis, was displaced will be referred to as Mode 2 biaxial tests. Tests where the XMD was held at a constant displacement while the MD was displaced will be referred to as Mode 3 biaxial

tests. All three modes of testing were performed on all geosynthetics tested. The geosynthetics tested along with the number of trials performed on each geosynthetic are shown in Table 29. More trials were performed for practicing with the biaxial testing device, but these are not included in Table 29 because they were not used for calculation of the elastic constants. The geogrid and geotextile tested in the uniaxial testing program were Geogrid B and Geotextile B.

Table 29 Summary of Materials Tested Biaxially

Geosynthetic Type	Manufacturer and Product	Generic Name	Trials by Mode (1,2,3)
Biaxial Geogrid	Tensar BX1100	Geogrid A (GgA)	6, 6, 6
Biaxial Geogrid	Tensar BX1200	Geogrid B (GgB)	3, 1, 1
Biaxial Geogrid	BOSTD E1616	Geogrid C (GgC)	3, 2, 1
Biaxial Geogrid	BOSTD E2020	Geogrid D (GgD)	3, 3, 2
Biaxial Geogrid	BOSTD E3030	Geogrid E (GgE)	3, 2, 2
Biaxial Geogrid	BOSTD RX1200	Geogrid F (GgF)	5, 1, 2
Triaxial Geogrid	Tensar TX140	Geogrid G (GgG)	6, 2, 2
Woven Geotextile	TenCate RS380i	Geotextile A (GtA)	3, 1, 2
Woven Geotextile	TenCate RS580i	Geotextile B (GtB)	4, 2, 1

Biaxial Testing Device

The biaxial testing device used for this project (Figure 48) was developed and built by the Western Transportation Institute (WTI) at Montana State University (MSU). The biaxial device is capable of testing cruciform samples with interior dimensions up to 450 mm by 450 mm. The length of the cruciform arms can be up to 600 mm. The device was specifically designed for testing geosynthetics under working load conditions. The device is capable of applying a constant rate of displacement in all four directions (mode 1 loading), which allows the center of the sample to remain in a constant location. The device is also capable of applying load in one principal direction while the other direction does not displace (mode 2 and mode 3 loading). The device is operated by controlling the displacement of the load plate (Figure 48), which causes displacement at the clamps via tension in the chains.

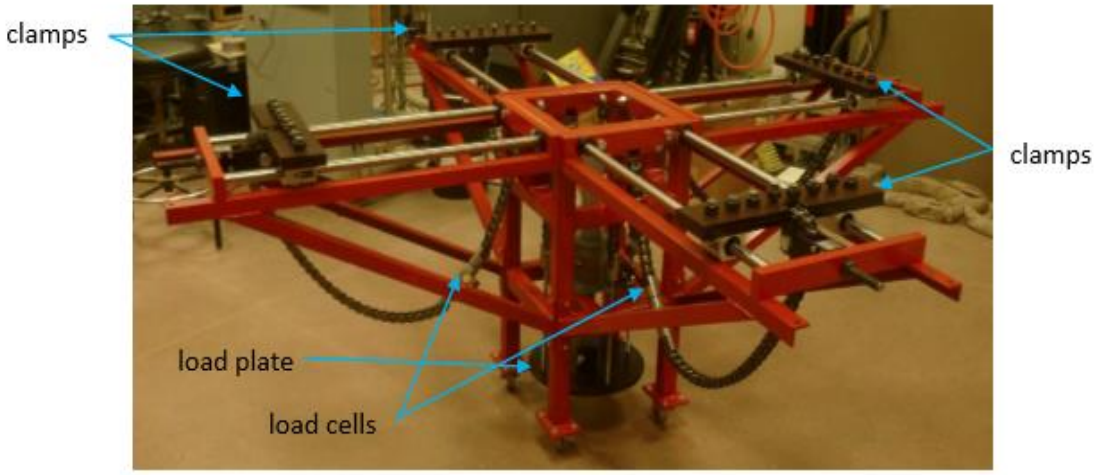

Figure 48 Biaxial Testing Device at MSU/WTI

The displacement of the load plate is controlled by the rotation of an electric motor that is connected to a gear reducer and a worm drive. The worm gear causes upward or downward displacement of the load plate (Figure 49).

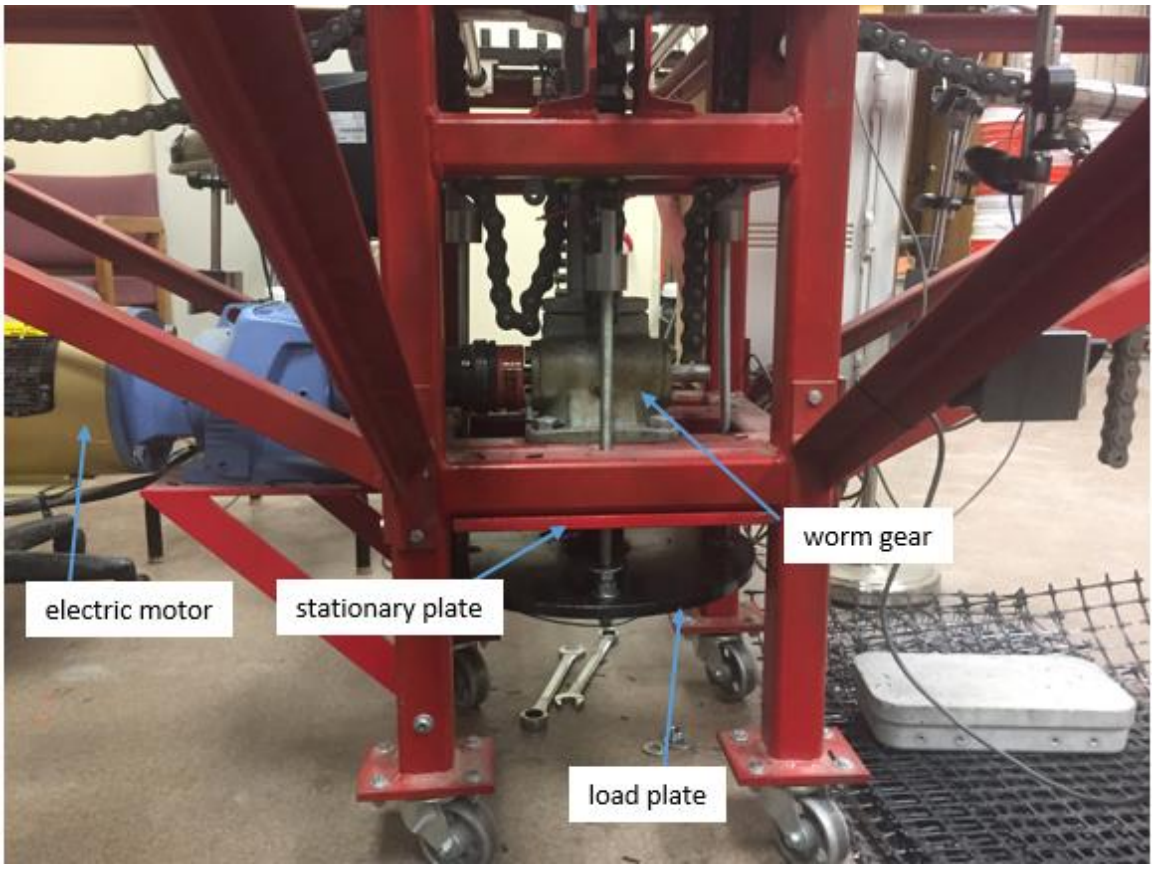

Figure 49 Biaxial Testing Device Bottom Half

A small control panel is used for choosing the direction and speed of the motor's rotation. The control panel has a digital readout for motor speed. The speed of the motor can be converted to displacement of the load plate by using the gear reduction ratio of 10:1 and the worm gear ratio of 100 rotations:1 inch. Thus 1000 rotations of the electric motor corresponds to 2.54 cm (1 inch) of displacement of the load plate.

For mode 1 loading, all four clamps are displaced simultaneously by being connected to the load plate that displaces downward. For mode 2 and mode 3 tests, one direction remains connected to the load plate while the other direction is disconnected from the black load plate and connected to the stationary red plate (Figure 50).

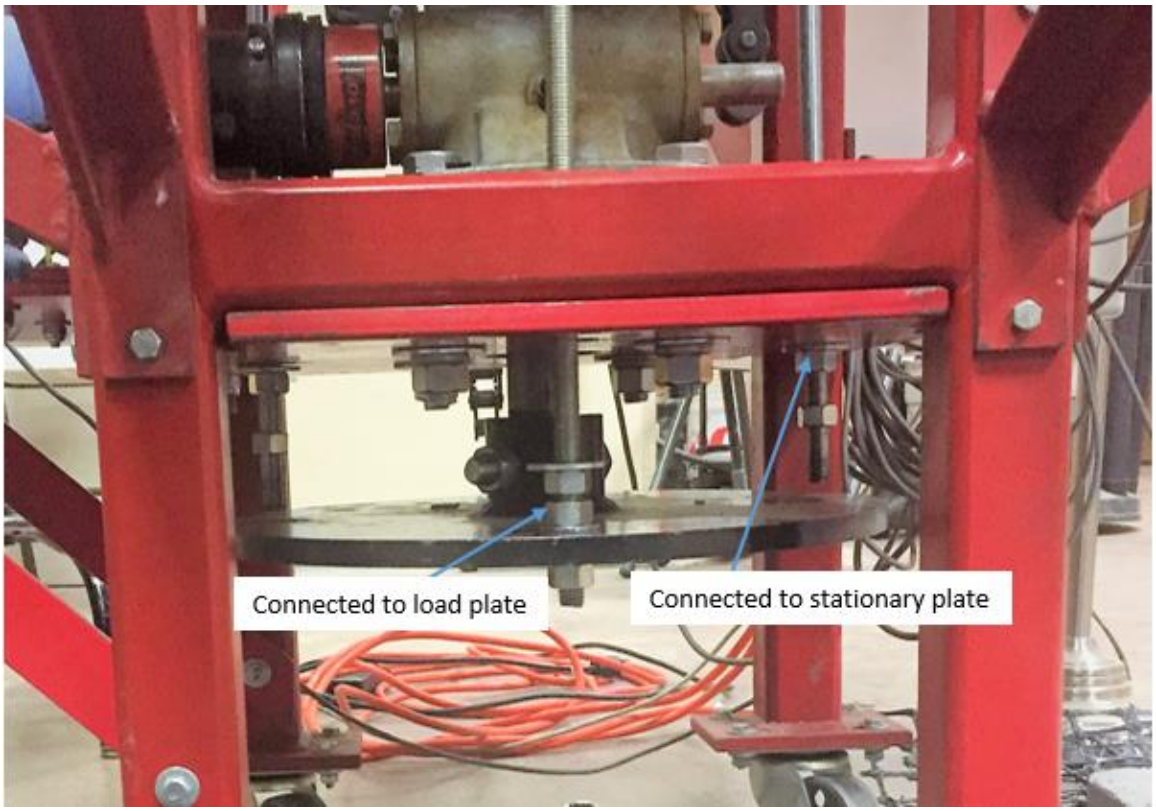

Figure 50 Biaxial Testing, Load Plate and Stationary Plate

The biaxial device has one load cell in each principal direction that is placed in the chain as shown in Figure 48. Linear variable differential transformers (LVDTs) are used to measure displacement of the material in the interior section of the biaxial sample at discrete points from which axial strain is calculated. The attachment and placement of LVDTs is discussed further in the Testing Setup section. The biaxial device is connected

to a laptop computer with a digital readout of the current load in both directions and current displacement in all four directions as measured by load cells and LVDTs, respectively.

Testing Setup

Geosynthetic samples used for biaxial tension tests were cut from large rolls. The samples were cut from the middle section of the geosynthetic roll to minimize any material defects that are more common near the edge of the roll. Samples were also visually inspected for any material defects from manufacturing. Samples were cut in the shape of a cruciform as shown in Figure 52. The materials were then laid flat on the floor with cinder blocks placed at the end of each cruciform arm to minimize the inherent curling that the samples have from being stored on a roll. Samples were kept under these blocks until the curling had decreased sufficiently for testing setup. Once the material was cut and flattened, the material was placed in the biaxial testing device. The four ends of the cruciform shaped sample were centered and placed in the clamps. For geogrids, ribs that interfered with the bolts use to tighten the clamps were snipped. For woven geotextiles, holes were melted in the geotextile such that the bolts could fit through the material (Figure 51).

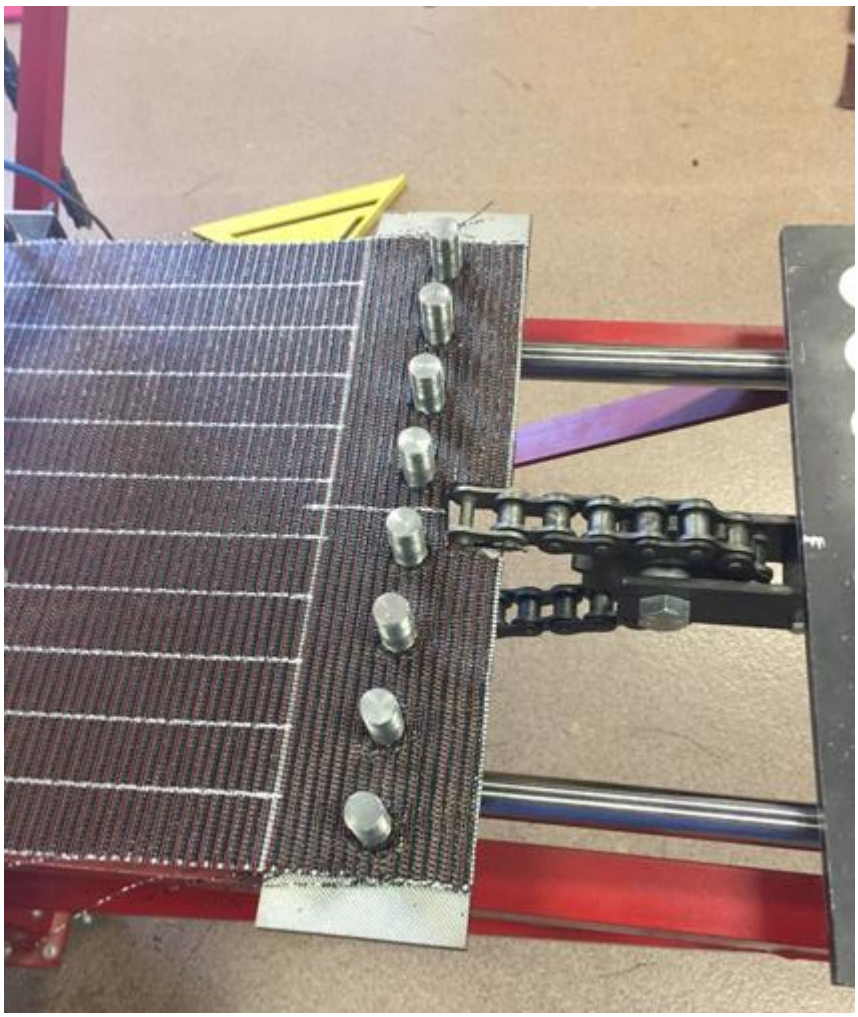

Figure 51 Woven Geotextile in End Clamp

The sample was carefully centered in each grip and the bolts were tightened to 70 N-m of torque using a torque wrench. The sample was centered in the device such that the interior portion of the geosynthetic was symmetric in both directions (Figure 52).

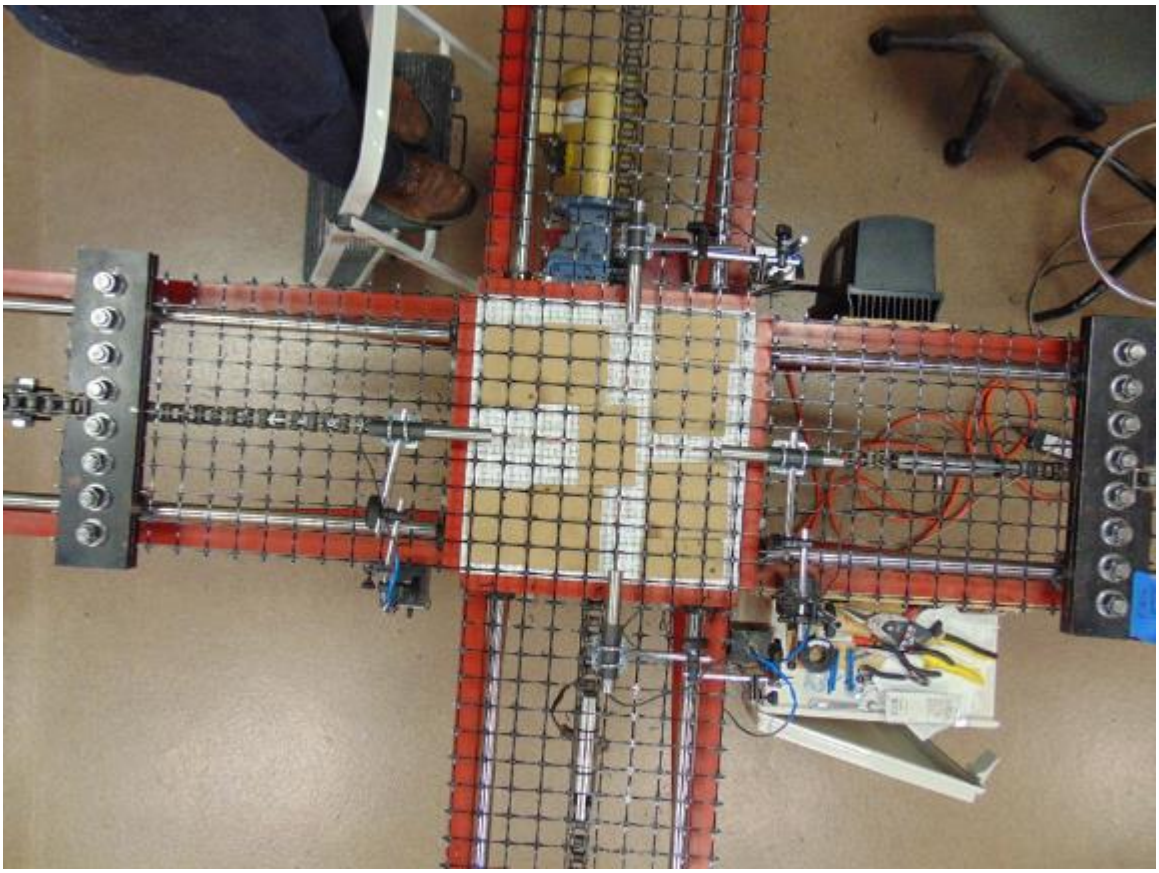

Figure 52 Biaxial Testing Device with a Biaxial Geogrid Setup

For geogrids, the ribs perpendicular to the direction of loading were cut in all four cruciform arms. For woven geotextiles, eleven slits were cut in all four cruciform arms (Figure 53). The cruciform arms were slit to reduce load reductions that are known to occur in biaxial tension tests between the applied load at the grip and the load in the interior portion of biaxial sample. This load reduction effect was documented in MSAJ (1995) and Bridgens and Gosling (2003) and was shown to have minimal effects with slit cruciform arms as discussed in the Literature Review section of this thesis. If cruciform

arms are left intact near the interior portion of the biaxial sample, this will also restrict movement in the orthogonal direction of the material which is undesirable.

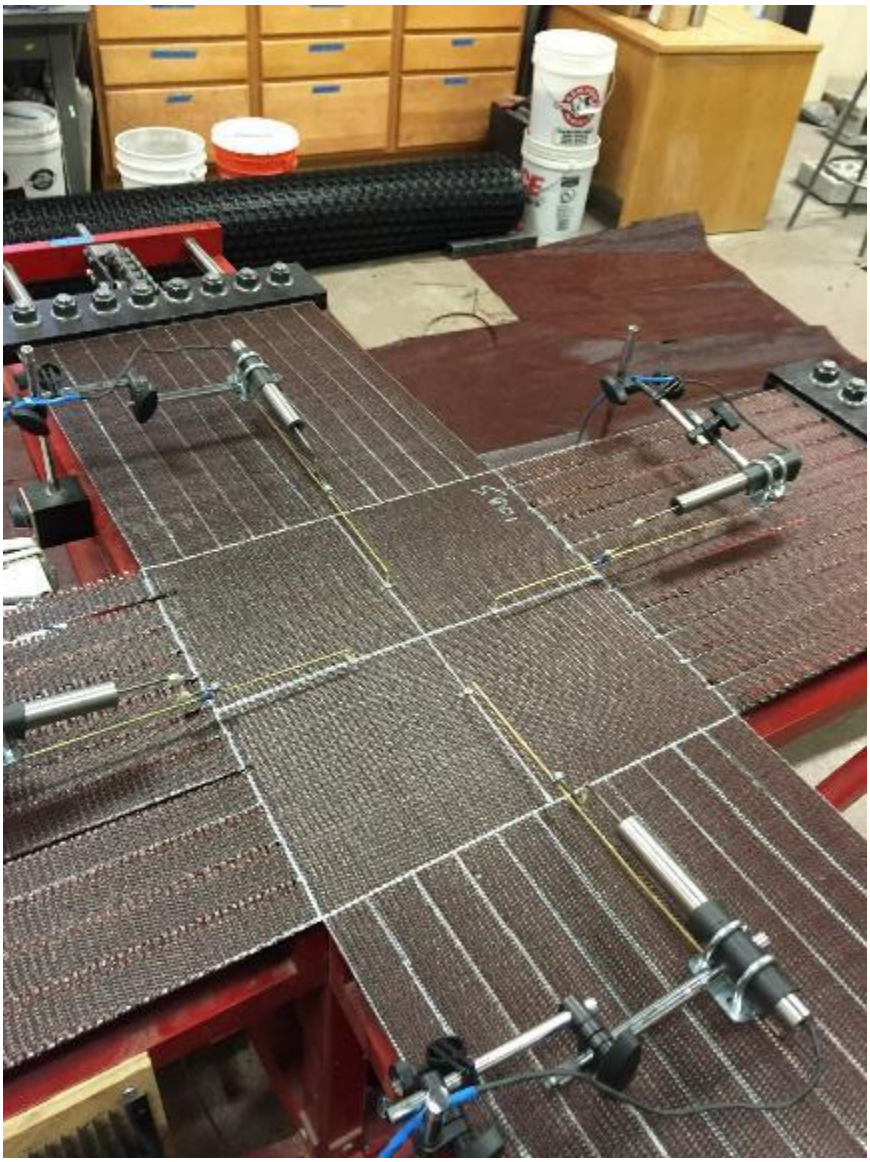

Figure 53 Biaxial Testing Device with a Woven Geotextile Sample

LVDTs were attached to the interior portion of the sample. For geogrids, LVDTs were attached at nodes (Figure 54), while for geotextiles LVDTs were attached in the woven interior portion (Figure 55). LVDT attachment was an experimental process that required several techniques and iterations before coming up with a system that was used. For geogrids, small holes were predrilled in the nodes where LVDTs would be attached. The arm of the LVDT had an electric terminal (red piece) on the end of it with a small hole in the middle (Figure 54). The electric terminal was securely attached to the arm of the LVDT using super glue. The hole in the electric terminal was lined up with the predrilled hole in the node and a small nail (1.2 mm x 15.9 mm) was hammered through the electric terminal hole into the predrilled hole in the node of the geogrid to connect the LVDT arm to the node (Figure 54). A small amount of super glue was then placed on the head of the nail to ensure no displacement would occur.

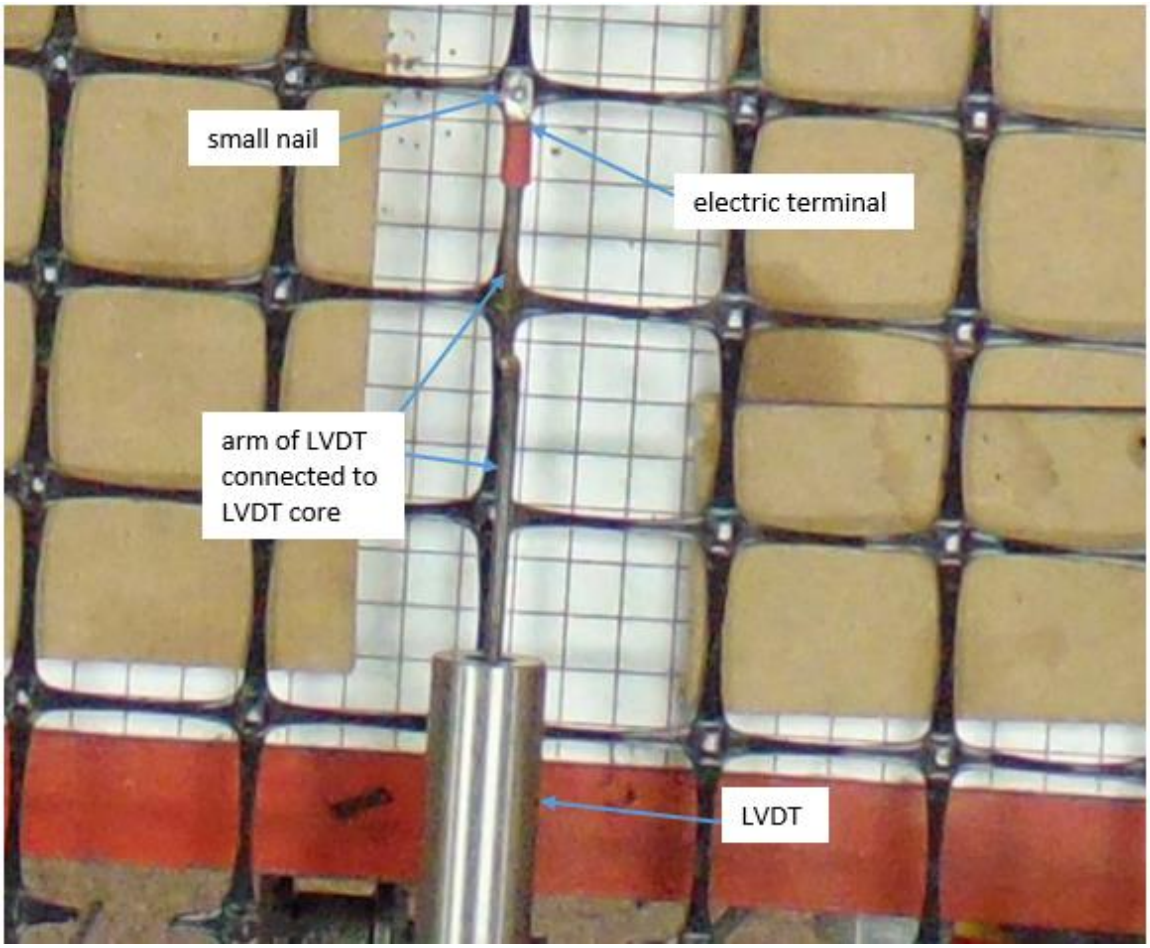

Figure 54 LVDT Attachment for Biaxial Geogrid Samples

For woven geotextiles, a sharp threaded rod was pushed through the sample and a nut was threaded on each side of the geotextile to lock the attachment point in place. The threaded rod was connected to the arm of the LVDT (Figure 55).

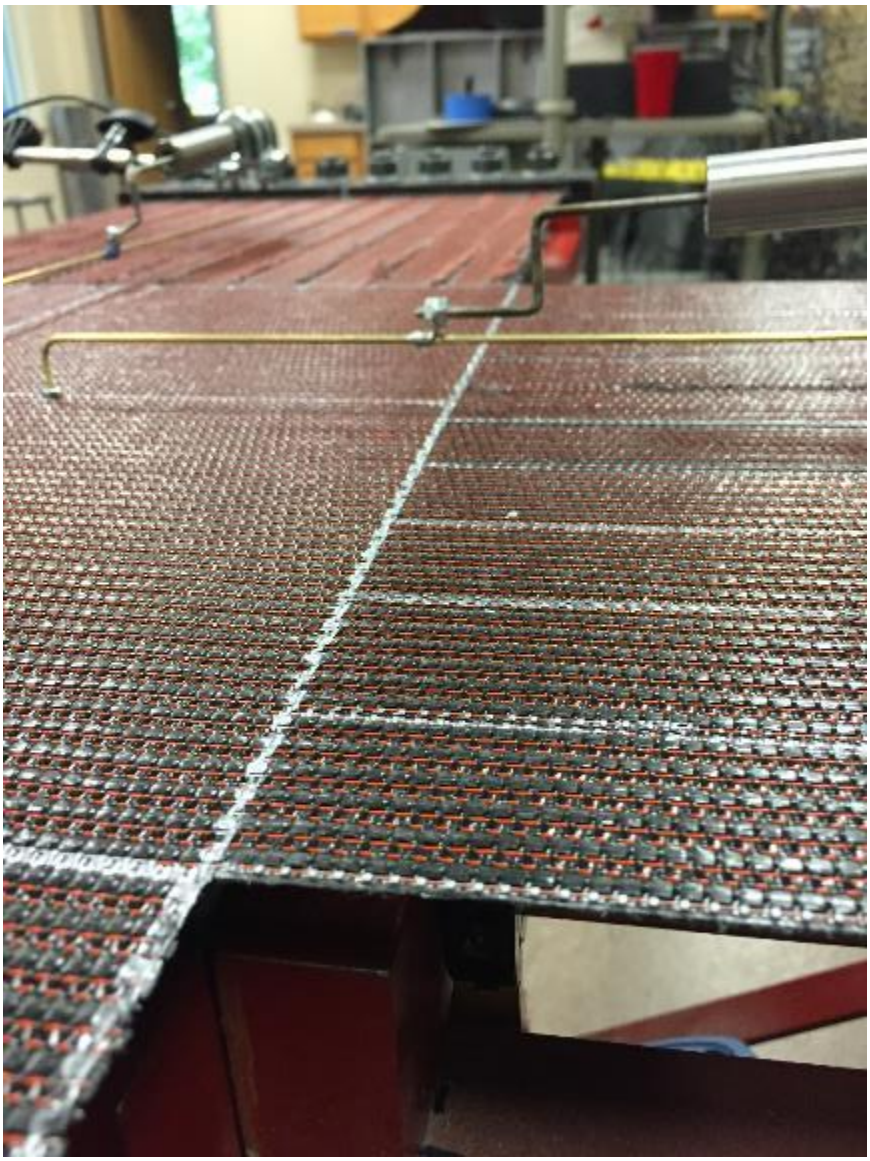

Figure 55 LVDT Attachment for Biaxial Woven Geotextile Samples

Great care was taken with the LVDT setup and attachment to minimize error in measurements of strain. Once all four LVDTs were attached, a seating load of 222 Newtons (50 lb.) in each direction was applied by tightening the bolts at the end of each arm (Figure 56).

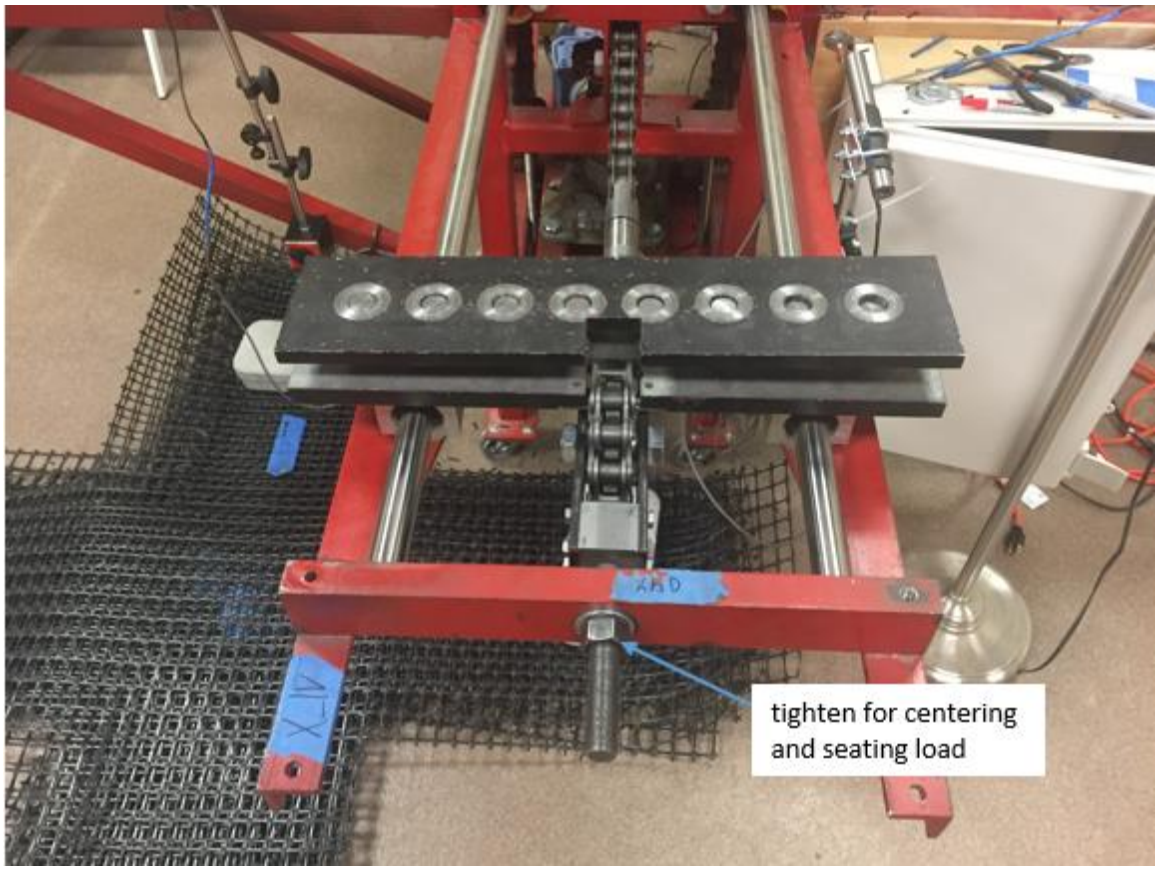

Figure 56 Biaxial Testing Device, Bolt for Applying Seating Load

When applying the seating load, the material was again carefully centered on the device. Wooden blocks were placed underneath the interior portion of the sample to minimize any displacement in the z-direction when tensioned (Figure 52). Once the seating load was applied, a gauge length in both directions was measured from the center lines of the nails used to attach the LVDT arm to the geogrid node. For geotextiles the gauge length was measured from centerline to centerline of the threaded rod. The sample width for geogrids was determined as outlined by ASTM D7556 and discussed in the uniaxial testing section (Figure 15). For geotextiles, the width was just simply measured

as the width of the sample. The LVDTs were then adjusted such that the inner core was parallel with the outer core and parallel with the geosynthetic material. It was then double checked that the seating load was still at 222 Newtons (50 lbs) before the test was started.

Recommendations for specimen dimensions of biaxial samples was examined by Bridgens and Gosling (2003) and MSAJ (1995) for structural membranes in the Literature Review section. The gauge points must be sufficiently far from edge of the interior portion such that any effects from the grips are not noticed and the instrumentation is placed within the zone of uniform stress and strain as observed by Krause and Bartolotta (2001) and Bridgens and Gosling (2003). Bridgens and Gosling (2003) and MSAJ (1995) both used smaller biaxial testing devices with smaller overall sample dimensions than was used for this thesis. The ratio of sample width to recommended gauge length for samples tested by Bridgens and Gosling (2003) was 2/3. The Japanese testing standard recommended sample widths of 48 cm or more and used gauge lengths ranging from 20 to 80 mm. McGown et al. (2004) conducted biaxial tests on geogrids using cruciform shaped samples with central areas of 100 to 220 mm square with 5 ribs in each direction but measured displacement using photogrammetric techniques. The biaxial geogrids tested had rectangular apertures, thus the XMD and MD directions had slightly different sample widths and gauge lengths. The samples were always symmetric with respect to each direction and the same sample size was used for each given material for all trials and all modes of loading. Sample dimensions used were decided based upon the available literature and the size and layout of the available biaxial

testing device. Typical interior sample widths ranged from 365 mm to 422 mm and gauge lengths ranged from 127 mm to 178 mm.

Testing Procedure

Biaxial tests were run with the motor set at a speed of approximately 3450 rotations per minute, which corresponds to a displacement of the load plate of 8.76 cm (3.45 inches) per minute. Initially it was desired to use ASTMD D7556 as a guideline for strain rate, but the biaxial device was not capable of producing a strain rate that satisfied this standard. The strain rate as outlined in ASTM D7556 should be 10 ± 3 % per minute. The motor was run at its maximum speed which produced strain rates of approximately 5 % per minute. Measured strain rates for trial biaxial tests are listed later in this chapter in Table 30.

A laptop computer and data acquisition system were connected to the testing device to record real time values of load and displacement in both directions. Using the measured gauge lengths in both directions, displacements that correspond to strains of 0.5, 1.0, 1.5, 2.0, 3.0 and 4.0 % were calculated for both directions. The motor was then switched on and run until the material reached the displacement corresponding to a strain of 0.5 %. The motor was then shut off and a timer for 20 minutes was started. This process was continued for all permanent strain limits. This procedure was used for all materials tested and for all modes of loading.

The procedure described had some inherent human error with reaching the permanent strain limits. To reach the permanent strain limits, the motor had to be stopped

manually at the desired displacement. This was difficult to do with high precision because once the switch for the motor was turned off, the motor would continue to spin while slowing down. This deceleration period would cause more displacement in the material. After lots of practice, this process was not very difficult, but it was still impossible to have identical values of permanent strain limits for each material and each trial. The permanent strain values were approximated as best as possible and recorded so this was not a large issue. Another problem encountered with the testing device was its inability to load materials to 3.0 and 4.0 % permanent strain for some of the stiffer geosynthetics tested. The motor did not have the power to load some of these materials to the upper strain limits, and the load cell reached its capacity of 8896 N (2000 lbs) for some materials. Tests were run to the highest level of permanent strain that was attainable for materials where these limitations were encountered. It was discovered that if the motor speed was slowed down after initially loading the material at full speed, the motor was capable of applying a little more displacement. When possible, this was done to load the material to one more strain limit.

Biaxial Testing Results

The results from Geogrid A will be presented in this section because the greatest number of trials for each mode were performed on this material. The results obtained for this material and the analysis process that follows were performed for all materials tested. The load per unit width versus strain plot for a mode 1 loading is shown in Figure 57. The X-direction is always the XMD or 1-direction and the Y-Direction is always the MD

or 2-direction. Geogrid A as well as all geogrids examined for this thesis did not have square apertures so it was not possible to have an equal distance between the device grips in both principal directions. The slight difference in values of strain between the two material directions (Figure 57) is due to this difference in total length of the sample between grips for principal directions.

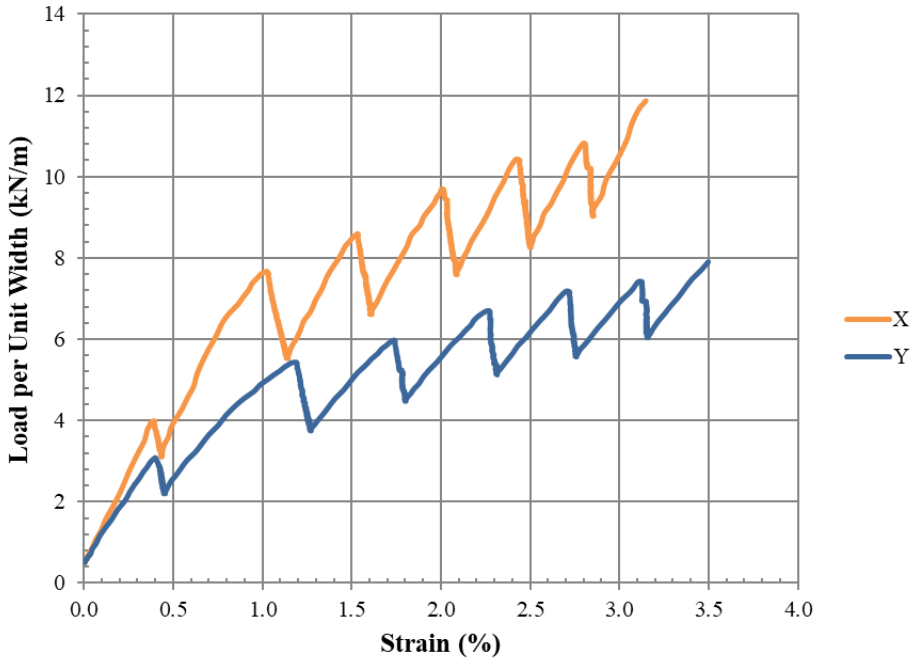

Figure 57 Mode 1 Test Results from Geogrid A

Mode 2 and mode 3 tests for Geogrid A are shown in Figure 58 and Figure 59, respectively. For the mode 3 test shown in Figure 59, the motor was reversed briefly to try and better approximate the permanent strain limit of 3.0 %, which is why the load per unit width vs. strain plot has an irregular shape. It was decided that approximating the

permanent strain limits would be sufficient given the biaxial testing device used, so this was not done for future materials.

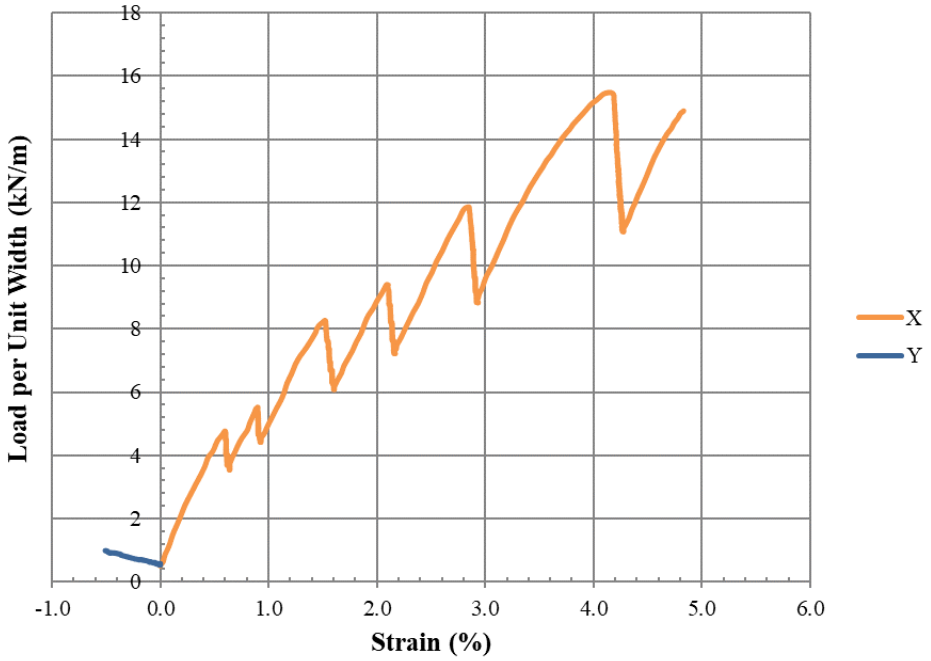

Figure 58 Mode 2 Test Results from Geogrid A

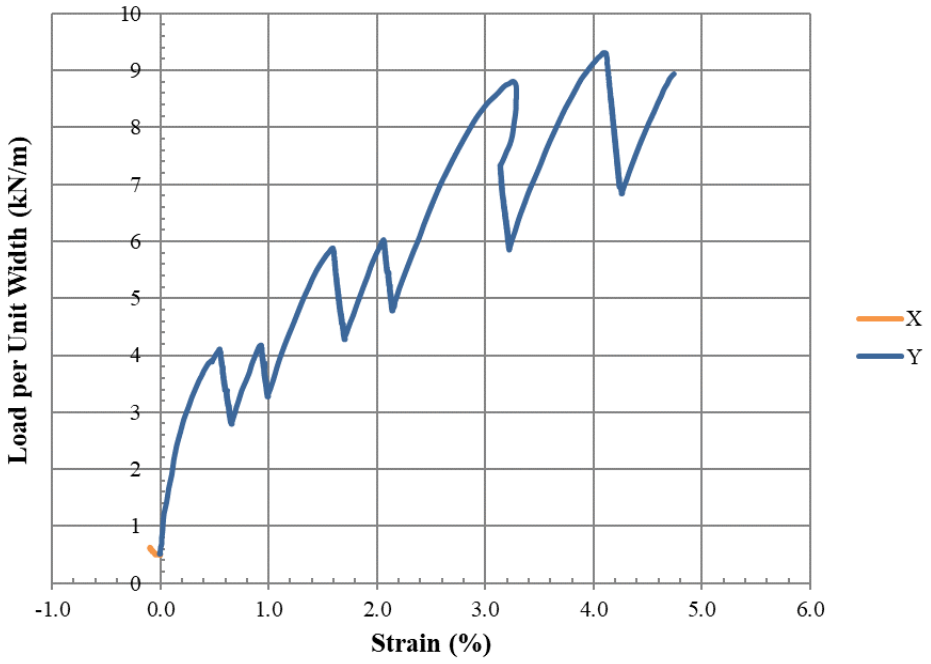

Figure 59 Mode 3 Test Results from Geogrid A

The load per unit width (stress) and strain data from biaxial tests was then examined closely to find the slope of the reloading curve after the stress relaxation and creep period of 20 minutes. The slope of the initial reloading portion of the load per unit width vs. strain was called a pseudo modulus. The goal was to characterize the resilient response for an orthotropic linear elastic model, meaning the stress-strain data used should be over a linear portion of the curve. As can be seen from Figure 57, Figure 58 and Figure 59, the stress-strain response is relatively linear initially after the 20 minute period of stress relaxation/creep. The slope can then be seen to become non-linear as plastic strain develops. Some load steps and trials also had some nonlinearities immediately upon loading that are most likely due to errors in testing setup and instrumentation. Thus, it was necessary to examine the stress-strain response after stress

relaxation/creep on a case by case basis to ensure the response was linear and representative of the resilient material response. The pseudo modulus was calculated using a best fit linear trendline of the stress/strain data after each stress relaxation/creep period as shown in Figure 60. The stress/strain interval selected for calculation of the pseudo modulus varied slightly from trial to trial in order to use the most linear portion of the reloading curve after stress relaxation/creep.

As mentioned in the testing procedure section, the stiffness of geosynthetics is dependent on strain rate (Perkins, 2000). The strain rate outlined in ASTM D7556 was not achievable with the biaxial testing device used for this testing. The strain rates for the data used for calculation of the pseudo modulus is shown in Table 30 for all six trials of mode 1 loading on Geogrid A. The strain rates vary between 2.99 and 7.59 % / minute and are almost all below the minimum value of 7.0 % per minute as outlined in ASTM D7556. The variability is attributed to several factors including the method in which pseudo modulus was calculated and imperfections in testing setup, instrumentation and the testing device. The electric motor used to control displacement (strain) has a short acceleration period and does not immediately rotate at its maximum speed. During this short acceleration period, the material does not experience a constant rate of strain. Since the pseudo modulus was calculated from the initial loading this means the strain rate is increasing then constant in the region of loading used for calculation of pseudo modulus. Since the pseudo modulus was calculated on a case by case basis, the strain interval was not always equal, meaning the strain rates shown in Table 30 should be expected to be variable.

Table 30 Strain Rate of Mode 1 Trials on Geogrid A

	Strain Rate (% / minute)											
Load	Trial 1		Trial 2		Trial 3		Trial 4		Trial 5		Trial 6	
Step	X	Y	X	Y	X	Y	X	Y	X	Y	X	Y
1	4.79	6.19	4.11	5.22	4.95	5.73	4.99	5.61	4.78	5.54	5.11	5.95
2	4.44	5.38	2.99	3.91	4.33	5.10	4.18	5.00	4.32	5.07	3.74	4.24
3	4.22	4.59	4.44	5.90	4.78	5.06	4.64	5.12	4.98	5.36	4.89	5.58
4	4.48	5.04	4.62	5.63	4.54	5.09	6.32	7.59	5.13	5.21	4.81	5.37
5	4.02	4.75	4.90	6.33	3.92	4.54	4.13	4.94	5.14	6.08	6.00	6.25
6	4.78	5.41	-	-	4.73	4.79	5.24	5.06	4.25	5.12	-	-

The first load step of the mode 1 trial performed on Geogrid A (Figure 57) was examined closer in Figure 60 for calculation of the pseudo modulus. Figure 60 is zoomed in data from Figure 55 for the loading after the first 20-minute period of stress relaxation/creep.

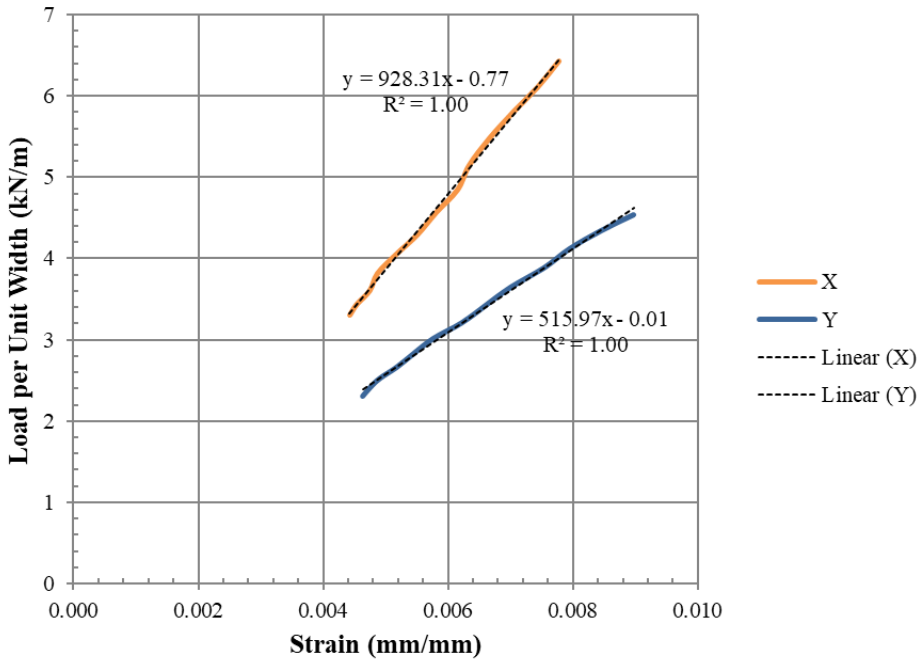

Figure 60 Mode 1 Test Results from Geogrid A, Zoomed in on Load Step 1

The slope of the best fit linear trendline (pseudo modulus) was used to calculate stress and strain inputs for the orthotropic linear elastic model described in the theory section for calculation of elastic constants. The strain was simply calculated as the interval of strain that the pseudo modulus was calculated over, while the stress was calculated as the strain multiplied by the pseudo modulus. This process was repeated for each level of permanent strain (load step) for all three modes of loading. For mode 1 loading, both directions exhibited a linear stress-strain response as is seen in Figure 60. For mode 2 and mode 3 loading, the direction with no applied displacement did not always yield a well-behaved linear stress-strain response (Figure 64). The reason for this is likely due to testing device or instrumentation limitations for such small displacements and loads that occur in the direction not being displaced. Mode 2 and mode 3 data was still used for calculation of elastic constants, but more carefully examined to remove outlying data. The zoomed in version of Figure 58 and Figure 59 is shown in Figure 61 and Figure 62 for mode 2 and mode 3 loading respectively.

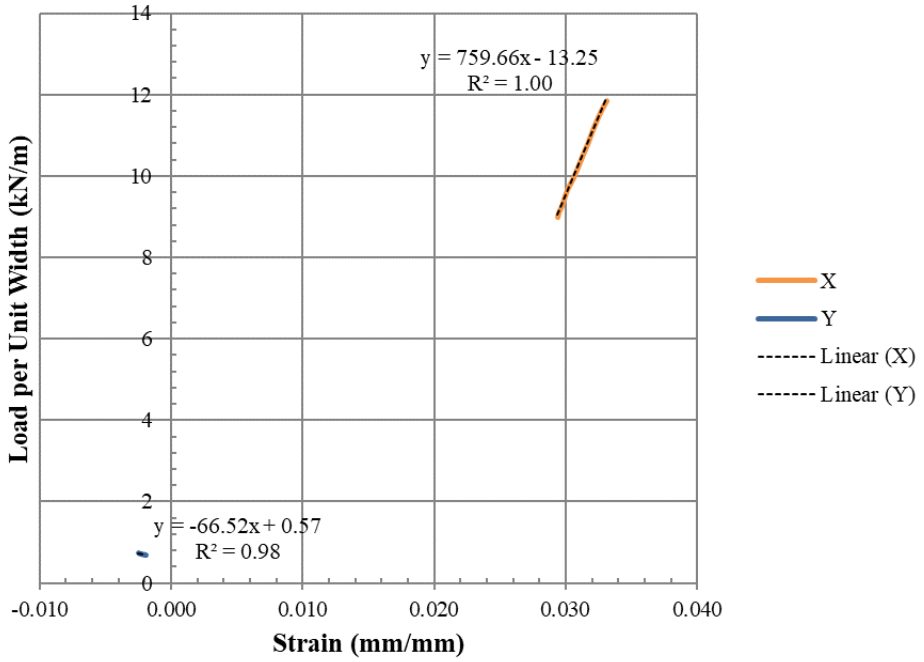

Figure 61 Mode 2 Test Results from Geogrid A, Zoomed in on Load Step 5

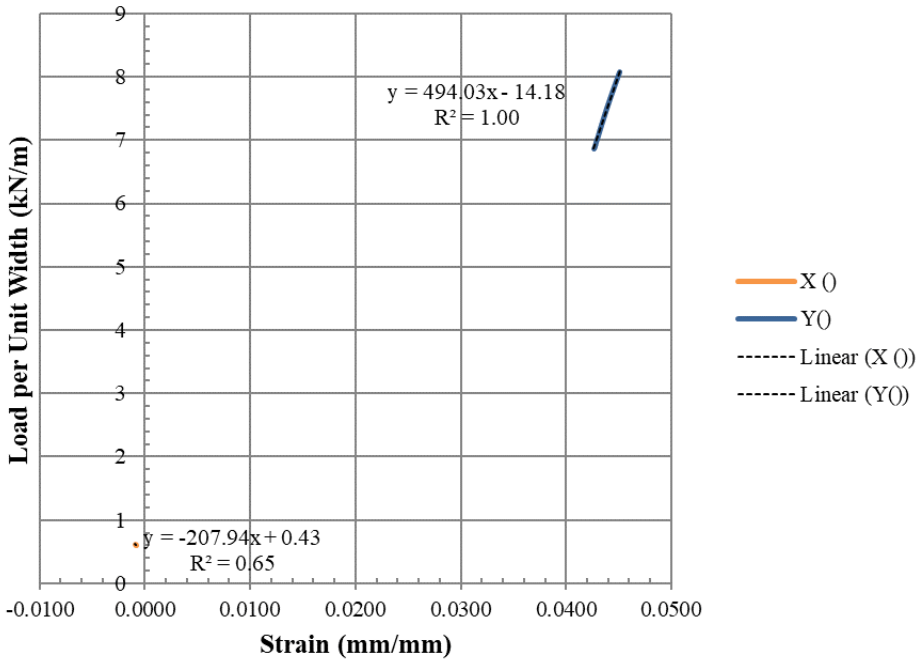

Figure 62 Mode 3 Test Results from Geogrid A, Zoomed in on Load Step 6

The direction not being loaded in Figure 61 and Figure 62 is zoomed in on Figure 63 and Figure 64, respectively.

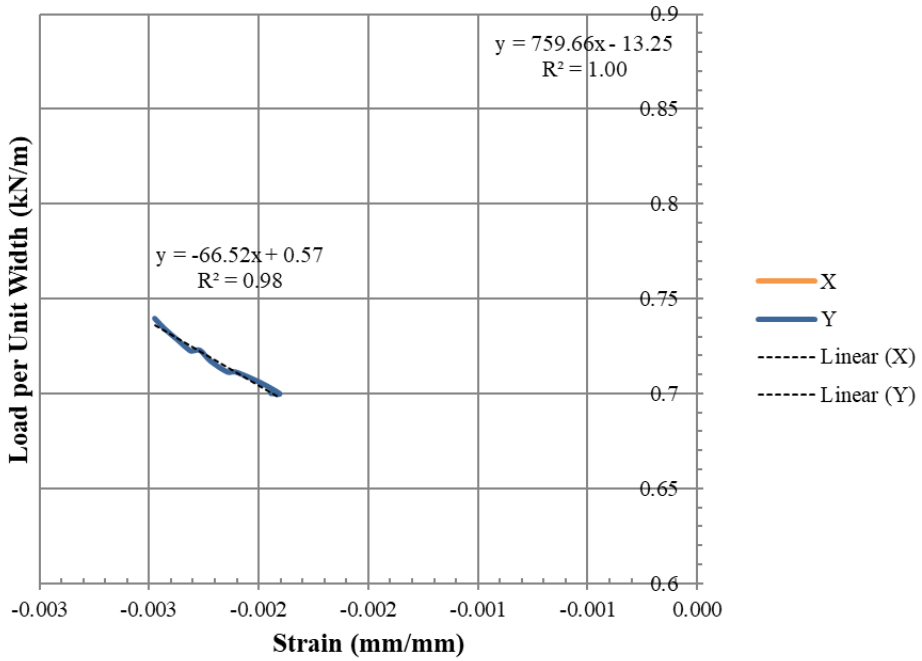

Figure 63 Mode 2 Test Results from Geogrid A, Zoomed in on Load Step 6 Y-Direction

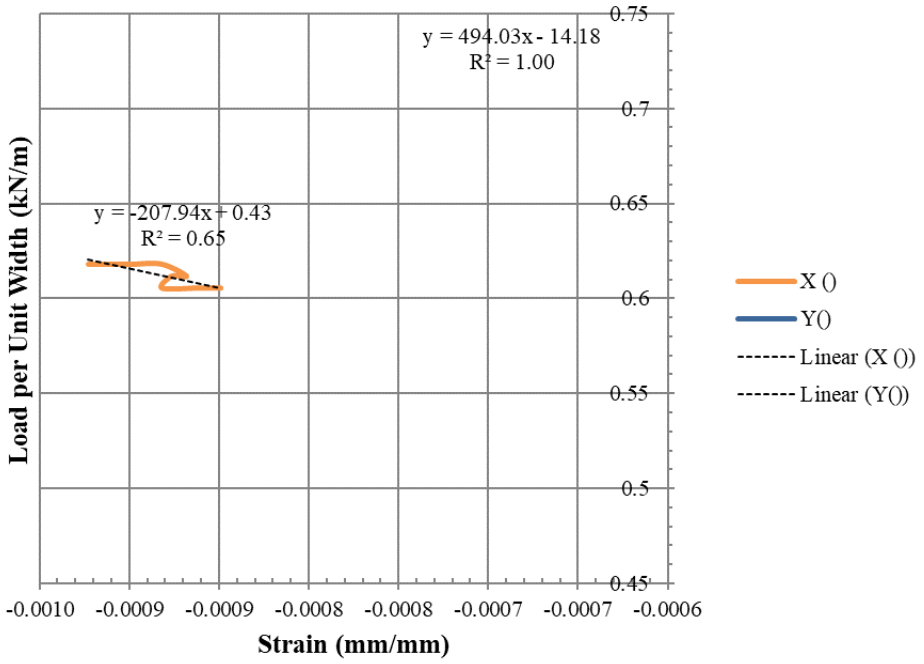

Figure 64 Mode 3 Test Results from Geogrid A, Zoomed in on Load Step 5 X-Direction

The pseudo modulus was used to calculate stress and strain values in the same way as for mode 1 loading. Since the level of permanent strain varied slightly, it was more convenient to examine the pseudo modulus plotted against load step instead of permanent strain. The pseudo modulus for mode 1 loadings on Geogrid A is plotted against load step and permanent strain in Figure 65 and Figure 66.

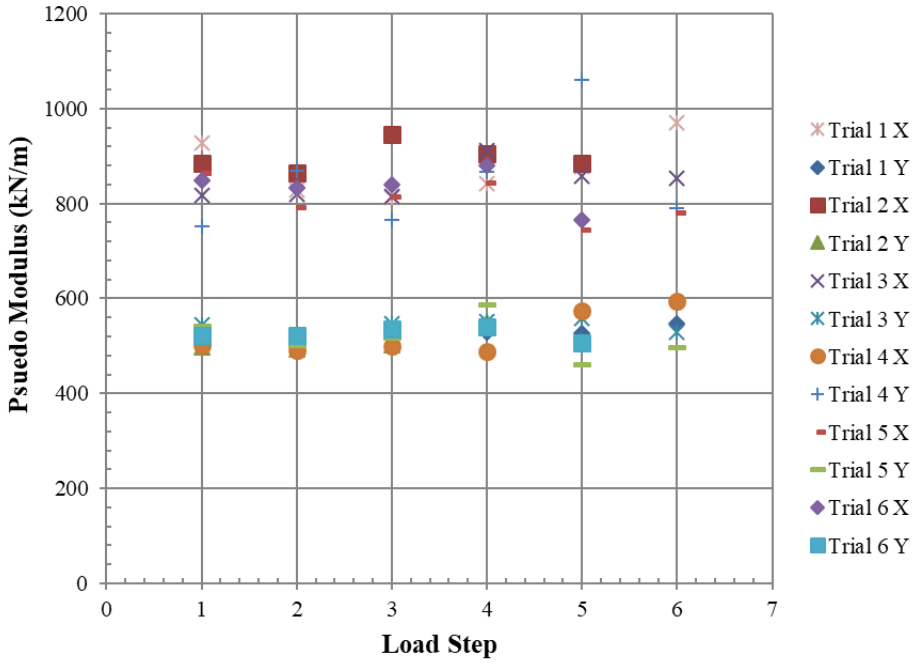

Figure 65 Pseudo Modulus vs. Load Step for Mode 1 Tests from Geogrid A

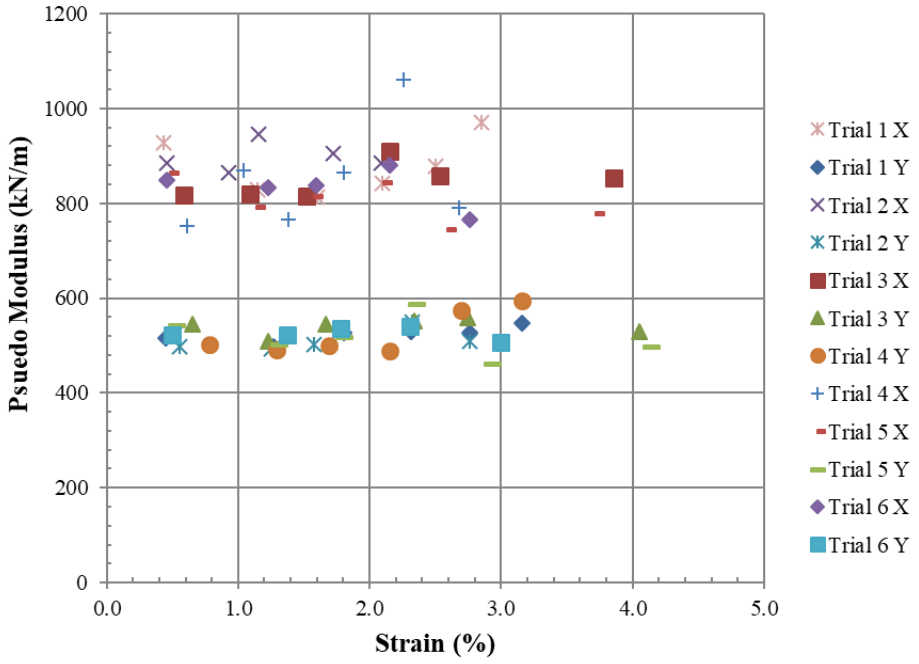

Figure 66 Pseudo Modulus vs. Strain for Mode 1 Tests from Geogrid A

The pseudo modulus remains relatively constant as permanent strain increases for Geogrid A. This matches the observations seen in the uniaxial testing program and Cuelho et al. (2005) where the modulus remained relatively constant with permanent strain for geogrids. The pseudo modulus for mode 2 and mode 3 loading on Geogrid A was also plotted against strain and load step as shown in Figure 67, Figure 68, Figure 69 and Figure 70.

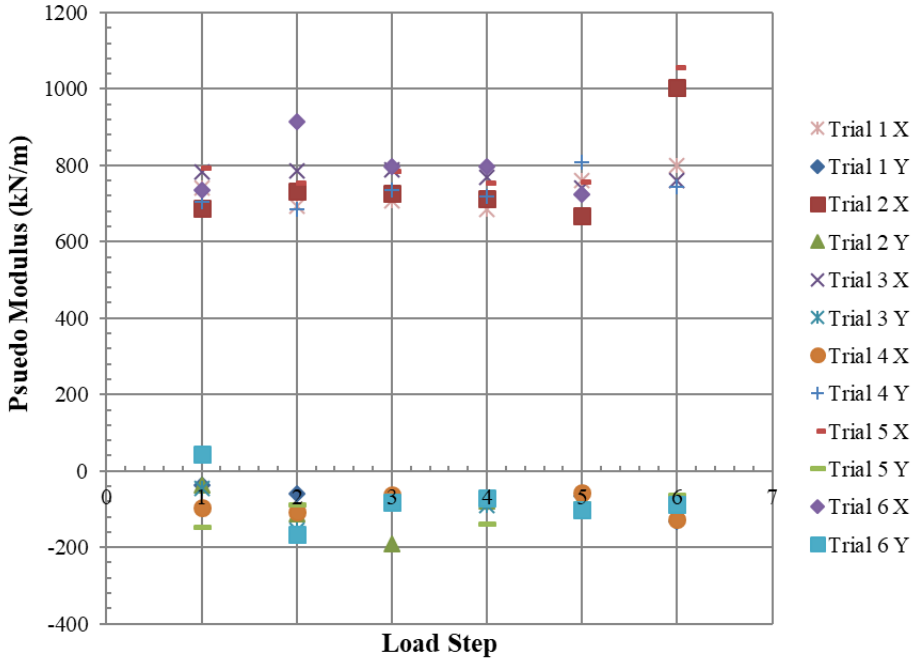

Figure 67 Pseudo Modulus vs. Load Step for Mode 2 Tests from Geogrid A

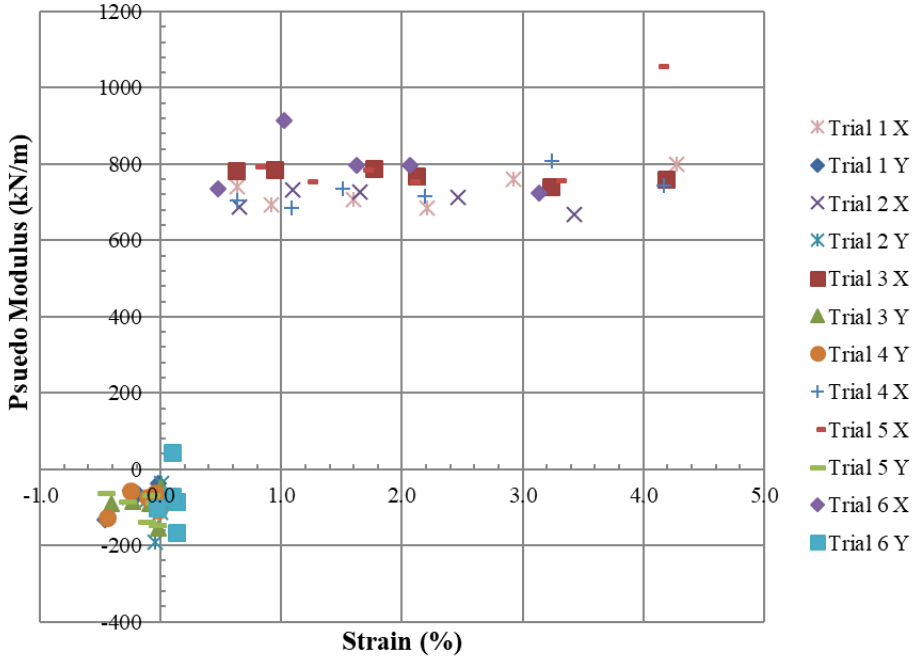

Figure 68 Pseudo Modulus vs. Strain for Mode 2 Tests from Geogrid A

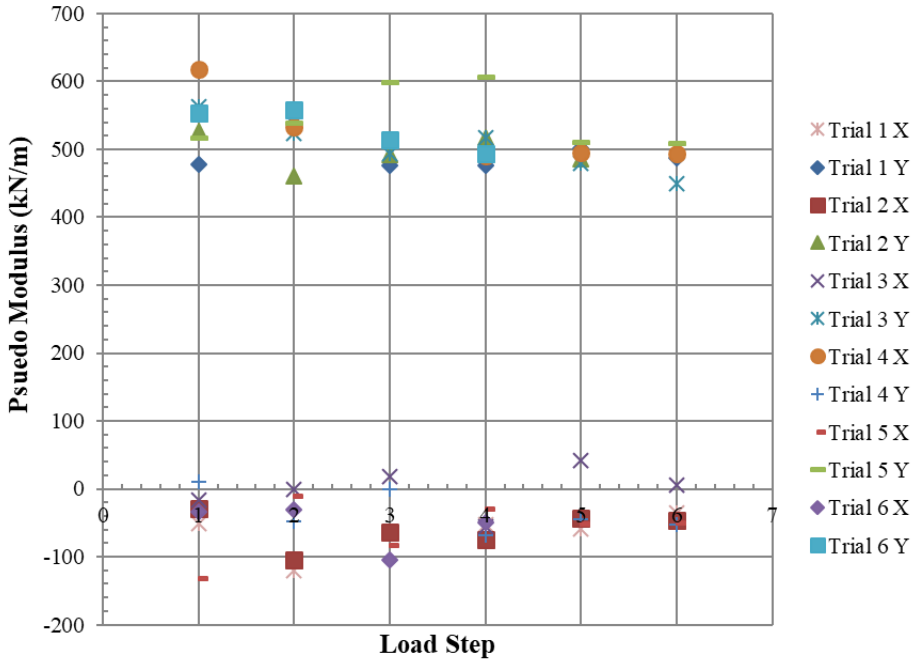

Figure 69 Pseudo Modulus vs. Load Step for Mode 3 Tests from Geogrid A

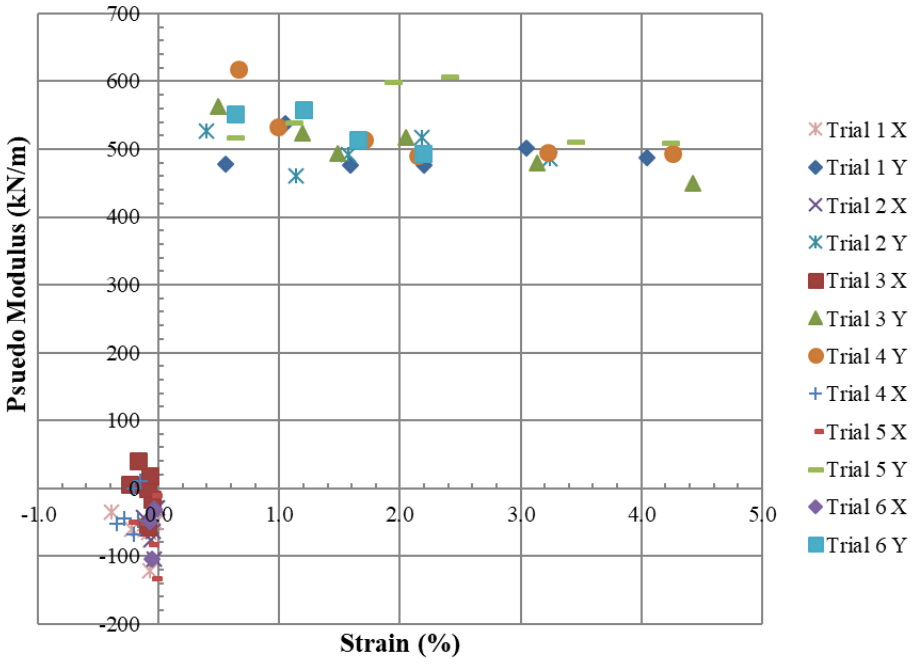

Figure 70 Pseudo Modulus vs. Strain for Mode 3 Tests from Geogrid A

Initially it was desired to use Section 8.3 from ASTM D7556 as a guideline to decide how many trials were necessary for each mode of loading and material. After performing 6 trials from all three modes on Geogrid A, it was discovered the biaxial testing procedure with the device used was not capable of satisfying this precision requirement. It was then decided to implement a less formal approach for the rest of the materials tested so that they could be tested within a reasonable timeline.

The number of trials for each mode of loading and each material (Table 29) was decided on a case by case basis based on the quality of data obtained. Load per unit width vs. strain and pseudo modulus plots were visually inspected to assess quality of the data. Pseudo modulus vs. load step plots (Figure 65, Figure 67 and Figure 69) were used to

identify outlier data, which was not used for the calculation of elastic constants. The outlier data eliminated for Geogrid A are shown in Table 31.

Table 31 Outlier Data for Geogrid A

Mode of Loading	Trial Number	Load Step
1	5	5, 6
1	4	1, 5
1	6	5
2	2	6
2	5	6
2	6	1, 2
3	3	5, 6
3	5	All

Elastic constants were calculated using the least squares technique described in the theory section of this report using the stress and strain data calculated from the pseudo modulus at each load step from all three modes of loading after outliers were removed. The least squares technique was used to minimize the stress terms or the strain terms to solve for the four elastic constants (modulus of elasticity in the XMD and MD and Poisson's ratio).

The least squares method relies on fitting the orthotropic linear elastic model to data from different modes of loading with an unequal number of trials performed. Having

a different number of trials for each mode of loading biases the results of the least squares regression to those modes with a higher number of trials, which undermines the goal of the method. To eliminate this bias, a single data set was created for each mode of loading and load step. This was accomplished by first taking an average of the pseudo modulus from all trials at each load step and for each mode of loading. The ratio of strain in the x-direction (1-direction) and strain in the y-direction (2-direction) was then taken for all trials at each load step and each mode of loading. The strain ratio was then averaged for all trials for each load step and mode of loading. This resulted in a single value for average strain ratio and average pseudo modulus for each load step and mode of loading. It was also recognized that if the stress/strain data used for calculation of elastic constants was not over an equal interval of stress or strain this would create a slight bias. The Japanese Testing Standard recommended that stress strain data over an equal load interval be used for the determination of elastic constants. For this thesis it was decided that using an equal strain interval of 0.2 % was appropriate because this is what was done for determination of uniaxial properties.

A stress-strain data set was created by assigning an arbitrary value of strain of 0.2 % to the strain value in the direction being loaded (x-direction for mode 1 (could also choose y-direction for mode 1), x-direction for mode 2, y-direction for mode 3). The strain in the other direction was then calculated based upon the average strain ratio for that given load step and mode of loading. The stress values were calculated using the average pseudo modulus multiplied by the strain for the given load step and mode of

loading. This then created a data set that contained just one value for stress and strain in both directions for each load step and mode of loading.

The elastic constants were then calculated using the stress and strain minimization techniques presented in the Theory section of this thesis with the results shown in Figure 71 and Figure 72. The XMD is denoted by the 1-direction and MD is denoted by the 2-direction. The results from wide-width cyclic tensile tests performed by Cuelho and Ganeshan (2004) are also shown on Figure 71 for reference. The tests performed by Cuelho and Ganeshan (2004) were performed in five load steps with permanent strain values of 0.5, 1.0, 1.5, 2.0 and 3.0 %. At each level of permanent strain 1000 cycles were performed with a magnitude of 0.2 % and at a strain rate of 16 % per minute (Cuelho, Ganeshan, 2004).

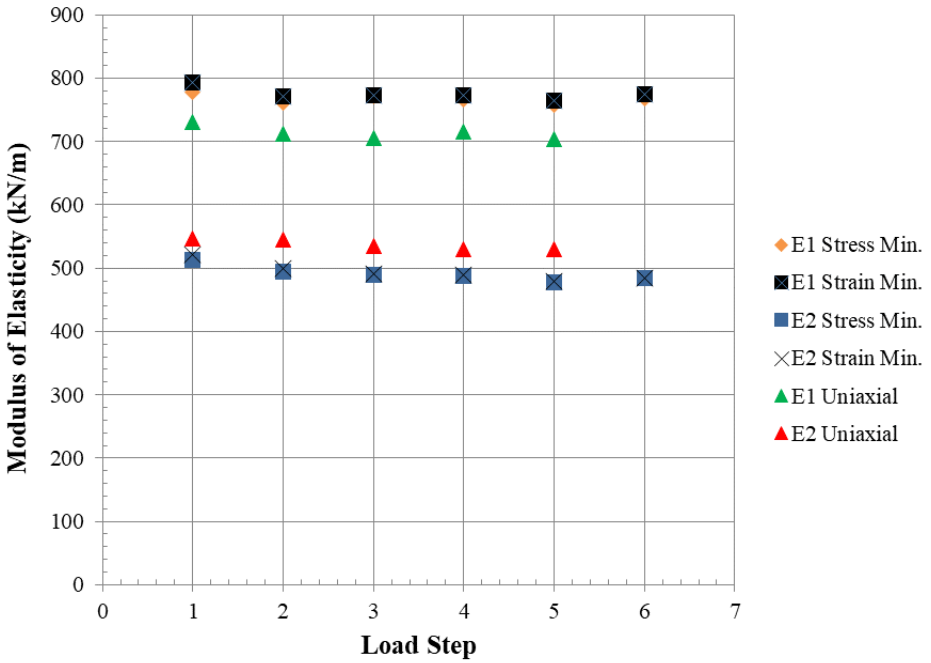

Figure 71 Modulus of Elasticity in Both Directions for Geogrid A by Load Step

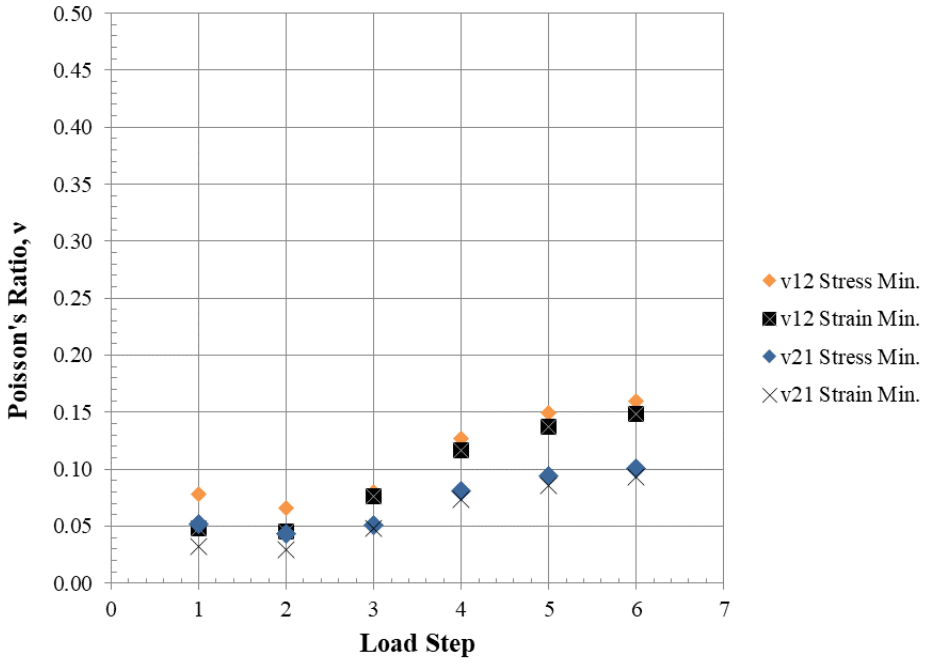

Figure 72 Poisson's Ratio in Both Directions for Geogrid A by Load Step

Observing Figure 71, the uniaxial modulus in the MD is slightly lower than the biaxial modulus, while the opposite is true for the XMD. It is important to remember that the biaxial modulus values are not expected to match the uniaxial values because they are from a different testing procedure with different cycle/hold times, strain rates and boundary conditions. The comparison between uniaxial and biaxial results was made only to confirm that the modulus of elasticity values being calculated from biaxial tests were reasonable. The increased stiffness observed in the XMD from biaxial tests in comparison to uniaxial could be due to the behavior of the junctions of geogrids under biaxial loading in comparison to uniaxial loading as discussed in the literature review and observed by McGown et al. (2004).

The Japanese Testing Standard states that both the stress and strain minimization are applicable for calculation of elastic constants. Both methods resulted in very similar values for modulus of elasticity as shown in Table 32 and Table 33, where the values from the two methods were averaged and an associated standard deviation and coefficient of variability was calculated. The values of Poisson's Ratio from stress and strain minimizations were compared in the same manner and had high coefficients of variability due to the low magnitude of Poisson's Ratio (Table 34 and Table 35). Previous research studies examined for this thesis only used one of the two methods, due to the fact that the Japanese Testing Standard states that either method is applicable. For this thesis, elastic constants were reported as an average of the two methods since there is no justification given in the Japanese Testing Standard to choose one over the other. All elastic constants reported in the remainder of this report will be an average of the values calculated using a stress and strain minimization.

Table 32 Average Modulus of Elasticity with respect to Load Step from Least Squares Stress and Strain Minimization for XMD of Geogrid A

Load Step	Average Modulus E_1 (kN/m)	Standard Deviation	Coefficient of Variability
1	786	11.18	1.42%
2	766	6.95	0.91%
3	772	1.47	0.19%
4	770	4.84	0.63%
5	761	5.42	0.71%
6	771	4.67	0.61%

Table 33 Average Modulus of Elasticity with respect to Load Step from Least Squares Stress and Strain Minimization for MD of Geogrid A

Load Step	Average Modulus E_2 (kN/m)	Standard Deviation	Coefficient of Variability
1	517	5.30	1.02%
2	496	3.66	0.74%
3	490	0.61	0.12%
4	489	1.29	0.26%
5	478	1.45	0.30%
6	484	0.79	0.16%

Table 34 Average Poisson's Ratio with respect to Load Step from Least Squares Stress and Strain Minimization for XMD-MD of Geogrid A

Load Step	Average Poisson's Ratio, v_{12}	Standard Deviation	Coefficient of Variability
1	0.063	0.021	33.31%
2	0.056	0.015	26.00%
3	0.078	0.003	3.80%
4	0.122	0.008	6.28%
5	0.143	0.009	6.26%
6	0.154	0.008	5.08%

Table 35 Average Poisson's Ratio with respect to Load Step from Least Squares Stress and Strain Minimization for MD-XMD of Geogrid A

Load Step	Average Poisson's Ratio, v_{21}	Standard Deviation	Coefficient of Variability
1	0.042	0.014	33.69%
2	0.036	0.009	26.16%
3	0.050	0.002	3.86%
4	0.077	0.005	6.63%
5	0.090	0.006	6.70%
6	0.097	0.005	5.55%

To examine how well the elastic constants fit the data measured from biaxial tension tests, the stress values in both direction were calculated using Equations (11) and (12) from the Theory section and shown again below. The stress values were calculated using the measured strain from biaxial tests and the elastic constants for each load step from Table 32, Table 33, Table 34 and Table 35. These calculated stress values were then compared to the measured stress values from biaxial tension tests. The calculated and measured stress values in both directions from all load steps for all trials from all three modes of loading after outliers were removed are shown on Figure 73.

$$\sigma_1 = \frac{E_1}{1-\nu_{12}\nu_{21}}\varepsilon_1 + \frac{\nu_{21}E_1}{1-\nu_{12}\nu_{21}}\varepsilon_2 \tag{11}$$

$$\sigma_2 = \frac{\nu_{12}E_2}{1-\nu_{12}\nu_{21}}\varepsilon_1 + \frac{E_2}{1-\nu_{12}\nu_{21}}\varepsilon_2 \tag{12}$$

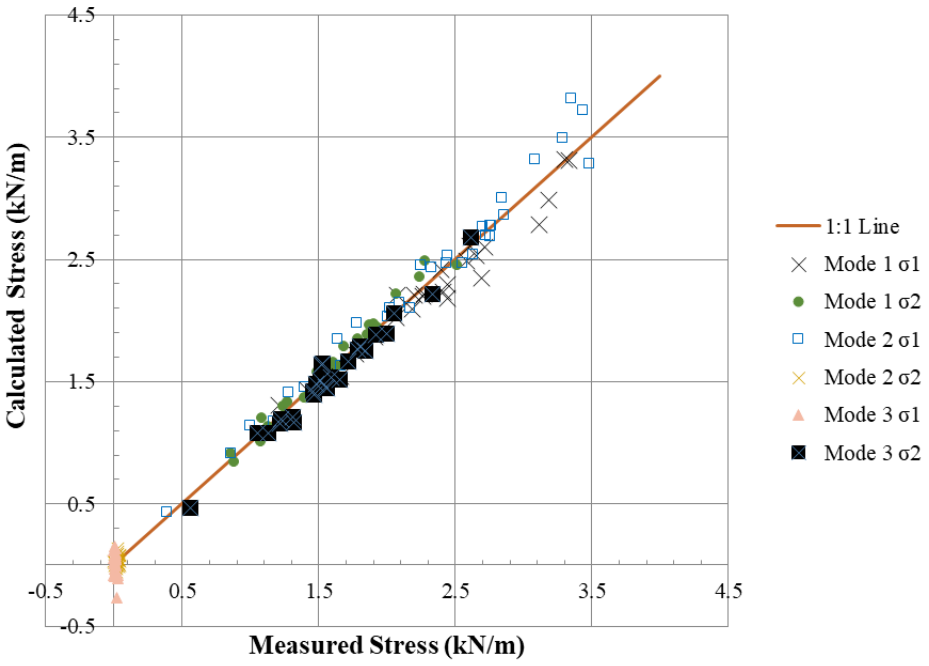

Figure 73 Comparision of Calculated and Measured Stress Values Using Elastic Constants for Each Load Step for Geogrid A

Using the measured and calculated stress values shown on Figure 73, a R^2 value was calculated to quantify how well the calculated stress values fit the measured stress values for each load step (Table 36).

Table 36 R^2 values for Fit of Calculated Stress Values to Measured Stress Values

Load Step	σ_1	σ_2
1	0.988	0.989
2	0.994	0.989
3	0.986	0.996
4	0.988	0.996
5	0.987	0.995
6	0.986	0.994

The comparison shown on Figure 73 with the associated R^2 values (Table 36), shows that the elastic constants used (Table 32, Table 33, Table 34 and Table 35) to describe the resilient response of Geogrid A fit the measured data. The direction with applied displacement (σ_1 and σ_2 for mode 1, σ_1 for mode 2 and σ_2 for mode 3) is described very well by the elastic constants as shown by how similar the calculated stress and measured stress values are on Figure 73. The direction with no applied displacement (σ_2 for mode 2 and σ_1 mode 3) has very low stress and strain values and the measured stress values were more variable than those in the direction being loaded. These low and more variable measured stress values lead to slightly larger differences between the calculated and measured stress values for σ_2 values from mode 2 and σ_1 values from mode 3 loading. Overall the high correlation between measured and calculated stress values (Table 36) combined with the fact that the modulus values are in the range of values calculated previously using uniaxial tests gives confidence to these values for elastic constants.

Observing Figure 71 and Figure 72, it was noted that the modulus of elasticity values appear to remain relatively constant with increasing levels of permanent strain (load step). This is encouraging as all previously calculated measures of stiffness for geogrids have shown little change in stiffness with increasing permanent strain. When examined closely, the modulus of elasticity in both directions does slightly decrease with load step (Table 32 and Table 33), while Poisson's Ratio slightly increases (Table 34 and Table 35). The slight decrease in modulus as permanent strain increases was also observed by Cuelho and Ganeshan (2004) for Geogrid A.

Since the elastic constants are relatively similar for all load steps examined, it was decided that it would be useful to also report a single set of elastic constants that could be used to describe the behavior of Geogrid A at all low levels of strain (0.5 – 4 %). To do this, the least squares method was then applied to all of the stress/strain data combined from each load step to calculate a single set of elastic constants. These values are plotted on Figure 74 and Figure 75 as a constant line in addition with the elastic constants plotted on Figure 71 and Figure 72 for comparison. The elastic constants calculated using the data from all load steps are shown in Table 37.

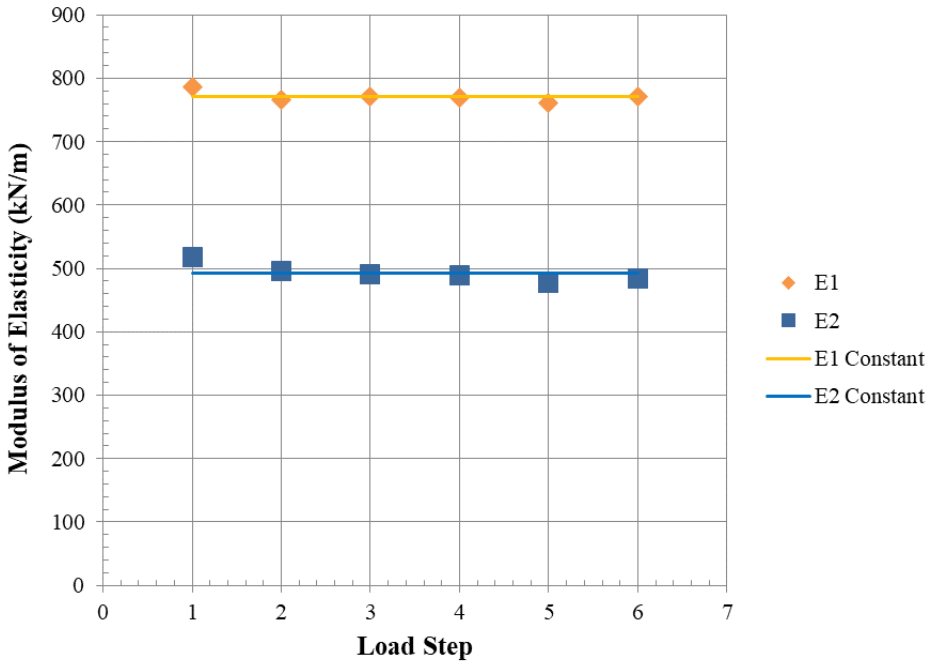

Figure 74 Modulus of Elasticity in Both Directions for Geogrid A

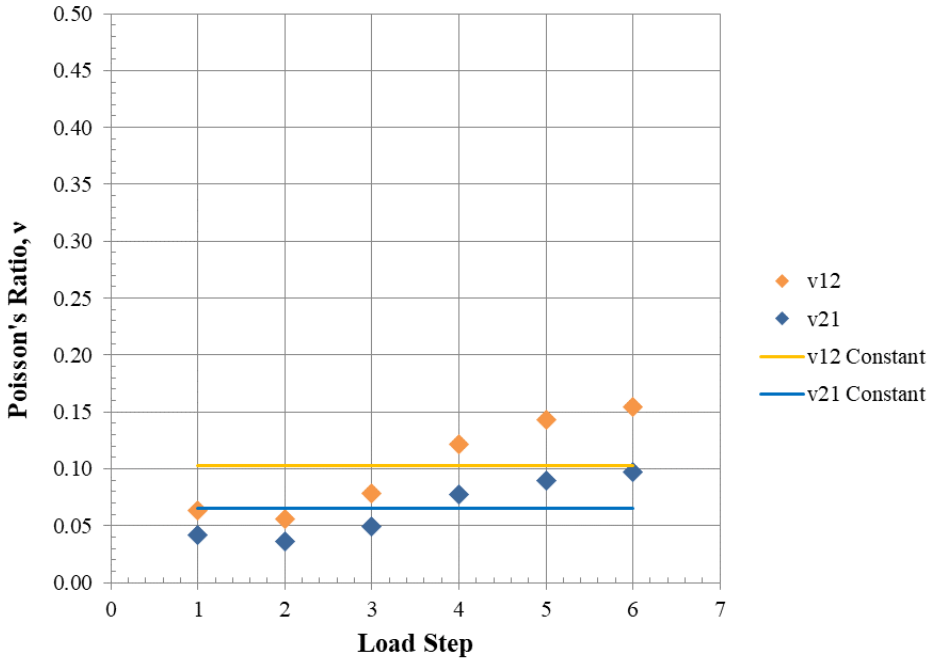

Figure 75 Poisson's Ratio in Both Directions for Geogrid A

Table 37 Elastic Constants for Geogrid A at Low Levels of Strain

Modulus of Elasticity	Modulus of Elasticity	Poisson's Ratio	Poisson's Ratio
E_1 (kN/m)	E_2 (kN/m)	ν_{12}	ν_{21}
771	493	0.103	0.066

The calculated and measured stresses were compared in the same manner as Figure 73 but using the elastic constants from Table 37 at all load steps. The comparison of calculated and measured stress values using a single set of elastic constants is shown in Figure 76.

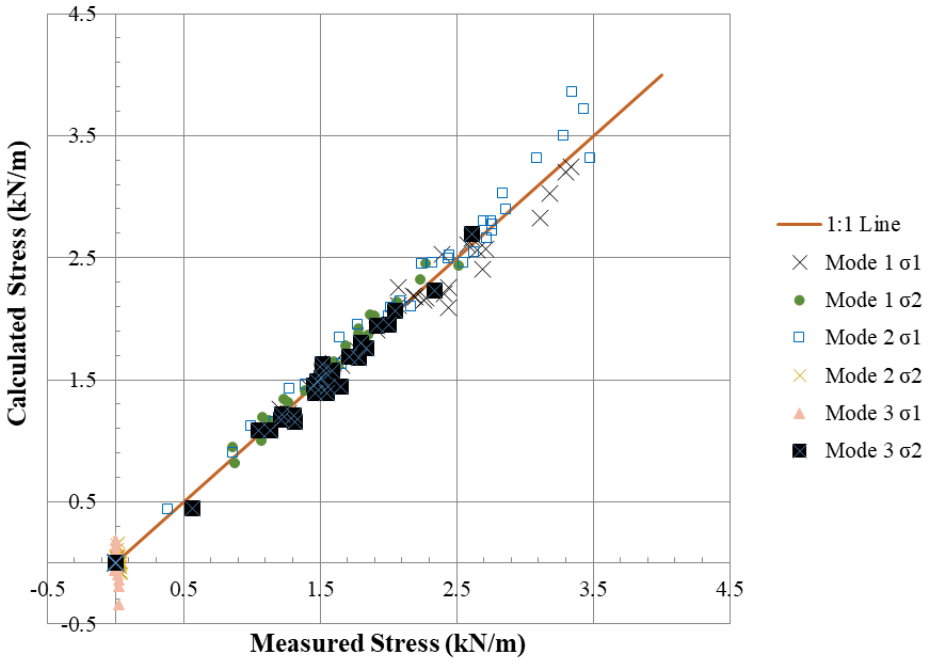

Figure 76 Comparision of Calculated and Measured Stress Values Using Single Set of Elastic Constants for Geogrid A

Using the measured and calculated stress values shown on Figure 76, a R^2 value was calculated for how well the calculated stress in both directions fit the measured stress. The R^2 values calculated were 0.987 and 0.992 for stress in the XMD and MD respectively. This indicates that the single set of elastic constants used to describe the resilient behavior of Geogrid A at low levels of strain fit the measured response well.

The same process as detailed for Geogrid A was carried out for all biaxial geogrids tested for this thesis. The elastic constants that resulted are shown on Figure 77, Figure 78, Figure 79, Figure 80 and Table 38 with the associated R^2 values. Elastic constants were not calculated for Geogrid G because the material behavior of this triaxial geogrid could not be fit to the constitutive model used to calculate elastic constants. The

testing of the triaxial geogrid is discussed in more detail in the recommendations for future testing section in chapter seven.

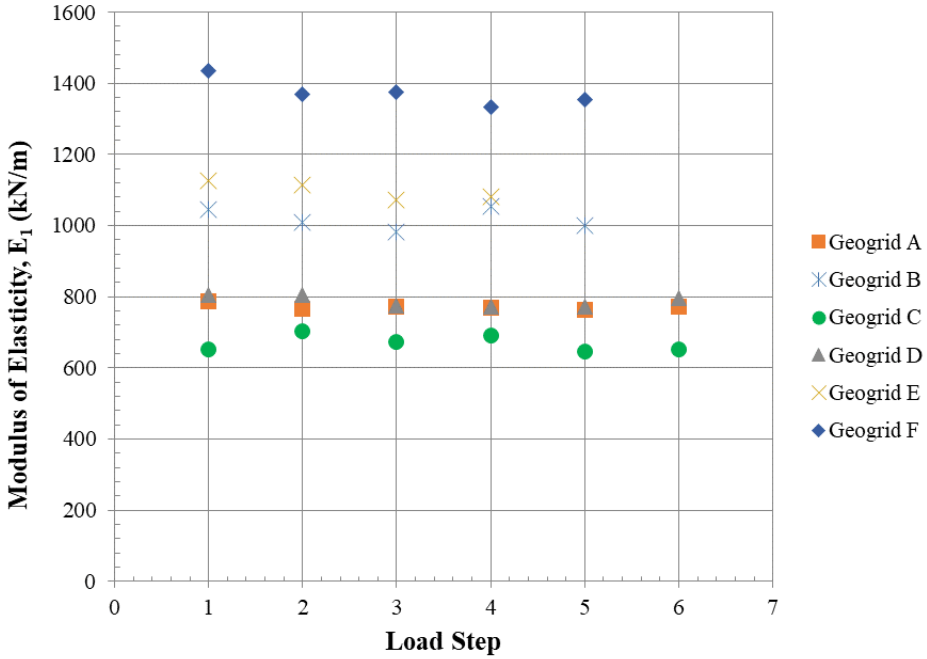

Figure 77 Modulus of Elasticity, E_1, vs. Load Step for All Geogrids

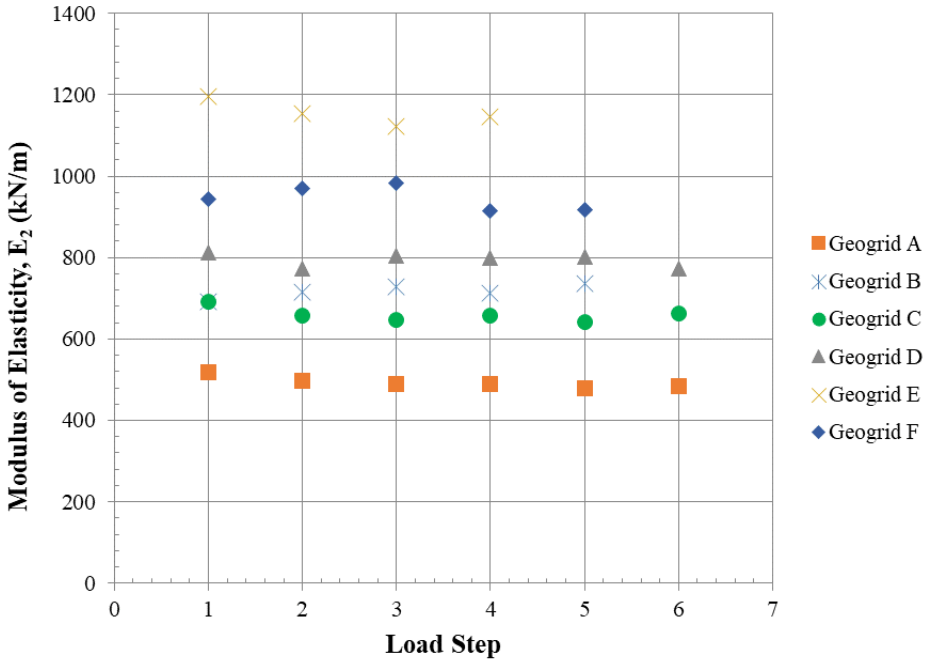

Figure 78 Modulus of Elasticity, E_2, vs. Load Step for All Geogrids

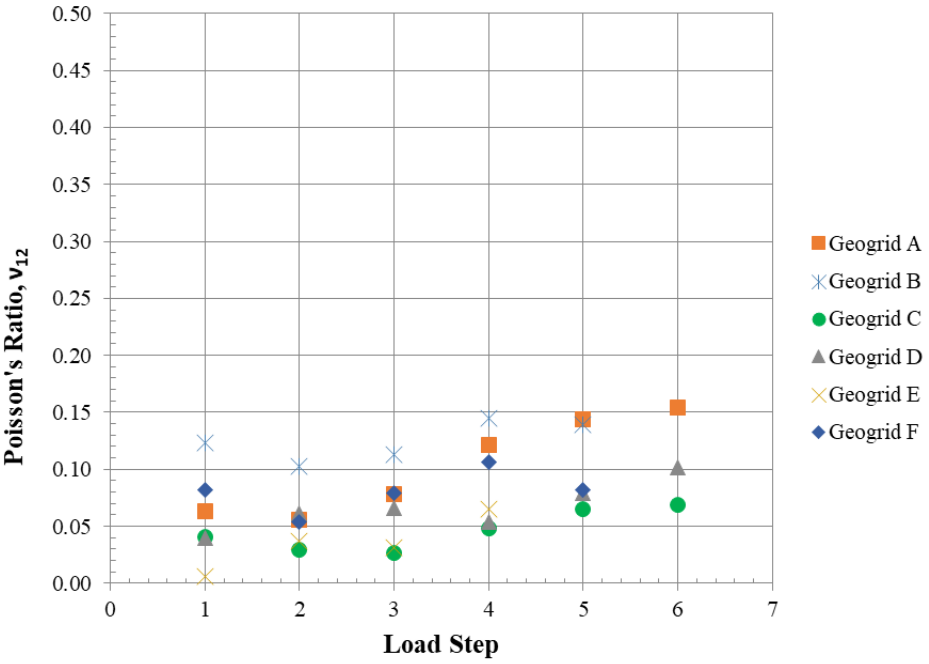

Figure 79 Poisson's Ratio, ν_{12}, vs. Load Step for All Geogrids

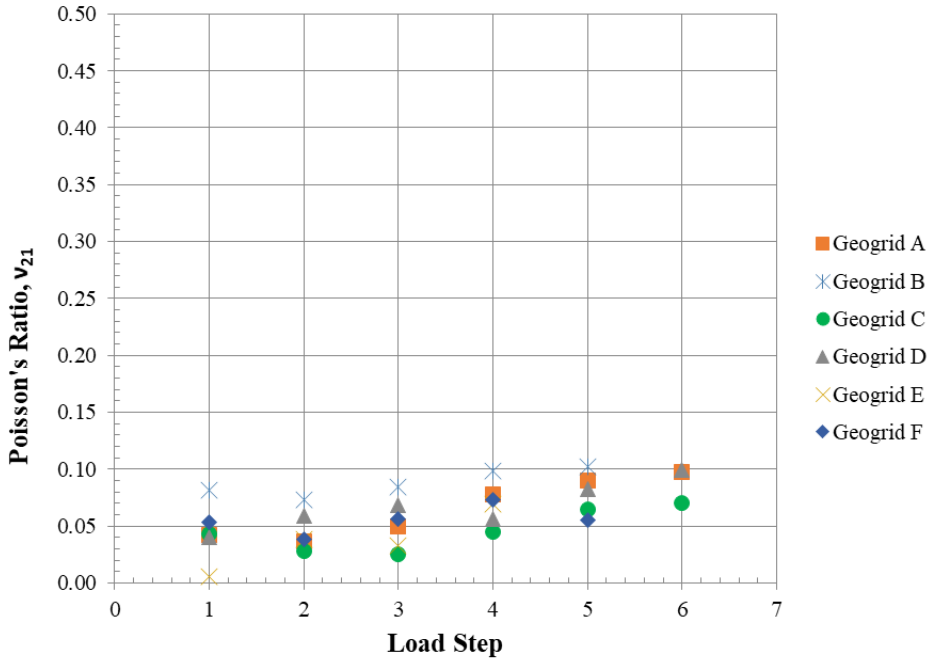

Figure 80 Poisson's Ratio, ν_{21}, vs. Load Step for All Geogrids

Table 38 Elastic Constants by Load Step for All Geogrids

Material	Biaxial Data					R^2		Uniaxial Data	
	Load Step	E_1 kN/m	E_2 kN/m	ν_{12}	ν_{21}	σ_1	σ_2	E_1 kN/m	E_2 kN/m
Geogrid A	1	786	517	0.063	0.042	0.988	0.989	730[1]	547[1]
	2	766	496	0.056	0.036	0.994	0.989	712[1]	545[1]
	3	772	490	0.078	0.050	0.986	0.996	705[1]	535[1]
	4	770	489	0.122	0.077	0.988	0.996	715[1]	530[1]
	5	761	478	0.143	0.090	0.987	0.995	703[1]	530[1]
	6	771	484	0.154	0.097	0.986	0.994		
Geogrid B	1	1045	690	0.124	0.082	0.984	0.989	1150[1]	860[1]
	2	1008	716	0.103	0.073	0.995	0.988	1095[1]	830[1]
	3	981	729	0.113	0.084	0.995	0.998	1085[1]	800[1]
	4	1055	711	0.145	0.098	0.985	0.996	1090[1]	805[1]
	5	1001	736	0.139	0.102	0.827	0.998	1085[1]	800[1]

	6	-	-	-	-	-	-		
Geogrid C	1	652	691	0.041	0.043	0.988	0.958		
	2	704	657	0.030	0.028	0.948	0.993		
	3	673	646	0.026	0.025	0.985	0.993		
	4	691	657	0.048	0.045	0.974	0.995	475[2]	450[2]
	5	646	641	0.065	0.065	0.996	0.999		
	6	651	664	0.068	0.070	0.996	0.993		
Geogrid D	1	804	811	0.0400	0.0404	0.987	0.992		
	2	805	773	0.061	0.059	0.989	0.986		
	3	776	803	0.066	0.068	0.983	0.982		
	4	772	799	0.054	0.056	0.986	0.990	565[2]	535[2]
	5	771	801	0.080	0.083	0.990	0.995		
	6	796	773	0.102	0.099	0.988	0.986		
Geogrid E	1	1125	1195	0.0056	0.0059	0.989	0.994		
	2	1113	1155	0.037	0.038	0.996	0.995		
	3	1073	1121	0.031	0.033	0.990	0.999		
	4	1081	1145	0.065	0.069	0.991	0.992	880[2]	810[2]
	5	-	-	-	-	-	-		
	6	-	-	-	-	-	-		
Geogrid F	1	1434	943	0.082	0.054	0.974	0.866		
	2	1369	969	0.054	0.038	0.974	0.769		
	3	1375	982	0.079	0.056	0.990	0.837		
	4	1334	916	0.106	0.073	0.988	0.858	980[2]	390[2]
	5	1355	918	0.082	0.055	0.957	0.889		
	6	-	-	-	-	-	-		

[1] Uniaxial Data From Cuelho and Ganeshan (2004) Cyclic Wide Width Tests
[2] Uniaxial Data From Valero et al. (2014) using ASTM D6637 Secant Modulus

The elastic constants for all geogrids fit the measured the data well as is seen in the high R^2 values. The elastic constants for all geogrids tested follow a very similar trend as Geogrid A with respect to having a modulus of elasticity in both directions that remains relatively constant with increasing permanent strain. For some geogrids examined the modulus of elasticity values decrease very slightly with load step, causing Poisson's ratio values to increase slightly with permanent strain, with Geogrid A showing

this trend most significantly. Poisson's ratio values for Geogrid E at load step 1 are an order of magnitude lower than those for other load steps for this material. To confirm that these low Poisson's ratio values are not a result of unreliable stress/strain data it would be desirable to conduct significantly more trials than was possible for this thesis. The biaxial values for modulus of elasticity were compared to uniaxial values when possible as shown in Table 38. The values from Cuelho and Ganeshan (2004) should be expected to be in the same range as biaxial values since these are both resilient values with fairly similar procedures. The values from Valero et al. (2014) however differ significantly from biaxial tests because these uniaxial values were calculated as a secant modulus at 2.0 % strain from a single stage monotonic loading. This highlights how misleading a secant modulus value can be if it is calculated over large strain intervals for geogrids that develop plastic strain and thus exhibit a nonlinear loading curve. This was examined by Cuelho and Ganeshan (2004) for Geogrid A in Figure 81. The nonlinear monotonic loading curve of geosynthetics has a large effect on the secant modulus with increasing permanent strain. This highlights the importance of calculating modulus values from initial loading over small intervals of strain where the loading curve is linear.

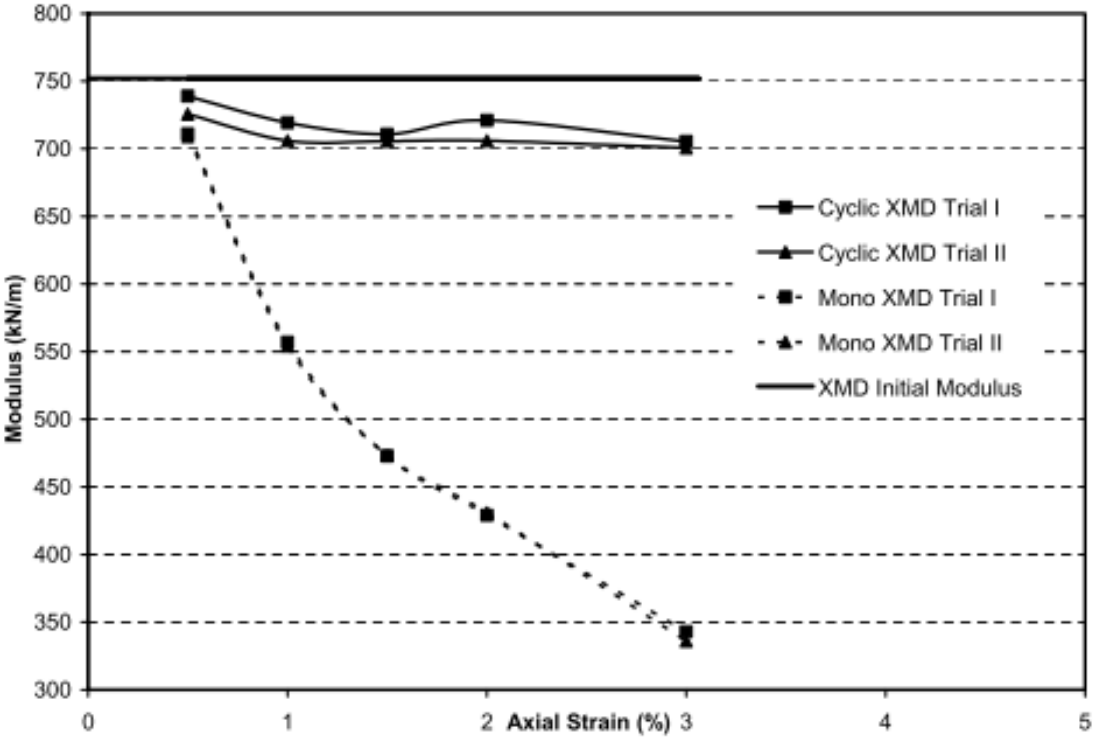

Figure 81 Modulus vs. Strain for Geogrid A from Different Types of Loading (Cuelho and Ganeshan, 2004)

Since the elastic constants only change slightly across the different load steps examined for the geogrids tested, a single set of elastic constants was also calculated for each geogrid to describe its resilient behavior at low levels of strain examined. These values are shown in Table 39.

Table 39 Elastic Constants for Low Levels of Strain for Geogrids

Material	Biaxial				R^2	
	E1 (kN/m)	E2 (kN/m)	ν12	ν21	σ1	σ2
Geogrid A	771	493	0.103	0.066	0.987	0.992
Geogrid B	1018	715	0.125	0.088	0.957	0.992
Geogrid C	670	659	0.0463	0.0456	0.980	0.990
Geogrid D	787	794	0.067	0.068	0.984	0.988
Geogrid E	1098	1155	0.033	0.035	0.991	0.989
Geogrid F	1373	946	0.081	0.056	0.976	0.849

The single set of elastic constants (Table 39) fit the measured data well and could be useful if constant values of elastic constants are desired to more broadly describe the elastic constants of geogrids at low levels of strain (0.5 % - 4.0 %).

In addition to the six geogrids tested biaxially, two woven geotextiles were also tested. The tests on woven geotextiles were performed using the same testing procedure and the data was analyzed in the same manner in order to generate elastic constants shown in Figure 82, Figure 83, Figure 84, Figure 85 and Table 40.

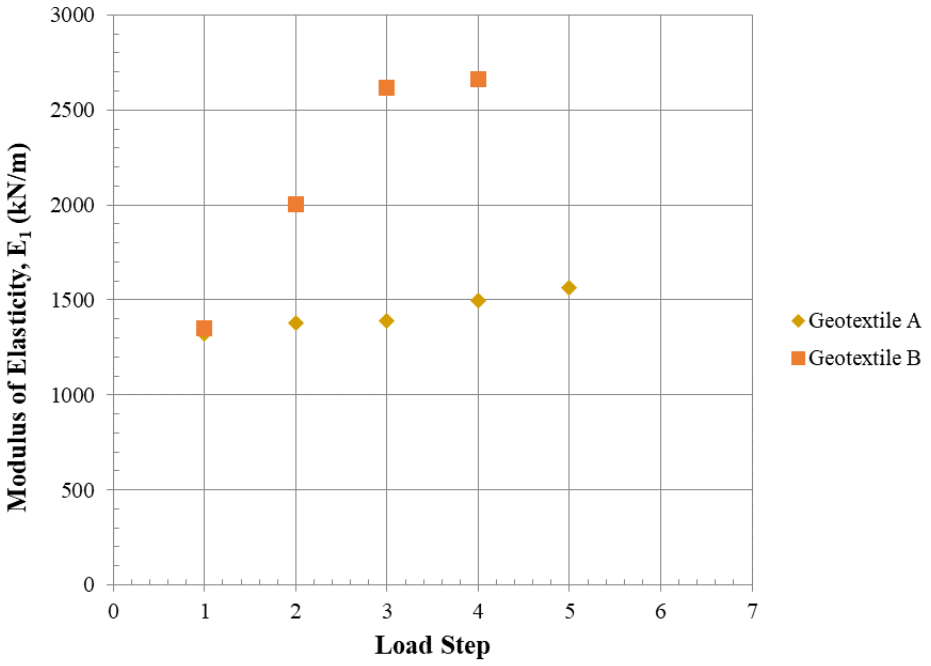

Figure 82 Modulus of Elasticity, E_1, vs. Load Step for All Geotextiles

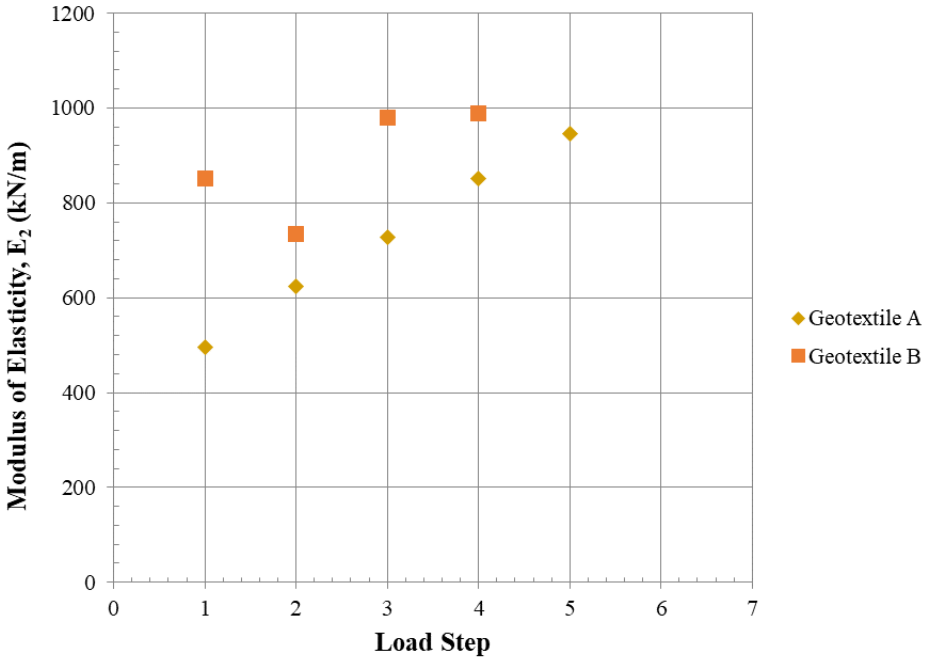

Figure 83 Modulus of Elasticity, E_2, vs. Load Step for All Geotextiles

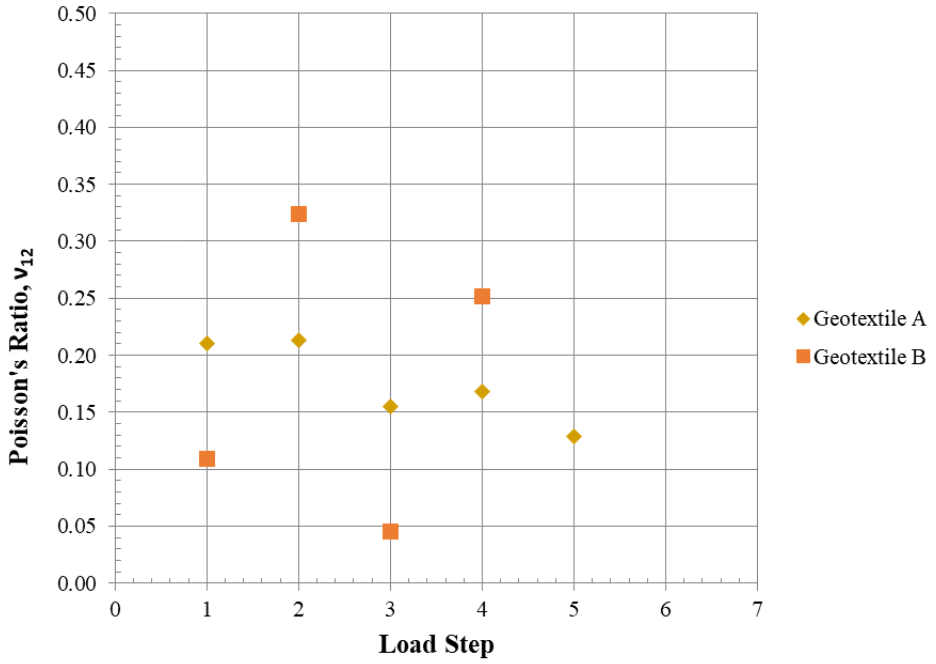

Figure 84 Poisson's Ratio, ν_{12}, vs. Load Step for All Geotextiles

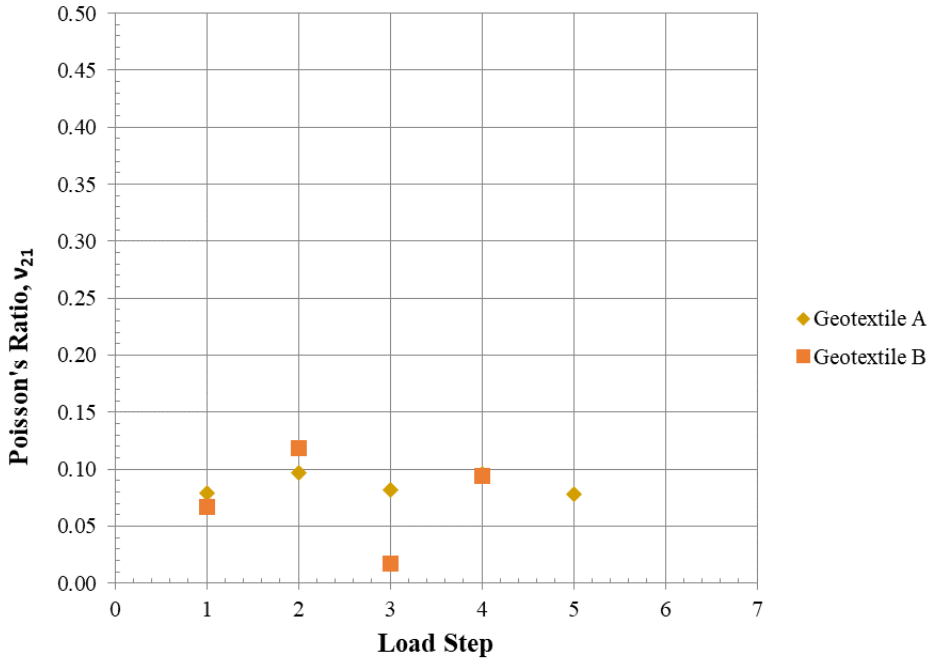

Figure 85 Poisson's Ratio, ν_{21}, vs. Load Step for All Geotextiles

Table 40 Elastic Constants by Load Step for All Geotextiles

Material	Biaxial Data					R^2		Uniaxial	
	Load Step	E1 kN/m	E2 kN/m	ν12	ν21	σ1	σ2	E1 kN/m	E2 kN/m
Geotextile A	1	1321	497	0.21	0.08	0.965	0.980		
	2	1381	624	0.21	0.10	0.958	0.955		
	3	1391	729	0.16	0.08	0.925	0.959		
	4	1497	852	0.17	0.10	0.823	0.975	875[1]	525[1]
	5	1567	946	0.13	0.08	0.549	0.953		
	6								
Geotextile B	1	1351	850	0.11	0.07	0.949	0.984	1114[2]	
	2	2003	734	0.32	0.12	0.944	0.995	1696[2]	
	3	2618	980	0.05	0.02	0.902	0.987	2001[2]	
	4	2660	988	0.25	0.09	0.482	0.997	2087[2]	
	5							2251[2]	
	6							2247[2]	

[1] From Manufacturer Technical Data Sheet, Secant Modulus from ASTM D4595
[2] From Uniaxial Testing Program Conducted for this Thesis

The elastic constants calculated for the two geotextiles tested fit the measured data well except for the final load step examined for both materials where low R^2 values were calculated. The Poisson's Ratio calculated for Geotextile B shows a complex response in comparison to that of the geogrids. The modulus of elasticity for the geotextiles increases with increasing permanent strain as was observed in the uniaxial testing program and by Cuelho et al. (2005). The modulus of elasticity values calculated from the biaxial data are higher than those calculated from uniaxial tests, but are in a similar range. This exemplifies the highly complex behavior of woven geotextiles and the interactions that occur between woven fibers under biaxial load/strain conditions. Although the geotextiles did not exhibit a constant stiffness with increasing load step, it

was still thought to be useful to have a single set of elastic constants that could be used to describe the behavior of the woven geotextiles at low levels of strain examined. The single set of elastic constants calculated for both woven geotextiles tested is shown in Table 41.

Table 41 Elastic Constants for Low Levels of Strain for Geotextiles

Material	Biaxial				R^2	
	E1 (kN/m)	E2 (kN/m)	ν12	ν21	σ1	σ2
Geotextile A	1438	752	0.163	0.085	0.873	0.757
Geotextile B	2225	883	0.191	0.076	0.554	0.937

CHAPTER SEVEN

SUMMARY AND RECOMMENDATIONS

Summary of Testing and Analysis

The uniaxial and biaxial testing programs implemented were successful in characterizing the resilient response of different geosynthetic materials. The uniaxial testing program was useful for creating a biaxial testing procedure on the experimental biaxial testing device available. The uniaxial results were able to show that the four different types of loading examined (cyclic stress relaxation, monotonic stress relaxation, cyclic creep and monotonic creep) simulated an equivalent resilient response on a biaxial geogrid and woven geotextile. The time to generate a representative resilient response in the lab with these four types of loading was shown to be relatively quick (20 minutes).

The biaxial testing procedure was developed using available literature, the uniaxial testing program results and considerations for the available biaxial testing device. The procedure used was able to generate data that fit an orthotropic linear elastic constitutive model that was used to calculate elastic constants for different geosynthetic materials. The elastic constants were successfully solved for using a least squares approximation for different geosynthetics. The elastic constants calculated using the least squares approximation were reasonable values based upon how well they fit the measured biaxial stress/strain data and their proximity to resilient uniaxial modulus values. The elastic constants calculated from biaxial tests are not expected to be identical to uniaxial values because the test conditions are different. Elastic constants calculated from biaxial

tests with an orthotropic linear elastic constitutive model provide a better representation of geosynthetic material properties than uniaxial tests because Poisson's ratio is included in the model. Thus, the elastic constants calculated are more applicable for predicting the stress/strain response of geosynthetics in field loading applications. The elastic constants were calculated from stress/strain data after stress relaxation and creep so that they can be used to describe a resilient response of geosynthetics expected in field loadings. The elastic constants were calculated from stress/strain data from three modes of loading and thus describe the response of geosynthetics in multiple field loading situations where geosynthetics experience simultaneous loading in both directions, or plane strain loading.

Recommendations for Future Testing

The uniaxial tests performed were modeled after an existing ASTM standard (D7556), and thus do not need significant modification or recommendations. The creep tests however do not have an existing standard and could be investigated further to confirm the conclusions drawn in this thesis. Due to time limitations, a robust uniaxial creep testing program was not possible for this thesis and thus a small number of trials were performed on only two materials. The creep properties of geosynthetics have been studied in the past but not in the same format as was investigated for this research. To examine the resilient response of geosynthetics after uniaxial creep, it is recommended that a procedure modeled after ASTM D7556 be developed and implemented on more materials with enough trials to determine if precision requirements in ASTM D7556 are met.

Ideally more trials on all materials tested biaxially would have been performed to try and quantify the precision of the data collected and what is possible with the given biaxial device. More trials performed on the geotextiles could have helped better understand the values of Poisson's ratio reported at different load steps. More trials on Geogrid E would also be helpful to confirm the very low Poisson's ratio values calculated for load step 1.

The biaxial tests on geosynthetics were modeled after the uniaxial testing program, ASTM D7556 and biaxial tension tests performed on structural membranes. The biaxial testing device used for this project was a relatively new testing device that had not been used for any formal testing programs or robust research previously. This created a lot of experimentation with the device in order to generate reasonably precise data that was useful for determining the material response of geosynthetics. Some improvements to the instrumentation and control of the device is necessary to generate data with higher precision. The LVDTs used to measure strain in the materials are accurate instruments, but attaching them to the geosynthetic at discrete points is not the best way to measure strain in the material. The setup of the LVDTs inherently introduces small amounts of human error that influence strain measurements between trials. It would beneficial to use video software to observe the strain of all nodes in the interior portion of the cruciform sample in order to generate a strain field. This type of approach would eliminate human error and save time associated with testing setup. The measurement of strain between discrete points also was problematic for the triaxial geogrid tested. The triaxial geogrid was tested in all three modes of biaxial loading using the developed

testing procedure. The data generated from testing the triaxial geogrid was very erratic and difficult to fit into the constitutive model. The data from the triaxial geogrid ultimately was not used for calculation of elastic constants due to the quality of the data. It was thought that the discrete measurement points of strain for the triaxial geogrid may have caused some the data to be confusing and if a strain field was calculated then a better representation of the material response could have been generated.

The mechanism through which the biaxial testing device created displacement in the material could also be improved on future biaxial testing devices. The electric motor was not ideal for loading materials because it is not technically creating a constant rate of strain for the initial loading of a material after stress relaxation or creep. This is due to the fact that the electric motor must accelerate to the desired speed before it operates at a constant speed. The same is true when the motor is turned off as it must decelerate before stopping. This deceleration causes difficulty in reaching the desired level of permanent strain precisely in the testing procedure used. The permanent strain limits used for biaxial tests were not precisely or consistently adhered to because of the human control of the displacement and the deceleration of the motor. A major improvement necessary for creating a more standardized testing procedure would be to setup the biaxial device so that a testing procedure with precise permanent strain limits could be programmed. An interface with feedback to the device control such as that on the uniaxial testing device would be ideal so that the strain limits are precisely followed. The measurement of load using load cells in the chains of the device was a smart way to design the biaxial testing device but caused some minor problems. The weight of the load cells in the chains and

the self-weight of the chain cause a slight sagging in the chain at low levels of load. The effect of this was not significant for this study because the data of interest was at loads corresponding to 0.5 % strain and above where the sagging is minimal. In the future, it may be desirable to measure load in all four directions if tests were performed on samples at a 45 degree orientation to confirm that the load is equal on both sides of a sample.

Another improvement that could be made on the biaxial testing device is the material gripping method. The material grips on the biaxial device did not cause any issues with the data collected but could be improved. The rigid plates that were bolted together to grip the material were very functional and cost-effective, but also required significant time for testing setup. The geosynthetic also had to be modified to fit in the grips for each testing sample and then manually centered in each grip. Eight bolts then had to be tightened on all four grips, ensuring the material stayed centered the entire time. This process was not difficult to perform but was much more time-intensive than using the gripping method available for the uniaxial testing device. A possible improvement to the biaxial testing device would be to have clamps more similar to those used in the uniaxial testing device.

Overall, the biaxial device used for this thesis was an adequate device designed in an intelligent and cost-effective manner for the testing of geosynthetics. However, the device in conjunction with the procedure developed and number of trials performed on each material was not able to produce the high quality, repeatable data that would be necessary to create a standardized testing procedure such as ASTM D7556. Some potential improvements could be made in the instrumentation for measuring strain and

controlling displacement. A photometric method for measuring strain would be recommended so that a strain field is generated instead of measuring strain at discrete points using LVDTs. A hydraulic loading mechanism that is controlled by a programmable procedure would eliminate the need for a human controlled procedure and a case by case analysis of data. This type of testing device would certainly be significantly more expensive but might be necessary for creating a biaxial testing procedure for simulating the resilient response of geosynthetics similar to the uniaxial ASTM D7556 testing procedure.

REFERENCES CITED

ASCE/SEI 55-10. (2010). Standard for Tensile Membrane Structures

ASTM D7556. (2010). Standard Test Methods for Determining Small-Strain Tensile Properties of Geogrids and Geotextiles by In-Air Cyclic Tension Tests.

ASTM D4595. (2015). Standard Test Method for Determining Tensile Properties of Geogrids by the Single or Multi-Rib Tensile Method.

ASTM D4439. (2017a). Standard Terminology for Geosynthetics.

ASTM D4595. (2017b). Standard Test Method for Tensile Properties of Geotextiles by the Wide-Width Strip Method.

Beccarelli, P. (2015). The Development of Biaxial Testing Devices and Procedures for Architectural Fabrics. In *Biaxial Testing for Fabrics and Foils: Optimizing Devices and Procedures* (pp. 73-118). Cham: Springer International Publishing.

Bridgens, B., & Gosling, P. (2003). *Biaxial fabric testing to determine in-situ material properties*. Paper presented at the Proceedings of the Int. Conf. on Structural Membranes.

Bridgens, B., & Gosling, P. (2004). *A new biaxial test protocol for architectural fabrics*. Paper presented at the IASS 2004 Symposium Montpellier: Shell and spatial structures from models to realisation.

Bridgens, B., & Gosling, P. (2010). *Interpretation of results from the MSAJ "testing method for elastic constants of membrane materials"*. Paper presented at the Tensinet symposium.

Chapra, S. C., & Canale, R. P. (1998). *Numerical methods for engineers* (Vol. 2): McGraw-Hill New York.

Checkland, P., Bull, T., & Bakker, E. (1958). A two-dimensional load-extension tester for fabrics and film. *Textile Research Journal, 28*(5), 399-403.

Cuelho, E. (1998). *Determination of Geosynthetic Constitutive Parameters and Soil/Geosynthetic Interaction by In-Air and In-Soil Experiments*. (Master of Science Master's), Montana State University, Bozeman, Montana.

Cuelho, E., & Ganeshan, S. (2004). Developing Test Protocols to Determine Geosynthetic Material Properties That Better Represent Traffic Loading Conditions. *Western Transportation Institute, Montana State University–Bozeman, USA*.

Cuelho, E., Perkins, S., & Ganeshan, S. (2005). Determining geosynthetic material properties pertinent to reinforced pavement design. In *Advances in Pavement Engineering* (pp. 1-12).

Haas, R., & Dietzius, A. (1913). *Stoffdehnung und Formänderung der Hülle von Prall-Luftschiffen*: Springer.

Hangen, Detert, & Alexiew. (2008). BIAXIAL TESTING OF GEOGRIDS: RECENT DEVELOPMENTS. *EUROGEO, 4*.

Klein, W. G. (1959). Stress-Strain Response of Fabrics Under Two-Dimensional Loading: Part I: The RL Biaxial Tester. *Textile Research Journal, 29*(10), 816-821.

Koerner, R. M. (2012). *Designing with Geosynthetics - 6Th Edition*: Xlibris US.

Krause, D. L., & Bartolotta, P. A. (2001). Biaxial Testing of High-Strength Fabric Improves Design of Inflatable Radar Domes.

Kupec, J., & McGown, A. (2004). The Biaxial load-strain behaviour of Biaxial Geogrids. *Geoasia04*.

McGown, A., Kupec, J., Heerten, G., & Voskamp, W. (2004). Current Approaches to the Determination of the Design Stiffness and Strength of Polymeric Biaxial Geogrids. *Vorträge der Baugrundtagung*, 123-130.

MSAJ. (1995). Testing Method for Elastic Constants of Membrane Materials. In (Vol. (MSAJ/M-02-1995), pp. 28). Toranomon, Minatoku, Toyko, Japan: The Membrane Structures Association of Japan.

Perkins, S. (2000). Constitutive modeling of geosynthetics. *Geotextiles and Geomembranes, 18*(5), 273-292.

Reichardt, C., Woo, H., & Montgomery, D. (1953). A two-dimensional load-extension tester for woven fabrics. *Textile Research Journal, 23*(6), 424-428.

Valero, S. N., Sprague, C. J., & Wrigley, N. E. (2014). *Full Scale Trafficking of Geogrid Reinforced Sections Under Realisitic Service Conditions*. Paper presented at the International Conference on Geosynthetics, Berlin, Germany.

Van Craenenbroeck, M., Puystiens, S., De Laet, L., Van Hemelrijck, D., & Mollaert, M. (2015). *Biaxial testing of fabric materials and deriving their material properties–A quantitative study*. Paper presented at the Proceedings of the International Association for Shell and Spatial structures (IASS) symposium.

APPENDICES

APPENDIX A

NONLINEAR LEAST SQUARES APPROXIMATION FOR SOLVING ELASTIC CONSTANTS

As discussed in the Theory section of this thesis, a nonlinear least squares approach was also used to calculate the elastic constants for a given data set of stress and strain values from biaxial tension tests. The nonlinear least squares approximation technique is an iterative process that was programmed using MATLAB. The technique is outlined in Chapra and Canale (1998) for approximation functions that have a nonlinear dependence on their parameters such as the approximation function shown by Equation (33).

$$f(x) = a_0(1 - e^{-a_1 x}) \tag{33}$$

In order to solve for the parameters (a_0, a_1) in the approximating function matrices must be setup as shown in Equation (34). Where [Z] is the matrix of partial derivatives of the function with respect to the parameters a_0 and a_1 (Equation(35)), [D] is a matrix calculated as the difference between the measurements (data) and the function values (Equation (36)) and [ΔA] is the changes in the parameter values (Equation 30).

$$\{D\} = [Z_j]\{\Delta A\} \tag{34}$$

$$[Z_j] = \begin{bmatrix} \frac{\partial f_1}{\partial a_0} & \frac{\partial f_1}{\partial a_1} \\ \frac{\partial f_2}{\partial a_0} & \frac{\partial f_2}{\partial a_1} \\ \frac{\partial f_n}{\partial a_0} & \frac{\partial f_n}{\partial a_1} \end{bmatrix} \tag{35}$$

$$\{D\} = \begin{Bmatrix} y_1 - f(x_1) \\ y_2 - f(x_2) \\ y_n - f(x_n) \end{Bmatrix} \tag{36}$$

$$\{\Delta A\} = \begin{Bmatrix} \Delta a_0 \\ \Delta a_1 \\ \Delta a_m \end{Bmatrix} \tag{37}$$

The nonlinear approach is used to solve [ΔA] using Equation (38). The unknown parameters are then updated using the [ΔA] values and the process is performed iteratively until [ΔA] is sufficiently small, thus the solution has converged.

$$\left[[Z_j]^T[Z_j]\right]\{\Delta A\} = \left\{[Z_j]^T\{D\}\right\} \tag{38}$$

Applying the nonlinear least squares approach to a stress and strain data set from biaxial tension tests is setup as follows. The nonlinear approach was only performed as a stress minimization since this resulted in the same values of elastic constants as the linear least squares stress minimization. The approximation functions used for stress are taken as Equations (11) and (12), where the approximating functions are related nonlinearly to the parameters (E_1, E_2, ν_{12}). The two Poisson's Ratio terms (ν_{12} and ν_{21}) can be related via the reciprocal constraint (Equation (9)).

$$\sigma_1 = \frac{E_1}{1-\nu_{12}\nu_{21}}\varepsilon_1 + \frac{\nu_{21}E_2}{1-\nu_{12}\nu_{21}}\varepsilon_2 \tag{11}$$

$$\sigma_2 = \frac{\nu_{21}E_2}{1-\nu_{12}\nu_{21}}\varepsilon_1 + \frac{E_2}{1-\nu_{12}\nu_{21}}\varepsilon_2 \tag{12}$$

The [Z] matrix is then setup by taking the partial derivatives of Equations (11) and (12) with respect to the parameters (E_1, E_2, ν_{12}). The [Z] matrix shown by Equation (39) will have n number of rows where n is the number of data points.

$$[Z] = \begin{bmatrix} \frac{\partial \sigma_1}{\partial E_1} & \frac{\partial \sigma_1}{\partial E_2} & \frac{\partial \sigma_1}{\partial \nu_{12}} \\ \frac{\partial \sigma_2}{\partial E_1} & \frac{\partial \sigma_2}{\partial E_2} & \frac{\partial \sigma_2}{\partial \nu_{12}} \end{bmatrix} \tag{39}$$

The [D] matrix then is the difference between the approximating function values ($\sigma_{1,\text{Calculated}}$) and the data values ($\sigma_{1,\text{Data}}$) for stress.

$$\{D\} = \begin{Bmatrix} \sigma_{1,\text{Calculated}} - \sigma_{1,\text{Data}} \\ \sigma_{2,\text{Calculated}} - \sigma_{2,\text{Data}} \end{Bmatrix} \quad (40)$$

The [ΔA] matrix is then solved using Equation (38). The parameter values are updated from the initial guess values using the [ΔA] matrix such that the process can be continued iteratively until [ΔA] is sufficiently small meaning the solution has converged on the "best fit" values for the elastic constants.

$$E_1 = E_1 + \Delta A(1)$$

$$E_2 = E_2 + \Delta A(2)$$

$$\nu_{12} = \nu_{12} + \Delta A(3)$$

The computer program MATLAB has a built-in function for solving nonlinear least squares problems. The "lsqnonlin" function in MATLAB can be used to solve nonlinear least-squares (nonlinear data-fitting) problems (MathWorks). The MATLAB function also requires an initial guess so that an iterative approach can be started. One potential advantage of this approach is that bounds can be imposed on the unknowns (elastic constants). This built-in function was also used for a stress minimization approach and resulted in the same values for elastic constants as the linear and nonlinear approaches.

APPENDIX B

LOAD PER UNIT WIDTH VS. STRAIN PLOTS FOR BIAXIAL TESTS

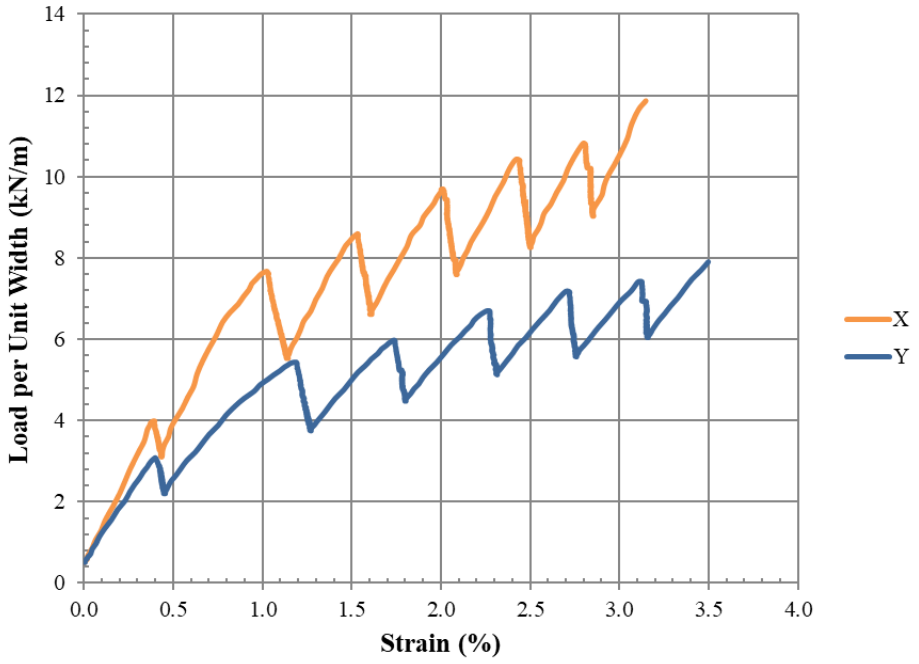

Figure 86 Geogrid A Mode 1 Trial 1

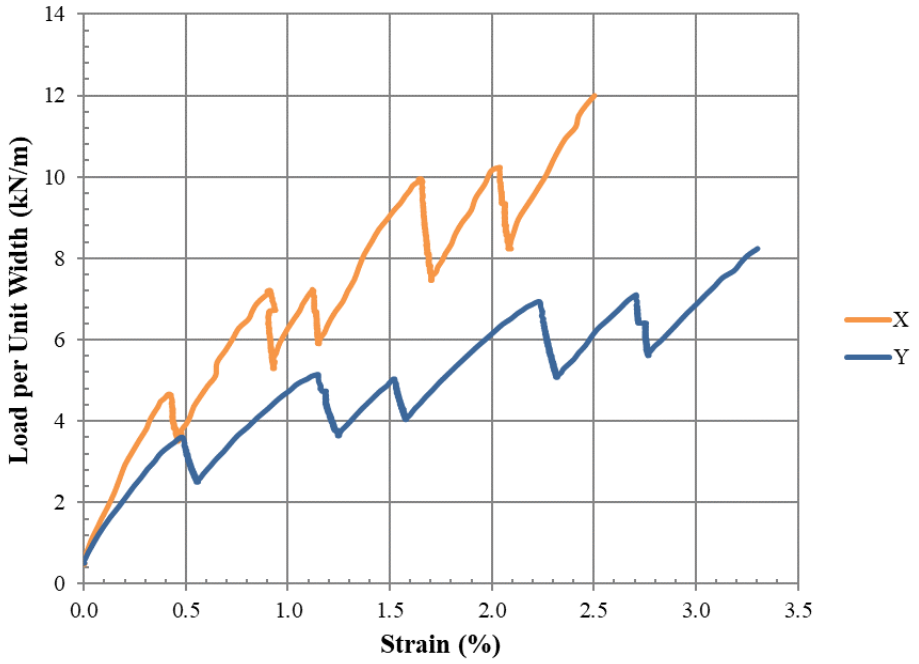

Figure 87 Geogrid A Mode 1 Trial 2

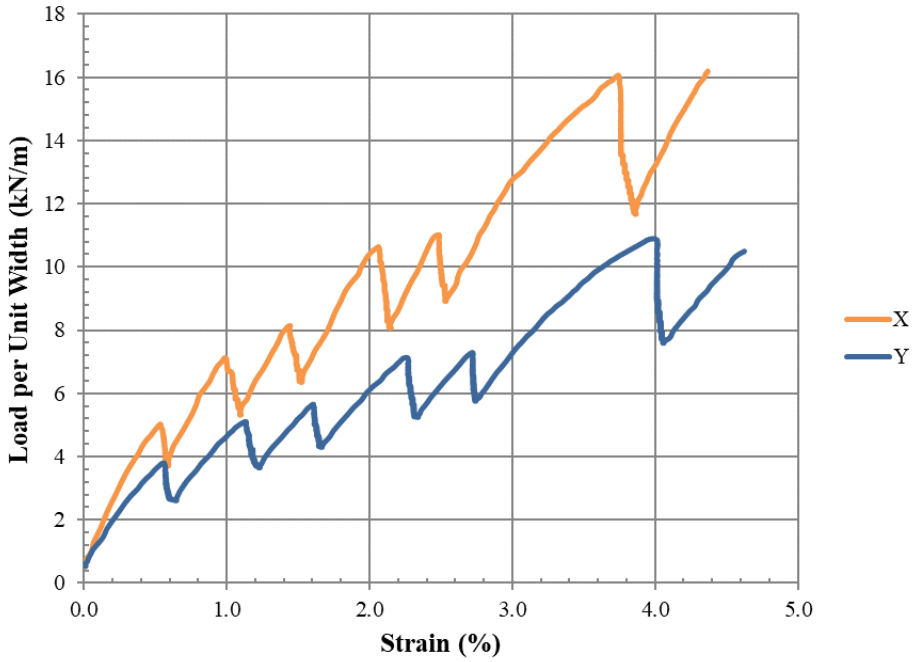

Figure 88 Geogrid A Mode 1 Trial 3

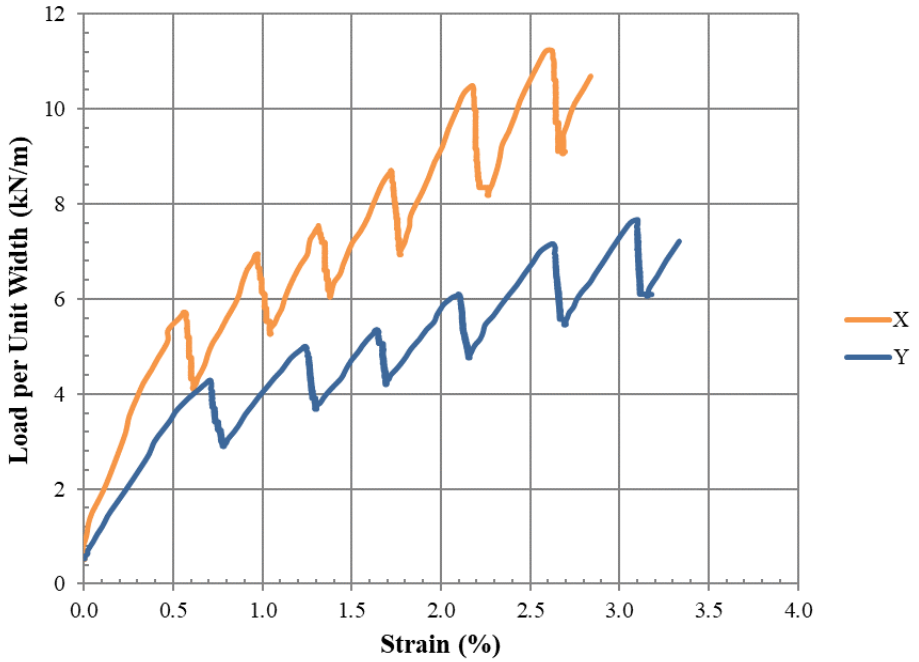

Figure 89 Geogrid A Mode 1 Trial 4

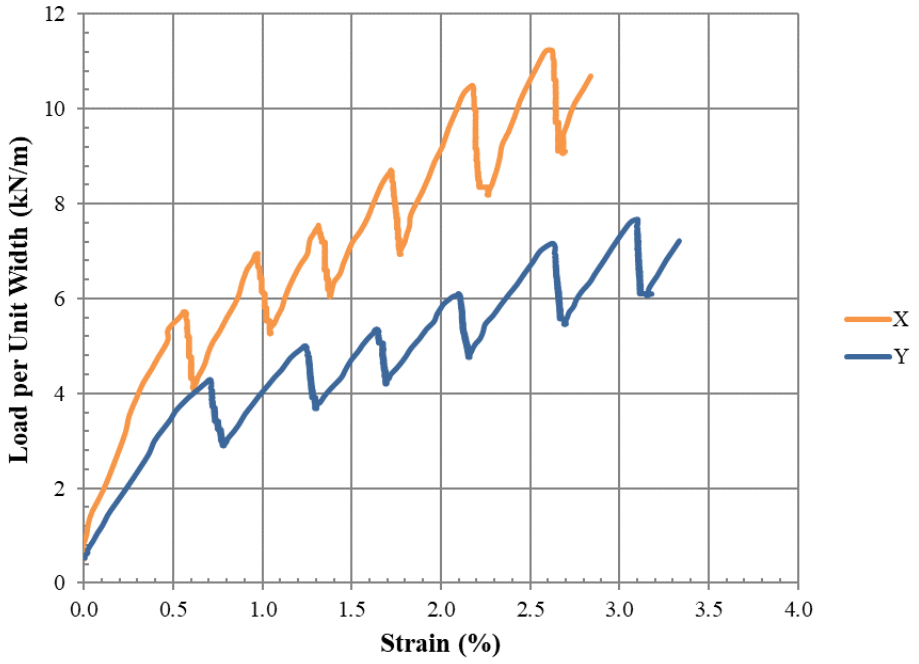

Figure 90 Geogrid A Mode 1 Trial 5

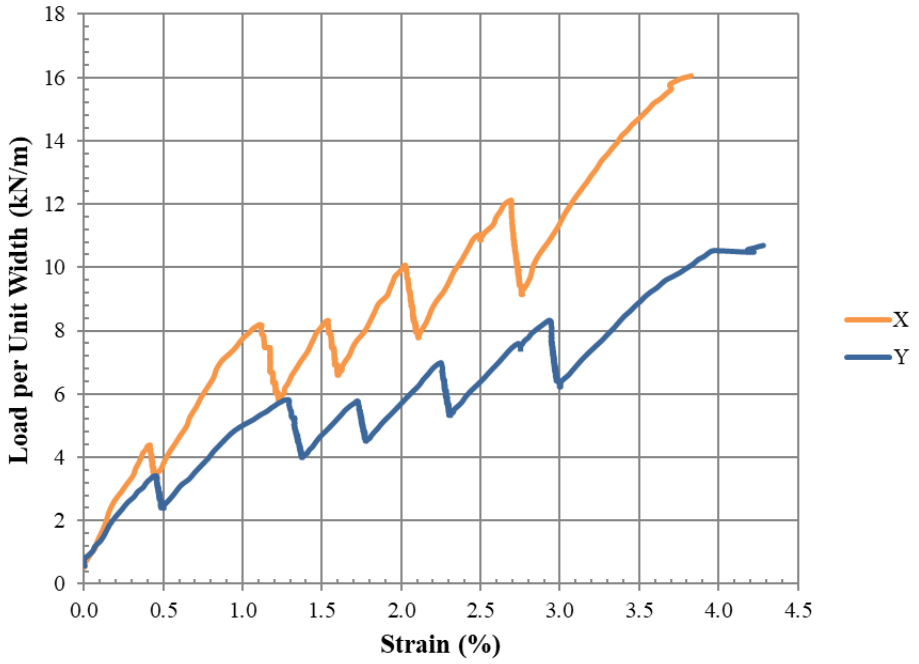

Figure 91 Geogrid A Mode 1 Trial 6

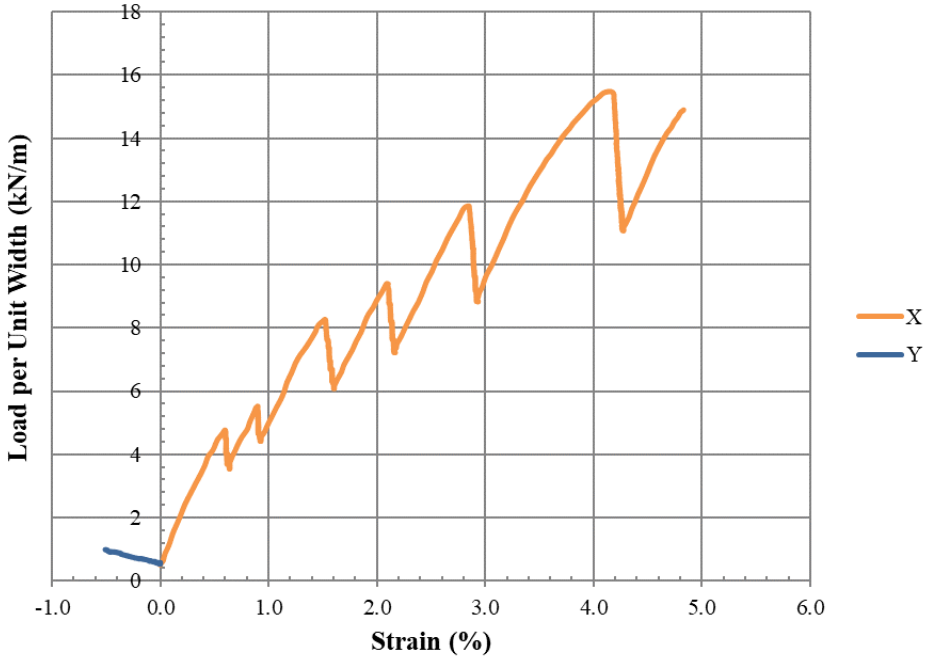

Figure 92 Geogrid A Mode 2 Trial 1

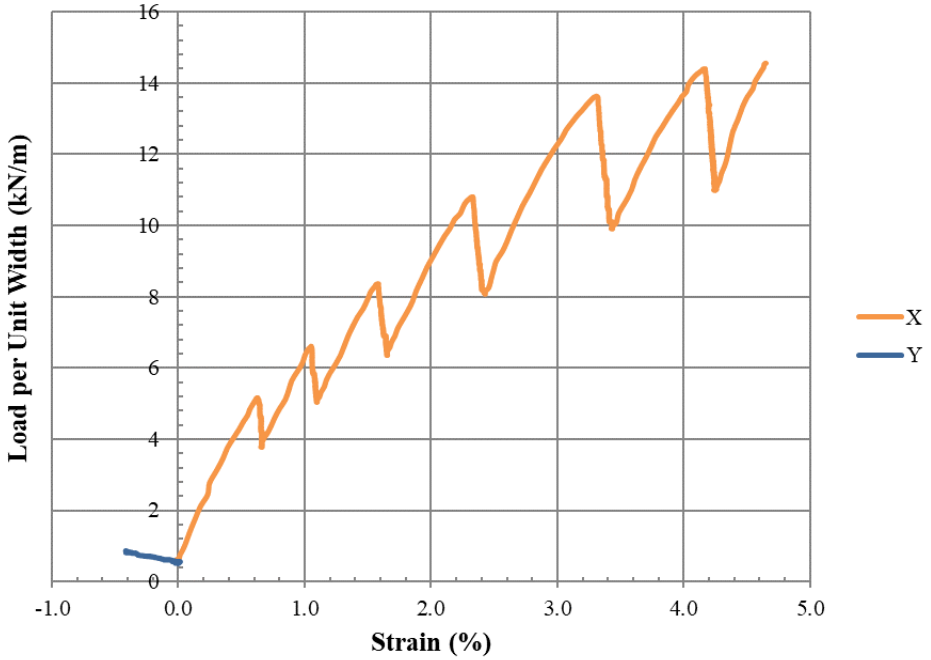

Figure 93 Geogrid A Mode 2 Trial 2

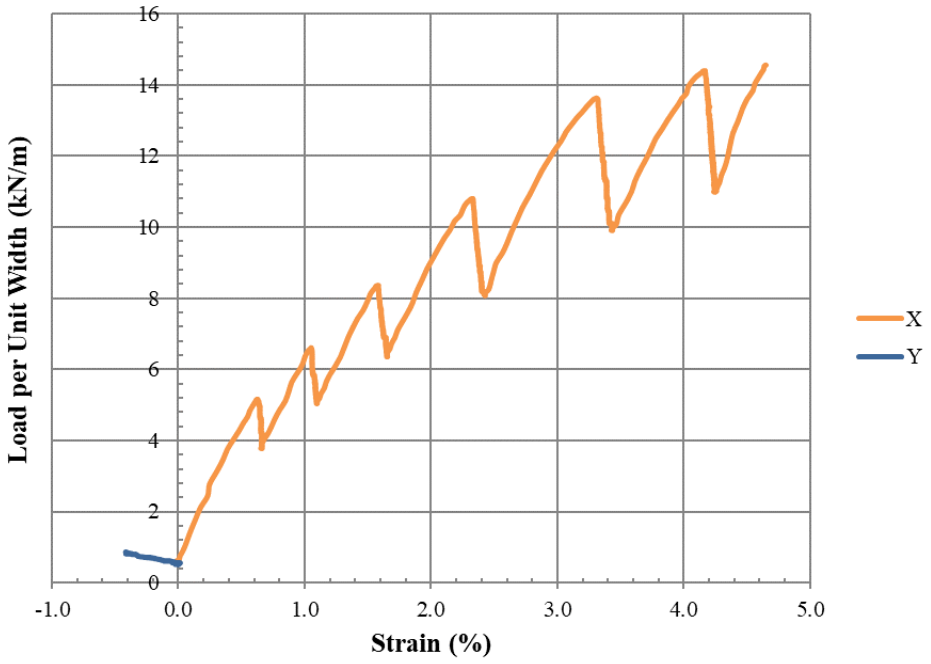

Figure 94 Geogrid A Mode 2 Trial 3

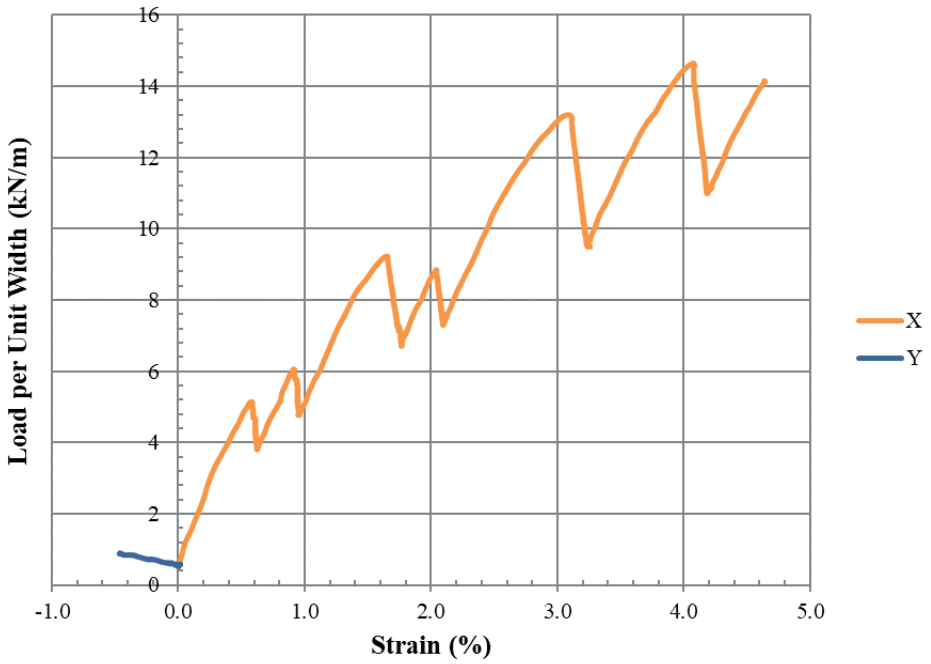

Figure 95 Geogrid A Mode 2 Trial 4

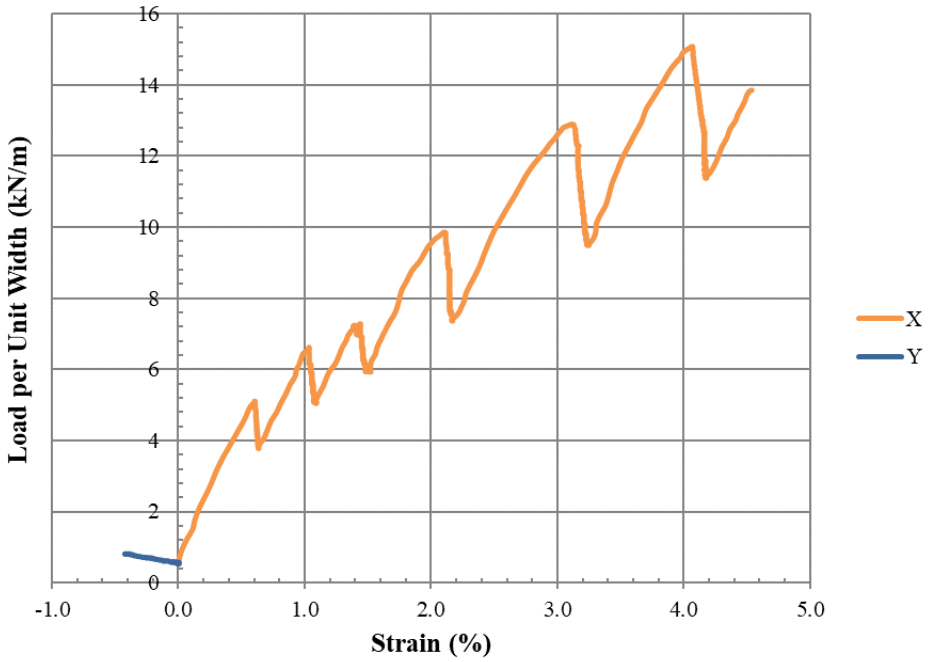

Figure 96 Geogrid A Mode 2 Trial 5

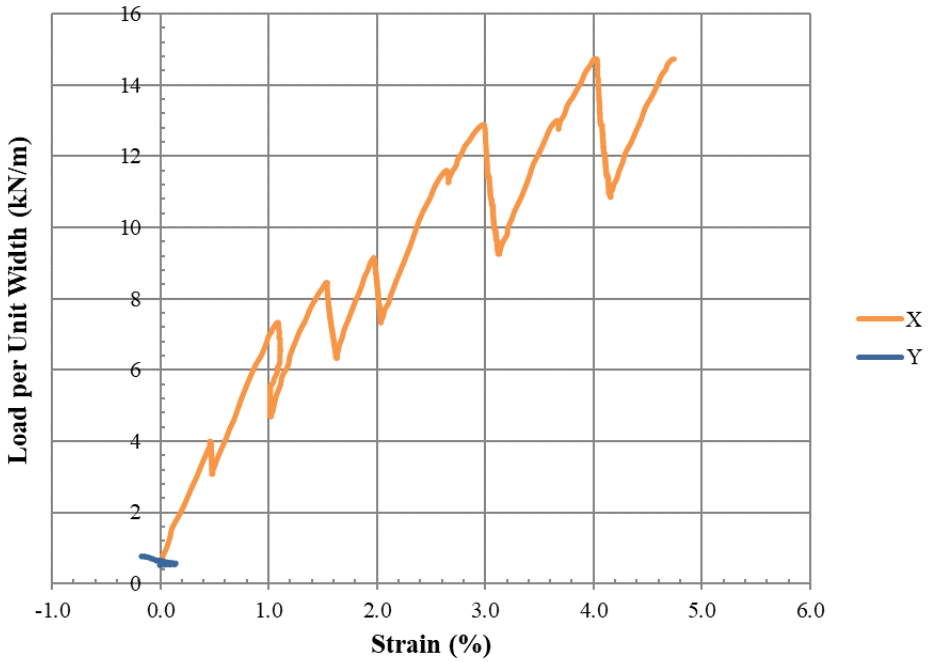

Figure 97 Geogrid A Mode 2 Trial 6

The irregularities seen on these load per unit width vs. strain plots between 2.0 % and 3.0 % strain and 3.0 % and 4.0 % strain are due to the motor stopping automatically then manually being restarted it at lower motor speeds to try to reach the next permanent strain limit. This process had to be repeated multiple times for other materials and is why the curve may appear irregular. This was acceptable because the only data of interest is the initial loading after stress relaxation/creep.

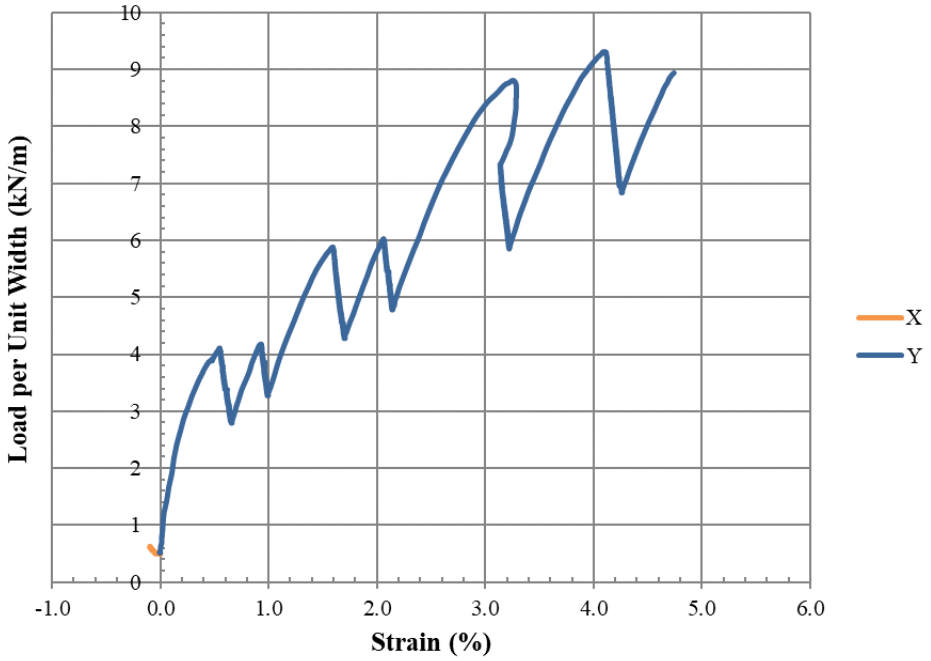

Figure 98 Geogrid A Mode 3 Trial 1

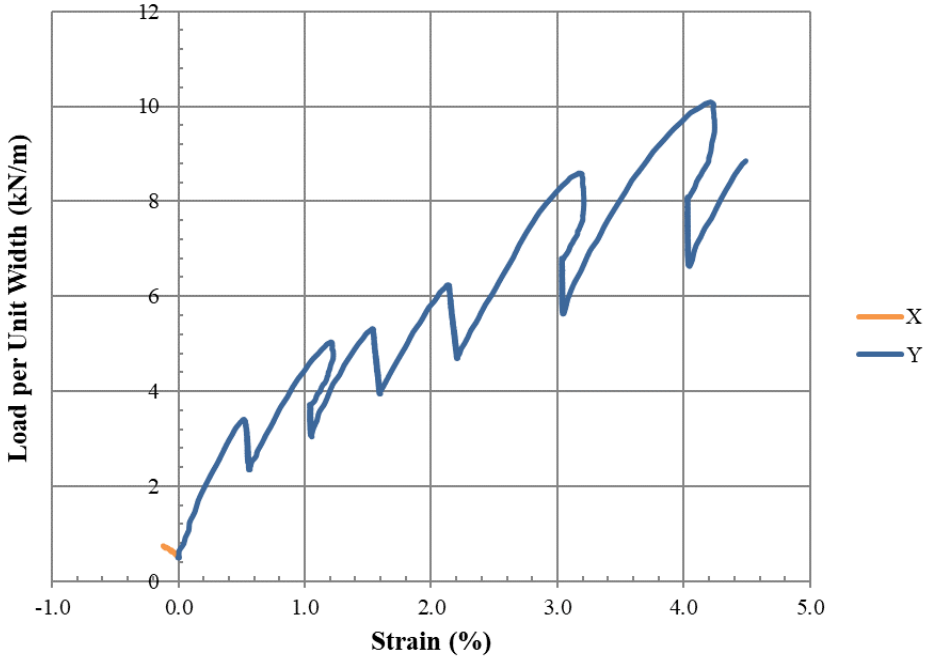

Figure 99 Geogrid A Mode 3 Trial 2

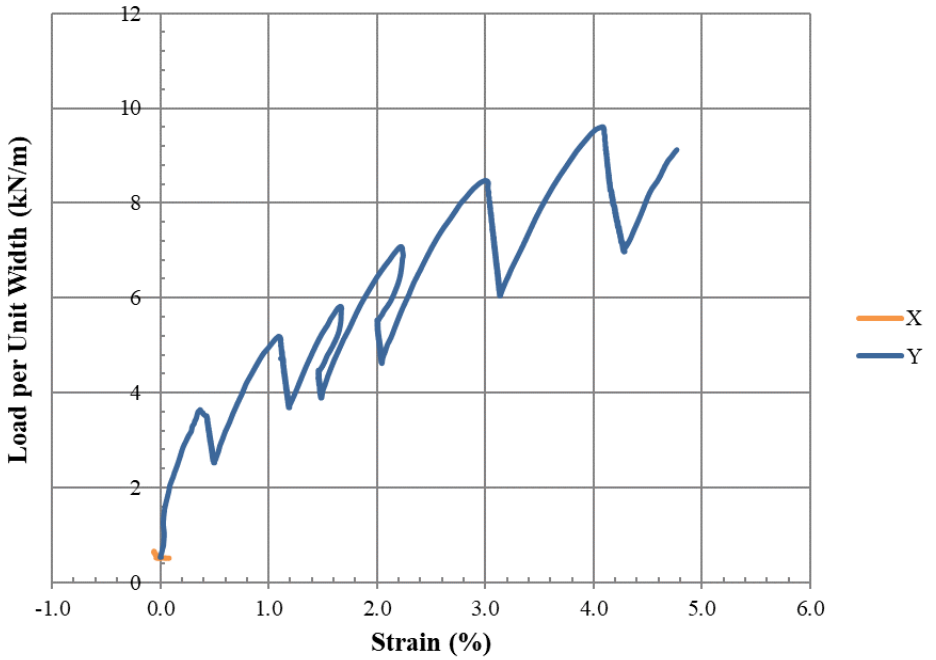

Figure 100 Geogrid A Mode 3 Trial 3

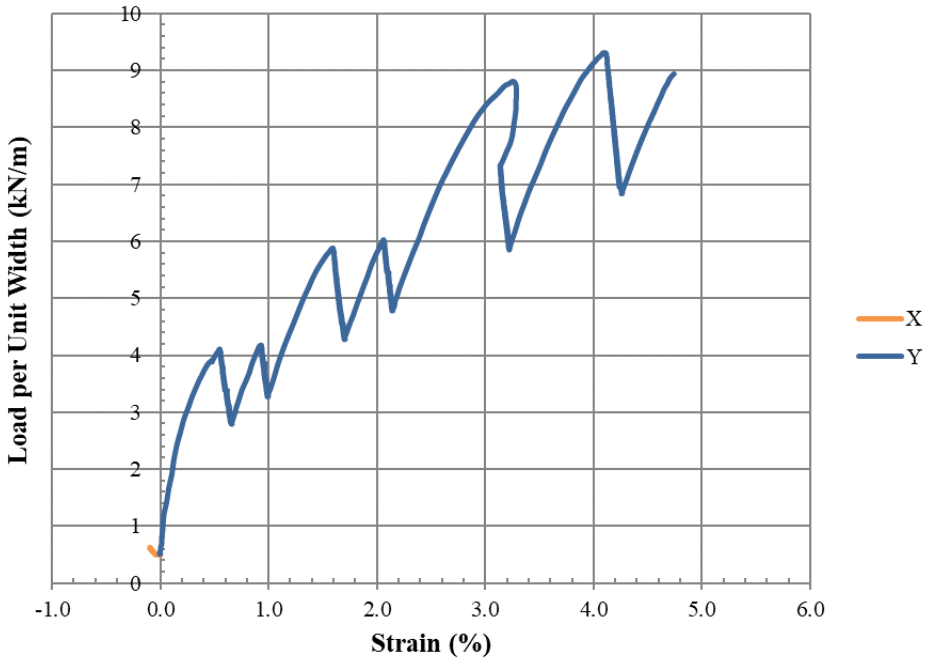

Figure 101 Geogrid A Mode 3 Trial 4

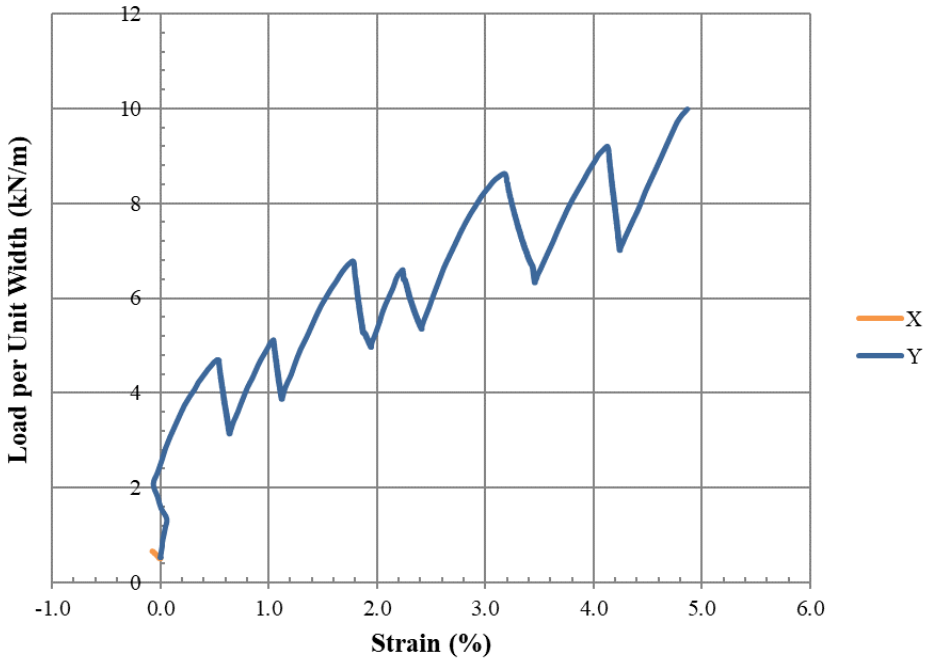

Figure 102 Geogrid A Mode 3 Trial 5

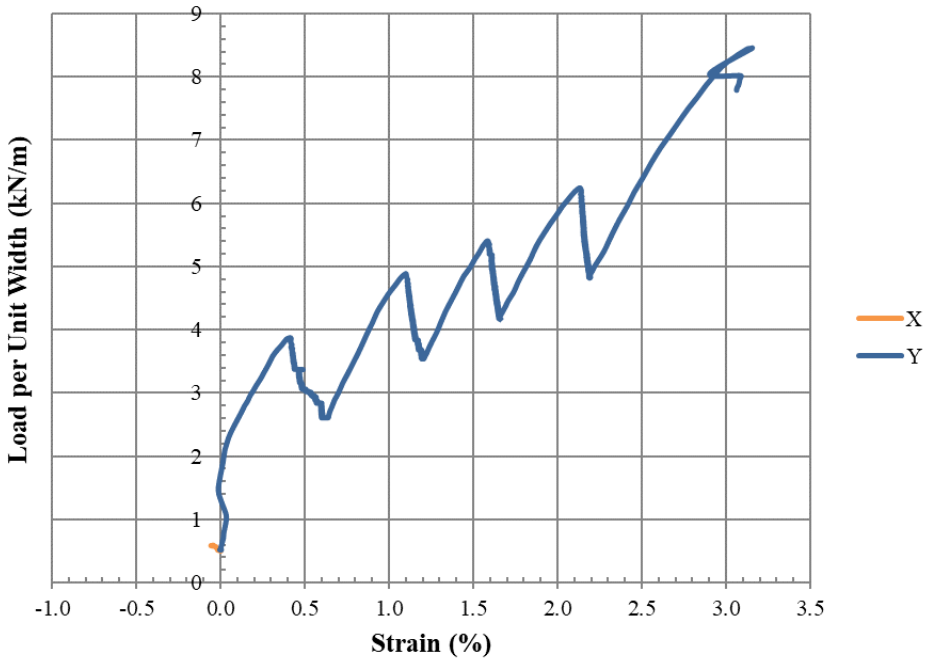

Figure 103 Geogrid A Mode 3 Trial 6

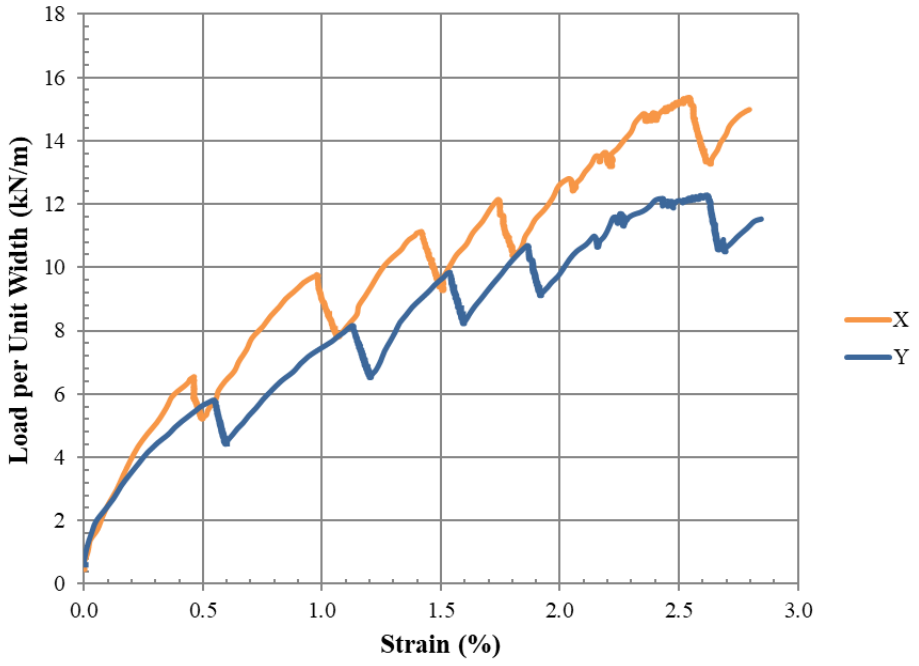

Figure 104 Geogrid B Mode 1 Trial 2

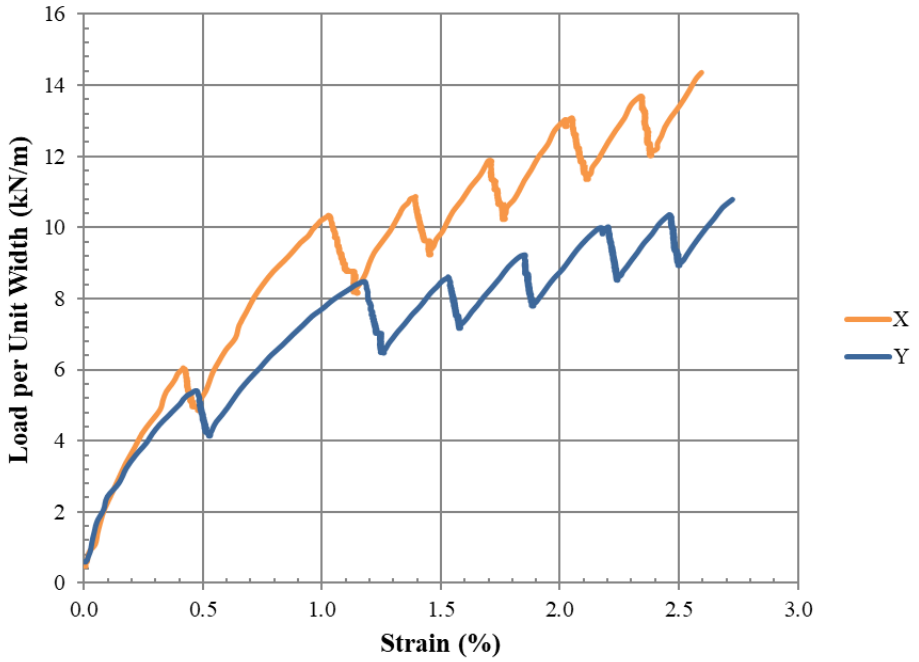

Figure 105 Geogrid B Mode 1 Trial 3

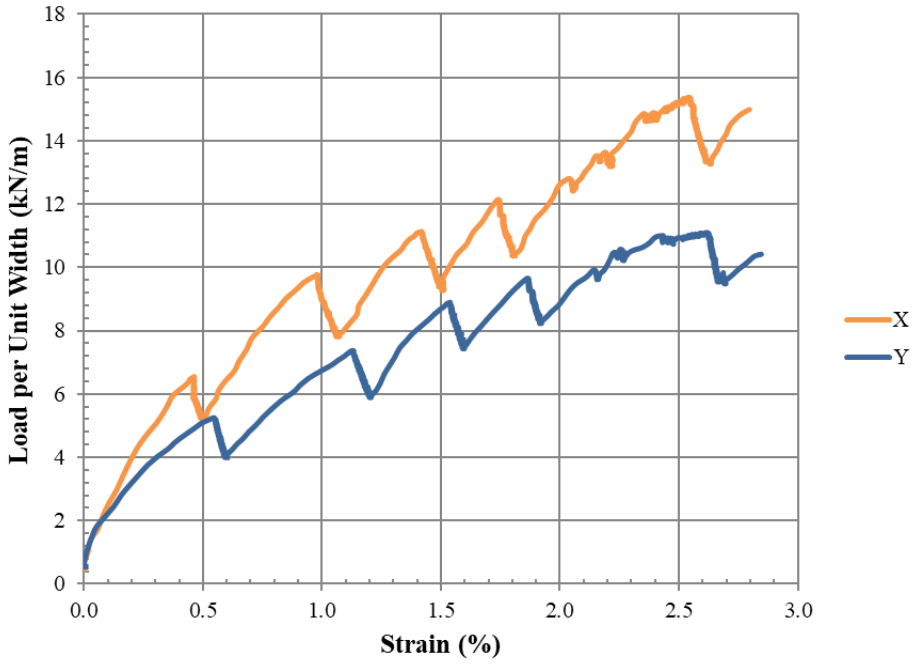

Figure 106 Geogrid B Mode 1 Trial 4

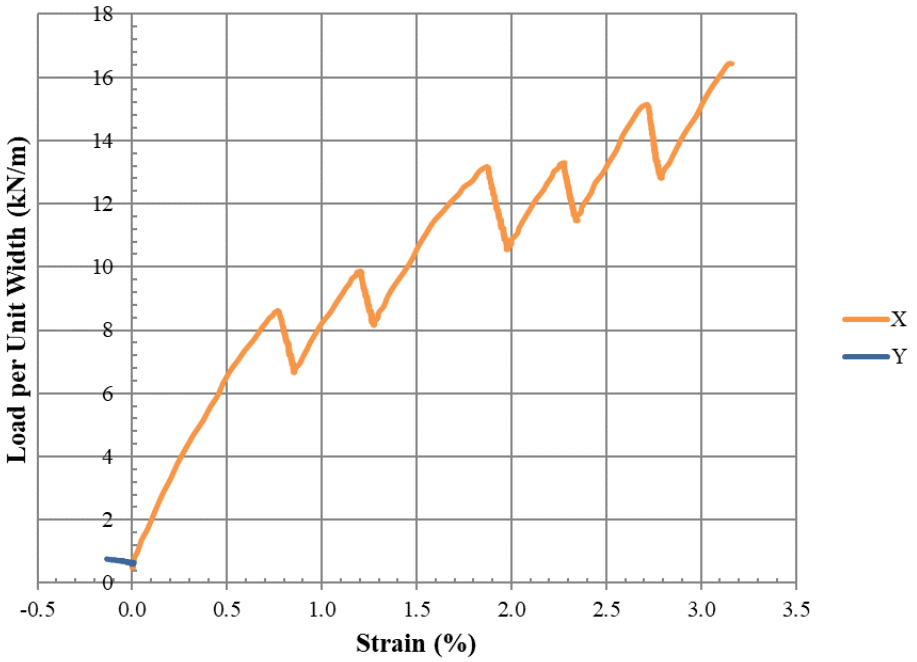

Figure 107 Geogrid B Mode 2 Trial 1

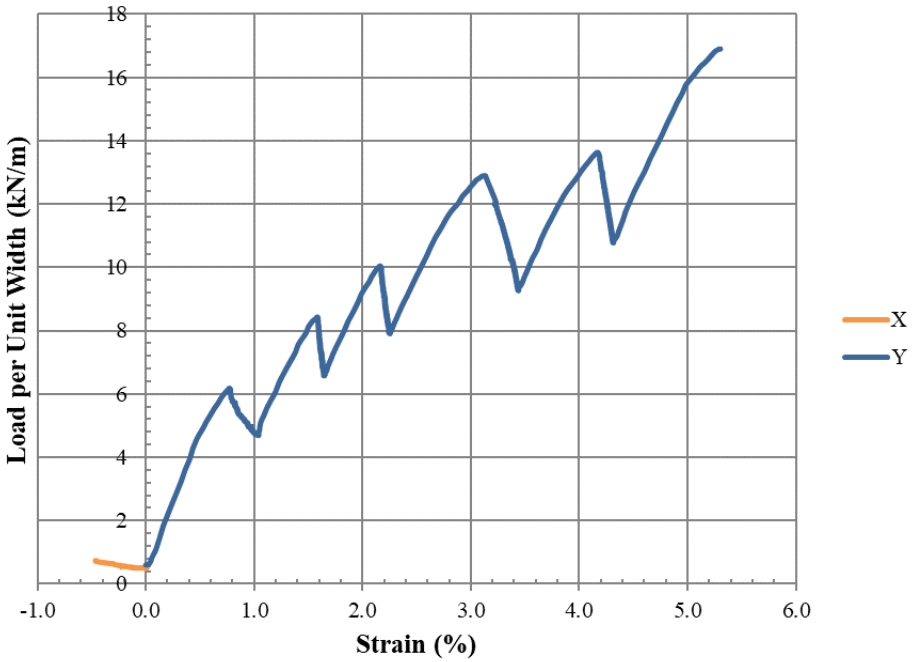

Figure 108 Geogrid B Mode 3 Trial 2

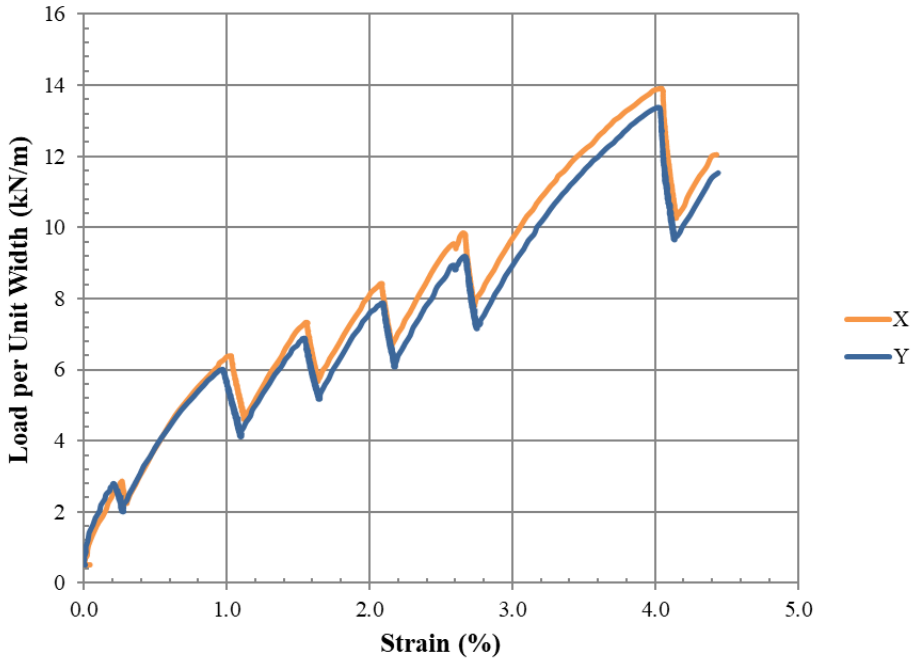

Figure 109 Geogrid C Mode 1 Trial 1

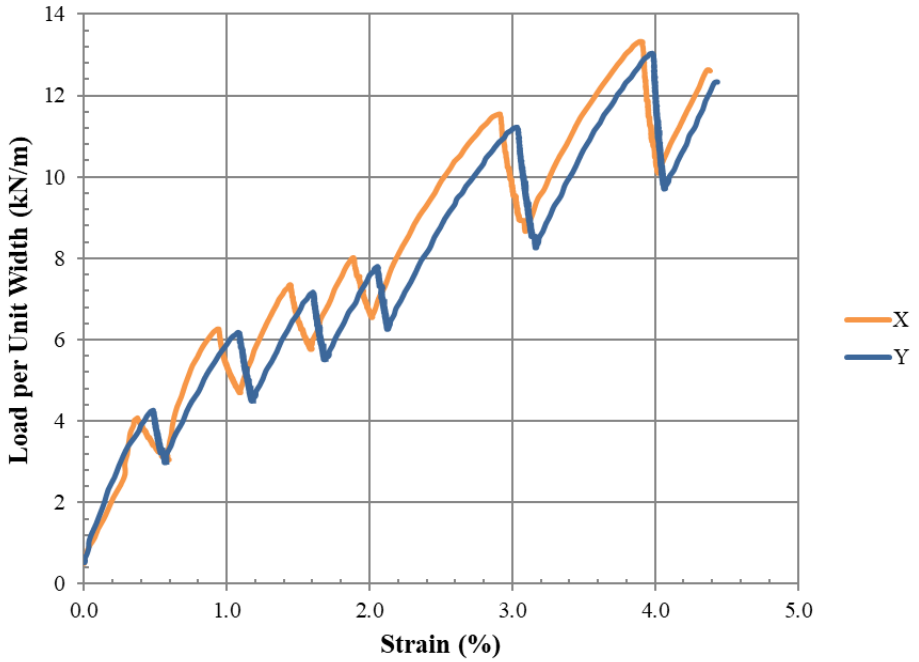

Figure 110 Geogrid C Mode 1 Trial 2

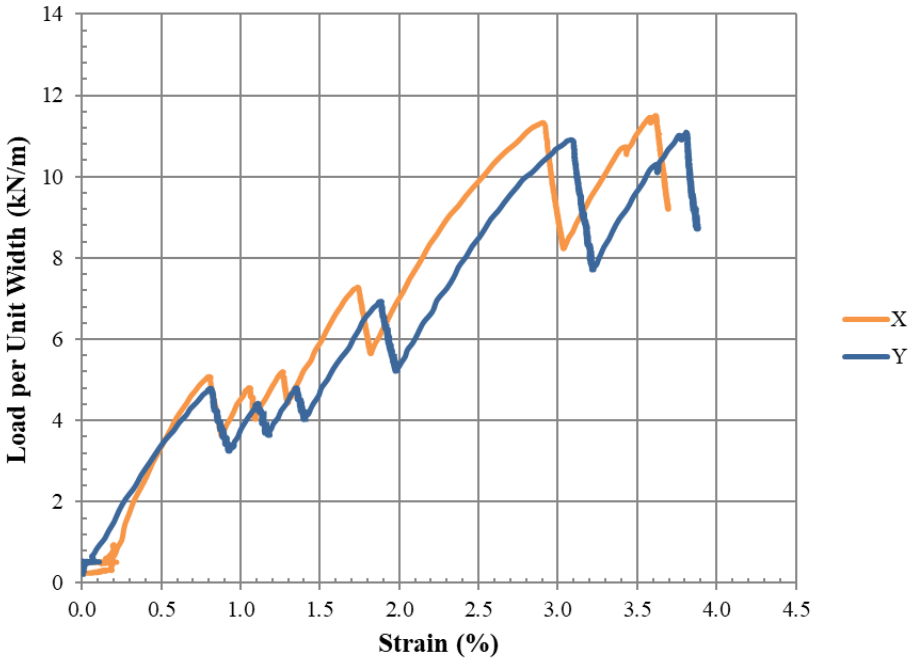

Figure 111 Geogrid C Mode 1 Trial 3

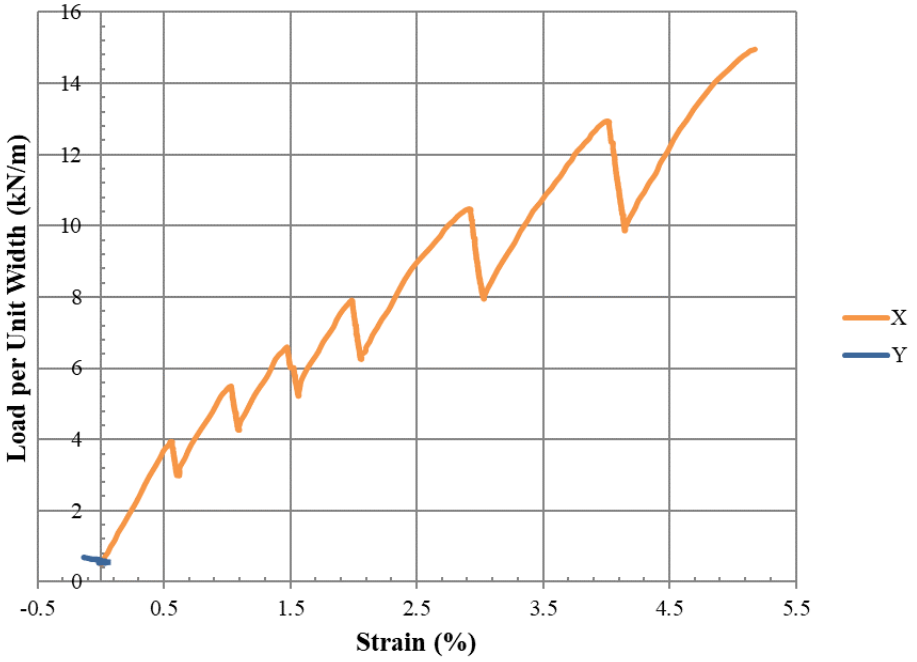

Figure 112 Geogrid C Mode 2 Trial 1

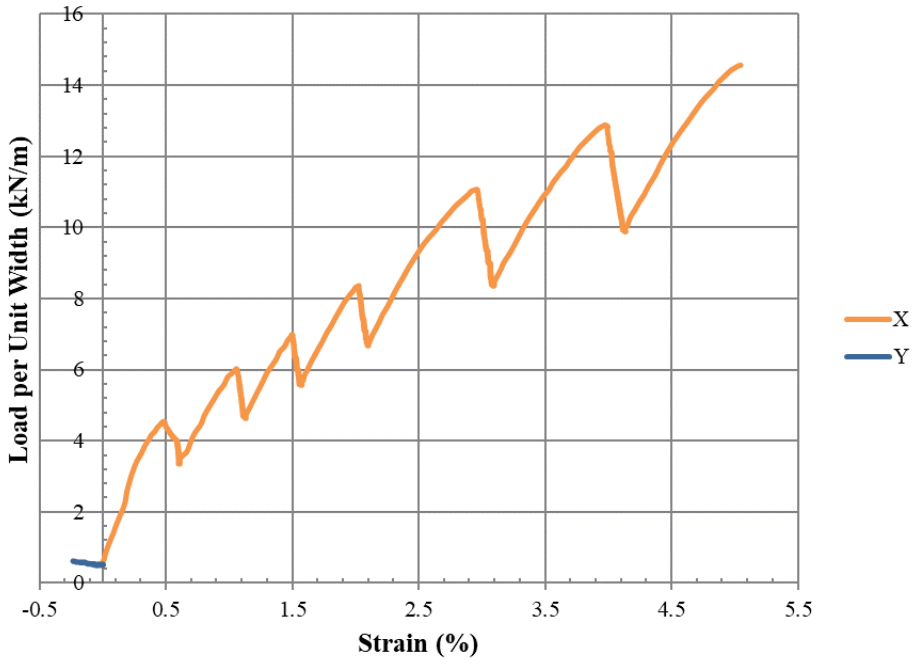

Figure 113 Geogrid C Mode 2 Trial 2

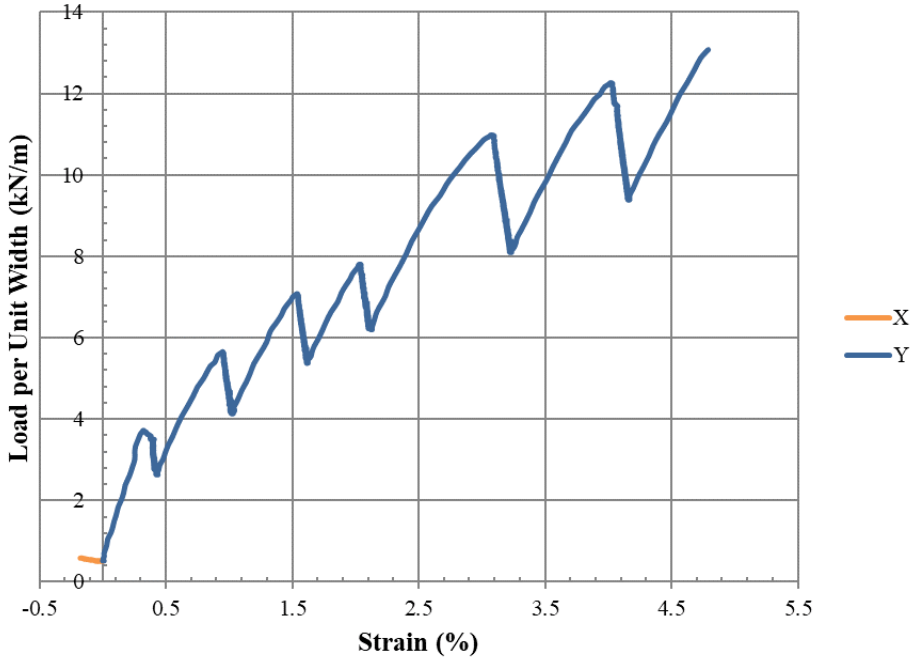

Figure 114 Geogrid C Mode 3 Trial 1

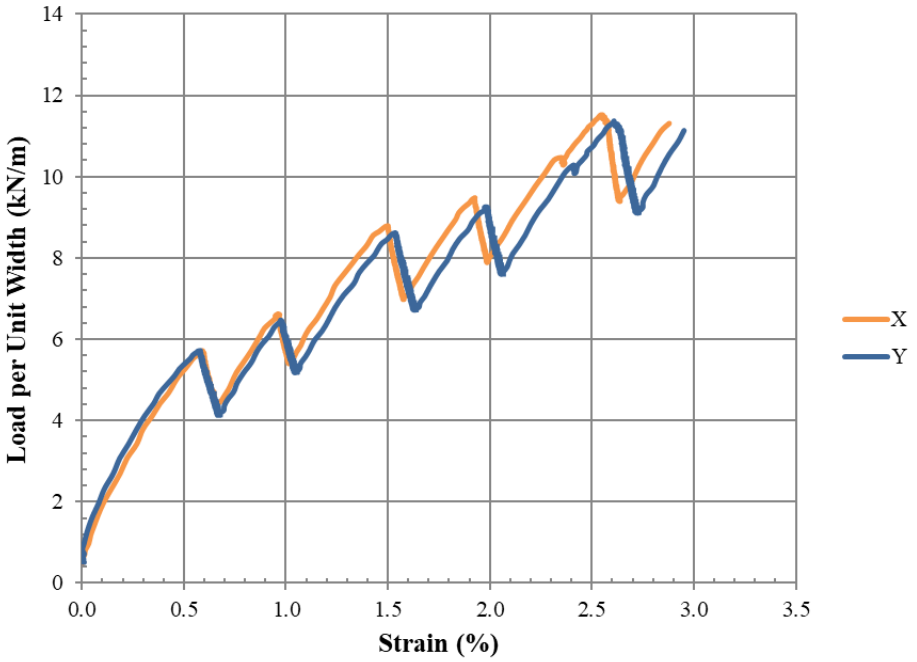

Figure 115 Geogrid D Mode 1 Trial 3

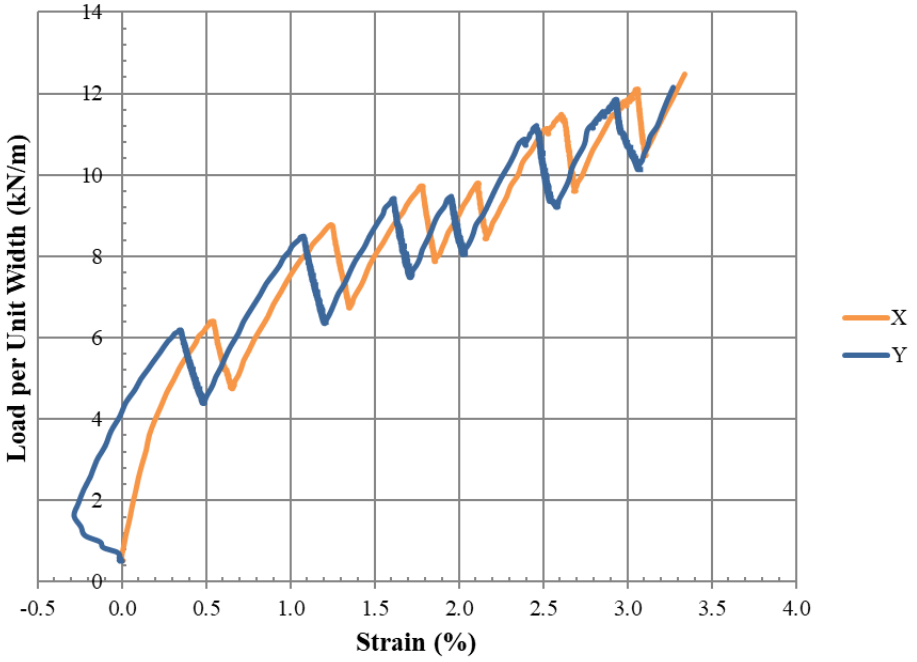

Figure 116 Geogrid D Mode 1 Trial 4

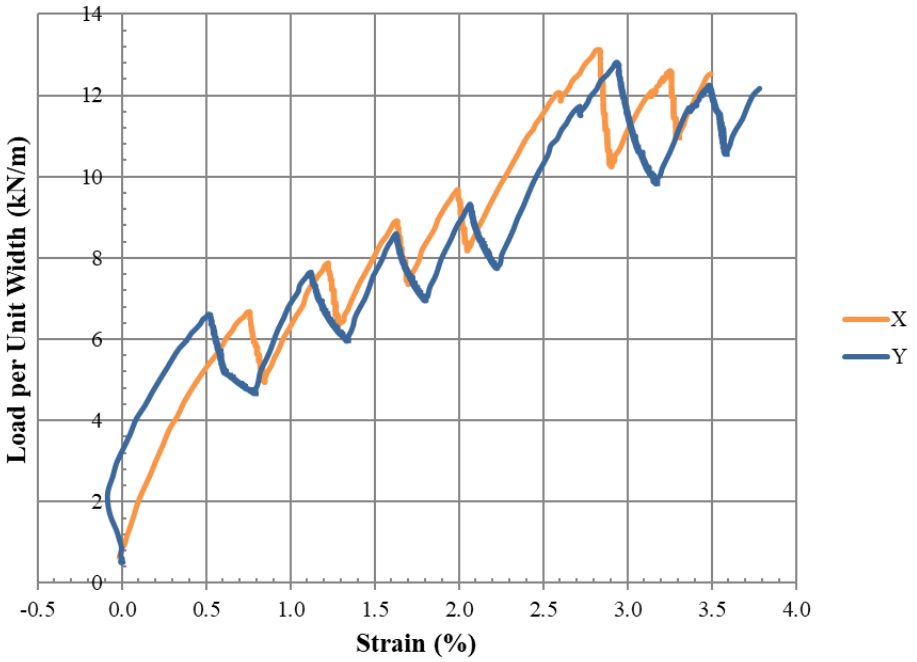

Figure 117 Geogrid D Mode 1 Trial 5

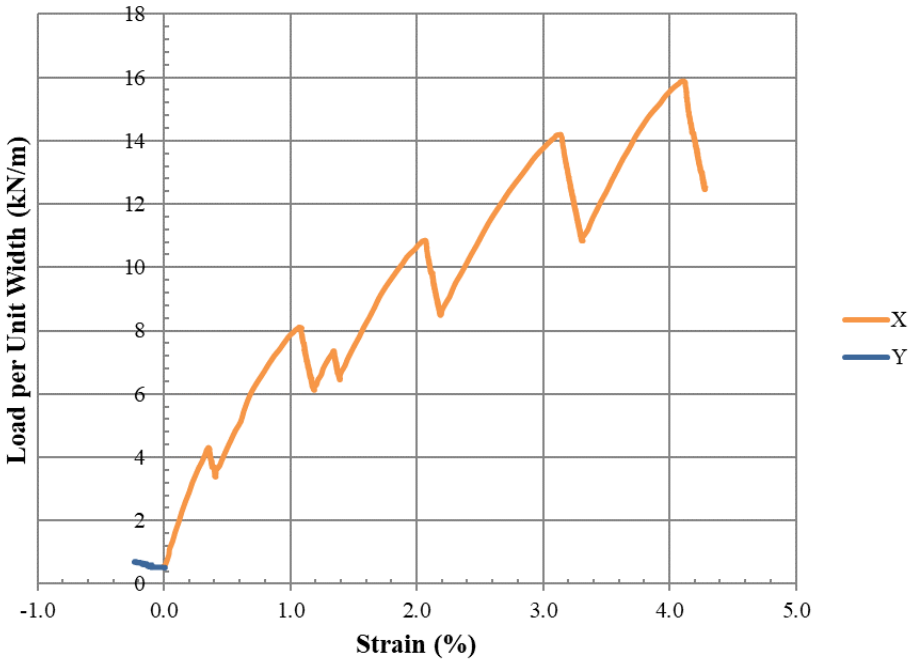

Figure 118 Geogrid D Mode 2 Trial 1

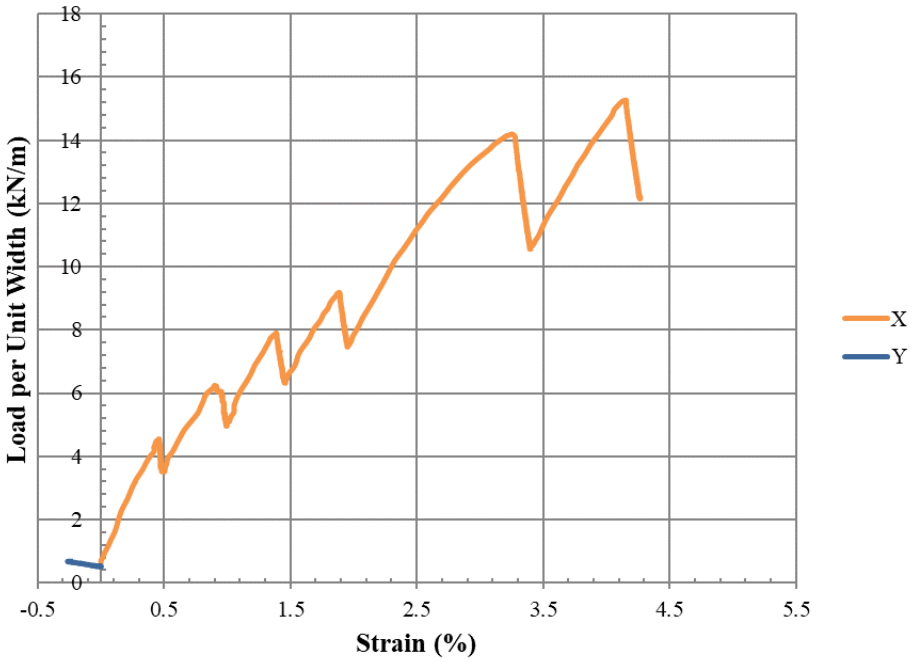

Figure 119 Geogrid D Mode 2 Trial 2

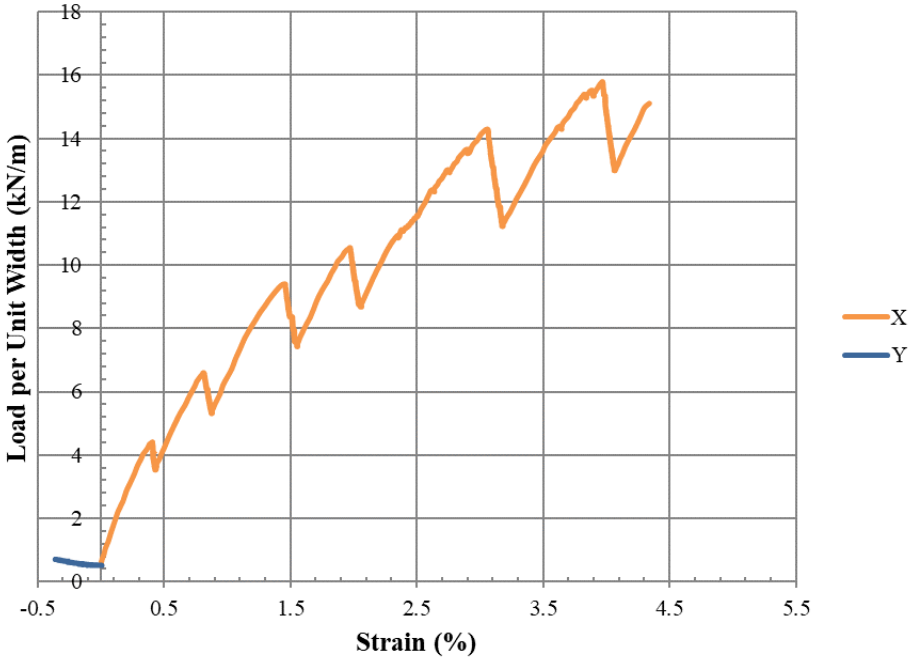

Figure 120 Geogrid D Mode 2 Trial 4

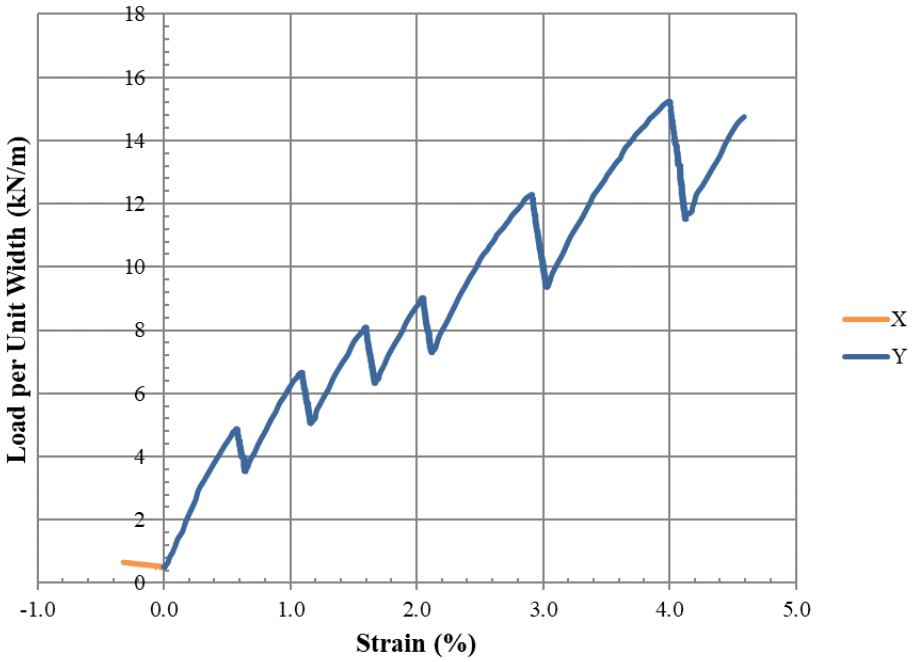

Figure 121 Geogrid D Mode 3 Trial 1

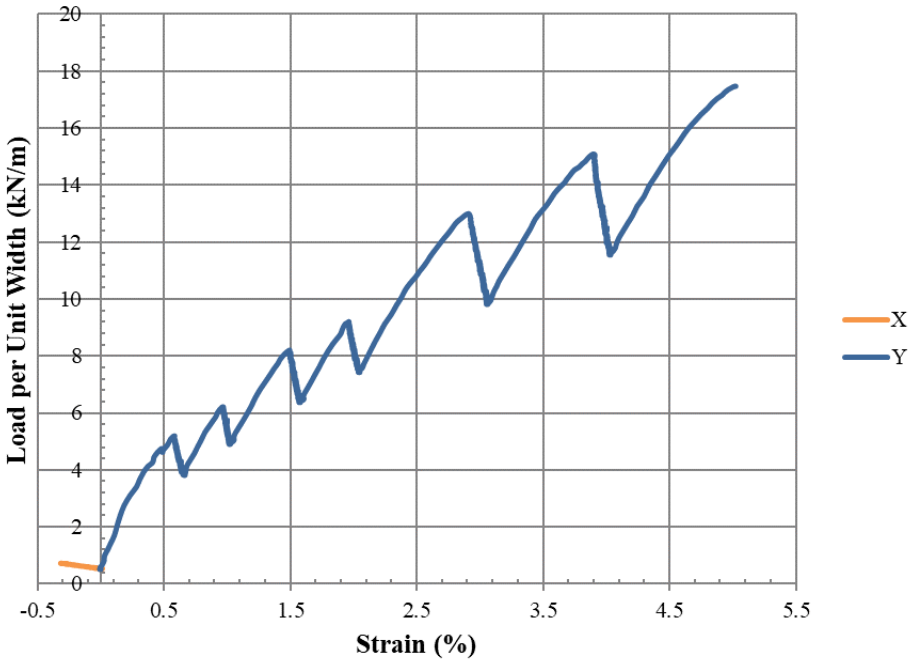

Figure 122 Geogrid D Mode 3 Trial 2

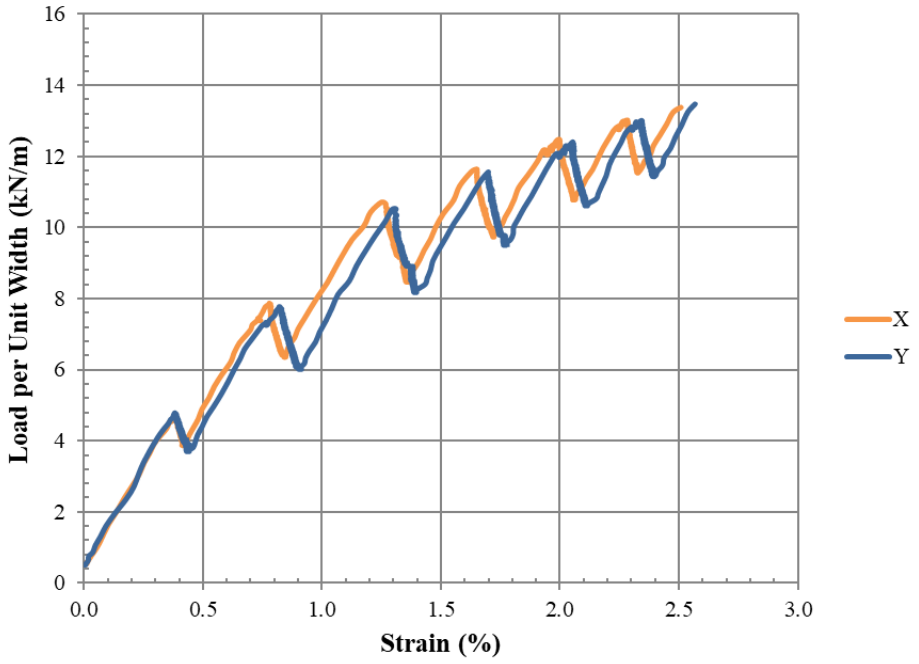

Figure 123 Geogrid E Mode 1 Trial 1

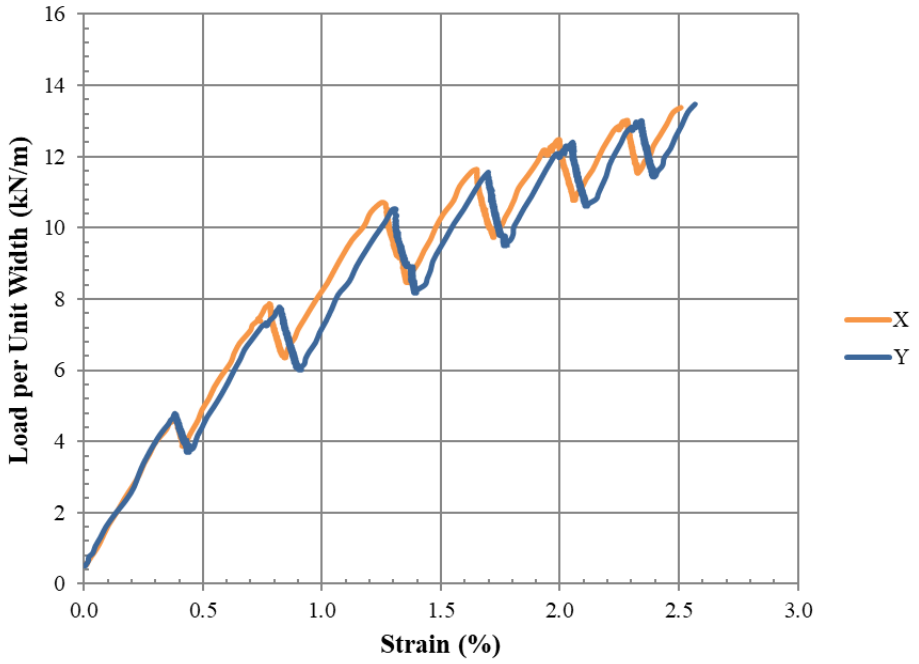

Figure 124 Geogrid E Mode 1 Trial 2

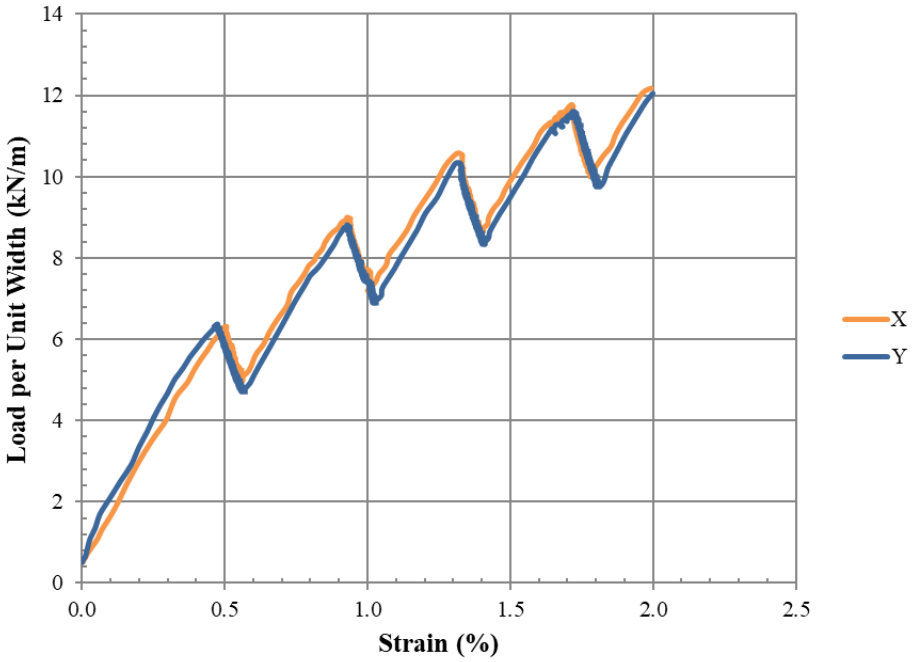

Figure 125 Geogrid E Mode 1 Trial 3

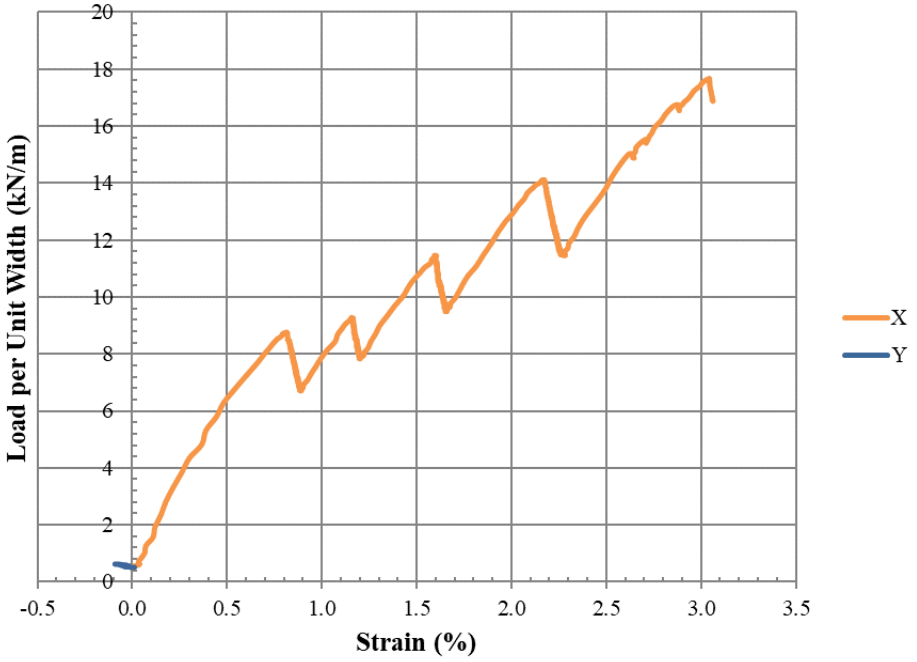

Figure 126 Geogrid E Mode 2 Trial 1

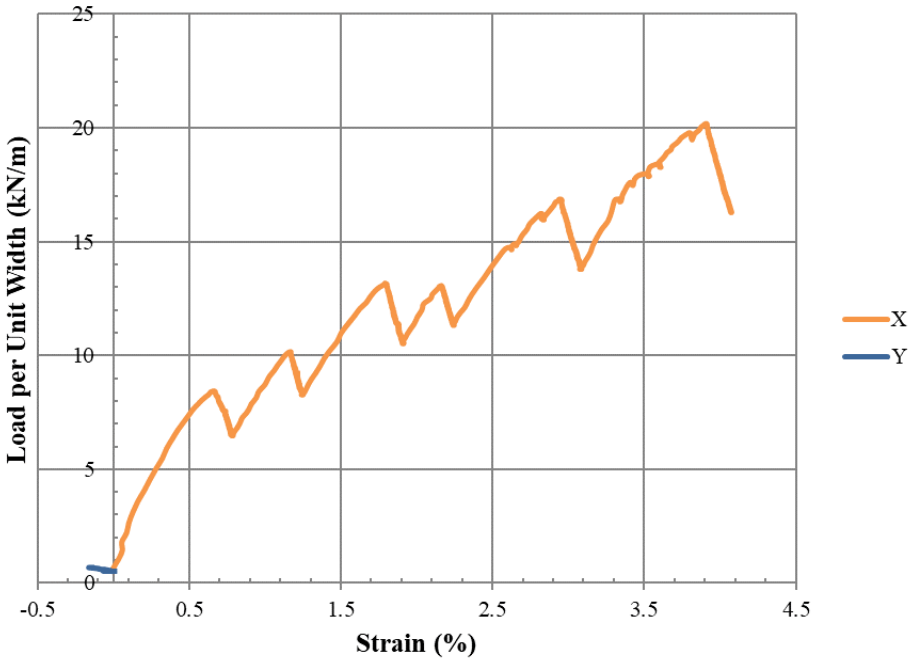

Figure 127 Geogrid E Mode 2 Trial 3

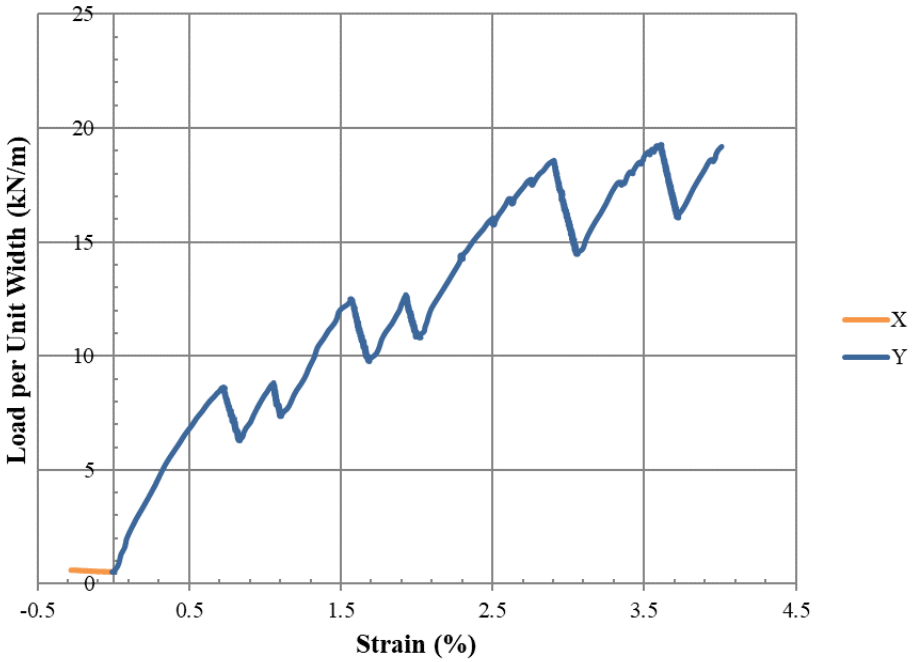

Figure 128 Geogrid E Mode 3 Trial 1

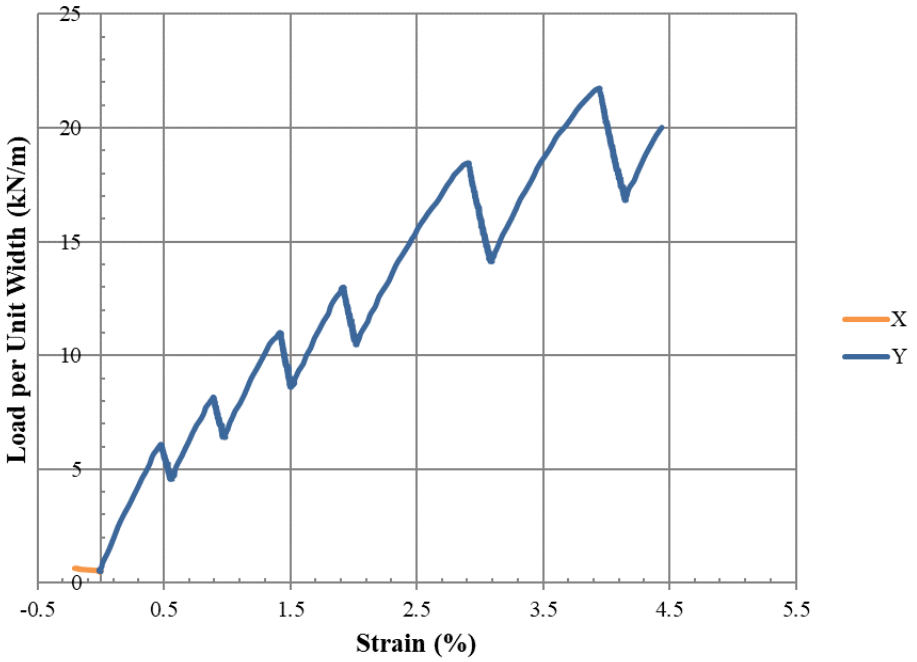

Figure 129 Geogrid E Mode 3 Trial 2

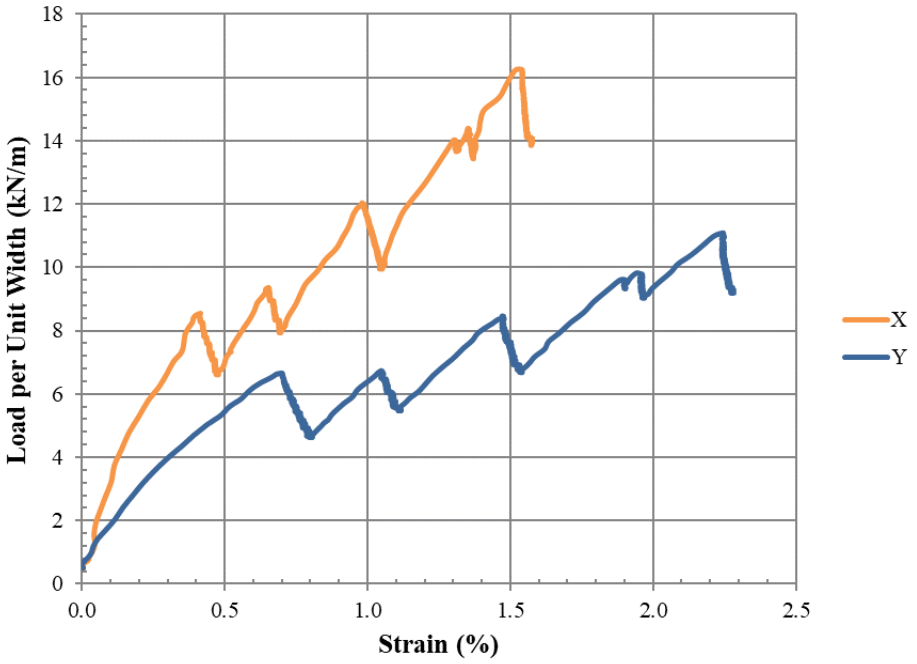

Figure 130 Geogrid F Mode 1 Trial 1

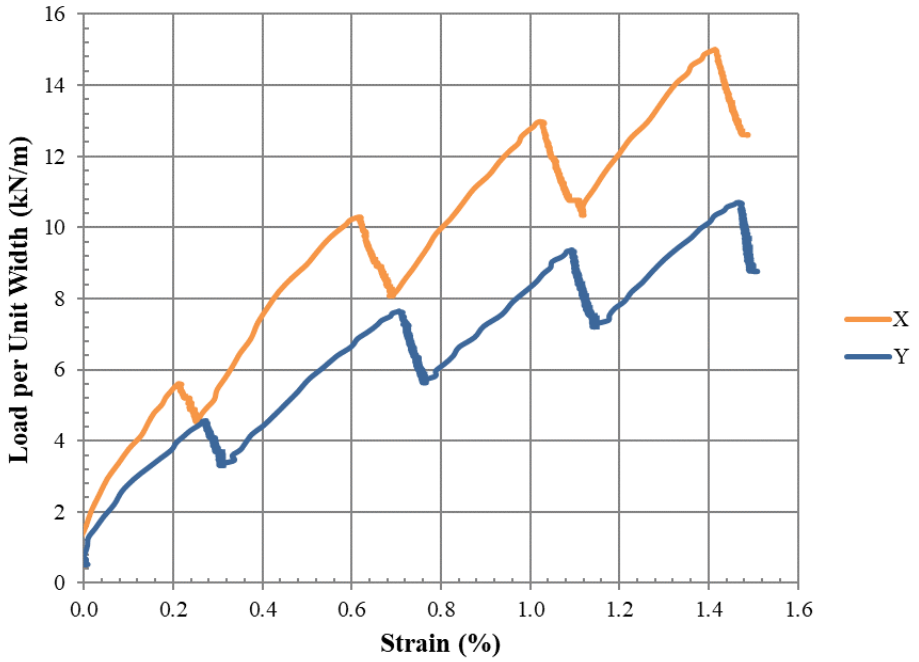

Figure 131 Geogrid F Mode 1 Trial 2

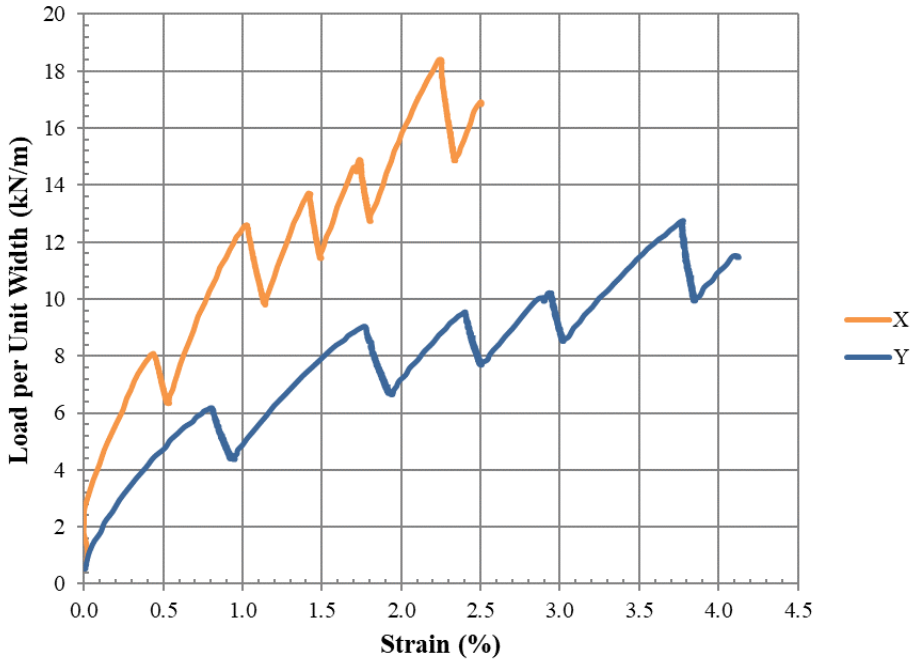

Figure 132 Geogrid F Mode 1 Trial 3

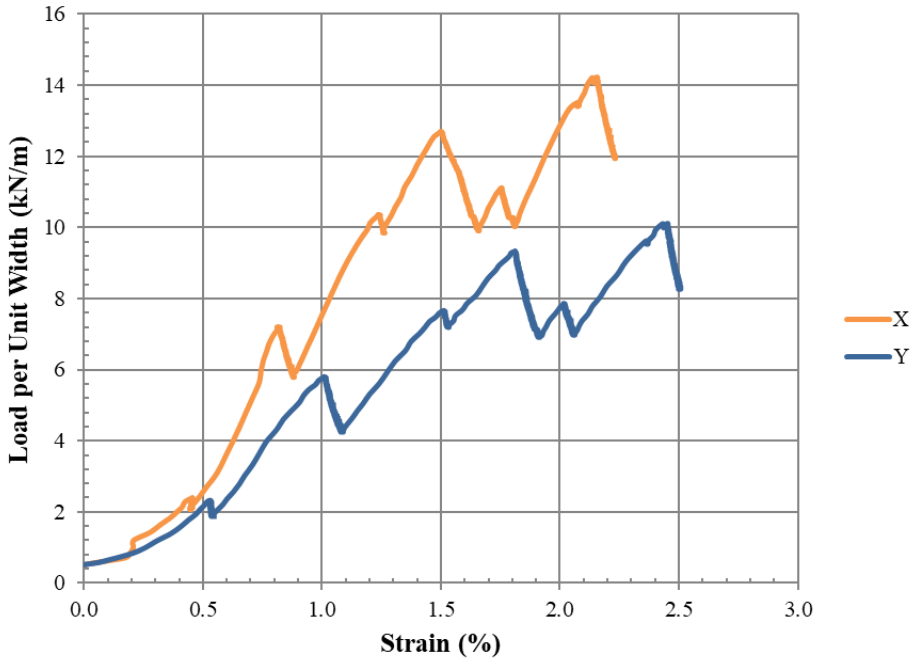

Figure 133 Geogrid F Mode 1 Trial 4

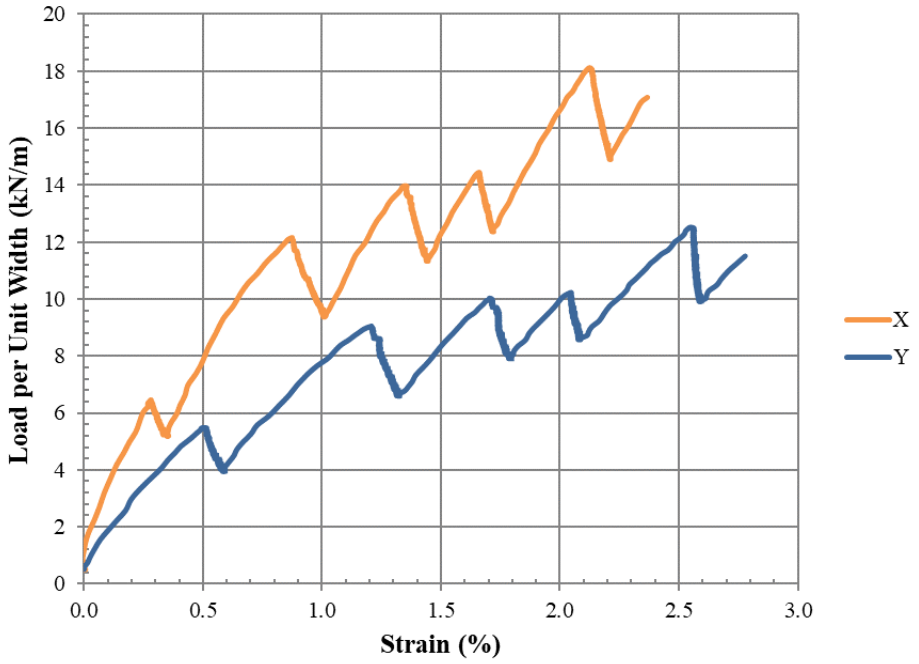

Figure 134 Geogrid F Mode 1 Trial 5

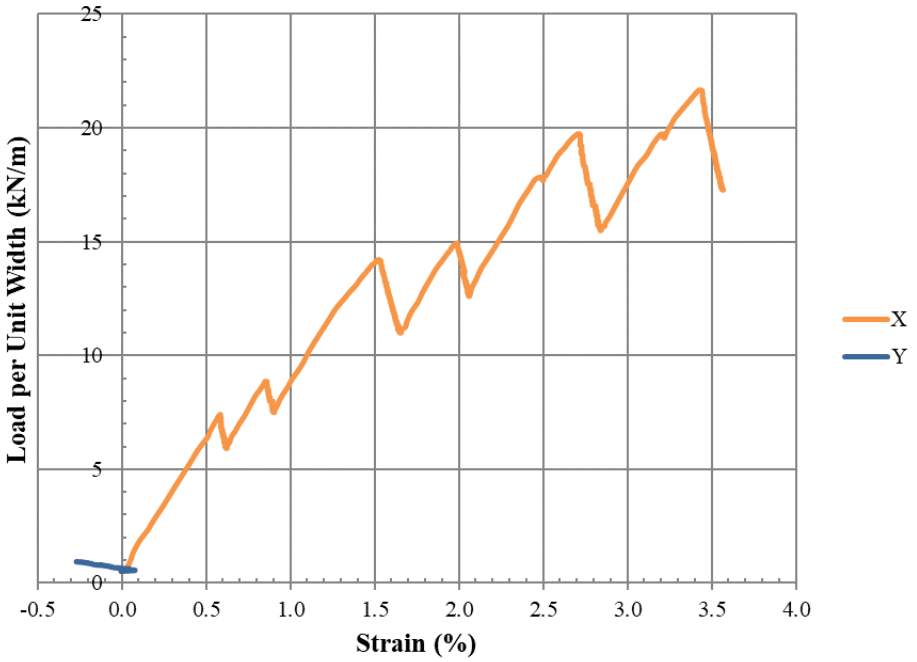

Figure 135 Geogrid F Mode 2 Trial 1

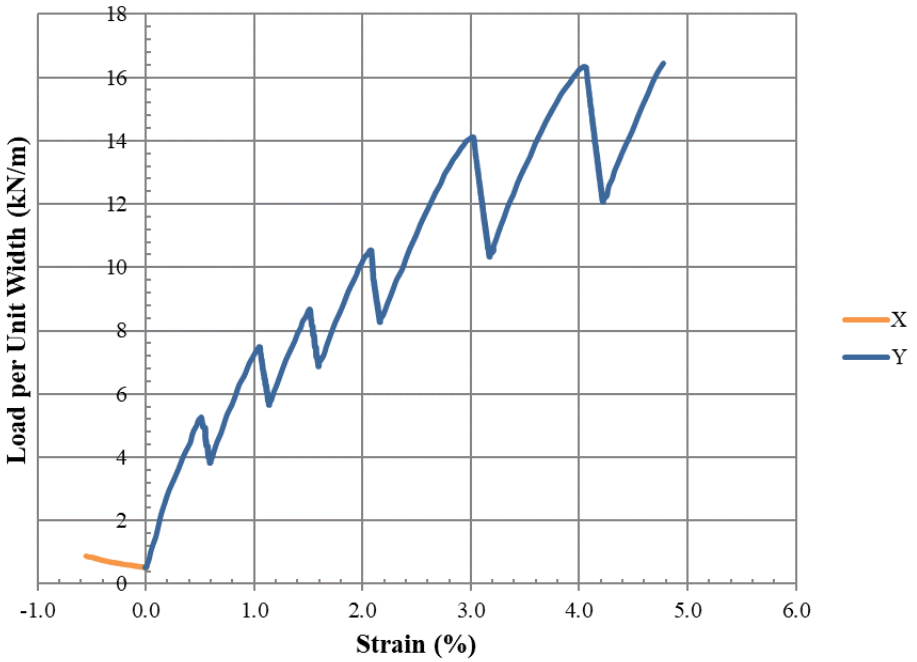

Figure 136 Geogrid F Mode 3 Trial 1

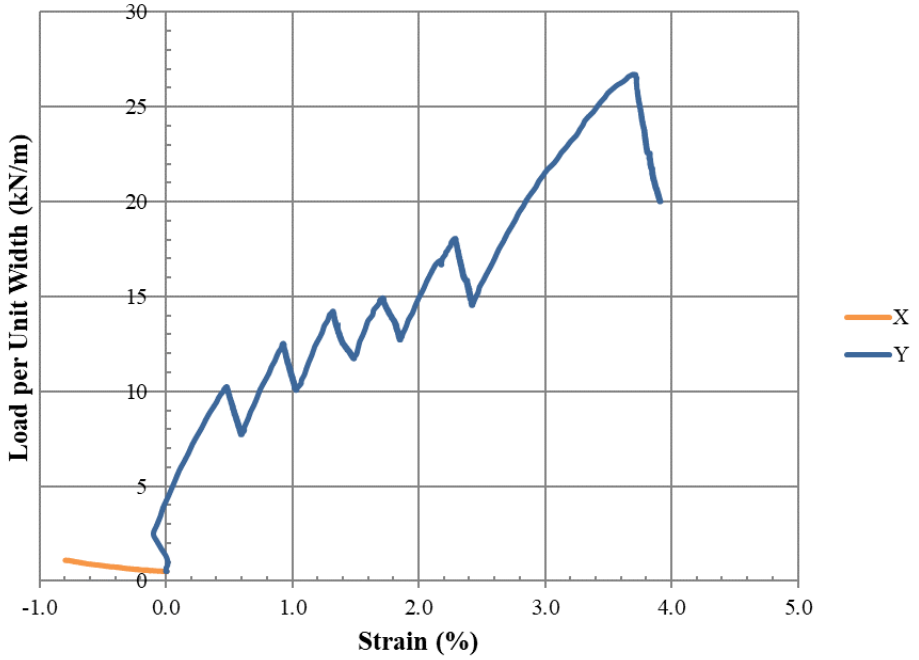

Figure 137 Geogrid F Mode 3 Trial 3

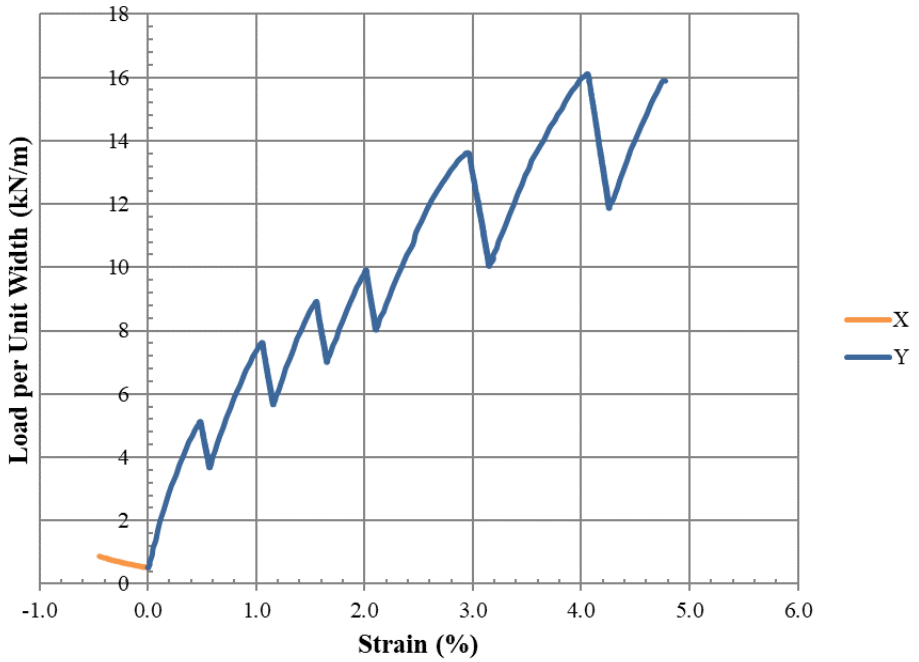

Figure 138 Geogrid F Mode 3 Trial 4

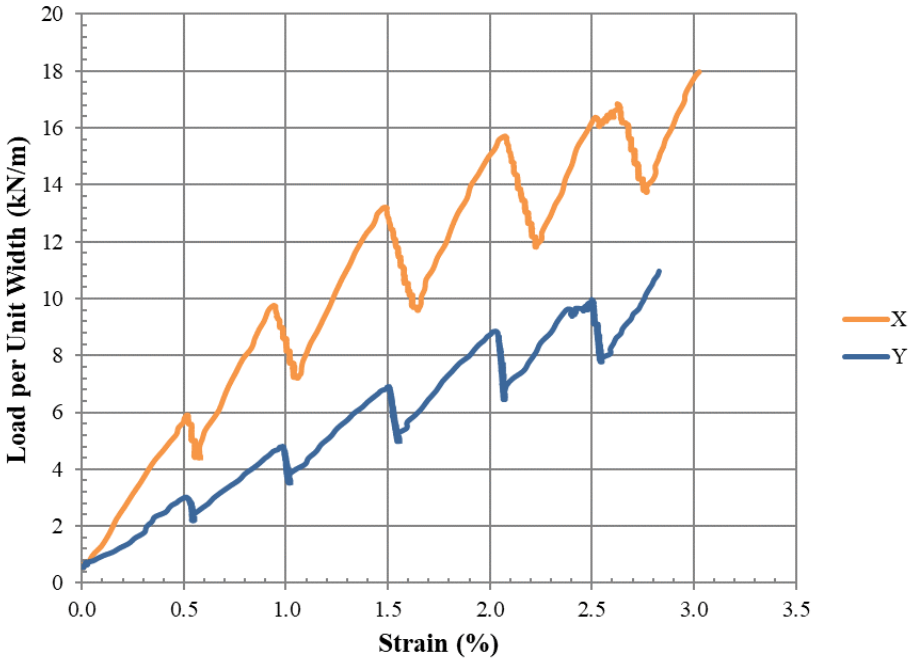

Figure 139 Geotextile A Mode 1 Trial 1

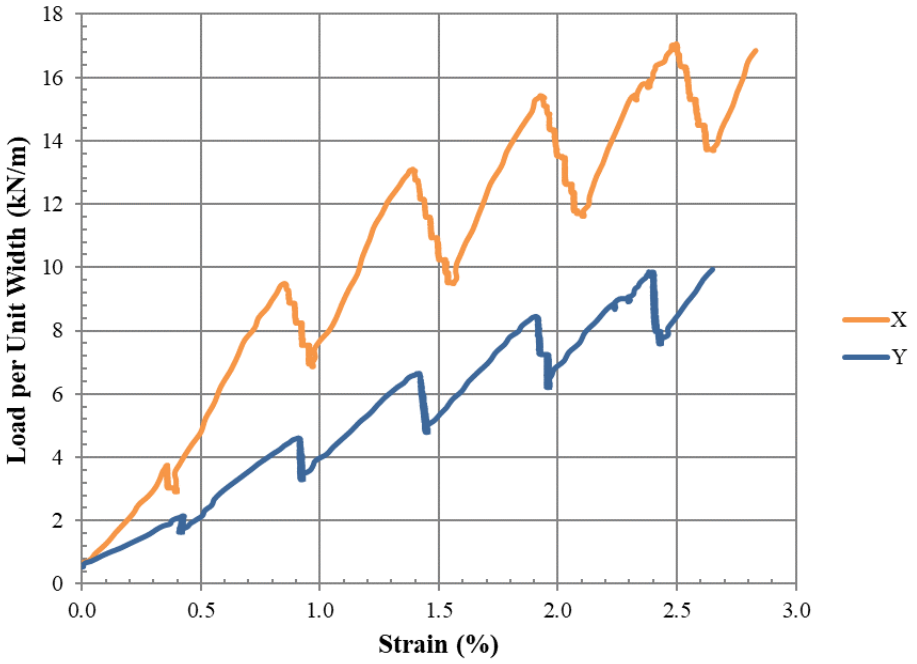

Figure 140 Geotextile A Mode 1 Trial 2

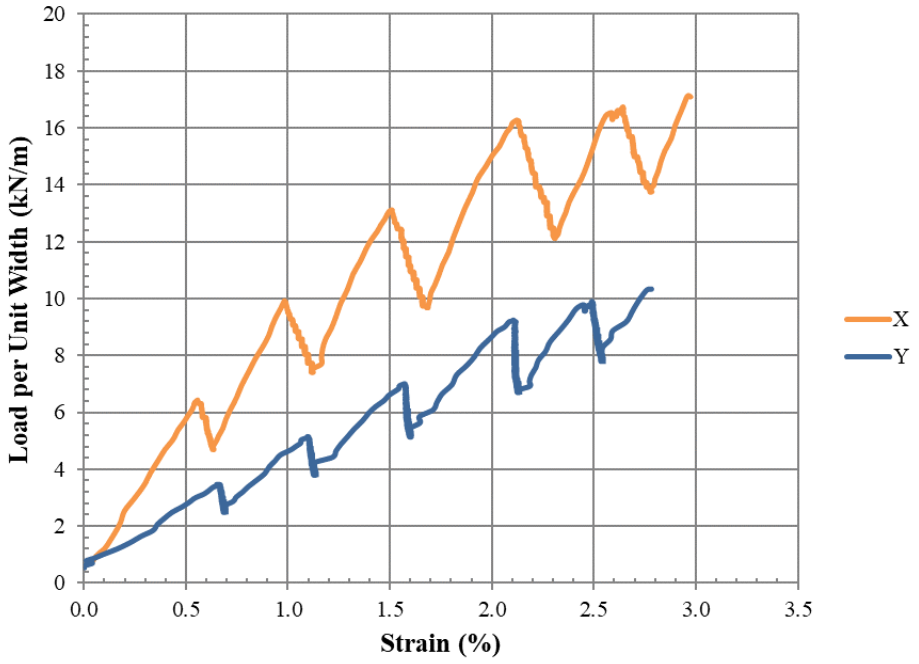

Figure 141 Geotextile A Mode 1 Trial 3

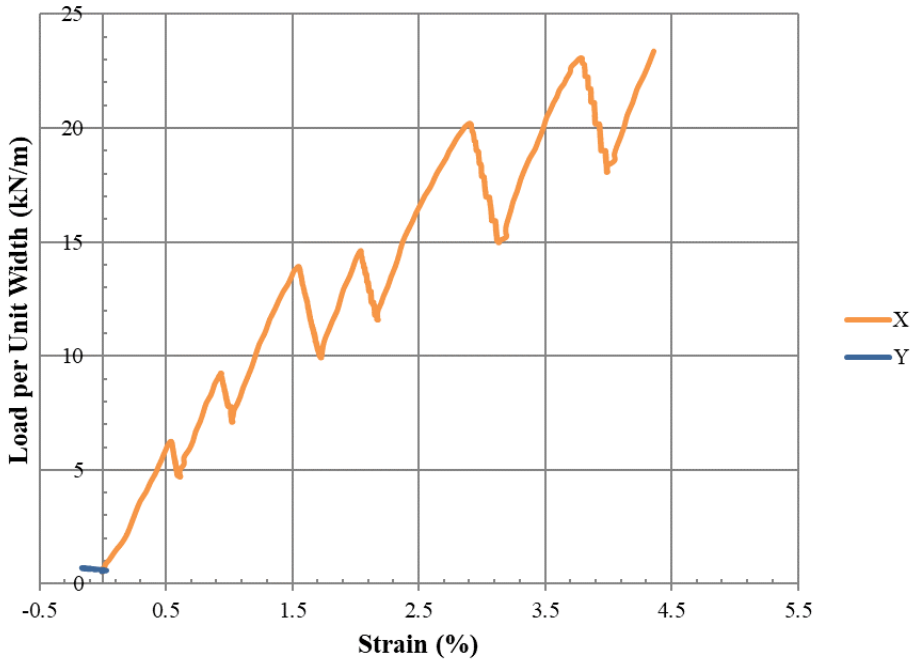

Figure 142 Geotextile A Mode 2 Trial 1

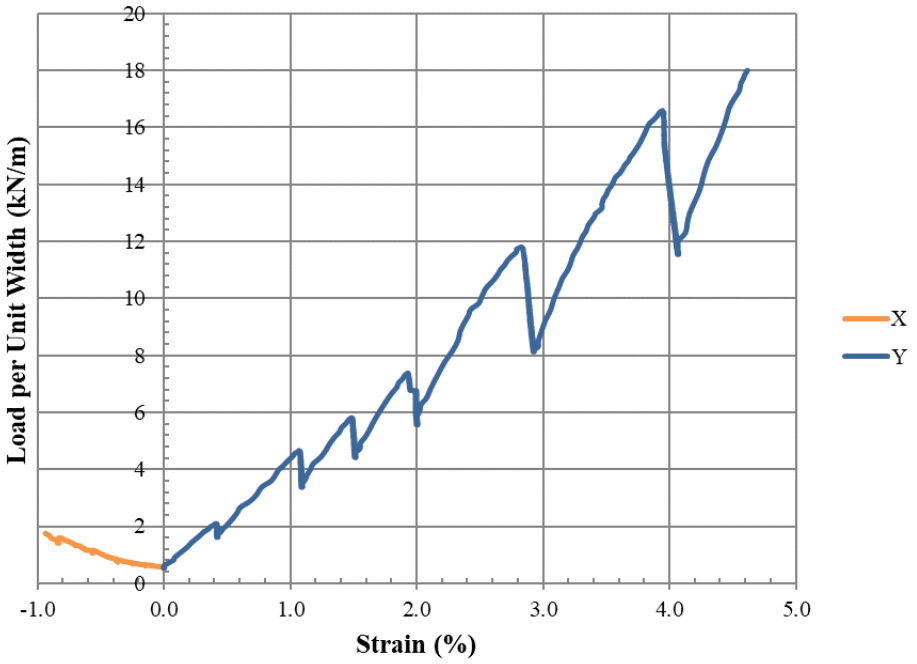

Figure 143 Geotextile A Mode 3 Trial 1

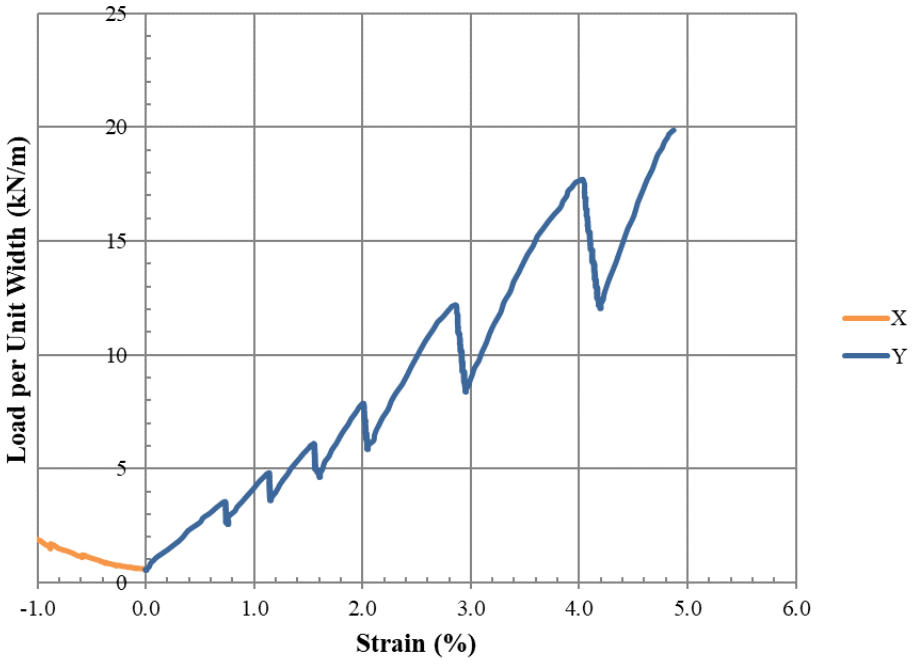

Figure 144 Geotextile A Mode 3 Trial 2

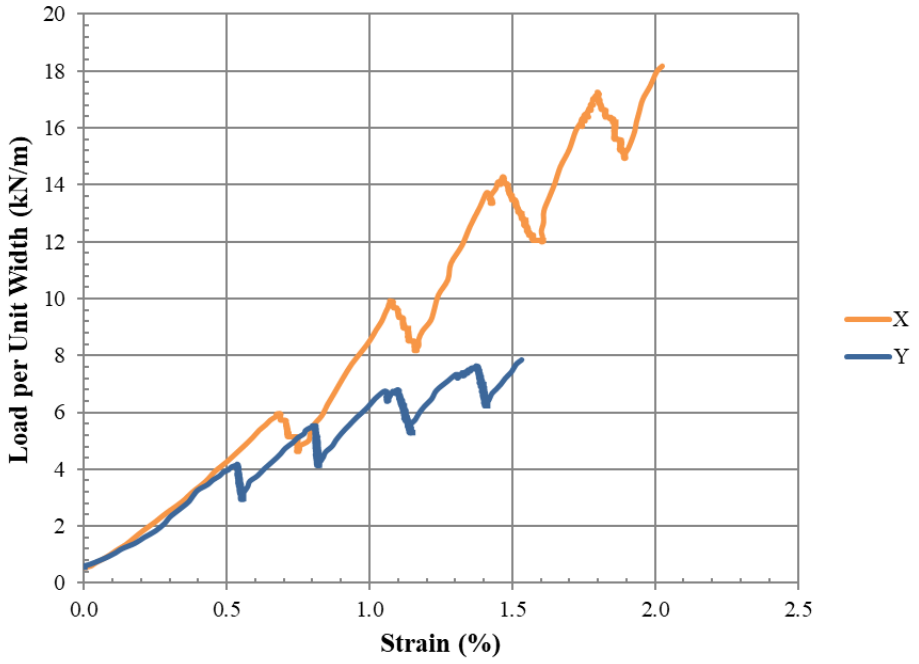

Figure 145 Geotextile B Mode 1 Trial 4

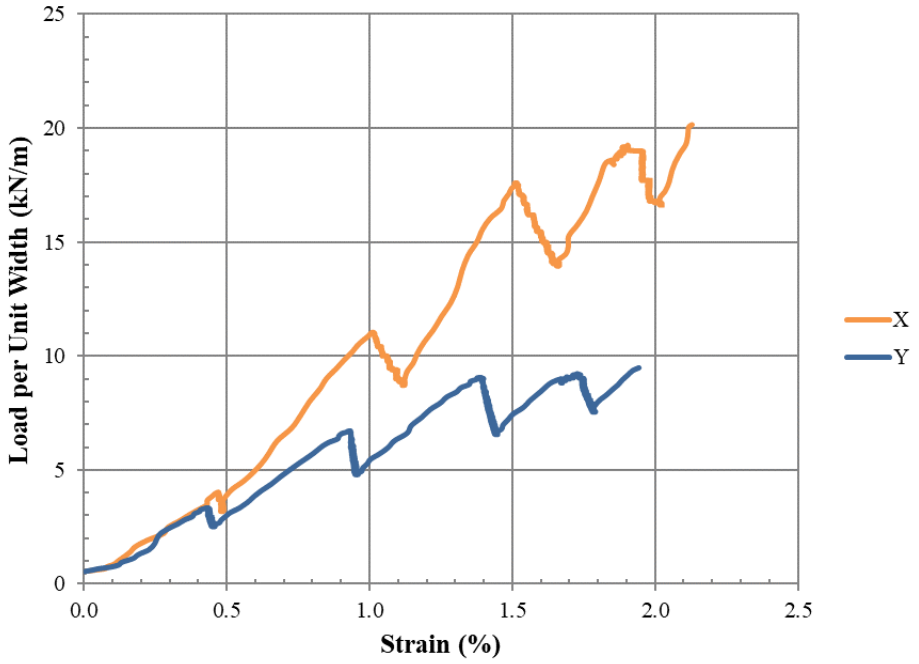

Figure 146 Geotextile B Mode 1 Trial 5

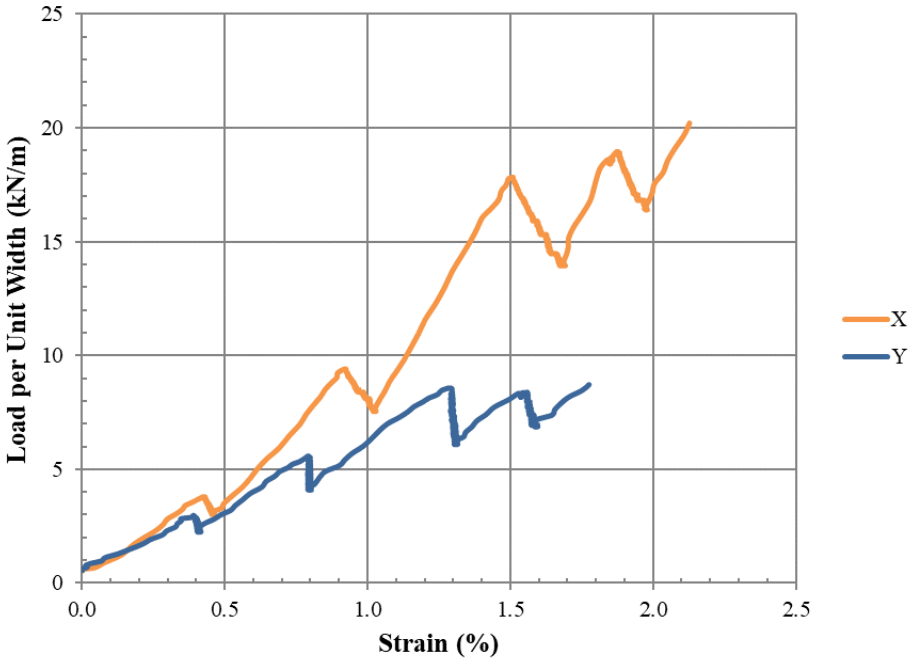

Figure 147 Geotextile B Mode 1 Trial 6

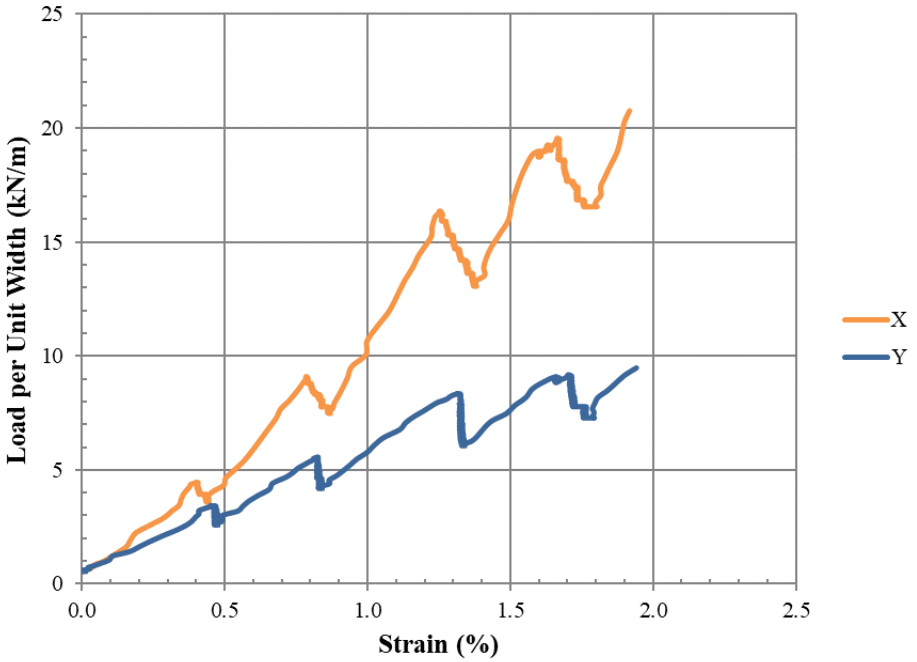

Figure 148 Geotextile B Mode 1 Trial 7

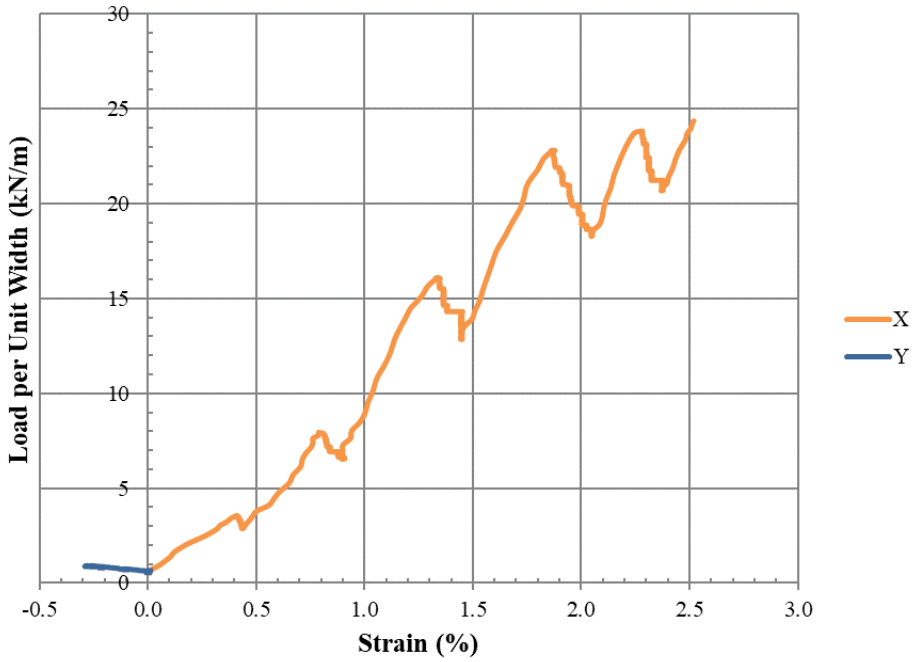

Figure 149 Geotextile B Mode 1 Trial 1

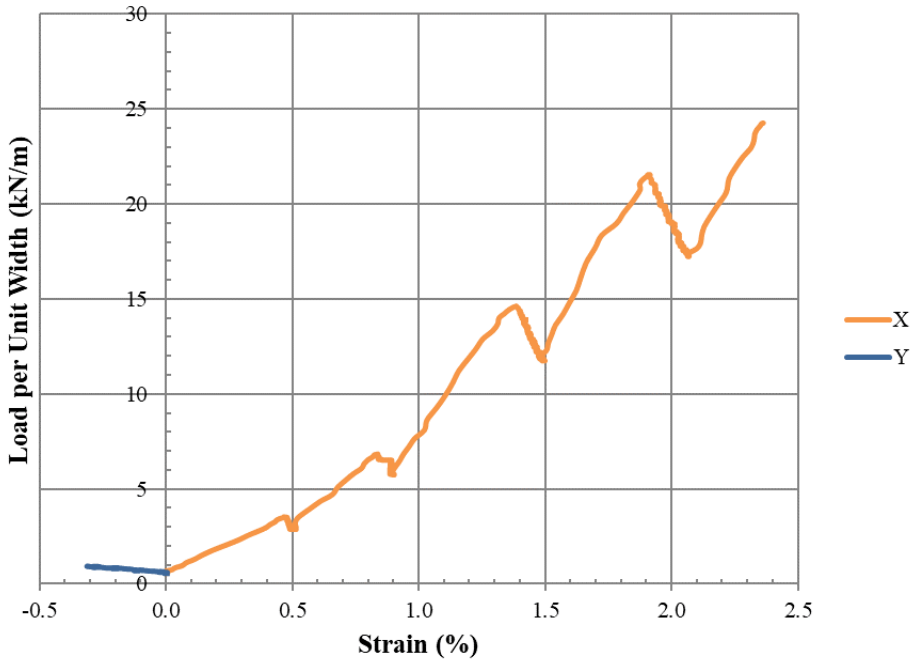

Figure 150 Geotextile B Mode 2 Trial 2

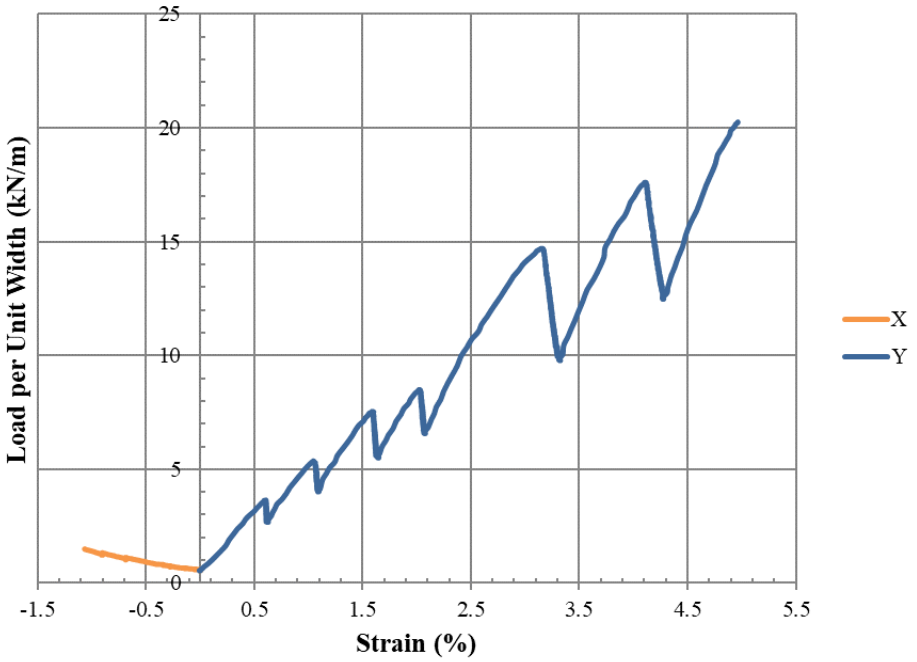

Figure 151 Geotextile B Mode 3 Trial 1

APPENDIX C

DRAFT OF TESTING STANDARD FOR DETERMINATION OF ELASTIC CONSTANTS FOR GEOSYNTHETICS USING IN-AIR BIAXIAL TENSION TESTS

Scope

This test method covers the determination of the elastic constants of geogrids and geotextiles subjected to small-strain biaxial tension tests meant to represent loads experienced by geosynthetics in field loadings such as reinforced pavement.

Terminology

Aperture – Openings in a geogrid, space between by ribs and nodes.
Cross-machine direction (XMD) - Direction of geosynthetic along the width of the roll, perpendicular to machine direction.
Cruciform sample – Shape of biaxial specimens tested, having an interior portion and four arms.
Elastic Constants – Modulus of elasticity and Poisson's ratio for XMD and MD.
Gauge Length – Distance between attachment points of LVDTs used for measurement of displacement within the interior portion of cruciform sample.
Geogrid - Geosynthetic formed by a regular network of integrally connected elements with apertures greater than 6.35 mm (1⁄4 in.) to allow interlocking with surrounding soil, rock, earth, and other surrounding materials to primarily function as reinforcement.
Geosynthetic - Product manufactured from polymeric material used with soil, rock, earth, or other geotechnical engineering related material as an integral part of a man made project, structure, or system.
Geotextile - Any permeable textile material used with foundation, soil, rock, earth, or any other geotechnical engineering related material, as an integral part of a man-made project, structure, or system
LVDT – Linearly varying displacement transducer, used to measure displacement in the interior portion of a cruciform sample.
Machine direction (MD) – Direction of geosynthetic along the length of the roll, perpendicular to the cross machine direction.
Mode 1 – Tests where both perpendicular directions were pulled in tension by an equal displacement.
Mode 2 – Tests where machine direction (MD), referred to as the Y or 2-Direction, was held at a constant displacement while the cross-machine direction (XMD), referred to as the X or 1-Direction, was displaced
Mode 3 – Tests where XMD was held at a constant displacement while the MD was displaced.
Node - Point where geogrid ribs are interconnected to provide structure and dimensional stability.
Rib - For geogrids, continuous elements of a geogrid, which are either in the machine or cross-machine direction as manufactured.

Summary of Test Method

In this test a cruciform shaped geosynthetic sample is loaded in tension to a prescribed level of permanent strain. The material is then held at this level of permanent strain such

that the material experiences stress relaxation and/or creep for 20 minutes. The material is then loaded to progressively higher levels of permanent strain with the same hold period of 20 minutes occurring at each level of permanent strain. The data collected during this period is load and displacement, which is used to calculate stress and strain. The stress and strain values are used to solve for the elastic constants of the geosynthetic using a least squares approximation for an orthotropic linear elastic constitutive model.

Apparatus Requirements

1. Must be capable of testing cruciform shaped samples of geotextiles and geogrids.
2. Must be capable of testing sufficiently large biaxial samples such that the behavior of the macrostructure of the geosynthetics can be captured.
3. Must be capable of applying an equal displacement in all four directions such that the center point of the sample remains in a constant location (mode 1 loading).
4. Must be capable of loading one direction while the other direction remains constant (mode 2 and mode 3 loading).
5. The gripping mechanism must be capable of holding the material without causing premature failure or slippage.
6. Instrumentation for measuring load and displacement must be included with device or attachable.

Sampling

Samples used for testing should be cut from near the center of geosynthetic rolls and visually inspected for any material defects or abnormalities. Once materials have been cut from a geosynthetic roll they should be flattened out using weights on all four ends of the cruciform shaped sample such that any curling of the sample is minimized.

Test Specimen

Exact test specimen size should be based upon the particular material. Geotextile samples can be cut to any size. The following dimensions should be used for both directions:
Width of material: 16 inches
Un-gripped length of crucible arm: 18 inches
Gauge length: 6 inches
Geogrid specimen sizes should be approximately those of a geotextile and will vary between products. The dimensions of specimens vary due to different geometry and aperture sizes. The specimen dimensions in each principal direction are made to match as closely as possible. Care should be taken to make the total distance between grips in both directions as close as possible.

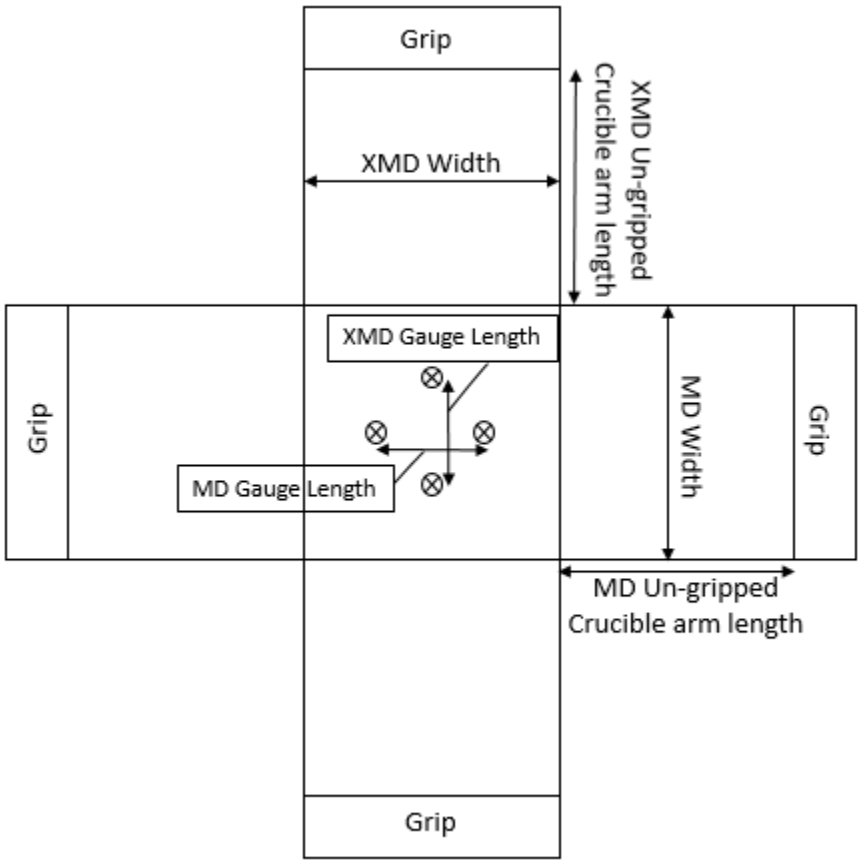

Figure 152 Biaxial Testing Specimen

Testing Setup For Geogrids

1. Make sure motor speed is set to its maximum speed of 3450 rpm. This should be done prior to placing specimen in device as it cannot be set precisely without having the motor spin.
2. Loosely place test specimen in biaxial testing device.
3. Cut necessary ribs at the end of the cruciform arm such that material can be centered in grip.
4. Align the specimen to be centered and square in each grip.
5. Tighten bolts on all four grips to 70 N-m of torque.
6. Snip the transverse ribs in cruciform arms (ribs perpendicular to direction of loading). The two rows of ribs closest to the interior portion of the sample should be snipped twice such that there is a clear gap.
7. Center the specimen on the device by adjusting the chain lengths and tightening screw at the end of each arm.
8. Once sample is approximately centered LVDT attachment can be started.

9. First place towers that hold LVDTs on the side of the biaxial device, ensuring they will not be in contact with the specimen at any point in the test.
10. Mark the location for LVDT attachment using a silver marker.
11. Drill a small hole in the nodes where LVDTs will be attached. It is helpful to place a block under the geogrid node for support when drilling the hole.
12. Align hole of electric terminal that is connected to LVDT arm with the hole drilled in the LVDT node and carefully hammer a small nail (1.2 mm x 15.9 mm) through these holes.
13. Ensure there is a small gap between the node and electric terminal and that the bottom of the nail is in the air (not in contact with device in anyway). If the nail is too long then the bottom of the nail should be cut to meet this condition.
14. Place a small amount of super glue on the nail head to ensure a rigid connection between nail and electric terminal. It is helpful to use a spacer to ensure the distance between the electric terminal and node is uniform between attachments and to hold the electric terminal in place while super glue dries.
15. Align LVDTs by adjusting the towers that hold LVDTs such that the inner core of the LVDT is straight and parallel with the outer core and is floating inside. Care should be taken with aligning LVDTs. It is also important that the LVDT is aligned such that is has enough measurement range to stay in range for the entire duration of test.
16. Place smooth blocking materials underneath the interior portion of the biaxial sample to ensure no displacement occurs out of plane. Care should be taken to avoid interference between blocking and LVDT attachment nails.
17. If a mode 2 or mode 3 test is being performed the rods should be disconnected from the load plate and connected to the stationary plate.
18. Apply a seating load of 50 lbs. in both directions. While applying the seating load precisely center the specimen on the testing device. This is done by tightening the bolt at the end of arms of the device. It can be helpful to look down ribs in all four directions to center and use device frame as a reference for centering specimen.
19. Count number of ribs (tensile elements) across the crucible arm in both directions such that a width can be calculated using method outlined in data analysis step 1.
20. Measure gauge length from centerline to centerline of nails used for LVDT attachment.
21. Calculate displacements in both directions that will correspond to permanent strain limits.
22. Ensure LVDTs are still properly aligned and 50 lb. seating load is still present.

Testing Setup For Geotextiles

1. Make sure motor speed is set to its maximum speed of 3450 rpm. This should be done prior to placing specimen in device as it cannot be set precisely without having the motor spin.

2. Loosely place test specimen in biaxial testing device.
3. Melt holes at ends of crucible arms so that bolts on grips fit through the specimen and it is centered and square in the grip.
4. Tighten bolts on all four grips to 70 N-m of torque.
5. Cut 11 slits of equal width along the crucible arms in the direction being loaded.
6. Center the specimen on the device by adjusting the chain lengths and tightening screw at the end of each arm.
7. Once sample is approximately centered LVDT attachment can be started.
8. First place towers that hold LVDTs on the side of the biaxial device, ensuring they will not be in contact with the specimen at any point in the test.
9. Mark the location for LVDT attachment using a silver marker.
10. Push the sharp threaded rod through woven fibers at the marked locations.
11. Place a nut above and below the geotextile on the threaded rod and tighten against each other to ensure a rigid connection.
12. Align LVDTs by adjusting the towers that hold LVDTs such that the inner core of the LVDT is straight and parallel with the outer core and is floating inside. Care should be taken with aligning LVDTs. It is also important that the LVDT is aligned such that it has enough measurement range to stay in range for the entire duration of test.
13. Place smooth blocking materials underneath the interior portion of the biaxial sample to ensure no displacement occurs out of plane. Care should be taken to avoid interference between blocking and LVDT attachment rods.
14. If a mode 2 or mode 3 test is being performed the rods should be disconnected from the load plate and connected to the stationary plate.
15. Apply a seating load of 50 lbs. in both directions and while doing this precisely center the specimen on the testing device. This is done by tightening the bolt at the end of arms of the device. It can be helpful to look down fibers in all four directions to center and use device frame as a reference for centering specimen.
16. Measure width of sample gripped.
17. Measure gauge length from centerline to centerline of rods.
18. Calculate displacements in both directions that will correspond to permanent strain limits.
19. Ensure LVDTs are still properly aligned and 50 lb. seating load is still present.

Testing Procedure

1. Make sure motor speed dial is set to its maximum speed of 3450 rotations per minute.
2. Make sure displacement values corresponding to permanent strain values are known.
3. Reset the data logging device (resend program) so that data being collected starts from scratch.

4. Turn the electric motor on so that it rotates forward (causing downward displacement of the load plate).
5. Turn off the electric motor as the displacement of the material approaches the value corresponding to the first level of permanent strain.
6. Once motor has stopped rotating, start a timer for 20 minutes.
7. Once 20 minutes has passed continue by repeating steps 4-6 for the desired levels of permanent strain.
8. Ensure that the material is loaded after the final 20 minute hold to a minimum value of 0.5 % strain above the final permanent strain limit.
9. Make sure to not exceed load limit of 2000 lbs. for load cells.
10. If electric motor is not capable of achieving upper levels of permanent strain it is helpful to lower motor speed after initially loading material at full speed such that the motor is capable of applying slightly more displacement.
11. Unload the material to seating load value or below.
12. Collect data from the trial performed.

Data Analysis

1. Convert measured load to load per unit width (stress) by dividing the measured load by the width it was applied over. For geogrids load per unit width should be calculated as outlined by section 11.2.2 of ASTM D7556, where the width that load will be divided by is calculated as the number of tensile elements per unit width (N_t) divided by the number of tensile elements being tested (N_r).

$$\sigma = \frac{Load}{N_r} * N_t$$

   N_t is determined by taking the average of three measurements from samples that are 95 % of the manufactured product roll width. Each measurement is performed by measuring the distance from the central point of the starting aperture (center line to center line aperture dimension divided by 2) to the center point of the aperture a distance equal to 95 % of the manufactured product roll width away from the starting aperture (this establishes the b value). As such, this measurement will result in fractional value. The number of tensile elements, N_c, within this distance, b, are counted and N_t is determined by dividing the N_c value by the b value (ASTM, 2010).
2. For both orthogonal directions, add the displacement at both LVDTs measured such that the displacement between the two LVDT attachment points is calculated.
3. From the displacement calculated in step 2, calculate strain in both orthogonal directions using the measured gauge lengths.
4. Examine load per unit width and strain data directly after 20 minute hold period.

5. Examine this data to ensure it is linear and fit a linear trendline to initial stress vs. strain data. The slope of the best fit linear trendline will be called a pseudo modulus. The stress/strain interval of the pseudo modulus varies slightly between trials but should be approximately 0.2 – 0.4 % strain and most importantly capturing the linear response. An example from a mode 1 trial is shown in Figure 153.

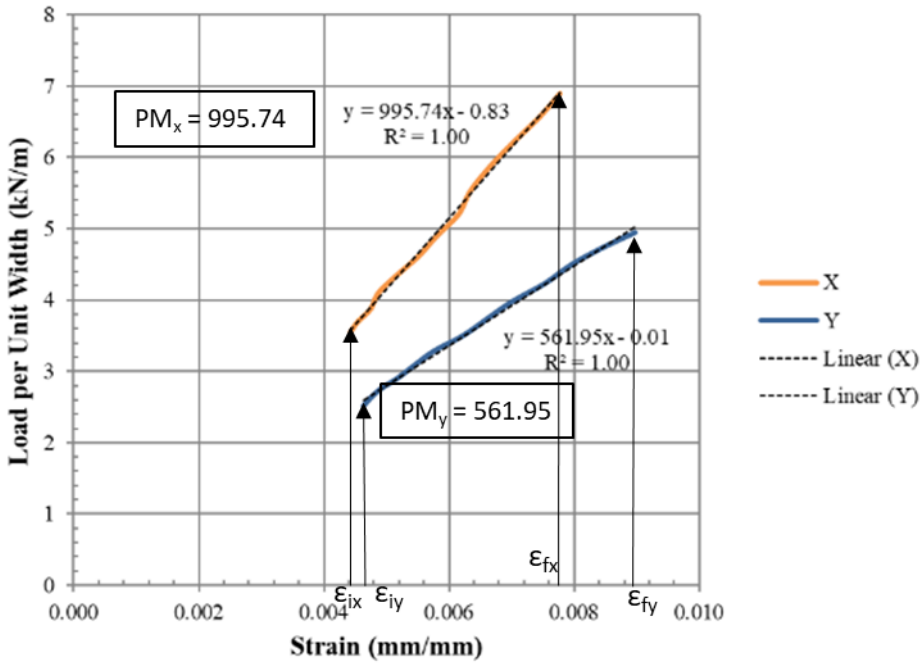

Figure 153 Determination of Pseudo Modulus for Mode 1 Loading

6. Calculate a value of stress and strain, where the strain value is the strain interval over which the pseudo modulus was calculated and is determined from the first and last data points of the interval (Equations 1 and 2) and the stress is the strain value multiplied by the pseudo modulus (Equations 3 and 4).

$$(1)\ \varepsilon_1 = \varepsilon_x = \varepsilon_{fx} - \varepsilon_{ix}$$

$$(2)\ \varepsilon_2 = \varepsilon_y = \varepsilon_{yx} - \varepsilon_{iy}$$

$$(3)\ \sigma_1 = \sigma_x = PM_x * \varepsilon_1$$

$$(4)\ \sigma_2 = \sigma_y = PM_y * \varepsilon_2$$

7. Perform steps 4-6 for all levels of permanent strain (load step).
8. Examine a plot of pseudo modulus vs. permanent strain (or load step) to examine any outlier values or trials. An example is shown in Figure 154.

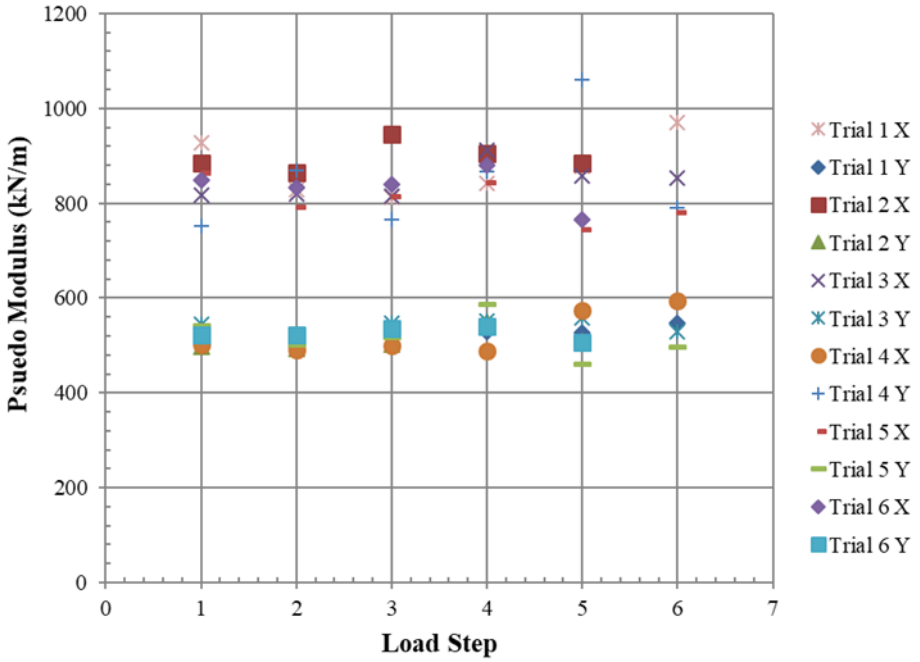

Figure 154 Pseudo Modulus vs. Load Step for Mode 1 Loading

9. Calculate an average value for pseudo modulus for each load step and mode of loading for both material directions (XMD and MD) as shown by Equations 5 and 6.

$$(5)\ \mathrm{PM}_{1,avg.} = \mathrm{PM}_{x,avg.} = \frac{\sum_i^n PM_{x,i}}{n}$$

$$(6)\ \mathrm{PM}_{2,avg.} = \mathrm{PM}_{y,avg.} = \frac{\sum_i^n PM_{y,i}}{n}$$

10. Calculate an average ratio of strain values (ratio between strain in XMD to strain in MD) for each load step and mode of loading.

$$(7)\ \left(\frac{\varepsilon_1}{\varepsilon_2}\right)_{avg.} = \frac{\sum_i^n \left(\frac{\varepsilon_1}{\varepsilon_2}\right)_i}{n}$$

11. For mode 1 loading, load step 1 assign an arbitrary value of 0.002 to strain in the XMD.

$$(8)\ \varepsilon_1 = 0.002$$

12. Calculate strain in the MD based upon the average strain ratio for mode 1, load step 1.

$$(9)\ \varepsilon_2 = \frac{\varepsilon_1}{\left(\frac{\varepsilon_1}{\varepsilon_2}\right)_{avg.}}$$

13. Calculate the stress in the XMD using the average pseudo modulus in the XMD for mode 1, load step 1.

$$(10)\quad \sigma_1 = \mathrm{PM}_{1,avg.} * \varepsilon_1$$

14. Calculate the stress in the MD using the average pseudo modulus in the MD for mode 1, load step 1.

$$(11)\quad \sigma_2 = \mathrm{PM}_{2,avg.} * \varepsilon_2$$

15. Repeat steps 11-14 for all load steps.
16. Repeat steps 11-14 for mode 2 loading.
17. Repeat steps 11-14 for mode 3 loading except assign an arbitrary value of 0.02 strain in the MD.
18. A data set with one value of stress and strain in the XMD and MD for all three modes of loading and all load steps should be generated from this process.

Calculation of Elastic Constants

An orthotropic linear elastic constitutive model was used to describe the behavior of geosynthetics subjected to biaxial tension tests. The resulting equation from this constitutive model is shown in matrix from by Equation (12) and algebraically by Equations (13) and (14).

$$(12)\qquad \begin{bmatrix}\sigma_1\\ \sigma_2\end{bmatrix} = \begin{bmatrix}C_{11} & C_{12}\\ C_{21} & C_{22}\end{bmatrix}\begin{bmatrix}\varepsilon_1\\ \varepsilon_2\end{bmatrix}$$

$$(13)\qquad \sigma_1 = C_{11}\varepsilon_1 + C_{12}\varepsilon_2$$

$$\sigma_2 = C_{21}\varepsilon_1 + C_{22}\varepsilon_2 \tag{14}$$

Constants C_{11}, C_{12}, C_{21} and C_{22} are defined by Equations (15), (16), (17) and (18)

$$C_{11} = \frac{E_1}{1-\nu_{12}\nu_{21}} \tag{15}$$

$$C_{22} = \frac{E_2}{1-\nu_{12}\nu_{21}} \tag{16}$$

$$C_{12} = \frac{\nu_{21}E_1}{1-\nu_{12}\nu_{21}} \tag{17}$$

$$C_{21} = \frac{\nu_{12}E_2}{1-\nu_{12}\nu_{21}} \tag{18}$$

The major and minor Poisson's ratio terms are related by Equation (19) and constrained by Equation (20).

$$\nu_{12} = \nu_{21}\,\frac{E_1}{E_2} \tag{19}$$

$$\nu_{12}\nu_{21} < 1 \tag{20}$$

A least squares approximation is used to solve for the elastic constants of geosynthetics using the data generated from biaxial tests. The least squares approximation can be performed as a stress or strain minimization. Reported values for elastic constants should be an average of the value obtained from stress and strain minimizations. The process for calculating elastic constants using a stress minimization is shown by Equations (21) through (27).

$$S = \sum\{(C_{11}\varepsilon_1 + C_{12}\varepsilon_2 - \sigma_1)^2 + (C_{21}\varepsilon_1 + C_{22}\varepsilon_2 - \sigma_2)^2\} \tag{21}$$

$$\frac{\partial S}{\partial C_{11}} = \frac{\partial S}{\partial C_{22}} = \frac{\partial S}{\partial C_{12}} = 0 \tag{22}$$

$$\begin{bmatrix} \sum(\varepsilon_1^2) & \sum(\varepsilon_1\varepsilon_2) & 0 \\ \sum(\varepsilon_1\varepsilon_2) & \sum(\varepsilon_2^2+\varepsilon_1^2) & \sum(\varepsilon_1\varepsilon_2) \\ 0 & \sum(\varepsilon_1\varepsilon_2) & \sum(\varepsilon_2^2) \end{bmatrix} \begin{bmatrix} C_{11} \\ C_{12} \\ C_{22} \end{bmatrix} = \begin{bmatrix} \sum(\sigma_1\varepsilon_1) \\ \sum(\sigma_1\varepsilon_2+\sigma_2\varepsilon_1) \\ \sum(\sigma_2\varepsilon_2) \end{bmatrix} \tag{23}$$

$$E_2 = C_{22} - \frac{C_{12}^2}{C_{11}} \tag{24}$$

$$\nu_{12} = \left[\frac{C_{11}}{C_{22}}\left(1 - \frac{E_2}{C_{22}}\right)\right]^{0.5} \tag{25}$$

$$E_1 = \frac{\nu_{12}^2 E_2}{1 - \frac{E_2}{C_{22}}} \tag{26}$$

$$\nu_{21} = \nu_{12}\,\frac{E_2}{E_1} \tag{27}$$

For a strain minimization Equations (13) and (14) are rearranged in terms of strain as defined in Equations (28) and (29).

$$\varepsilon_1 = \frac{\sigma_1}{E_1} - \frac{\sigma_2}{E_2}\nu_{21} \tag{28}$$

$$\varepsilon_2 = \frac{\sigma_2}{E_2} - \frac{\sigma_1}{E_1}\nu_{12} \tag{29}$$

Constants are defined by Equations (30) through (32)

$$E_{11} = \frac{1}{E_1} \tag{30}$$

$$E_{22} = \frac{1}{E_2} \tag{31}$$

$$E_{12} = \frac{\nu_{12}}{E_1} = E_{21} = \frac{\nu_{21}}{E_2} \tag{32}$$

Least Squares is applied in a similar manner as for the stress minimization as shown in Equations (33) through (35). The elastic constants are calculated using Equations (36) through (39).

$$S = \sum[\{(E_{11}\sigma_1 - E_{12}\sigma_2) - \varepsilon_1\}^2 + \{(E_{22}\sigma_2 - E_{12}\sigma_1) - \varepsilon_2\}^2] \tag{33}$$

$$\frac{\partial S}{\partial E_{11}} = \frac{\partial S}{\partial E_{22}} = \frac{\partial S}{\partial E_{12}} = 0 \tag{34}$$

$$\begin{bmatrix} \sum(\sigma_1^2) & \sum(-\sigma_1\sigma_2) & 0 \\ \sum(-\sigma_1\sigma_2) & \sum(\sigma_2^2 + \sigma_1^2) & \sum(-\sigma_1\sigma_2) \\ 0 & \sum(-\sigma_1\sigma_2) & \sum(\sigma_2^2) \end{bmatrix} \begin{bmatrix} E_{11} \\ E_{12} \\ E_{22} \end{bmatrix} = \begin{bmatrix} \sum(\sigma_1\varepsilon_1) \\ \sum(-\sigma_1\varepsilon_2 - \sigma_2\varepsilon_1) \\ \sum(\sigma_2\varepsilon_2) \end{bmatrix} \tag{35}$$

$$E_1 = \frac{1}{E_{11}} \quad (36)$$

$$E_2 = \frac{1}{E_{22}} \quad (37)$$

$$\nu_{12} = E_1 * E_{12} \quad (38)$$

$$\nu_{21} = \nu_{12} \frac{E_2}{E_1} \quad (39)$$

The elastic constants are calculated at each load step using the data set of stress and strain values from all three modes of loading for that given load step as described in Step 19 in the Data Analysis section. If a single set of elastic constants is desired then data sets from all load steps should be combined.